Synthetic Approaches Utilizing Zeosils: Inorganic Insertion Compounds and Hierarchical Pore Structures

Von der Naturwissenschaftlichen Fakultät der Universität Hannover

zur Erlangung des Grades

Doktorin der Naturwissenschaften

– Dr. rer. nat. –

genehmigte Dissertation

von

Dipl.-Ing. Geanina Ramona Nechifor

geboren am 22. Dezember 1976

in Resita (Rumänien)

2005

Referent: Prof. Dr. Peter Behrens
Korreferent: Prof. Dr. Jürgen Caro
Tag der Promotion: 20. Juli 2005

Erklärung

Hiermit erkläre ich gemäß §6.b der gemeinsamen Ordnung der naturwissenschaftlichen Fachbereiche der Universität Hannover für die Promotion zum „Doktor der Naturwissenschaften“, dass ich die Dissertation unter dem Titel „Synthetic Approaches Utilizing Zeosils: Inorganic Insertion Compounds and Hierarchical Pore Structures“ selbst verfasst und die benutzten Hilfsmittel und Quellen vollständig angegeben habe.

Gemäß §6.c erkläre ich weiterhin, dass diese Dissertation noch nicht veröffentlicht und in keiner Form als Prüfungsarbeit verwendet wurde.

Hannover, den 18.05.2005

Dipl-Ing. Geanina Ramona Nechifor

Acknowledgements

And now, that I reached the end, I would like to acknowledge those people, family, friends and colleagues, that stood by me in these last three years. It is a tradition to do so, even if the words will never be able to express my real gratitude to them.

Let me start by first thanking my family, who even if never completely understood what I'm doing so far from them, supported me always and believed I'm going to make it.
To my husband, Marcello, thanks for your permanent encouragement and for your support during all these years. I cannot tell you how happy I am to have you by my side.

Prof. Behrens, thank you for giving me the chance to enter your group and together with this, into the captivating world of zeolites, so new for me. Thank you also for all our discussions (never giving up talking English to me) and for the opportunity to participate to many conferences that allowed me to find out more about the world of research.

Special thanks to Birgit and Songül, so good friends from the beginning. You showed me the other side of Hannover, the one outside work. And thanks Birgit for always finding the time for my TGA measurements.

To all my colleagues, past and present, Dr. Andreas Schneider, Dr. Michael Wiebcke, Olaf, Clemens, Hans, Stephan (all doctors now), Carsten, Petra who welcomed me in Germany and made me feel as home. I will always remember our badminton evenings!
Special thank to Ralph and Monika, who shared with me their experience with zeosils.
But thanks also to the younger colleagues, Stefan, Katrin, Boris, Ilka, Michael, Kay, who brought fresh ideas and enthusiasm to our group.
I wish you all the best.

I would like to express my acknowledgment to the people in Leuven, who hosted me in their labs for three months. Thank to Prof. Martens, who accepted me there and gave me the opportunity to learn about zeogrids and zeotiles.
My gratitude to Prof. Cristine Kirschhock, for always finding time for me and for our discussions.

Special thanks to Sebastien and Alex, to Bogdan, Steliana, Roxana, Raluca, Angelica and Andrei, who guided me through the “labyrinth” of the Institute from Leuven.
Best wishes to you all.

With regard to the Raman and TGA experiments, I am very grateful to PD Dr. Claus Rüscher from the Institute of Mineralogy, Hannover; and to Sonja Locmelis from AK Binnewies, thanks for sharing with me the “strategy” of melting quartz-ampoules.

Last but not least I would like to thank the Graduate Program sponsored by the State of Niedersachsen for bringing together people of so many nationalities and creating this multicultural experience. Kalpana, Andrea, Adrian, Paras, Marc, Rana, Muayad, Murshed, Nisath, Ling, Alexander, to all of you, my best wishes for the future.

Table of contents

Abstract

In the first part of this work, insertion compounds of inorganic substances of porosils are described. Porosils possess pure silica microporous crystalline frameworks; a special class of porosils are zeosils, which possess channel-type voids. After previous work in our group on small and medium pore zeosils, the focus here is on large and extra-large pore zeosils, having channels which are circumscribed by 12 or 14 [SiO_4] tetrahedra, respectively. The chosen zeosils are ITQ-4 (IFR), SSZ-24 (AFI), CIT-5 (CFI) and UTD-1(OH). Different inorganic species, as iodine, selenium, mercury(II) halides and gold(III) chloride were used as guest components. On the basis of the different pore characteristics of the crystalline host materials, different stabilities of the insertion compounds were observed, which are related to the strengths of host-guest interactions. More important, it was also possible to observe different degrees of guest-guest interactions. Extra-large pore zeosils as UTD-1 also allowed for the insertion of gold(III) chloride, which cannot be introduced into medium and large pore zeosils.

The second part of the work deals with the synthesis of novel porous materials with a hierarchical pore structure, the so-called zeodyes. They were prepared using the “clear solution” and an azo-dye as surfactant. The clear solution is a nanoslab suspension, containing slab particles with dimensions of 1.3 x 4.0 x 4.0 nm, which possess the crystalline structure of Silicalite-1. The synthesis conditions were optimized in order to obtain stable and ordered structures. The newly synthesized materials have layered structures. They were investigated with powder X-ray diffraction and UV-vis spectroscopy. Upon template removal, materials with hierarchical pore structures (combined micro- and mesoporosity) were obtained, as shown by nitrogen adsorption experiments.

Keywords: zeosil, insertion, meso-microporous materials

Kurzzusammenfassung

Im ersten Teil dieser Arbeit werden Insertionsverbindungen von anorganischen Substanzen in Porosilen beschrieben. Porosile besitzen rein silicatische mikroporöse kristalline Gerüste; eine Unterart sind die Zeosile, die kanalförmige Hohlräume haben. Während frühere Arbeiten in unserem Arbeitskreis sich mit Zeosilen beschäftigten, die kleine und mittlere Poren aufweisen, basiert die vorliegende Arbeit auf Zeosilen mit großen oder sehr großen Poren, die Zwölfer- oder Vierzehner-Ringöffnungen zeigen. Es handelt sich hierbei um die Zeosile ITQ-4 (IFR), SSZ-24 (AFI), CIT-5 (CFI) und UTD-1(OH). Verschiedene anorganische Moleküle wie Iod, Selen, Quecksilber(II)-Halogenide und Gold(III)-Chlorid wurden als Gastmoleküle verwendet. Sie werden in evakuierten Ampullen über die Gasphase in die Hohlräume der mikroporösen Siliciumdioxid-Wirte eingelagert. Anhand der definierten Porenabmessungen der kristallinen Materialien lassen sich unterschiedliche Stabilitäten der Insertionsverbindungen auf der Basis der Stärke der Wirt-Gast-Wechselwirkungen erklären. Insbesondere werden aber auch unterschiedliche Gast-Gast-Wechselwirkungen beobachtet. Zeosile mit sehr großen Porenabmessungen wie UTD-1 erlauben auch die Insertion von Gold(III)-Chlorid, das nicht in die Zeosile mit mittelgroßen und großen Poren eingelagert werden kann.

Das zweite Teil der Arbeit beschäftigt sich mit der Synthese von Siliciumdioxid-Compositen, die eine hierarchische Porestruktur aufweisen, den sogenannten “zeodyes“. Sie wurden mit Hilfe der "clear solution" und einem Tensid, das eine Azofarbstoffgruppe enthält, aufgebaut. Die “clear solution“ ist eine Suspension von "nanoslabs"; sie enthält plättchenförmige Partikel mit Abmessungen von 1.3 x 4.0 x 4.0 nm mit der Kristallstruktur des Silicalit-1. Die Synthesebedingungen wurden optimiert, um die gewünschten Strukturen in stabiler Form zu erhalten. Die erhaltenen Azotensid-Silica-Composite sind lamellar aufgebaut. Die Systeme wurden mit Röntgenpulverdiffraktometrie und UV-Vis-Spektroskopie analysiert. Nach der Templat-Entfernung wurden Materialien mit hierarchischer Porenstruktur (Mikro- und Mesoporen erhalten, wie mittels Stickstoffadsorptionsuntersuchungen gezeigt wurde.

Schlagworte: Zeosil, Adsorption, meso-mikroporöse Materialien

1. INTRODUCTION

The controlled synthesis and the application of new host-guest compounds with tailored properties has become an important goal in the recent solid-state chemistry. Among the host systems used, crystalline microporous materials are more and more applied, since their well-defined voids allow specific arrangements of the guest species [SD90] [BS96] [OZ92]. Such microporous materials have frameworks consisting of channels or cages with diameters in the range from 2 to 10 Å, which allow rather small molecules to enter, but avoid the formation of bulk phases. By the use of microporous pure silica modifications (zeosils) as hosts in the insertion experiments, the host-guest interactions become very weak and so, the properties of the insertion compounds are mainly determined by guest-guest interactions. Rather, these interactions between the inserted guest species can be controlled by the pore system. The dimensions (channel diameters, interconnection of channels) of the host-pore system regulate the arrangement of the occluded guest molecules; the geometry of the pores system may allow for or eliminate interactions between the guest molecules. Inside the void system, the guest species can be stabilized as atoms, clusters or molecules. This depends on the space offered by the host, so practically on the host dimensionality.

Different types of molecules have been successfully loaded into such zeolites, including organic [JA02] [SW02], organometallic [OG89] [BP97] and inorganic species [OZ92] [WI98], resulting in composite materials with new properties.

Lately, many investigations have focused on the insertion of different inorganic species into medium pore zeosils, when different stabilities of the insertion compounds were observed. The state of the guest molecules inside the void system of these hosts was found to be nearly unperturbed, with molecules that resemble those present in gaseous phase or in non-coordinating solvents.

So far, only a limited number of application experiments using large or extra-large pore zeosils (like the 12-membered ring (MR) ITQ-4 and SSZ-24 or the 14 MR CIT-5 and UTD-1) have been reported. Here, we tried to evaluate the sorption capacity of these microporous materials and compare it with the one found for the medium-pore zeosils [WI98], in order to establish the potential benefits of these larger pores in processing large molecules.

Next, the synthesis of novel hierarchical pore systems is described. The “dual-templating” procedure used by a group in Leuven for the preparation of zeogrids and zeotiles, provides the basis of this work. By using different molecules as secondary templates (azo-dyes) and various

synthesis conditions, new materials were synthesized, the so-called zeodyes. Their double-porosity characteristic, their stability and the advantage in circumventing diffusion problems make them interesting materials for further applications, with regard to traditional zeolitic materials.

2. GENERAL CONSIDERATIONS

2.1. Porous inorganic materials

A substance can be described as porous if one part of its total volume is occupied by pores. When talking about porous inorganic materials, one should first clearly define a length scale associated with the pore sizes. In this sense, the most accepted one is the definition proposed by IUPAC (International Union of Pure and Applied Chemistry) in the early 1970's [EV72] [RA94]. With regard to this proposal, porous materials can be divided in three categories, as follows:

- microporous materials, with pores in the range up to 20 Å,
- mesoporous materials, with pore sizes between 20 and 500 Å, and
- macroporous inorganic materials, having pores larger than 500 Å.

In the category of microporous materials, ultra-micropores, with dimensions up to 10 Å, and super-micropores, having diameters between 10 and 20 Å, can be further distinguished [RR99]. Porous gels and glasses lie, due to their pore size, in between the meso- and the macroporous range.

Having a definition of the various porous inorganic materials, we will take now a closer look to materials interesting for the insertion experiments discussed in this work, namely crystalline microporous oxides. The physicochemical properties of zeolites made them one of the most interesting class of minerals for scientists since their first description [CR56]. The Greek name of zeolites, „ζειν", to boil, and „λιθος", stone, describes the behavior of zeolites upon fast heating, when they seem to boil because of the fast water loss. The many different silicate zeolite structure types can be summarized with the general formula: $A_{(4-w)y/x}^{x+}[Si_{1-y}T_y^{w+}O_2]*zH_2O*nM$, where A represents mono- or divalent cations, T tetra, tri-, di- or monocovalent cations tetrahedrally coordinated by oxygen, and M neutral atomic or molecular guest species. The zeolites consist of corner-sharing $[TO_4]$ tetrahedrons, where T represents Si or Al. The Si/Al ratio lies between 1 and ∞. In the aluminosilicate framework, $[AlO_4]$ tetrahedra are negatively charged because of the trivalent state of aluminum. The charge of the whole framework can be compensated by mono- or divalent cations present within the cavities. More than 130 different topologies of zeolites and similar substances are known up to now. These structure types are described by a three letter code and are listed in the „Atlas of Zeolite Structure Types" issued by the International Zeolite Association (IZA) [BM01]. Only about one

quarter of them occurs naturally, the others are synthetic. The main properties of zeolites are their crystal lattice, their framework density (FD) (defined as the number of T atoms per 1000 $Å^3$), and finally, their channel and cage system. Zeolite channels are classified according to the number of oxygen- or T-atoms forming the window together with the geometrical dimensions of the two channel openings. Cages are, per definition, voids bigger in diameter than the normal channel system. They are only accessible through the channel system [GS99].

A sub-classification of the porous tectosilicates was done by Liebau et.al. [LG86] and based on geometrical and chemical considerations. They described as "porosils" the all-silica members of this class [GS99]. Porosils have a neutral tetrahedral [SiO_2] framework and thus no framework-charge balancing cations. As a consequence, the materials are hydrophobic and have a higher thermal stability than the conventional alumino-silicate zeolites [GM98].

Porosils are further subdivided in clathrasils and zeosils, depending on the pore geometry, which is cage-like or channel-like, respectively [LG86]. The cages in clathrasils are bound by not more than 6-membered ring (MR) units, suppressing properties such as sorption/desorption of organic molecules. In contrast, zeosils have at least 8 MR windows with a pore width larger than 4 Å. For small molecules, such apertures are large enough to penetrate. Since the porosity of the different zeolite (zeosil) structure types is created only after the calcination of the as-synthesized material, their specific properties become obvious only after the removal of the organic template.

Porous inorganic materials are showing, due to their large inner surface, interesting adsorption, catalytic and ion-exchange properties. Classical applications of these materials are therefore in the area of separation and cleaning processes, heterogeneous catalysis, and ion-exchange. Due to their charged framework, the zeolites are hydrophilic and so they easily adsorb polar molecules. Strong electrostatic interactions are present between the zeolite host and the adsorbed molecules. On the other hand, porosils, due to their uncharged framework and hydrophobic character, have a strong preference for the sorption of unpolar molecules. In the host-guest compounds, there are only weak van der Waals interactions between the zeosil framework and the adsorbed species.

Many new zeolite topologies have been synthesized in the last years, including uni- and tridirectional 10- or 12-membered ring (MR) pores. But their application in catalysis and sorption experiments is typically limited to molecules with diameters smaller than 0.8 nm. Reactants with larger sizes cannot diffuse into their pores (channels) and can thus not be selectively processed [MD99]. Therefore, the synthesis of microporous materials with larger pores represents an important goal. The recently synthesized large and extra-large pore zeosils

SSZ-24 [NA93], CIT-5 [BD98b] [WY97] and UTD-1 [BG95] [FT96] having 12 and 14 MR channels, respectively, are the materials that provide the basis of the present work. They were used in application experiments as host molecules for sorbing inorganic unpolar molecules.

2.2. Synthesis of microporous materials

2.2.1. Hydrothermal synthesis of zeosils

The synthesis of zeolites started with the pioneering work of Barrer and coworkers in the late 1940's [BA82]. The zeolites, typically aluminosilicate zeolites, were synthesized using a sol-gel method in an aqueous solution in a temperature range between ambient and about 300 °C under autogenous pressure. In a typical synthesis procedure, the starting materials, the silica source together with the alumina and the cation source, were mixed together while the pH was maintained above 7. The general problem of this synthesis route was that zeolites with different stoichiometries were obtained. The question was then how to predict the structure produced, i.e. how to make the different components react in such a way to give the product with the desired stoichiometry and crystal structure. The sol-gel method was developed further by using a structure-directing agent (SDA) which acts as a kind of template for the zeolite cavities. Typically SDAs are small organic amines or ammonium ions. After synthesis, the SDA removal has to be performed by thermal and oxidative decomposition or by extraction.

A typical hydrothermal synthesis involves mixing the silicate and aluminate solutions in the presence of inorganic and/or organic cations or molecules as well as water and a mineralizing agent to form an aluminosilicate hydrogel. To obtain pure silica zeosils, no alumina source is needed. Thus, the reaction mixture containing the SDA, silica source, water and a mineralizing agent is heated to 80 to 200 °C for some time (hours, days or even weeks). Many reviews on the hydrothermal gel method are available [BA82], [GI92].

Since every type of SDA is distinct in its properties, its influence on the structure type formed during the hydrothermal synthesis is very important. Although the nucleation and crystal growth to a stable crystallite are still mysterious, the host-guest interactions between the organic molecule and the silica precursors during the early stages of crystallization strongly influence the assembly of the inorganic framework. Despite the fact that the most important parameters, as composition of the reaction mixture, temperature, pressure and pH value can be varied in a wide range, and so the kinetics and thermodynamics can too, some general and qualitative conclusions can be drawn about the role of these organic molecules in the formation of the microporous SiO_2 frameworks. The SDAs can act in three different ways [DL92]:

(i) as mere pore fillers, which are occluded during synthesis in the small voids and do not influence the crystallization actively,

(ii) as structure-directing agents in a narrower sense, which direct the formation of the microporous materials towards certain frameworks [LZ95]; in this way different topologies can be obtained when using the same SDA, depending on the kinetic and the thermodynamic of the reaction, and

(iii) true templates, which only direct one zeolite topology. The SDAs used in the hydrothermal syntheses can be either neutral or charged. They have to be soluble in the reaction mixture and need to possess a sufficient chemical stability under the synthesis conditions. The size and the shape of the SDA determine the size and shape of the pores, so spherical molecules favour cage-like voids, whereas chain-like molecules lead predominantly to one-dimensional channels. SDAs with branched chains typically form intersecting channel systems. For almost every structure type, there are several different SDAs, indicating the flexibility of the silica framework.

There are also SDAs which direct different structure types under various synthesis conditions. So, together with the size and the shape of the SDA, some other parameters like temperature, pressure, pH, concentration of the template and of the silica source and the ratios between these two play an important role in the formation of a specific porous material.

In order to mobilize the silica, so-called mineralizing agents are necessary. As silica is insoluble in neutral water but dissolves in basic solutions, these mineralizing agents typically are bases, e.g. NaOH or Na_2CO_3. When no mineral bases are present in the reaction mixture, the basicity of the synthesis solution depends only on the Brønstedt basicity of the SDA. Under acidic conditions, fluoride anions can also serve as mobilizing agents for silica, in the so-called "fluoride-route" [GK86]. F^- ions can also become incorporated as co-guest molecules in the small cavities of the porous structure.

Different phases can be prepared using the same SDA by just varying the ratio between water and the silica source. Thus, the effect of the water content in the synthesis mixture can modify in some extent the structure-directing ability of the SDA and very different pore architectures can be made by using the same SDA [GM98].

2.2.2. Synthesis of zeogrids and zeotiles from clear-solution

A special method for the synthesis of porous materials, developed in the late 1970's and called the "clear solution" process, occurs in a liquid phase which is transparent for the human eye and therefore denoted as a clear solution (in contrast to the opaque gel phase typically occurring in zeolite syntheses) [UK79] [UM80] [UK84] [KU81] [SS93] [SS94a] [SS94b]. The clear solution is prepared at room temperature by the hydrolysis of tetraethylorthosilicate (TEOS) in concentrated TPAOH (tetrapropylammonium hydroxide) aqueous solution. The Si : TPA molar ratio is 25 : 9 and the Si : water content is 25 : 440 [RK99b] [KR04]. As shown by extensive research by a zeolite group from Leuven, the clear solution contains nanoslabs having dimensions of 1.3 x 4.0 x 4.0 nm in the *a*, *b* and *c* crystallographic directions, and has a framework connectivity which is similar to that of Silicalite-1. Each nanoslab contains between 396 and 432 Si atoms [RK99b]. The as-synthesized nanoslabs contain the TPA^+ ions at the intersections of the straight and zigzag channels of the MFI-like structure. The clear solution is stable at room temperature [PS94], but under heating to 100 °C for one or two days, the nanoslabs aggregate to form large Silicalite-1 crystals [RK98]. The formation and the structure of Silicalite-1 nanoslabs was characterized and published in 1999 by Ravishankar et.al. and by Kirschhock et.al. [RK99a] [RK99b] [KR99a] [KR99b] [KR99c].

The Silicalite-1 nanoslabs were then used by the Leuven group as building units in the synthesis of new materials, the so-called zeogrids and zeotiles.

Formation mechanism

Surfactant molecules belong to a class of substances called amphiphilic. They are characterized by a polar head and a non-polar, often hydrocarbon tail. When dissolved in water or in any other polar solvent, these molecules arrange themselves in such a way that the polar head is dissolved in the polar solvent, while the opposite end is kept isolated from the solvent. At this point, the solution looks like particles of solute randomly distributed through the solvent. As the concentration of the surfactant in solution increases, the molecules take on different arrangements or phases. When a certain concentration is reached, the so-called critical micelle concentration (cmc), micelles can form. They can take different shapes, like spheres, rods or disks. The surface of a micelle is in fact a layer of polar heads dissolved in the polar solvent. The inner part is formed by the hydrophobic ends, normally hydrocarbon tails. The micelles can have different sizes, but the smallest has a diameter that equals two times the length of the hydrocarbon tail. The temperature has an influence on the formation of the micelle in such a way that it starts to form only above a certain temperature. Together with this, the shape of the surfactant has an influence on the size and the shape of the micelle. It is known that in aqueous solutions surfactants form liquid-crystal phases, the so-called lyotropic phases. The type of lyotropic phase depends on the surfactant concentration (Figure 2.2.2.1.).

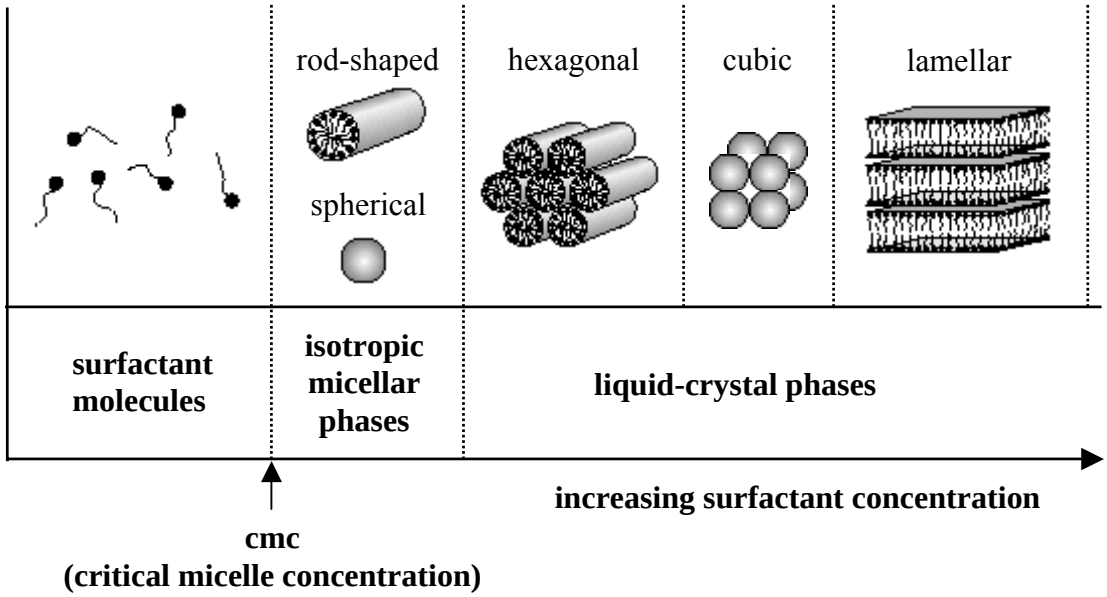

Fig. 2.2.2.1. Lyotropic phases.

In the synthesis of M41S mesoporous silica materials by means of CTAB (cetyltrimethylammonium bromide) surfactant, low surfactant concentrations yield to hexagonal MCM-41, whereas a high surfactant concentration leads to lamellar MCM-50 [ZL96]. In between, the cubic MCM-48 is obtained in a narrower CTMABr concentration window [BG97]. Zeogrids were formed by the precipitation of Silicalite-1 nanoslabs in the presence of a surfactant (a solution of CTAB, cetyltrimethylammonium bromide, in ethanol). The synthesis takes place at room temperature and results in the formation of a layered material exhibiting a characteristic repeat distance of 3.0 nm. The explanation given for the formation of the zeogrid structure was that, during precipitation, the surfactant was intercalated in between the nanoslabs. The repeat distance can then be interpreted as the thickness of the nanoslab, 1.3 nm, plus the thickness of the surfactant layer, measured to be 2.7 nm (Fig. 2.2.2.2.). After TPA and surfactant evacuation by calcination at 400 °C, a porous material, containing ultra- (20 %) and super-micropores (80 %), was obtained. The elimination of the surfactant from between the layers causes the fusion of the nanoplates, whereby empty spaces are formed in between the nanoslabs. These spaces represent the super-micropores. The ultra-micropores present in the final structure of the zeogrid materials are appearing after the evacuation of the structure-directing agent (TPA^+) from the channel intersections of the former Silicalite-1 nanoslabs [KR04].

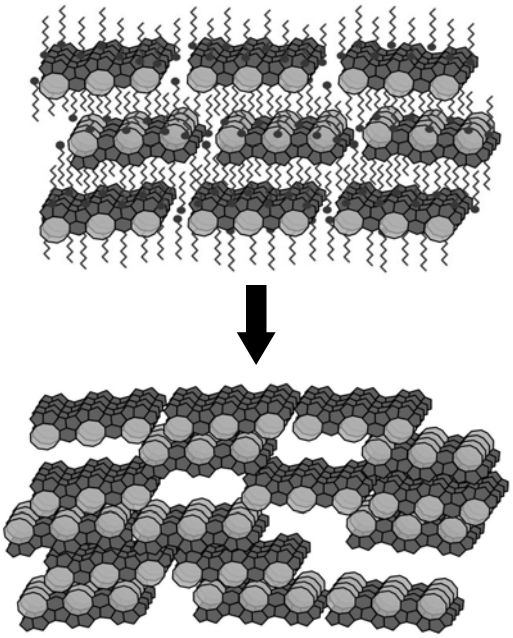

Fig. 2.2.2.2. Schematic representation of the formation of the zeogrid structure [KR04].

The other type of material synthesized using the clear solution is the zeotile-type. These materials were obtained when the nanoslab suspension was heated before the addition of the surfactant. Three different types of zeotiles have been synthesized by using different synthesis conditions, like temperature, time, or by using different molecules as secondary surfactant templates (solutions of CTAB in water or powdered CTAB, or triblock copolymers under acidic conditions). A review of the three synthesis methods to obtain zeotile-type materials is given in Table 2.2.2.3.

Table 2.2.2.3. Synthesis parameters to obtain zeotile materials [KR04].

Zeotiles	secondary template	*T* / °C	time
Zeotile-1	CTAB, aqueous solution	25	20 min
Zeotile-2	CTAB, powder	100	3 days
Zeotile-4	P123 copolymer, acidic conditions	90	4 days

The as-synthesized materials were subject to surfactant extraction and afterwards calcination. The three zeotiles have different structures: zeotile-1 and zeotile–4 are hexagonal, where zeotile-2 has a cubic structure. They are all microporous-mesoporous materials. Zeotile-2 has a mesostructure which is similar to the cubic mesoporous MCM-48 phase, with the difference that the walls of zeotile-2 are composed of zeolitic microporous Silicalite-1 units, corresponding to the nanoslabs.

The zeogrid and zeotile structures were analysed using high-resolution transmission electron microscopy (HR-TEM), X-ray diffraction and scanning electron microscopy (SEM), and their porosity was studied using nitrogen adsorption experiments. The extraction of the surfactant and the calcination processes were mainly described on the basis of the thermogravimetric results [KR04].

These new synthesized materials, due to their double-porosity characteristics and higher stability, can extend the application area of the simple zeolitic materials. Their hierarchical pore system circumvent diffusion problems that may appear when using normal zeolitic materials. In the present work, following the synthesis methods to obtain zeogrid and zeotile materials, by using special surfactants (“azo-surfactants”), novel interesting layered materials were obtained.

2.3. Insertion compounds

As described in the previous chapter of the present work, zeosils find their main application as highly selective adsorbents for sorbing unpolar molecules from wet gas streams or aqueous solutions. In basic research, zeosils can be used as geometrically structuring media, when the host pore system can be filled with guest molecules. Due to the electroneutrality of the zeosils, the host-guest interactions are very weak. The dimensions (channel diameters, interconnection of channels) of the host pore system then regulate the arrangement of the inserted molecules in a purely geometric fashion; especially, the geometry of the pore system may allow for or eliminate interactions between the guest species.

This idea was tested by the insertion of several different inorganic species into zeosils. For example, the insertion of sulphur [WF99a] or selenium [WF99b] into the zeosil host decadodecasil 3R (DDR) with cage-like voids leads to compounds containing S_7 and Se_6 rings, respectively, instead of the more stable chalcogen rings with eight atoms, which would be too large to fit into the cages. The confinement of selenium into the nearly cylindrical channels of $AlPO_4$-5 was also investigated by Poborchii et.al. [PK99]. It was found that selenium was incorporated as Se chains and Se_8 rings. A large number of other studies regarding the Se-loading into different zeosils have been published, e.g. selenium incorporated into the channels of mordenite [PK97] [BP85].

For the insertion of mercury halides HgX_2 (X: Cl, Br, I) [BH01] [WP02] and halogens (Br_2 and I_2) [WP96], a larger variety of zeosil hosts with ten-membered ring channels, (channel diameter of ca. 5.5 Å), was employed. In case of mercury(II) halides insertion compounds in medium pore zeosils, the interactions between the guest species and the electroneutral SiO_2 framework are very weak. Together with this, no indication of any significant guest-guest interaction between the occluded molecules was found. The HgX_2 molecules were in an almost unperturbed state, similar to the one in gaseous phase or in non-coordinating solvents [WP02].

Interesting results were obtained for the insertion compounds of iodine, where it was possible to control the guest-guest interactions by the different dimensionalities of the pore system of the zeosil hosts [WP96] [FB99]. First of all, the characteristic colours of the zeosils after insertion give indications about the degree of interaction between the occluded iodine molecules. For example, iodine in DDR has a violet colour, similar to the one of gaseous iodine; I_2–TON is violet to dark blue, indicating iodine molecules interacting in one dimension; and MFI containing I_2 was red-brown. This colour resembles that of liquid iodine and indicates

interactions in three dimensions, however, interrupted by the MFI silica framework. UV-vis and Raman spectroscopy were further used to investigate these interactions.

Here, we extend the investigations on insertion compounds based on zeosils with larger pore diameters, ITQ-4, CIT-5, SSZ-24 and UTD-1, having twelve- or fourteen-membered ring windows and channel diameters between 6 and 10 Å. All the pore systems consist of uni-dimensional channels. These large and extra-large pore zeosils have become available only in the recent years.

2.4. Structures of host materials

Four all-silica porous materials, ITQ-4 (IFR), SSZ-24 (AFI), CIT-5 (CFI) and UTD-1 have been considered for the assembly of insertion compounds. The letters between the brackets indicate the topology code of these materials as provided by the International Zeolite Association (IZA). Fig. 2.4.1. depicts the structure of these zeosils as well as the dimensionality and channel diameters of their pore systems [BC97b] [BM91] [WY97] [FT96]. Silicalite-1, with its 10 MR pores, is considered as a medium-pore zeosil. Here, it is used as a representative of this class in order to compare its insertion behavior, which has been extensively studied [WP96] [WP02] [WI98], with that of the other four zeosils. These can be considered as large pore (ITQ-4, 12 MR; SSZ-24, 12 MR) or extra-large pore (CIT-5, 14 MR; UTD-1, 14 MR) zeosils. They all have one-dimensional channel systems, which consist of channels running parallel to each other. MFI, on the other hand, has a three-dimensional channel system that contains two types of channels, a linear and a sinusoidal one (see Fig. 2.4.2.). These various pore dimensions of the host materials give us the opportunity to study the effect of the host pore dimensionality on the guest-guest interactions and also to see how the guest molecules are arranged inside the channels with regard to the intermolecular interactions between them.

zeosil	structure [http://www.iza-structure.org]	channel dimensionality	channels
ITQ-4 [BC97a]	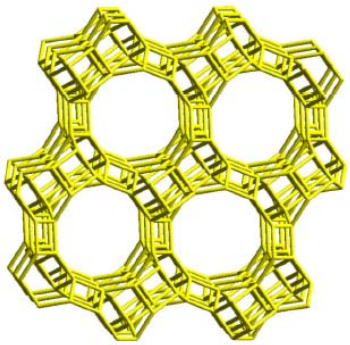	one-dimensional	12 MR 6.2 x 7.2 Å 

SSZ-24 [BC83]	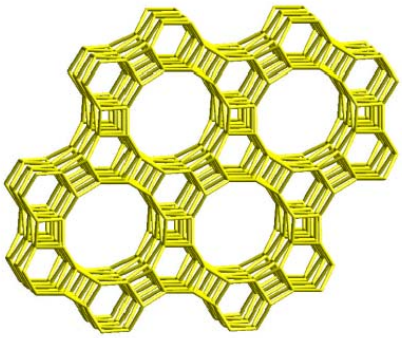	one- dimensional	12 MR 7.3 x 7.3 Å 
CIT-5 [WY97] [YW98]	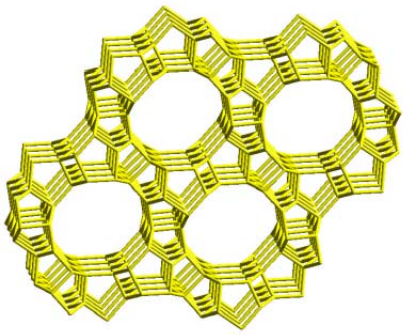	one- dimensional	14 MR 7.2 x 7.5 Å 
UTD-1 [WB99b]	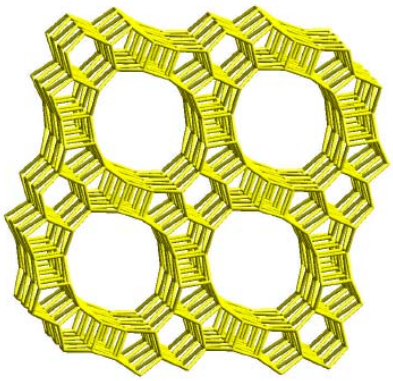	one- dimensional	14 MR 7.5 x 10.0 Å 

Fig. 2.4.1. Structures and pore dimensions of the large and extra-large pore zeosils.

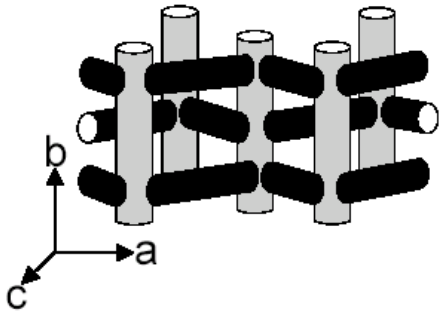

Fig. 2.4.2. Intersecting three-dimensional channel system of the MFI topology [KL78] [OK81].

2.5. Guest compounds for insertion experiments

2.5.1. Iodine

The main properties of iodine are summarized in Table 2.5.1.1. [CO73a]. At ordinary temperatures the element is a black crystalline solid with a slight metallic luster containing I_2 molecules. The van der Walls forces between the diatomic molecules are stronger in the case of iodine as compared to the other halogens. The molecules persist throughout the solid, liquid and gaseous phases. The melting and boiling points are low.

Table 2.5.1.1. Properties of iodine.

Property	iodine, I_2
molecular weight / g/mol	253.8090 [AW70]
size / Å: length Φ (min/max)	6.97 4.30 [GO95]
volume / $Å^3$	80 [GO95]
colour: solid liquid gas	black-greyish brown violet [GO95]
boiling point / °C	185.24 [TT60]
melting point / °C	113.60 [TT60]
crystal structure	orthorhombic, space group *Cmca* [BK67]
molecules per unit cell	4
unit cell dimensions / Å	a = 7.136, b = 4.686, c = 9. 784
intramolecular distance / Å	2.715 ± 0.006
intermolecular distance / Å	3.496 – 4.412

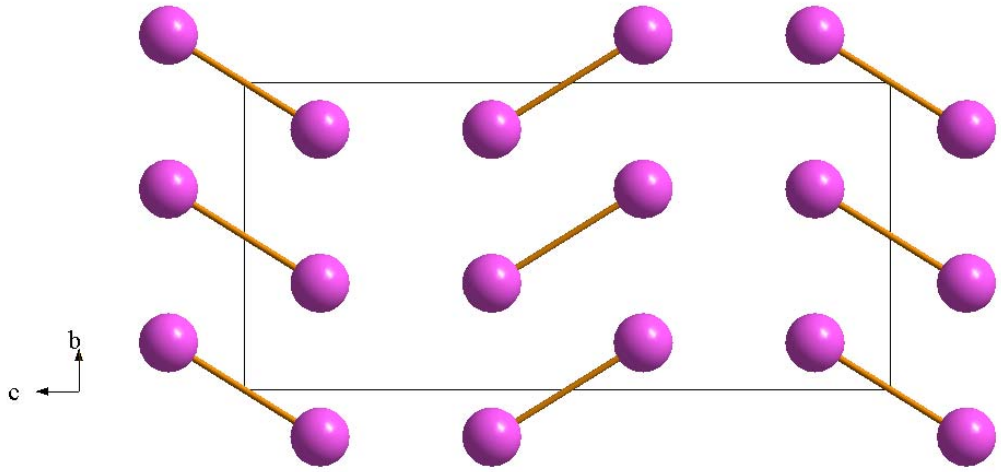

Fig. 2.5.1.2. Structure of solid iodine viewed along [100] [PM92].

The molecular structure of solid iodine, depicted in Fig. 2.5.1.2., is unique, i.e. there are no allotropic modifications under normal pressure. In solid iodine, the intramolecular bond distance is 2.715 Å (110 K), considerably longer than the one in the gaseous molecule, 2.666 Å, which can be traced back to intermolecular interactions. The shortest intermolecular I···I distances have been determined to be 3.496 and 3.972 Å, respectively [BK67]. These values are considerably shorter than twice the van der Waals distance corresponding to 4.30 Å. Each iodine atom is involved in two nearly perpendicular chains. The short I···I distances are found only in the *b* plane, whereas the distance between the layers along *c* (4.412 Å) is close to the van der Waals distance [BK67]. This can explain the anisotropy of iodine. In excellent agreement with the above mentioned bond distances, recently reported high-accuracy EXAFS measurements of gaseous (at 450 K), liquid (at 393 K) and solid iodine (at 300 K) confirm spectroscopically that, when going from gaseous to liquid and solid iodine, the intramolecular bond distance increases, the determined values are 2.681 Å, 2.696 Å and 2.720 Å, respectively [BC97a].

Iodine melts at 113.60 °C forming a brown liquid and vaporizes at 185.24 °C, the result being a violet-coloured gas, containing isolated I_2 molecules. Iodine dissolves in non- or weakly-coordinating solvents like CS_2, $CHCl_3$, CCl_4 or cyclohexane, giving also a violet colour, characteristic for isolated I_2 molecules. But in solvents like water, ethanol, acetone, the colour is

red-brown, due to the formation of charge-transfer complexes of iodine with the solvent molecules.

2.5.2. Selenium

The allotropy of selenium has not been studied as extensively as that of sulphur, but six modifications have been identified [CO75]. Selenium exists in several solid allotropes, namely amorphous, trigonal [UC69], rhombohedral [MI77] [MI80], orthorhombic [NT81] and α-, β- and γ-monoclinic [BU51] [MP53] [FJ80] selenium.

α- and β-monoclinic selenium are obtained by slow or rapid evaporation, respectively, of carbon disulphide or benzene solutions of black, vitreous selenium at room temperature. The unit cells of both crystalline modifications contain four Se_8 molecules at very similar intermolecular distances. In both cases, each of the Se_8 molecules is non-planar and puckered into the shape of a crown in which the Se-Se bond distance is 2.34 Å (Fig. 2.5.2.1.). This distance corresponds to a single bond and there is no evidence of double bond character. The Se-Se-Se angle is about 105.7°. Both α- and β-monoclinic selenium are appreciably soluble in carbon disulphide, giving a dark red solution, and both transform readily to the grey metallic form, but there is no clearly defined transition temperature, nor is there any evidence for a direct α→β transformation. At 170-180 °C all these modifications change into grey hexagonal selenium.

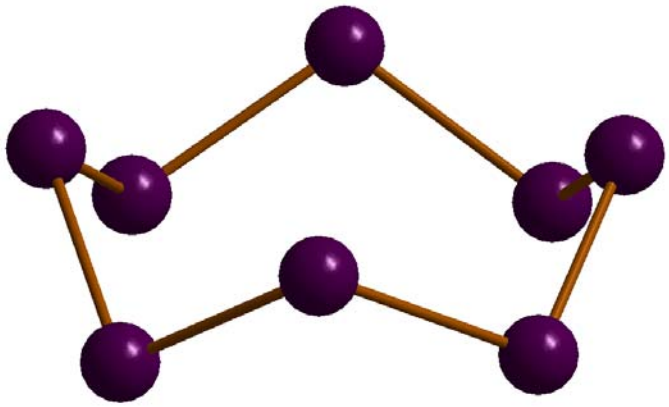

Fig. 2.5.2.1. Structure of Se eight-ring [CU72].

The trigonal modification is commonly known as grey selenium and has a metallic lustre. Grey or metallic selenium is the thermodynamically most stable form of the element. It is formed by heating any other modification, by slowly cooling molten selenium or a saturated solution of amorphous selenium in hot aniline, and by condensing selenium at a temperature close to the melting point of the element (220 °C). It is the only modification that conducts electricity. Its structure consists of infinite helical chains (Fig. 2.5.2.2.) in which branching does not occur, the

Se-Se bond distance being 2.373 Å and the bond angle 103.1° [CU67]. The shortest Se-Se distance between two chains is 3.436 Å. Grey selenium is insoluble in carbon disulphide.

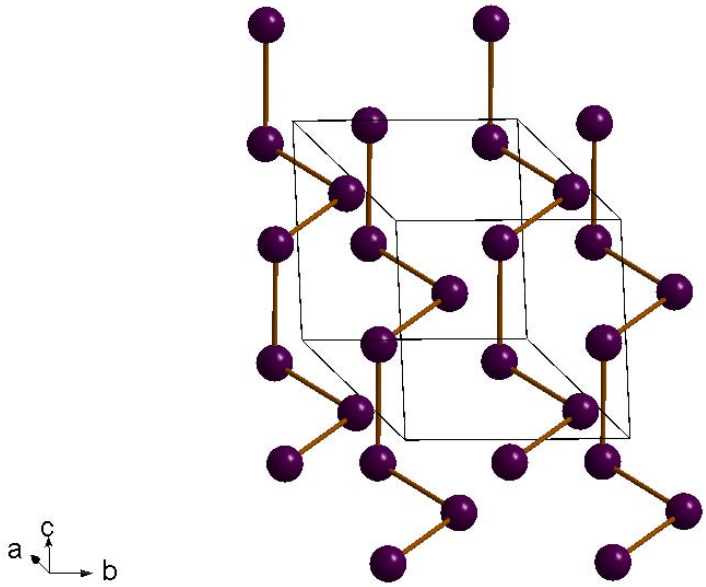

Fig. 2.5.2.2. Chain structure of grey metallic selenium [KH77].

The structure of the rhombohedral selenium, composed of Se_6 molecules, is depicted in Fig. 2.5.2.3. Different studies, like DSC and X-ray measurements, revealed that the rhombohedral phase is irreversibly converted to the polycrystalline trigonal phase at temperatures above 105 °C [MI80].

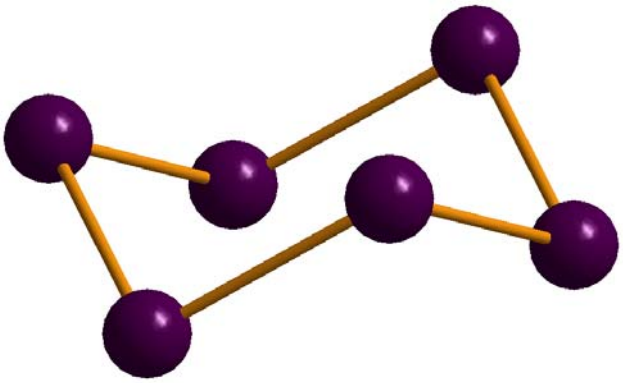

Fig. 2.5.2.3. Structure of Se six-ring [MI80].

Red amorphous selenium has a chain structure similar to that of hexagonal selenium, although it is deformed [RK52]. In spite of its relationship to hexagonal selenium, this modification does not conduct electricity and it's only very slightly soluble in carbon disulphide. This Se

modification is stable under ambient conditions, but when heated up to 60-80 °C it transforms into hexagonal selenium.

Vitreous black selenium, soluble in carbon disulphide, is the ordinary commercial form of the element; it is a brittle, opaque, dark red-brown to bluish-black lustrous solid and is obtained when molten selenium is cooled suddenly. It does not melt sharply, but softens at about 50 °C and rapidly transforms to hexagonal selenium at 180-190 °C. Vitreous selenium is much more complex than any other modification and the polymer rings may contain up to 1000 atoms [KR51]. The transformation to hexagonal selenium occurs at room temperature [CO75].

Apart from these well-known six Se modifications, the literature indicates some other additional phases, which are not however confirmed. Miyamoto [MI77] mentions as a crystalline phase another trigonal modification with a different molecular structure (rings instead of chains). Unger and Cherin [UC67] refer, apart from the well-known monoclinic modifications, to a triclinic one, the so-called β'-phase, and Donohue [DO74] observed another three cubic-crystallized modifications.

An overview of the crystallographic data of selenium modifications is given in Table 2.5.2.4.

Table 2.5.2.4. The crystal structures of the allotropes of selenium.

	symmetry	space group	*a*	*b*	*c*	*β*
α-selenium [CU72]	monoclinic	$P2_1/n$	9.054	9.083	11.601	90.81
β-selenium [BU52]	monoclinic	$P2_1/a$	12.85	8.07	9.31	93.13
grey selenium [KH77]	hexagonal	$P3_121$	4.368	4.368	4.958	-
cyclohexa-selenium [MI80]	rhombohedral	*R*3-bar	11.362	11.362	4.429	-

Liquid selenium forms at temperatures of 220.5 °C, has a black colour and consists of Se_8-rings and chains having up to 1000 Se atoms. In the molten state, the viscosity of selenium decreases rapidly with increasing temperature, indicating that the chain length of selenium polymers in the melt is progressively reduced with increasing temperature.

It is apparent from vapour density determinations that Se_8 molecules are present below 550°C; the vapour is yellow at the boiling point (685 °C) and dissociation to Se_6, Se_2 (above 900°C) molecules and to atomic selenium occurs with increasing temperature. A mass spectrometric study [YP68] of selenium vapour has provided evidence for the existence of Se_4 and Se_7 molecules in the vapour, in addition to those mentioned above.

The different Se modifications and their phase transformations as well as the formation of the gaseous phase are important details to analyze and understand the different possible structures of the guest species of selenium in zeosils.

2.5.3. Mercury(II) halides

Mercury(II) halides HgX_2 (where X: Cl, Br, I) represent an interesting class of guest species. These materials form low-dimensional structures in the solid state (molecular crystals are formed by $HgCl_2$, $HgBr_2$ and the yellow modification of HgI_2, whereas red HgI_2 possesses a layered structure) and are readily volatilized, so that the insertion can be carried out easily by vapour transport.

The chemistry of mercury(II) compounds is dominated by twofold coordination, which is more frequently for mercury than for any other transition metal. The dominating effect of linear (or nearly linear) twofold coordination is also present in the bulk solid state structures, depicted in Fig. 2.5.3.1.

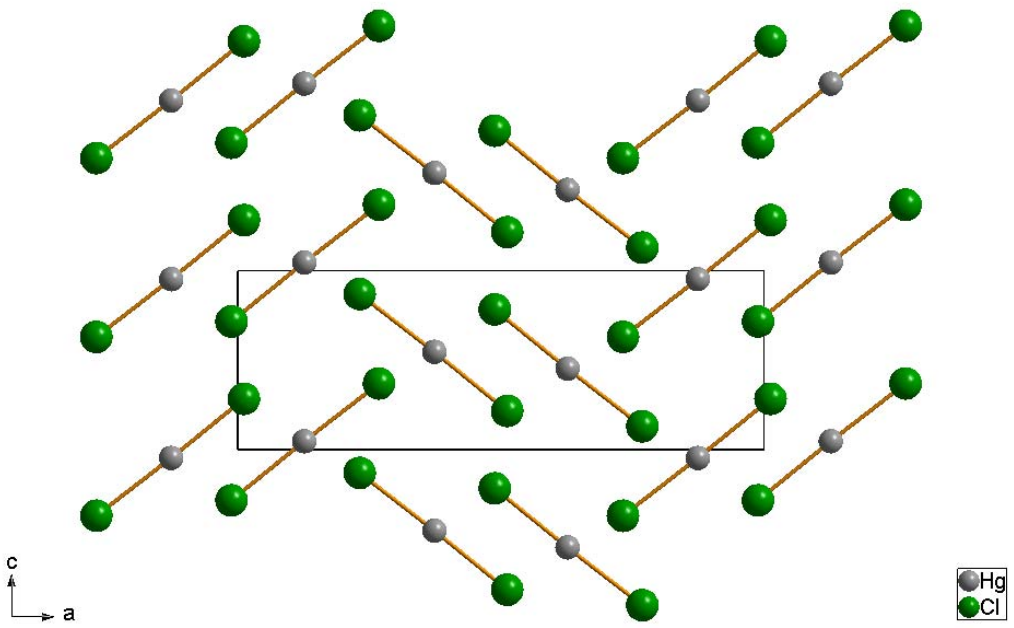

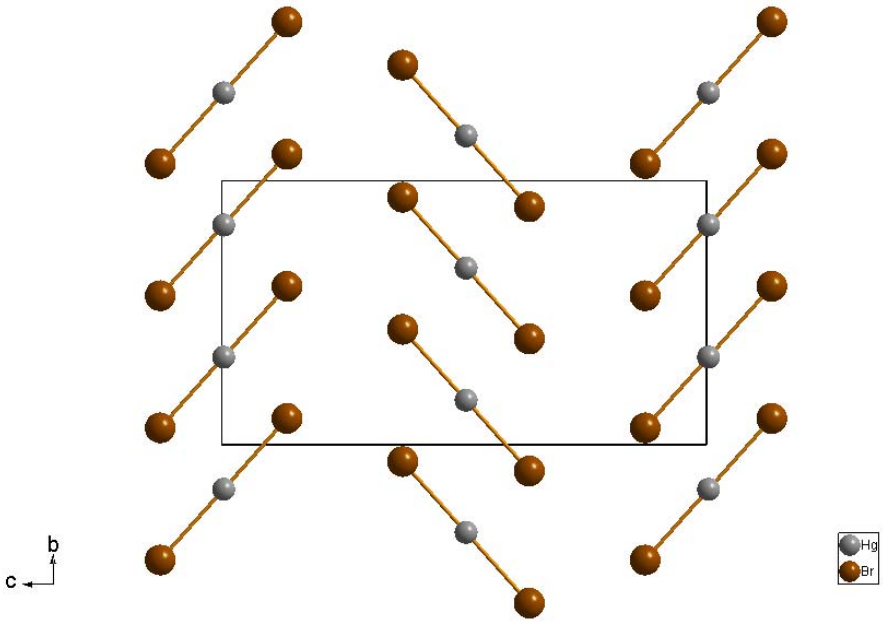
b
c
Hg
Br

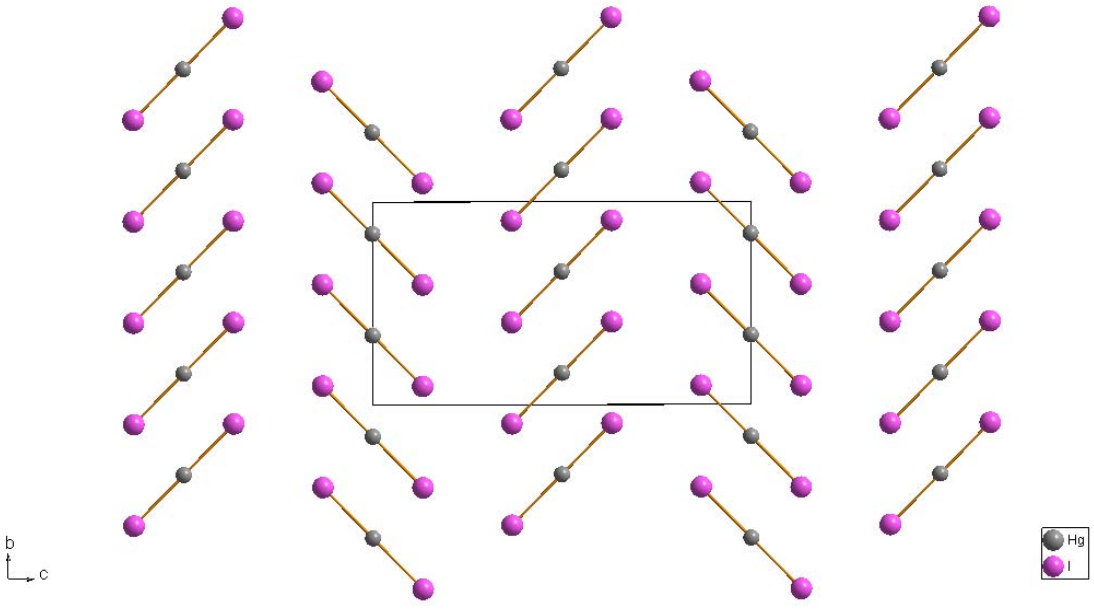
b
c
Hg
I

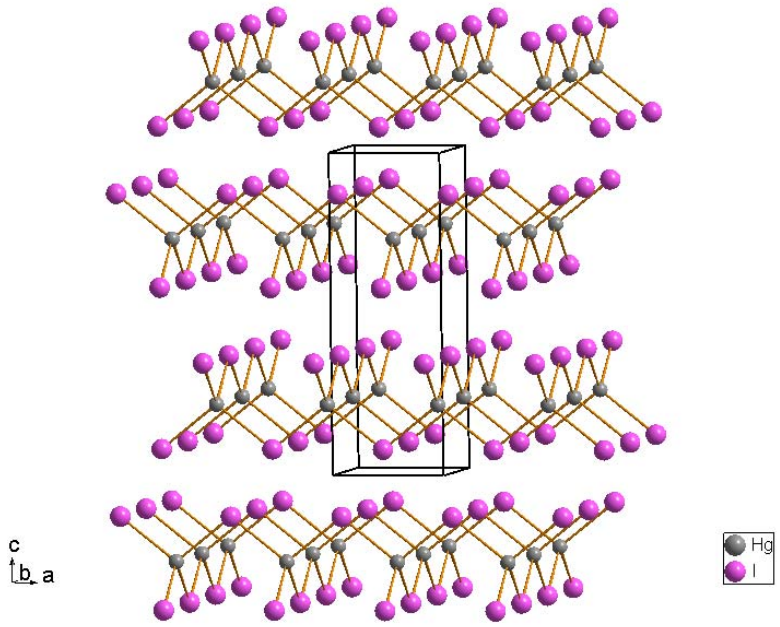

Fig. 2.5.3.1. Structure of the solid mercury(II) halides, $HgCl_2$ [SS80], $HgBr_2$ [PG90], yellow [JV67] and red [DM87] HgI_2.

$HgCl_2$, $HgBr_2$ and the yellow modification of HgI_2 (stable above 399 K) are "molecular solids" with a structure around the mercury atom that can be described as a strongly distorted octahedron. In contrast, in the red modification of HgI_2 (the thermodynamically stable form at room temperature), a tetrahedral coordination is found for Hg [DM87]. Solid mercuric chloride contains discrete linear Cl–Hg–Cl molecules; these are arranged in sheets, stacked one above another along the *c* axis [WE62]. Although mercury is often said to achieve distorted six-coordination, the four more distant chlorines are more remote at 3.34 and 3.63 Å than the sum of van der Walls' radii (3.30 Å). The Cl····Cl approaches are fairly close, however. Mercuric bromide has a related structure in which linear Br–Hg–Br units may be distinguished; these are arranged in layers in a deformed version, which is immediate in between a molecular and a layer structure. Instead of being regularly octahedrally coordinated, the metal atoms have two close and two more distant neighbors; bromine atoms are in a distorted version of the mixed hexagonal-cubic close-packing arrangement. Bromine atoms are about 3.74 Å apart, close to the sum of their ionic radii. There are at least three crystalline forms of mercuric iodide; the one stable at room temperature, the red α-form, has an infinite layer structure in which iodine atoms are in a distorted cubic close-packing, and mercury occupies ¼ of the tetrahedral holes (more precisely, ½ of those between every other pair of layers). Above 129 °C, the yellow β-form is

stable, with a structure like that of $HgBr_2$. Jeffrey et.al. [JV67] have confirmed the existence of another, orange, form, prepared by rapid evaporation of a warm solution of red HgI_2 in acetone. Unfortunately, twinning of the crystals precluded a full structure determination, but similarities to the α-form were apparent [CO73b]. The properties of mercury(II) halides are presented in Table 2.5.3.2.

Table 2.5.3.2. Physical properties of mercury(II) halides [CO73b].

property	$HgCl_2$	$HgBr_2$	HgI_2
molecular weight / g/mol	271.6	360.4	554.4
size / Å [GO95]: length Φ (min/max)	 8.18 3.60	 8.70 3.90	 9.46 4.30
volume / $Å^3$ [GO95]	65	78	98
melting point / °C [TT65]	277	241	257
boiling point / °C [TT65]	304	319	354
transition temperature / °C [TT65]			129 (red → yellow)
colour: solid liquid gas	white white white	white white white	α: red / β: yellow yellow white
molecular structure d(Hg–X) / Å [TI58]	linear 2.29 ± 0.02	linear 2.41 ± 0.02	linear 2.59 ± 0.02
crystal structure	orthorhombic [SS80] *a* = 12.776 *b* = 5.986 *c* = 4.333	orthorhombic [PG90] *a* = 4.628 *b* = 6.802 *c* = 12.476	(i) red, tetragonal [DM87] *a* = 4.370 *b* = 4.370 *c* = 12.443 (ii) yellow, orthorhombic [JV67]

d(Hg–X) / Å	2.23, 2.27 3.34 (2), 3.63 (2)	2.48 (2) 3.23 (4)	*a* = 4.702 *b* = 7.432 *c* = 13.872 (iii) orange: see text (i) 2.78 (4) (ii) 2.62 (2), 3.51 (4)

Electron diffraction experiments on HgX_2 vapours (X = Cl, Br, I) have shown that linear monomeric X–Hg–X species are present (Table 2.5.3.2.). At high temperatures (above 1000 °C), appreciable dissociation into halogen and either HgX or Hg occurs; this process is reversible.

2.5.4. Gold(III) chloride

The crystal structure of gold(III) chloride as determined by Clark et.al. [CT58] is based on a monoclinic unit cell containing two planar dimmeric Au_2Cl_6 molecules (Fig. 2.5.4.1.). In an Au_2Cl_6 molecule, each gold atom is coordinated by two bridging and two terminal chlorine atoms lying at the corners of a slightly deformed square. The bridging bonds are only 0.1 Å longer than the terminal ones.

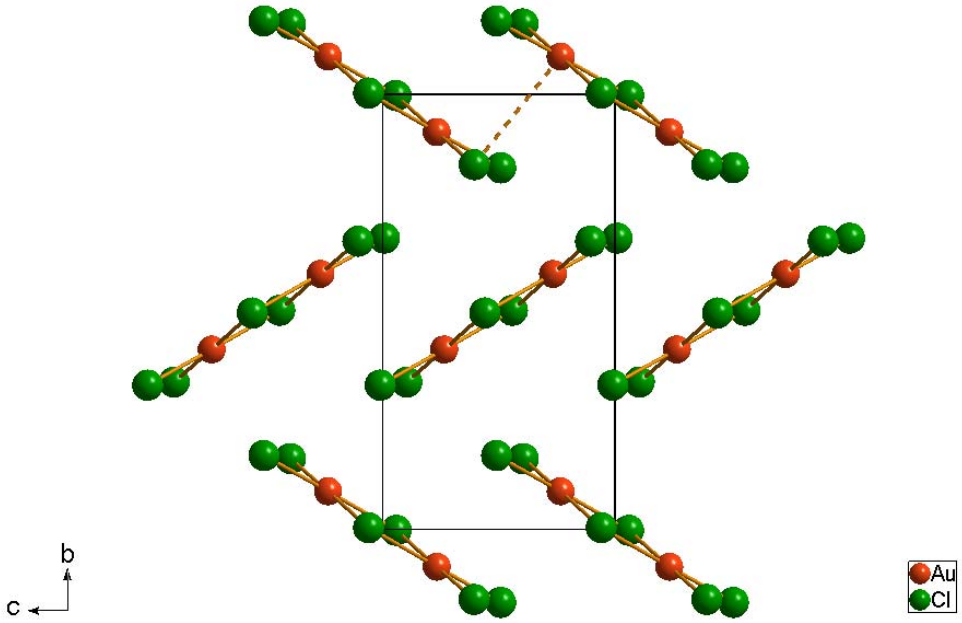

Fig. 2.5.4.1. Crystal structure of gold(III) chloride viewed along [100] [CT58].

The shape of the Au_2Cl_6 molecule is shown in Fig. 2.5.4.2. Table 2.5.4.3. reports the structural parameters of Au_2Cl_6 as bond distances and angles [CT58]. The symbols Cl^T and Cl^B denote a terminal and a bonding chlorine atom, respectively.

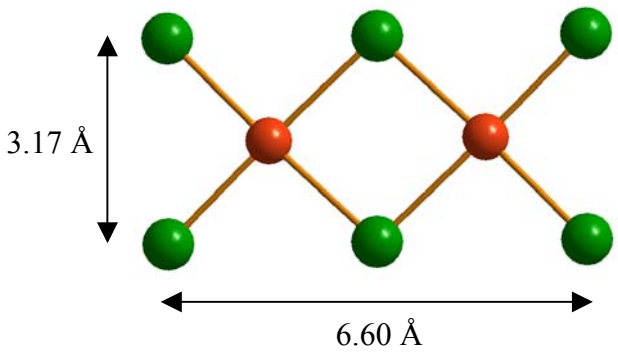

Fig. 2.5.4.2. Structure and dimensions of an Au_2Cl_6 molecule [CT58].

Table 2.5.4.3. Distances and angles in the solid state structure of Au_2Cl_6 [CT58].

$Au - Cl^T$ / Å	$Au - Cl^B$ / Å	Au – Au / Å	$Cl^T - Au - Cl^T$ / °	$Cl^B - Au - Cl^B$ / °	$Cl^T - Au - Cl^B$ / °
2.24	2.33	3.41	90	86	92

We now report reactions which, based on the known chemistry of Au_2Cl_6, will play an important role in the formation of gold(III) chloride inserted zeosils. It is known that weak heating causes sublimation of the brown Au_2Cl_6 (s):

$$Au_2Cl_6\ (s) \rightarrow Au_2Cl_6\ (g)$$

Heating at higher temperatures causes decomposition of Au_2Cl_6 and formation of the yellow AuCl and Cl_2.

$$Au_2Cl_6\ (g) \rightarrow 2\ AuCl\ (s) + 2\ Cl_2\ (g)$$

At temperatures above 160 °C, the solid $AuCl_3$ is stable only in the presence of chlorine gas. The stability of gold(III) chloride versus temperature is a function of the chlorine pressure. Under a chlorine pressure of 1 atm, the brown gold(III) chloride dissociates to a yellow solid at 280 °C. The above behavior is due to the reduction of gold(III) to gold(I) and metallic gold according to the reactions:

$$AuCl_3\ (s) \rightarrow AuCl\ (s) + Cl_2\ (g) \qquad [CS65]$$

$$2\ AuCl\ (s) \rightarrow 2\ Au\ (s) + Cl_2\ (g) \qquad [FB28]\ [SO56]$$

2.6. Azo-dyes

Azo-dyes were discovered in the 19th century and represent by far the largest class of colouring materials. They find applications in the industry, e.g. in the textile industry, were azo-dyes are used for colouring wool, cotton, linen, silk, but also for oils, waxes, wood, paper and so on. However, the importance of these substances has decreased in the last years after the discovery of the carcinogenic characteristics of azo-dyes.

The name azo-dye relates to the main functional group of their structure, the azo group, which consists of two nitrogen atoms connected by a double bond (R–N=N–R). Azo compounds can have an aliphatic structure, corresponding to colourless materials, e.g. azo-methane (H_3C–N=N–CH_3), or an aromatic one, e.g. azobenzene (H_5C_6–N=N–C_6H_5), where the nitrogen double bond is conjugated with aromatic rings. The last case characterizes coloured compounds, the azo-dyes.

The azo-dyes used in this work are amphiphilic entities which allows them to take part in self-aggregation processes occurring in aqueous solutions. Such amphiphilic azo-dyes ("azo-surfactants") can form micellar and lyotropic phases in aqueous solutions [TA73], and they can also control the arrangement of inorganic phases, e.g. amorphous silica [GL99] [MU04]. In the azo-surfactants used here, amphiphilicity is introduced by the presence of a polar trimethylammonium head-group and an unpolar alkyl tail. They can be shortly described by the formula $C_mAzoC_nTMA^+$, where C_m and C_n represent the number of carbon atoms in the alkyl tail and the alkyl spacer, respectively (Fig. 2.6.1.)

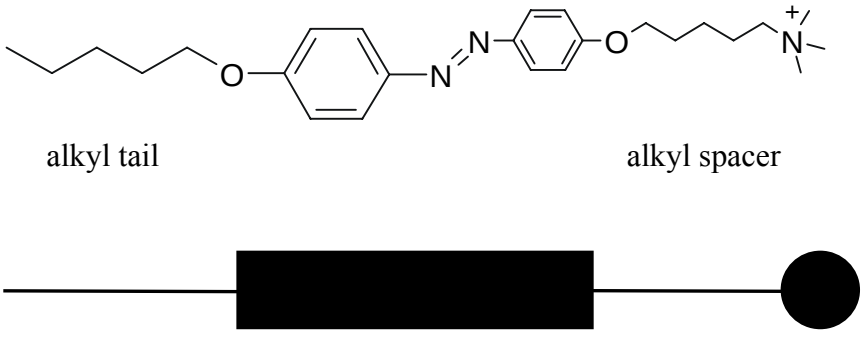

Fig. 2.6.1. Chemical formula of an azo-surfactant molecule having an alkyl spacer and an alkyl tail; below: schematic representation of an azo-surfactant molecule.

The azo-group has the same geometry as the ethylene group and exhibits cis-trans isomerism. Under light irradiation, a controlled cis-trans isomerization is possible. The trans isomer is more stable than the cis isomer.

An important characterization method for azo-dyes is the UV-vis spectroscopy (Fig. 2.6.2.).

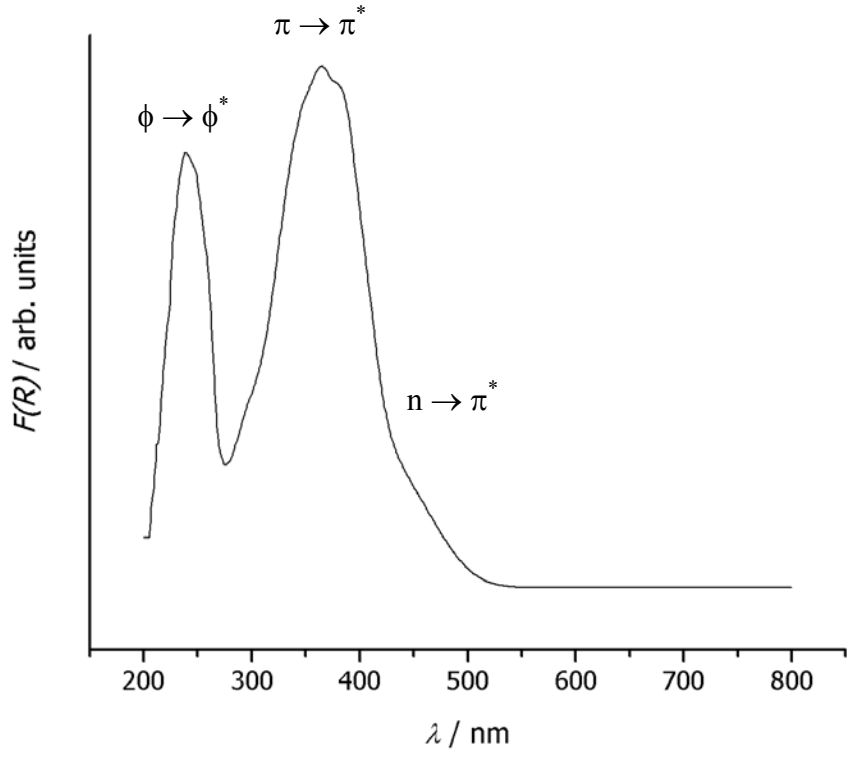

Fig. 2.6.2. UV-vis absorption spectrum of the zeodye prepared using the azo-surfactant $C_8AzoC_6TMA^+$.

The free electron pairs present at the nitrogen atoms can give rise to a weak n–π^* absorption band in the UV-vis spectrum of azo-dyes. This band is typically observed at 435-455 nm. Of higher intensity in the UV-vis spectra of these materials is the π–π^* band, which relates to the corresponding molecular orbitals localized at the N=N double bond. Values between 316 and 380 nm are typical for the wavelength characterizing this absorption band. Finally, a third band of lower intensity can be detected in the spectrum, and this was attributed to ϕ–ϕ^* transitions involving the excitation of π electrons in the phenyl rings. It typically appears in the near-UV region of the spectra.

These results can be explained on the basis of the molecular orbital theory [BJ66] [KB68] [JY58]. Fig. 2.6.3. shows the orbital diagram of an azo-dye system. The three highest occupied

orbitals (ϕ_1 ϕ_2 π_1) are depicted together with the three lowest not-occupied ones (ϕ_1^* ϕ_2^* π_1^*) and the n-orbitals, n_s and n_a, present due to the free electron pair at the nitrogen atoms.

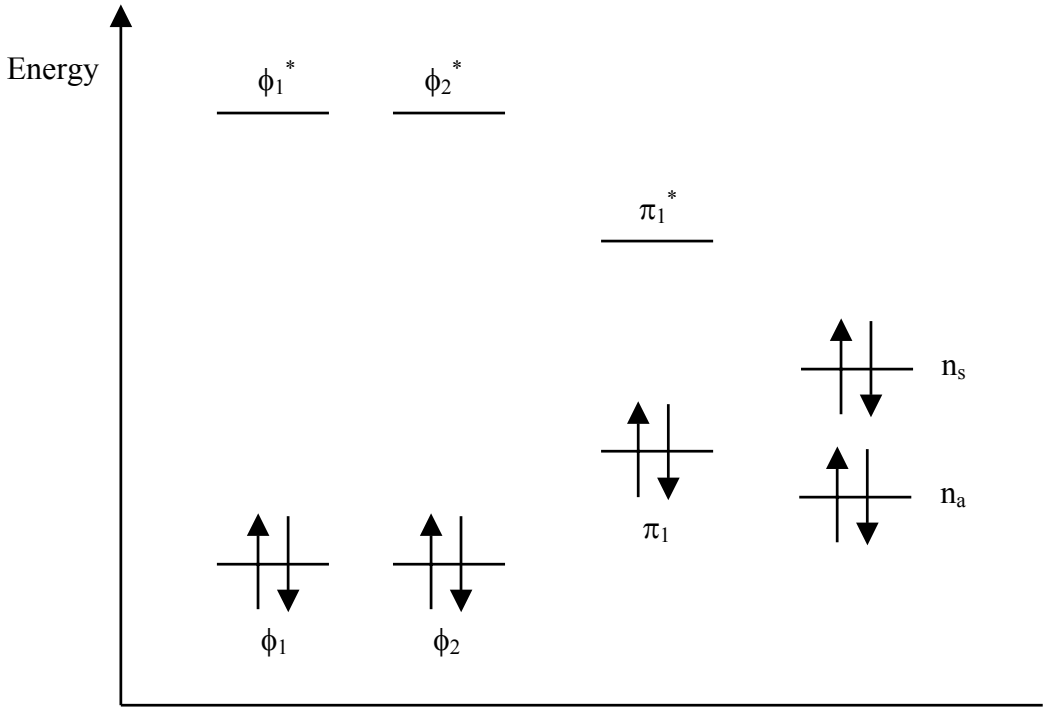

Fig. 2.6.3. Schematic orbital diagram of an azo-dye molecule.

When mixed with a silica precursor, azo-surfactants form layered materials with walls constructed typically of amorphous silica. Azo-dye molecules can either aggregate in a parallel (H-aggregate) or in a head-to-tail (J-aggregate) fashion (see Chapter 4.2.). Absorption spectra of the aggregates show differences when compared to the individual molecules [CS98] [SO99] [OS00] [MB70] [RE41] [RN99]. Aggregation is indicated by a shift of the π–π^* absorption band in the UV-vis spectrum of the dye with respect to the absorption band in aqueous solution. This shift can be explained with the help of the molecular exciton theory [FR31] [DA62]. From the position of this band in the spectrum we can determine the type of aggregate formed. For example, the pure azo-dye monomer in ethanol gives a band at 358 nm; whereas the band is shifted to 380 nm in the case of a J-aggregate and to 315 nm for a H-aggregate [GL99].

Due to their light-stability, their rather uncomplicated synthesis [UF03] and the large number of possible combinations of their structure, azo-dyes have meanwhile become an important tool in the chemistry of advanced organic materials, e.g. as molecular switches [GL99] [MU04].

3. EXPERIMENTAL

3.1. Insertion compounds

The synthesis of the insertion compounds is a multi-step procedure involving first the preparation of the host material using organic molecules as structure-directing agents (SDAs). This is followed by the removal of the organic part occluded in the pores (channels) by an oxidative combustion (calcination) and finally, the insertion of the guest material takes place (Scheme 3.1.). After the removal of the template, the host materials maintain a high crystallinity, as judged from X-ray diffraction.

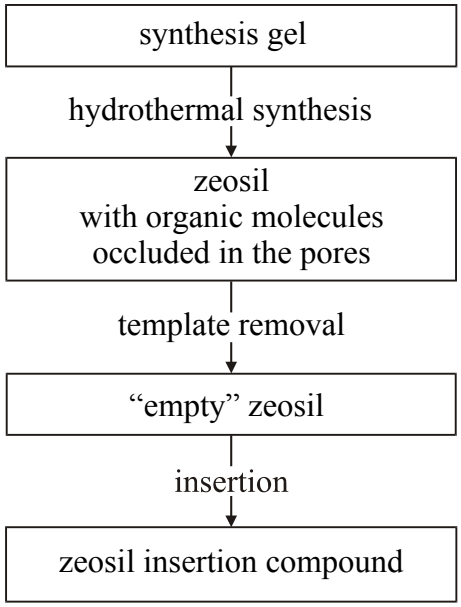

Scheme 3.1. Synthetic procedure for the insertion of zeosils.

3.1.1. Synthesis and characterization of host materials

A. Synthesis of zeosils

The hydrothermal syntheses of the host materials were carried out in home-built autoclaves. They consist of stainless steel lined (Fig. 3.1.1.1.) with chemically inert Teflon containers (Fig. 3.1.1.2.) and can be used at temperatures up to 470 K and pressures up to 200 bars.

Fig. 3.1.1.1. Autoclave - steel cover.

Fig. 3.1.1.2. Autoclave – Teflon interior.

Practically, for the 10 ml autoclaves, a maximal volume of 9 ml water, and for the 50 ml ones, 35 ml water can be filled inside. For the synthesis of zeosils, all autoclaves had a filling level of approximately 90 %, which means 8 and 30 ml of the reaction mixture, respectively. The filled autoclaves were placed in a forced-air oven (Model UT6 from Heraeus) with a high constancy of temperature (± 1 K) which excluded temperature variations during the synthesis period. For the procedure in which the autoclaves had to be rotated during synthesis, the oven was equipped with a mounting plate and an engine which permitted the rotation of the 10 ml autoclaves with 65 revolutions/minute.

For the synthesis of porous materials, the composition of the reaction mixture as well as the critical parameters, like temperature, pressure and reaction time, were varied in order to achieve preferably large crystals with high yields. Zeosil synthesis in general takes place in the temperature range between 150 and 200 °C. The first experiments were carried out in 10 ml free

volume autoclaves and once the synthesis parameters had been optimized with respect to the above mentioned goals, the reactions were up-scaled to volumes of 50 or 125 ml [JA02].
NaOH or HF were used as mineralizing agents for the hydrothermal syntheses. The use of HF has some advantages over a base like NaOH. First, the final porous materials made by the HF-route have fewer defects when compared with materials from basic reaction mixtures, and secondly, due to their SiO_2 composition and very low concentration of Si–OH groups, the materials are strictly hydrophobic [CV99].
The calcination process takes place in air and the temperature is chosen in order to ensure the complete combustion of the SDA, while maintaining a high crystallinity of the host material. After calcination, the zeosils are colourless, except for UTD-1, which has a grey colour due to cobalt oxide species blocking the pores. These are removed by washing with diluted hydrochloric acid.

Synthesis of Silicalite-1

[JA02] [GK86] [FL88] [GO95] [KM98] [BD98a] [PI99] [HU00]

The pure silica MFI, Silicalite-1, was synthesized in hydroxide as well as in fluoride medium, using tetrapropylammonium bromide (TPABr) as structure-directing agent. The molar ratio of the reactants for the synthesis with NaOH was:

$$1\ SiO_2 : 0.05\ TPABr : 0.08\ NaOH : 14\ H_2O.$$

In a typical synthesis, 43 ml of a 0.35 M tetrapropylammonium bromide solution (15 mmol), 24.4 ml of a 1 M sodium hydroxide solution and 10.6 ml water (totally 4.14 mol water, including the water from the SDA and NaOH solutions) were mixed. Then, 18 g (300 mmol) Cab-osil® M-5 were added. The whole reaction mixture was transferred into an 200 ml autoclave (40 % filling level). This was held at 180 °C for 12 days; thereafter, the crystalline material was filtered off and washed with water and acetone to give 18.88 g of high quality MFI crystals. After calcination at 600 °C for 3 hours, a colourless product was obtained. The weight loss during the calcination step was 12 %.
For the synthesis taking place with HF as mineralizing agent, the molar ratio considered was:

$$1\ SiO_2 : 0.12\ TPABr : 0.1\ HF : 0.1\ NH_4F : 37\ H_2O.$$

Practically, 0.9 g (24 mmol) ammonium fluoride were dissolved in 150 ml water; to this solution, firstly, 7 g (26 mmol) tetrapropylammonium bromide, and secondly, 13.7 g (228 mmol) Cab-osil® M-5 were added. After stirring for around 2 hours, the pH was adjusted with 1 ml (23 mmol) of a 40 % HF solution, to a pH value of ca. 5 to 6. The whole mixture was then

transferred into a 200 ml autoclave (80-90 % filling volume), heated to 160 °C and kept at this temperature for 21 days. After filtrating and washing with water and acetone, 14.09 g of pure MFI crystals were obtained. Calcination at 600 °C for 4 hours, accompanied by a weight loss of 12 %, gave colourless MFI crystals.

Chemicals used:

tetrapropylammonium bromide	Fluka	purum, > 98 %
Cab-osil® M-5	Fluka	200 ± 25 m^2/g, $H_2O \leq 3$ %
sodium hydroxide	Merck	> 98 %
hydrofluoric acid	Fluka	puriss. p.a
ammonium fluoride	Riedel-de Haën	> 96 %

Synthesis of benzylquinuclidine hydroxide

[JA02] [AP97]

Benzylquinuclidine is needed as structure-directing agent for the synthesis of ITQ-4. The correct name for quinuclidine is 1-azabicyclo[2,2,2]-octane. Practically, 25.10 g (226 mmol) quinuclidine were dissolved in 250 ml methanol. 26.7 ml (225 mmol) benzyl bromide were slowly added and the clear solution was heated under reflux to gave a colourless solid. After washing with ether, 63.19 g (224 mmol) benzylquinuclidine bromide were obtained (yield 99.5 %). For the ion-exchange from bromide to hydroxide, the solid was dissolved in 200 ml water and transferred to an exchange column containing the strong basic ion-exchanger Lewatit M 500 KR (hydroxide form). The final concentration of the benzylquinuclidine hydroxide solution was detected during titration with 0.01 M HCl using phenolphthalein and was found to be 1.52 M.

Chemicals used:

quinuclidine	Fluka	purum, ≥ 97 %
benzyl bromide	Fluka	purum, ≥ 98 %
Lewatit M 500 KR / OH	Bayer	

Synthesis of ITQ-4

[JA02] [AP97]

A well crystallized product of ITQ-4 with high yield was prepared by a hydrothermal procedure, for which the following molar ratio was employed:

$$1\ SiO_2 : 0.5\ SDA : 0.5\ HF : 12\text{-}30\ H_2O.$$

Here, the synthesis is described briefly: 8.20 g tetraethoxysilane, 13.04 g of a 1.52 M *N*-benzylquinuclidine hydroxide solution and 1.12 g water were mixed together and then stirred for 24 hours. After five hours stirring, the clear solution started to get turbid. After 24 hours of stirring, the hydrolysis of TEOS should be completed and the ethanol formed should be evaporated. The decrease in weight was observed to be 10.68 g, from which 7.26 g were due to the evaporation of ethanol. The missing water, 3.42 g, was substituted. After adding 0.70 g of a 48 % HF solution, the reaction mixture became viscous and was transferred into Teflon-lined steel autoclaves. They were heated to 150 °C in the oven and kept at this temperature for 13 days. During all this time the autoclaves were rotated with 65 revolutions/minute. 2.854 g fine crystals were obtained. They were calcined at 600 °C for four hours, with a weight loss of 19 %. The final product was colourless.

Chemicals used:

N-benzylquinuclidine hydroxide	synthesis see page 37	
tetraethoxysilane	Fluka	≥ 98 %
hydrofluoric acid, 48%	Fluka	puriss. p.a.

Synthesis of *N*(16)-methylsparteinium hydroxide

[JA02] [NA93] [LD94]

N(16)-methylsparteinium hydroxide was used as SDA in the syntheses of zeosils SSZ-24 and CIT-5. It was obtained through the methylation of (–)-sparteine, followed by the ion-exchange of *N*(16)-methylsparteinium iodide. The correct chemical name for (–)-sparteine is dodecahydro-7,14-methano-2H,6H-dipyrido[1,2-a:1',2'-e]diazocine.

N(16)-methylsparteinium iodide was synthesized from (–)-sparteine using the following procedure: 25 g (59 mmol) of (–)-sparteine sulphate pentahydrate were added to 60 ml of a 3 M

NaOH solution. The suspension was stirred until the crystals were completely dissolved and two phases were formed. The organic phase was extracted three times with 35 ml portions of diethyl ether and the combined extracts were dried over solid KOH (85 %) and filtered. The solvent was then evaporated at room temperature under vacuum. The recovered (–)-sparteine was dissolved in 115 ml acetone containing 14.75 ml (235 mmol) of methyl iodide. The reaction mixture was stirred in the dark for 24 hours, and the yellow product formed was filtered after previous addition of 50 ml of diethylether. 17.75 g (47 mmol) solid product were finally obtained (80 % yield). 10 g of the recovered solid were recrystallized from hot acetone/diethylether and a small amount of methanol to give 7.60 g of slightly yellow crystals. A strongly basic anion-exchange resin (Dowex 1X8), in the hydroxide form, was used to convert the iodine salt to the corresponding hydroxide form. Typically, 7.6 g of *N*(16)-methylsparteinium iodide were dissolved in 100 ml water and exchanged in the ion-exchange column. After washing the column with an additional 100 ml distilled water, the aqueous solution was evaporated in a rotavapor until an oily, slightly yellow solution was obtained. The concentration of this solution was determined by titration with 0.01 M HCl against phenolphthalein and was found to be 1.193 mmol/g.

Chemicals used:

sparteine sulphate pentahydrate	Fluka	purity ≥ 99%
sodium hydroxide	Merck	≥ 98%
methyl iodide	Merck	≥ 99%
DOWEX 1X8	Serva	

Synthesis of SSZ-24

[JA02] [NA93] [LD94] [GB96] [VP99] [BD98b]

SSZ-24 was synthesized from gels of composition

$$1\ SiO_2 : 0.3\ MSOH : 40\ H_2O$$

for the procedure taking place in hydroxide medium, and

$$1\ SiO_2 : 0.5\ MSF : 10.5\ H_2O,$$

in fluoride medium, using *N*(16)-methylsparteinium cation (MS) as structure-directing agent. The synthesis temperature was 175 °C, the synthesis time ten days and it was successful only

when the gel was mixed during heating. For this purpose, the autoclaves were rotated inside the forced-air oven with 65 revolutions/minute for some days. The synthesis in static conditions gave only an amorphous product.

A typical synthesis in hydroxide medium takes place as follows: 5.71 g of *N*(16)-methylsparteinium hydroxide solution with a concentration of 1.193 mmol/g was mixed with 10.39 g water. 3.41 g Ludox® AS-40 (40 % suspension of colloidal silica gel in water) were added afterwards and the mixture was stirred until a homogeneous gel was obtained. The solution was then allowed to age for one hour. One third from this gel, together with 0.031 g SSZ-24 seed crystals, was transferred into a 10 ml Teflon-lined autoclave (95 % filled level) and heated in the oven at 175 °C for 10 days. During all this time the autoclave has been rotated with 65 revolutions/min. The white crystals were recovered by filtration, washed with water and acetone and dried in air at room temperature. Ca 1.87 g white crystals were obtained. Careful recrystallization of the structure-directing agent in order to increase its purity was necessary to obtain pure SSZ-24 materials. To remove the occluded organic molecule, the sample was heated to 650 °C in air and kept at this temperature for six hours. After the calcination step, the weight loss was 14.1 %.

When mixing *N*(16)-methylsparteinium hydroxide with the same molar amount of HF, *N*(16)-methylsparteinium fluoride and water are formed. For the reaction in fluoride medium, 12.51 g from a *N*(16)-methylsparteinium hydroxide aqueous solution with a concentration of 2.15 mmol/g, 11.20 g tetraethoxysilane and 10.85 g water were mixed together. In order to achieve the water ratio of 10.5, only 5.7 g water were necessary. The reaction mixture was stirred for 22 hours in order to evaporate all the ethanol formed after the hydrolysis of TEOS. During this time, also a part of the water evaporated. After 22 hours of stirring, a weight loss of 15.36 g was observed; this represents 9.91 g ethanol, and the rest is water. Finally, 0.31 g water were added to achieve the intended molar ratio of 10.5. To this liquid reaction mixture, 1.13 g of a 48 % HF aqueous solution were added and within a few seconds the whole mixture became viscous, almost solid. The gel, together with 0.039 g seed crystals, was transferred into a 10 ml autoclave and heated to 175 °C under rotation for three days and static for the last two days. The solid product was recovered by filtration and dried in air for 12 hours at 50 °C. The calcination of the as-synthesized sample took place at 650 °C for 7 hours, giving a weight loss of 13.2 %.

Chemicals used:

N(16)-methylsparteinium hydroxide	synthesis see page 38	
Ludox® AS-40	Aldrich	
tetraethoxysilane	Fluka	≥ 98 %
hydrofluoric acid	Fluka	puriss. p.a.

Synthesis of CIT-5

[JA02] [BD98b] [WY97] [YW98] [KT00]

As SSZ-24, CIT-5 was synthesized with *N*(16)-methylsparteinium cation as structure-directing agent. The main differences between the two synthesis procedures are the different water content and the addition of different seed crystals. CIT-5 synthesis can take place in hydroxide or fluoride medium and it's successful only if the synthesis gel is mixed during heating. Otherwise, only an amorphous phase is obtained.

High-silica CIT-5 was prepared as a single phase by combining 6.44 g *N*(16)-methylsparteinium hydroxide aqueous solution with a concentration of 1.36 mmol/g with 4.38 g Ludox® (40 % suspension) and 14.28 g water under rapid stirring, to form a gel with the following molar ratio:

$$1\ SiO_2 : 0.3\ MSOH : 40\ H_2O.$$

The gel was aged under stirring for one hour and one third of it was transferred into a 10 ml Teflon-lined steel autoclave containing 0.031 g CIT-5 seed crystals. The autoclave was heated for 10 days at 175 °C. During this time, it was rotated with 65 revolutions/min. The white crystals formed were washed with deionized water and acetone. 0.63 g solid product were obtained. After calcination at 650 °C for 6 hours, the weight loss was 12.6 %.

The molar ratio used for the reaction in fluoride medium was:

$$1\ SiO_2 : 0.5\ MSF : 19\ H_2O.$$

For this purpose 10.84 g aqueous *N*(16)-methylsparteinium hydroxide solution (concentration 2.56 mmol/g), 11.56 g tetraethoxysilane and 17.02 g water were mixed. The reaction mixture was stirred for 26 hours in order to finalize the hydrolysis of TEOS and the total evaporation of ethanol. The weight loss after this time was 13.07 g, corresponding to 10.23 g ethanol and 2.84 g water. The amount of water in the reaction mixture was supplemented in order to achieve again the molar ratio of 19. Finally, 1.16 g of a 48 % HF solution was added. The result was the solidification of the reaction mixture. This was homogenized with a spatula and then transferred

into a 10 ml Teflon-steel autoclave and heated for 7 days at 175 °C. The autoclaves were rotated in the oven during the first four days, and left to stay static during the last three days. The final product was washed with water, suction filtered and dried at 50 °C for 12 hours. After calcination at 650 °C for six hours, the weight loss was approximately 12 %.

Chemicals used:

N(16)-methylsparteinium hydroxide	synthesis see page 38	
Ludox® AS-40	Aldrich	
tetraethoxysilane	Fluka	≥ 98 %
hydrofluoric acid	Fluka	puriss. p.a.

Synthesis of bis(pentamethycyclopentadienyl)cobalt (III) hydroxide, [Co(cp^*)$_2$]OH

[JA02] [KK80] [KK81] [RE82] [CV90] [SH79]

The metal complex [Co(cp^*)$_2$]PF_6, necessary in the synthesis of UTD-1, was prepared according to the cited literature. The complex was then converted to the hydroxide derivative by ion exchange. Practically, 9.0 g of [Co(cp^*)$_2$]PF_6 (yellow powder) were dissolved in a mixture of acetone, methanol and water with the ratio:

10 acetone : 5 methanol : 1 water (volumetric ratio).

100 g of the strongly basic anion exchanger Lewatit MP 500 were brought into an exchange column. The mixture containing the metal complex was passed over the ion exchanger. The yellow fraction was collected and, after filtration, a clear orange solution was obtained. The aqueous solution was evaporated in a rotavapor in order to obtain a concentration in between 0.5 to 1 M. The final concentration of the [Co(cp^*)$_2$]OH solution was determined by titration with 0.01 M HCl, using phenolphthalein as indicator, employing the following procedure: ca 0.05 to 0.1 g from the orange solution containing a few drops of phenolphthalein were titrated with 0.01 M HCl. A 0.56 mmol / 1 g solution concentration was obtained.

Chemicals used:

Lewatit MP 500	Bayer	
sodium hydroxide	Merck	> 98 %

Synthesis of UTD-1

[JA02] [BG95] [FT96] [BG96] [BB97] [RB98] [WB99a]

UTD-1 was prepared in hydroxide or in fluoride medium by using bis(pentamethyl-cyclopentadienyl)cobalt(III) hydroxide as structure-directing agent. UTD-1 was obtained as a single phase product using the following molar ratio:

$$1\ SiO_2 : 0.13\ [Co(cp^*)_2]OH : 0.09\ NaOH : 57\ H_2O.$$

The reaction took place at 150 °C for 14 days. With longer times and higher temperatures, dense phases develop at the same time. Practically, 0.12 g NaOH were dissolved into 1.08 g deionized water. To this solution, 0.23 g of the 0.56 mmol/g SDA ($[Co(cp^*)_2]OH$) solution were added under stirring, followed by the gradual addition of 0.06 g Cab-osil® M-5. The solution was allowed to age for one hour before being transferred to a 10 ml Teflon-lined steel autoclave (95 % filled level). The autoclave was heated under static conditions to 150 °C for 14 days. UTD-1 crystals were isolated by suction filtration and dried at 90 °C for two hours. Finally, 0.32 g of light yellow crystals were obtained. The addition of seed crystals or the rotation of the autoclaves during the hydrothermal synthesis leads to lower yields and decreased quality of the UTD-1 crystals [JA02]. The light yellow as-synthesized UTD-1 was calcined at 550 °C for six hours. The decrease in weight was about 8.9 to 10.5 %. In the end, a light grey or bluish grey material which still contains cobalt oxide was obtained. This was removed by firstly treating the calcined material with 50 ml of a 12 M HCl solution (for every 0.3 g of calcined UTD-1) at room temperature for 4 hours and secondly, employing 60 ml of a 7 M HCl solution (per 0.3 g UTD-1) at 60-70 °C for 12 hours. A colourless material was obtained as final product.

UTD-1 can also be synthesized in fluoride medium. However, after calcination and extraction with hydrochloric acid, the material does not become porous, which was explained by Jäger [JA02] and Hartl [HA02].

Chemicals used:

decamethylcobalticinium hydroxide	synthesis see page 42	
Cab-osil® M-5	Fluka	200 ± 25 m^2/g, $H_2O \leq 3$ %
sodium hydroxide	Merck	> 98 %
hydrofluoric acid	Fluka	puriss. p.a.
ammonium fluoride	Riedel-de-Haën	> 96 %

An overview of all synthesis and calcination procedures to obtain microporous materials is given in the table below.

Table 3.1.1.3. Synthesis and calcination of zeosils.

zeosils	SDAs	reaction mixture SiO_2:SDA: NaOH/HF:H_2O	reaction temp. T / °C	reaction time t / d	calc. temp. T / °C	calc. time t / h
Silicalite-1 (OH)	tetrapropyl-ammonium bromide	1 : 0.05: 0.08 : 14	180	12	600	3
Silicalite-1 (F)	tetrapropyl-ammonium bromide	1 : 0.12 : 0.1 : 37	160	21	600	4
ITQ-4 (F)	benzylquinu-clidine hydroxide	1 : 0.5 : 0.5 : 12~30	150	13	600	4
SSZ-24 (OH)	*N*(16)-methyl-sparteinium hydroxide	1 : 0.3 : - : 40	175	10	650	6
SSZ-24 (F)	*N*(16)-methyl-sparteinium hydroxide	1 : 0.5 : 0.5 : 10.5	175	5	650	7
CIT-5 (OH)	*N*(16)-methyl-sparteinium hydroxide	1 : 0.3 : - : 40	175	10	650	6
CIT-5 (F)	*N*(16)-methyl-sparteinium hydroxide	1 : 0.5 : 0.5 : 19	175	7	650	6

UTD-1 (OH)	decamethyl-cobalticinium hydroxide	1 : 0.13 : 0.09 : 57	150	14	550	6

B. Characterization of zeosils

Silicalite-1

Fig. 3.1.1. shows the X-ray diffraction patterns of as-synthesized and calcined Silicalite-1. The space group and the lattice parameters are presented in Table 3.1.2., where the *d*-spacing and the indexing of the experimental patterns are given in appendices A1 and A2 for the as-synthesized and the calcined material, respectively.

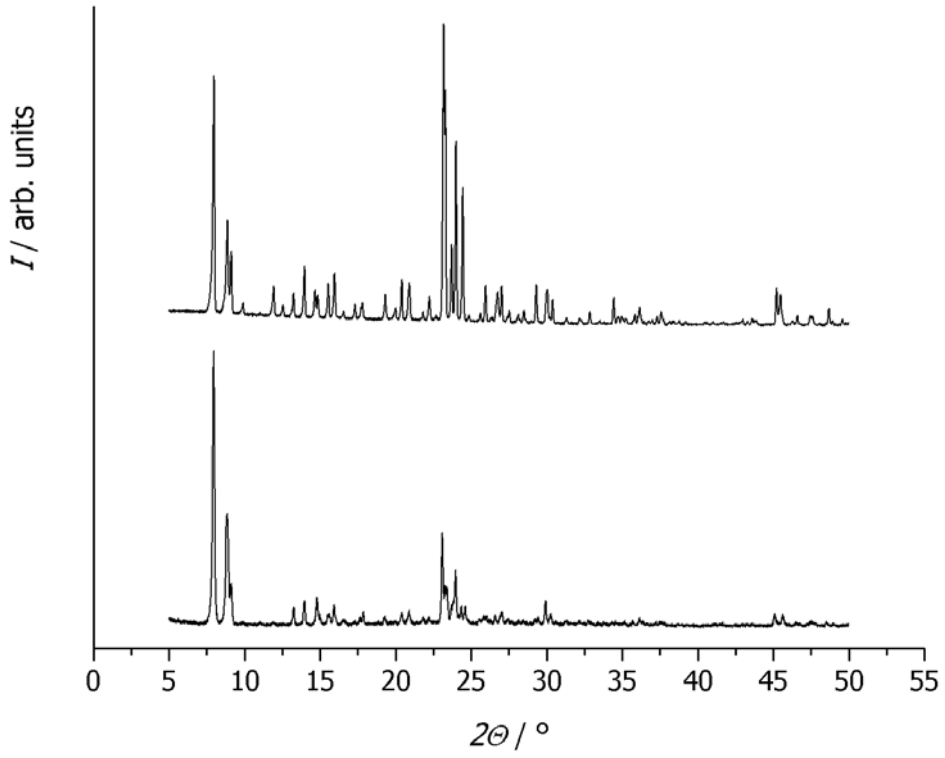

Fig. 3.1.1. Powder X-ray diffraction patterns of as-synthesized (upper trace) and calcined (lower trace) Silicalite-1.

Table 3.1.2. Structural properties of Silicalite-1.

structure type	crystal system	space group	lattice parameters
Silicalite-1 as-synth.	orthorhombic	*Pnma* (No. 62)	a = 20.020 Å b = 19.916 Å c = 13.3664 Å
Silicalite-1 calc.	monoclinic	$P1\ 2_1/n\ 1$ (No. 14)	a = 19.847 Å b = 20.059 Å c = 13.33 Å β = 90.43°

ITQ-4

The X-ray powder diffraction patterns of the as-synthesized and calcined ITQ-4 (see Fig. 3.1.3.) could be indexed and the unit cell parameters are presented in Table 3.1.4. and appendices A5 and A6.

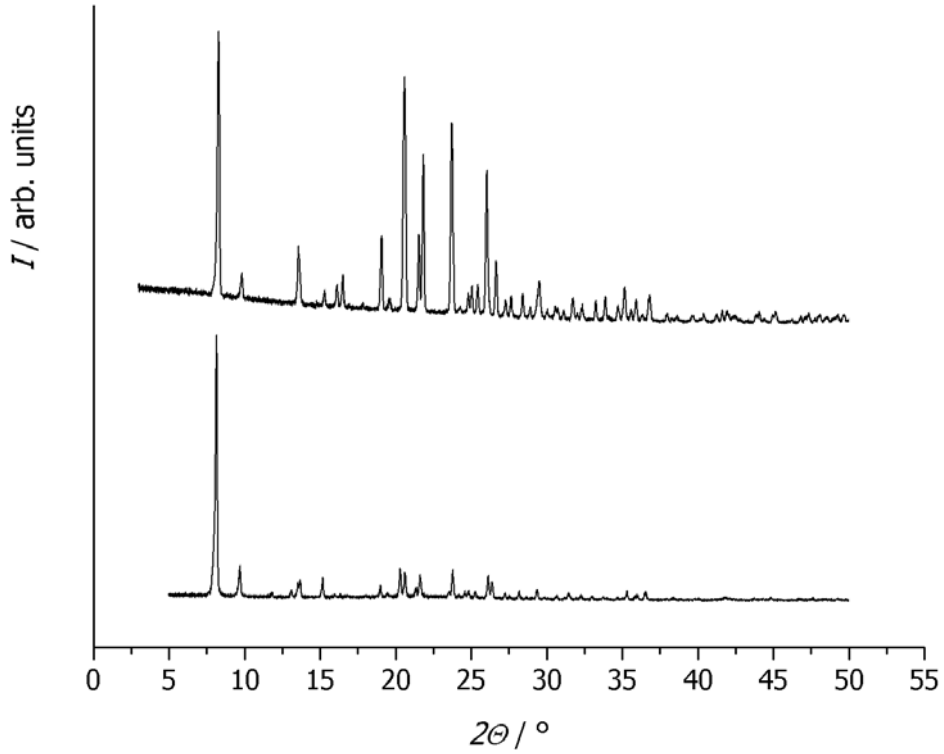

Fig. 3.1.3. Powder X-ray diffraction patterns of as-synthesized (upper trace) and calcined (lower trace) ITQ-4.

Table 3.1.4. Structural properties of ITQ-4.

structure type	crystal system	space group	lattice parameters
ITQ-4 as-synth.	monoclinic	*I* 1 2/*m* 1 (No. 12)	*a* = 18.476 Å *b* = 13.425 Å *c* = 7.7065 Å *β* = 101.618
ITQ-4 calc.	monoclinic	*I* 1 2/*m* 1 (No. 12)	*a* = 18.644 Å *b* = 13.4922 Å *c* = 7.6385 Å *β* = 101.953°

SSZ-24

Fig. 3.1.5. shows the X-ray diffraction patterns of the as-synthesized and calcined SSZ-24.

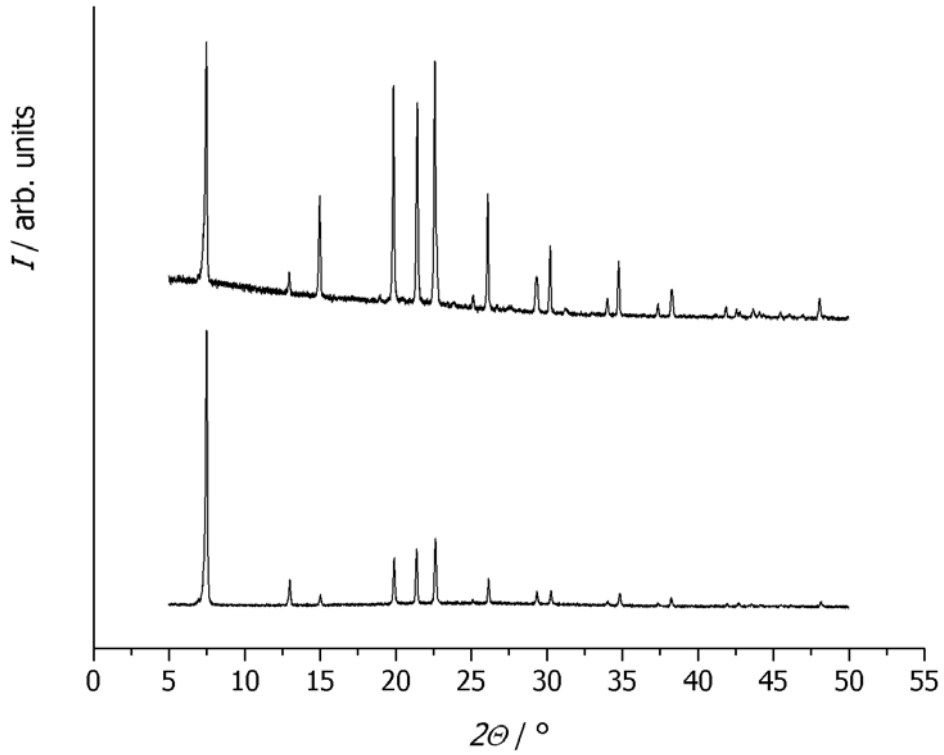

Fig. 3.1.5. Powder X-ray diffraction patterns of as-synthesized (upper trace) and calcined (lower trace) SSZ-24.

The indexing of these experimental patterns is presented in Table 3.1.6. and appendices A8 and A9.

Table 3.1.6. Structural properties of SSZ-24.

structure type	crystal system	space group	lattice parameters
SSZ-24 as-synth.	hexagonal	*P*6 (No. 168)	$a = b = 13.636$ Å $c = 8.280$ Å
SSZ-24 calc.	hexagonal	*P*6 (No. 168)	$a = b = 13.624$ Å $c = 8.312$ Å

CIT-5

The as-synthesized and calcined CIT-5 can be both described as having an orthorhombic symmetry (Table 3.1.8., appendices A14 and A15). The respective X-ray diffraction patterns are depicted in Fig. 3.1.7.

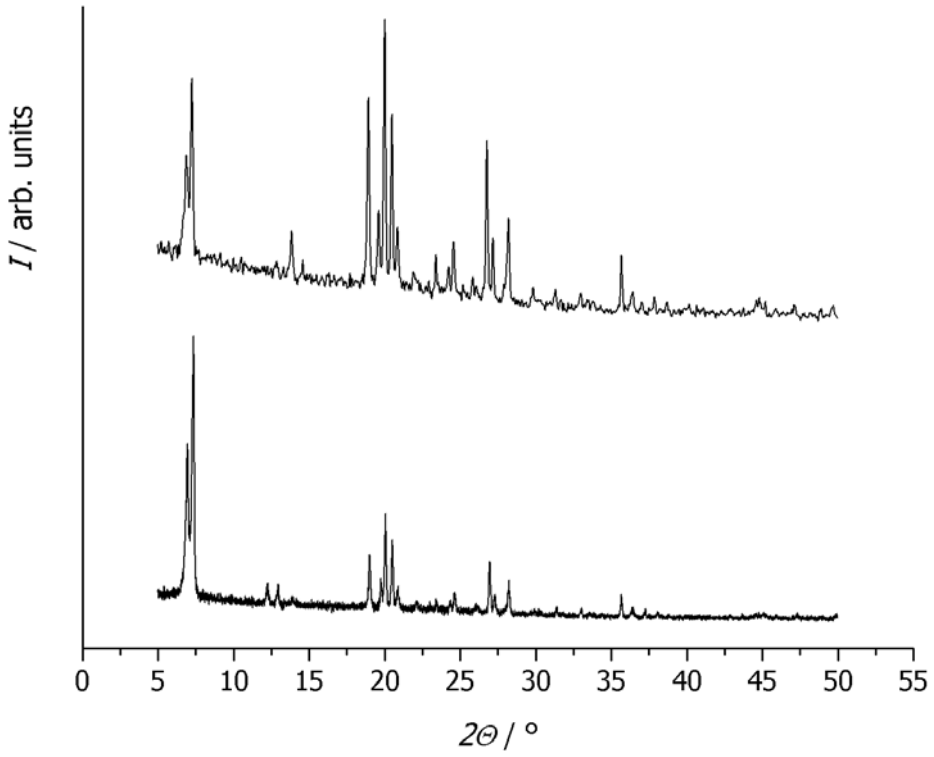

Fig. 3.1.7. Powder X-ray diffraction patterns of as-synthesized (upper trace) and calcined (lower trace) CIT-5.

Table 3.1.8. Structural properties of CIT-5.

structure type	crystal system	space group	lattice parameters
CIT-5 as-synth.	orthorhombic	*Imma* (No. 74)	a = 13.780 Å b = 5.0329 Å c = 25.536 Å
CIT-5 calc.	orthorhombic	*Im2a* (No. 46)	a = 13.709 Å b = 5.0358 Å c = 25.580 Å

UTD-1

The introduction of [Co(cp^*)$_2$]OH to the high silica (Si/Al > 350) gels, results in the formation of a novel crystalline phase, UTD-1. Fig. 3.1.9. shows the XRD powder patterns of the as-synthesized and calcined UTD-1 (after the extraction of cobalt oxide), obtained in hydroxide medium. The lattice parameters of the monoclinic as-synthesized UTD-1(OH) were refined in the space group *P*2. The X-ray powder diffraction pattern of the calcined and then extracted UTD-1 can be indexed using a monoclinic unit cell with the space group *P*2, but the UTD-1 system free from the cobalt complex can be also described as a disordered material possessing an orthorhombic lattice in space group *Bmmb* (see Table 3.1.10.). For the further insertion experiments of UTD-1, only the orthorhombic setting will be considered for the calcined zeosil.

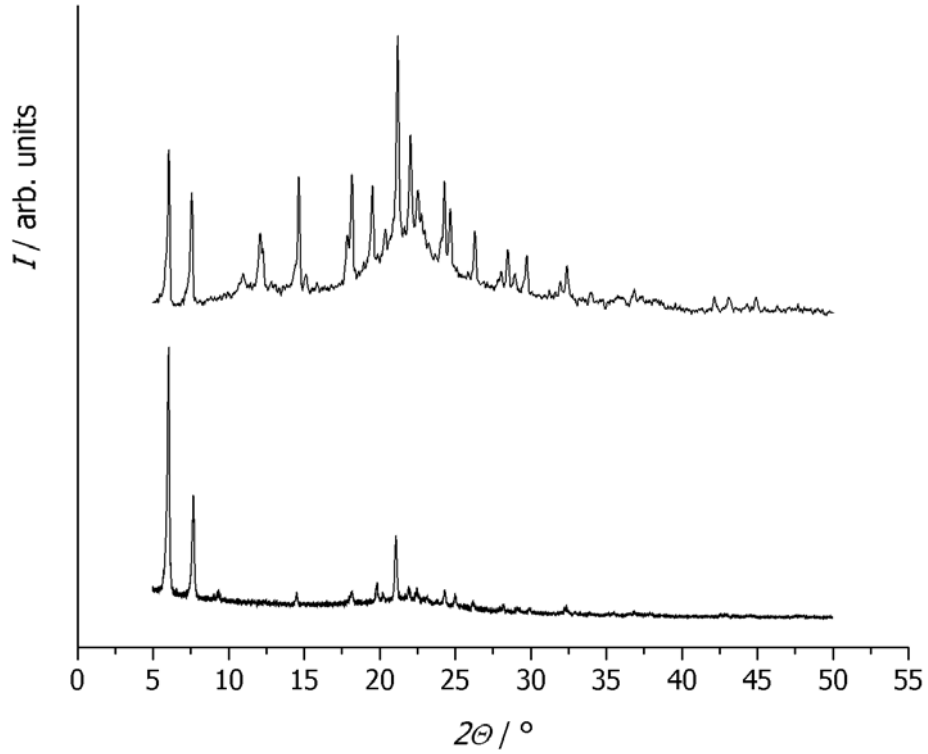

Fig. 3.1.9. Powder X-ray diffraction patterns of as-synthesized (upper trace) and calcined/extracted (lower trace) UTD-1.

Table 3.1.10. Structural properties of UTD-1.

structure type	crystal system	space group	lattice parameters
UTD-1 as-synth.	monoclinic	*P*2 (No. 3)	*a* = 14.85 Å *b* = 8.373 Å *c* = 30.37 Å *β* = 101.54°
UTD-1 calc.	monoclinic orthorhombic	*P*2 (No. 3) *Bmmb* (No. 63)	*a* = 14.6 Å *b* = 8.1 Å *c* = 30.3 Å *β* = 105.1° *a* = 19.017 Å *b* = 8.421 Å *c* = 22.978 Å

3.1.2. Insertion experiments

The host compounds, namely the zeosils Silicalite-1, ITQ-4, SSZ-24, CIT-5 and UTD-1 were prepared and calcined as described in detail in Chapter 3.1.1.A. Guest molecules were inserted into microporous SiO_2 hosts via gas phase. For the insertion, the powdered zeosil and varied quantities of the freshly smashed guest compound were put in an evacuated glass (or quartz-glass) tube in such a way that the host was placed at the bottom of the ampoule, whereas the guest was held loosely at the top by fine quartz-wool (Fig. 3.1.2.1.)

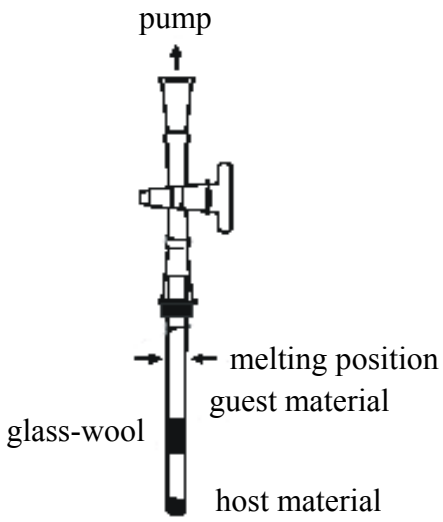

Fig. 3.1.2.1. Filling of ampoules.

In the case of guests materials which are air- or moisture-sensitive, the preparation of the samples was carried out in the inert atmosphere of a glove-box, having water vapour content less than 1 ppm. The tubes, containing first only the zeosil, were washed one time with argon and then disconnected from the melting installation. After transfer into the glove-box, they were finally filled with the guest compound under argon atmosphere. The closed ampoules were again transferred to the vacuum-line, evacuated and sealed under vacuum by melting with an oxygen-gas flame. In the case of non-sensitive guest compounds, after washing the tube one time with argon, the ampoule was removed from the melting installation, the guest material was added on the glass-wool. Thereafter, the tube was connected again to the melting device (position shown by an arrow in Fig. 3.1.2.2.) and under vacuum, sealed.

Fig. 3.1.2.2. Melting installation.

The ampoules used have an outer diameter of 10 mm with a wall thickness of 1 mm and are 20 cm long. They were sealed under a pressure of 10^{-5} mbar and heated in a tube furnace for approximately one week. The position of the tube inside the oven is shown in Fig. 3.1.2.3. After the insertion time, the ampoules were slowly cooled down to ambient temperature. The characteristic of this method is the strict division of the guest and the host material. Thus, a direct mixing of host and guest compounds can be avoided. Due to the temperature gradients, this arrangement caused the guest compounds to be collected at one end of the ampoules when the samples were cooled down after the insertion experiments. Reaction temperatures and times were varied in order to achieve a high loading.

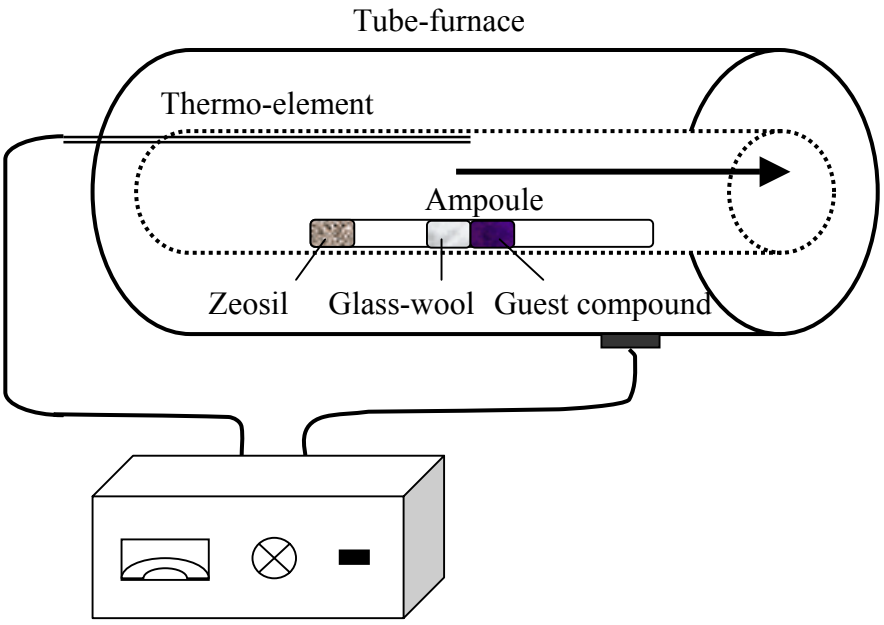

Fig. 3.1.2.3. Set-up for the insertion experiment in the oven.

The insertion of iodine was performed in glass ampoules. Approximately 100 mg zeosil were used, and after a previous dehydratation of the host inside the glass-tube, 1 g of freshly smashed iodine was filled over the glass-wool. Due to the fast sublimation of iodine, even at room temperature, the zeosil's colour was observed to change immediately from white to violet, due to the insertion of iodine molecules into the voids of the guest. The ampoule was then sealed and heated in the oven at 160 °C for five days. After this period, the ampoule was slowly cooled down to room temperature. Due to the instability of the iodine loaded zeosils under atmospheric conditions, the ampoules were opened in the glove-box. All insertion samples were stored and measured under argon atmosphere.

For the sorption experiments with selenium, quartz ampoules were used since temperatures higher than 500 °C (under vacuum) were necessary to bring selenium into the gaseous phase (boiling point: 684.9 °C, under normal pressure). For the insertion, 150 mg of the zeosil host were filled into the quartz tube and quartz-wool was used to fix the guest compound. The zeosil powder was first dehydrated by heating it under vacuum for some minutes, and then washed one time with argon. The ampoule was afterwards disconnected from the melting device and 500 mg of the guest material, selenium, were added on the quartz-wool. The tube containing now the host and the guest materials was sealed under vacuum and heated at 550 °C for ten days. After this time, the ampoule was cooled down to room temperature in such a way that the side containing the guest compound was brought close to one end of the furnace (shown with an

arrow in Fig. 3.1.2.3.). Due to the temperature gradient, was avoided condensation of selenium on the outer surface of the zeosil during cooling. In this way, the excess of guest material, which was not loaded into the cavities of the host, could condense at the opposite end of the quartz-tube. The ampoule was finally opened and the selenium–loaded zeosil was removed. All samples were stored and measured under ambient conditions.

The insertion of mercury halides was performed via gas phase, in evacuated and closed glass tubes. Before sealing, the open tubes containing only the host material, were dried under forced hot air. Even if the zeosils are hydrophobic materials, it was observed that without this step, the inserted samples become dark grey. This is probably due to the remaining traces of water which cause a reduction of the mercury(II) halides during insertion. Typically, 100 mg host material and 600 mg of the mercury halide (halide: chloride, bromide, iodide) were used for each experiment. The tubes were placed in an oven, with the host compound kept in the middle of the tube-furnace and the guest close to one end of the oven. This set-up avoids condensation of the bulk halide on the zeosils's surface during cooling. Insertion temperatures were chosen according to the volatility of the guest component: 360 °C in case of $HgCl_2$, 340 °C when using $HgBr_2$ and 380 °C for HgI_2. After five days insertion time, the ampoules were slowly cooled down to 150 °C and kept at this temperature for another two days. In the end, they were left to cool down slowly to room temperature. The ampoules were opened in the glove-box and the insertion samples were stored under argon atmosphere. The characterization techniques were carried out in closed sample-holders or capillaries, prepared in the glove-box.

For gold(III) chloride insertion experiments another device was used, because in this case, due to the decomposition of the guest compound at higher temperatures, chlorine was also added. The ampoule station had in this case also a chlorine inlet with a control device for the chlorine pressure. The procedure was similar to the one described before. After the tube was evacuated and washed with argon, 60 mg of the powdered gold(III) chloride were added over the quartz-wool in the glove-box and the closed ampoule was connected to the chlorine port. The tube was once again evacuated, washed with chlorine and then partially evacuated. Under a chlorine pressure of 500 mbar, the ampoule was finally sealed.

Due to the limited stability of the insertion compounds, all the characterization methods took place in sealed tubes or capillaries, with the exception of the loaded samples based on selenium as guest material.

A survey of all insertion experiments is given in the table below.

Table 3.1.2.4. Insertion parameters. Melting and boiling points are given as comparison.

guest compound	melting point T_m / °C	boiling point T_b / °C	insertion temperature T_i / °C	insertion time t_i / d
I_2	113.5	184.35	160	5
Se	217	684.9	550	10
$HgCl_2$	276	302	360	5
$HgBr_2$	236	322	340	5
HgI_2	259	354	380	5
$AuCl_3$	254	subl. 265	220	10

3.2. Zeodyes synthesis from clear solution

3.2.1. Preparation of Silicalite-1 nanoslab suspension

Silicalite-1 nanoslab suspension used in this work was prepared according to the literature [KR04] as follows: 3.657 g tetraethylorthosilicate (TEOS) were hydrolyzed in 3.209 g aqueous tripropylammonium hydroxide solution (TPAOH) under stirring. The hydrolysis of TEOS, recognized by the homogenization of the two liquids and by the temperature increase (70 °C), occurred within ca. 10 minutes. After 10 more minutes, 3.133 g water were added and the stirring was continued for another 24 hours. These amounts correspond to reactants molar ratios of 25 TEOS : 9 TPAOH : 400 H_2O and has as results the formation of 10 g half-nanoslab suspension. This was stored at 5 °C. The difference in the synthesis of half-nanoslab or nanoslab suspensions consist in the different amounts of water used. For example, in order to obtain half-nanoslab suspensions, as mentioned before, the water part should be 400, but when synthesizing nanoslab suspensions it should be 440 [RK99b] [KR04] or 480 [PS94].

Chemicals used:

TEOS	Acros	98 %
TPAOH aqueous solution	Alfa	40 wt.- %

3.2.2. Synthesis of zeodyes

The purpose here was the synthesis of a new class of porous materials, called zeodyes, starting from a Silicalite-1 half-nanoslab suspension and different types of azo-dyes. For the syntheses of zeodyes, the composition of the reaction mixture as well as the critical parameters, like temperature, pressure and time, were varied in order to obtain materials with better ordering, in high yields. The azo-dyes were synthesized in our group by B. Ufer [UF03]. Different types of azo-dyes were used, having alkyl chains of different lengths and/or various head groups. Best results were obtained in the case of azo-dyes with trimethylammonium as head group. The recipe for the preparation of these materials will be described as here. Typically, Silicalite-1 half-nanoslab suspension was added dropwise to a solution of azo-dye in ethanol, under stirring. It is known that in the presence of ethanol, a coupling of half-nanoslabs into nanoslabs takes

place [KR04]. An immediate flocculation occurred during the addition of the clear solution, and a milky viscous liquid was obtained. The whole emulsion was stirred for some hours, and then left to stay static, while the temperature was maintained constant. The stirring and the temperature program employed for the different azo-dyes is given in Table 3.2.2.1.

Table 3.2.2.1. Overview of synthesis temperatures and times for the preparation of zeodyes.

azo-dye	temperature / °C	stirring time / static time
C_3AzoC_2TMABr	96 (in autoclave) 20 (RT)	2 hours / 3 days 2 hours / 1 day
C_4AzoC_2TMABr	96 (in autoclave) 75 60 60 60 60	2 hours / 3 days 2 hours / 2 days 15 min. / 1 day 1 hour / 1 day 2 hours / 1 day 1 day / -
C_8AzoC_6TMABr	96 (in autoclave) 70 70 60 60 20 (RT)	2 hours / 1 day 2 hours / 1 day 2 hours / 2 days 2 hours / 1 day 1 day / - 2 hours / 1 day
$C_{10}AzoC_8TMABr$	70 20 (RT)	2 hours / 1 day 2 hours / 1 day

Due to the low solubility of the azo-dyes in ethanol, which becomes less when the alkyl chain becomes longer, the concentration of the azo-dye solution at room-temperature was quite low. The solubility can be improved by heating the solution. Different concentrations of the azo-dye solutions in ethanol were considered, as well as different ratios between azo-dye and clear solution.

The precipitate formed after the addition of the clear solution was recovered by filtration or centrifugation, washed with ethanol and water and dried at 60 °C for two hours. The amounts of

reactants used in the syntheses of the zeodyes as well as the amounts of product obtained in the end are given in the table below. These data refer to optimized synthesis procedures.

Table 3.2.2.2. Amounts of reactants and zeodyes produced.

azo-dye	$m_{\text{azo-dye}}$ / mg	concentration / % azo-dye in EtOH	m_{CS} / mg	ratio azo-dye : CS	m_{zeodye} / mg
C_3AzoC_2TMABr	14	1.8	108.2	0.13	32
C_4AzoC_2TMABr	203	3.3	602	0.34	196
C_8AzoC_6TMABr	245	3.6	878	0.28	297.7
$C_{10}AzoC_8TMABr$	375	1.5	1051	0.36	327.4

Another procedure for the synthesis of zeodyes was evaluated. It consisted in adding dropwise the azo-dye/ethanol solution into the half-nanoslab suspension. When using the same temperature/stirring program, no differences were noticed between the two respective products.

Synthesis of zeodye-3.2 (based on C_3AzoC_2TMABr as surfactant)

14 mg of the azo-dye C_3AzoC_2TMABr were dissolved in 768 mg ethanol, giving a concentration of the azo-dye solution of 1.8 %. 100 mg half-nanoslab suspension were added and the emulsion formed was stirred at room temperature for two hours and then left to stay static for another day. After this time, the yellow precipitate was recovered by centrifugation, washed three times with ethanol, dried for two hours at 60 °C and then at ambient temperature. The final material was investigated using X-ray powder diffraction, thermogravimetry and UV-vis spectroscopy.

Synthesis of zeodye-4.2 (based on C_4AzoC_2TMABr as surfactant)

Into 5.984 g ethanol, heated at 60 °C, 203 mg of the azo-dye C_4AzoC_2TMABr were added, giving a solution with a concentration of 3.3 %. To this hot solution, 602 mg half-nanoslab suspension were given under energic stirring. Stirring was necessary to assure the good mixing of the two reactant solutions. A yellow precipitate was formed immediately after the addition of the nanoslab. The milky liquid was stirred for another two hours and then left to stay static until the next day. After this period, the precipitate was centrifuged two times and washed with

ethanol, dried in the oven for two hours at 60 °C and then left to dry at room-temperature. 196 mg of a yellow powder were finally obtained. The product was analyzed by X-ray powder diffraction, thermogravimetry and UV-vis spectroscopy. One part of the zeodye-4.2 was afterwards calcined using the procedure described in chapter 3.2.3.

Synthesis of zeodye-8.6 (based on C_8AzoC_6TMABr as surfactant)

245 mg of C_8AzoC_6TMABr azo-dye were dissolved into 5.917 g ethanol at 70 °C. After good stirring, the solution became clear and was added dropwise over 878 mg half-nanoslab suspension. The whole mixture was stirred for two hours at 70 °C and then left to stay under static conditions for another two days, while maintaining the same temperature. The precipitate was recovered by filtration, washed with ethanol on the filter paper and left to dry. 297.9 mg of a yellow powder were obtained. Chapter 4.2 describes the characterization of this product.

Synthesis of zeodye-10.8 (based on $C_{10}AzoC_8TMABr$ as surfactant)

Into 1.051 g of half-nanoslab suspension, a solution with the concentration 1.5 % $C_{10}AzoC_8TMABr$ azo-dye in ethanol was added dropwise. The temperature was 70 °C and the stirring time two hours. After the sample was left for another 22 hours at static conditions, the emulsion was filtered, washed with ethanol and water and then dried at 60 °C for two hours. The synthesis gave 327.4 mg zeodye-10.8, that was further analyzed as all the other products.

3.2.3. Calcination of zeodyes

The as-synthesized zeodye, ground to give very fine particles, was loaded at the bottom of a U-tube made out of glass or quartz-glass. The calcination took place in a vertical tube furnace, with a heating rate of 0.5 °C/min. In the first step, the solid was heated under O_2 flow from ambient temperature to 150 °C and kept at these conditions for three days. After this step, the sample had still a yellow colour. It is denoted as intermediary zeodye. In the second calcination step, the sample was heated to 400 °C under N_2 flow, kept at this temperature for one day and then cooled down to room temperature. At this stage, the zeodye had a black colour, due to the carbonaceous residues left after the pyrolysis of the organic molecules. The last calcination step consisted in heating the sample to 400 °C for two days, under O_2 flow. The final zeodye

(zeodye calcined) had a white colour, which proves the total elimination of the azo-dye molecules that caused the initial yellow colour. For all three calcinations steps, the gas flow was 50 mL/min.

3.3. Characterizaton techniques

X-ray powder diffraction (XRD)

XRD was used to study the composition, phase purity and structure of the as-synthesized and calcined zeosils and zeodyes, as well as of the loaded zeosils. Room-temperature powder X-ray diffraction patterns of the samples which did not contain cobalt were obtained in a 2Θ transmission geometry with a CuKα_1-radiation on a Stadi P diffractometer from STOE. The samples were stored in special round sample-holders, in between two plastic foils or in capillaries having diameters of 0.5, 0.7 mm. The diffractometer was equipped with a nickel filter and a Ge(111) crystal monochromator. Data were recorded in steps of 0.1 to 0.5°, with total measurement times from 2 to 14 hours, in angle ranges between 5 and 50°. X-ray intensities were recorded with a PSD-detector and the evaluation of the data was performed using the WinXPOW program from STOE (version 1.08). Due to the fluorescence of cobalt when using the CuKα1-radiation as X-ray source, the cobalt containing samples were measured on a Theta Theta diffractometer from STOE equipped with a secondary monochromator and a scintillation counter. For the measurement, the samples were pressed in a flat sample holder with diameters of 10 or 17 mm. The WinXPOW software from STOE was used in order to remove the reflections caused by the CuKα2-radiation.

Thermogravimetric analysis (TG/DTA)

TG was performed to quantify the weight losses undergone by materials when subjected to increasing temperatures. In addition, differential thermal analysis (DTA) allowed evaluation of the endo- or exothermicity linked to the respective weight losses. The measurements were done using a STA-429 device from the company Netzsch, with a heating rate of 5 °C/min., under air, helium or argon atmosphere. The temperatures were raised up to ca. 900 °C. Al_2O_3 was used as a reference substance and the sample holders were made of Al_2O_3, too. For the loaded zeosils, at specific temperatures, the guest materials leave the host and by the respective weight loss, one can determine the degree of loading.

Nitrogen adsorption

When a solid porous material under vacuum is exposed to a gas, the gas adsorbs as a function of its chemical properties, of the chemical properties of the solid, but also of the physical properties of the measuring system considered, e.g. pressure of the gas, temperature, volume. After the adsorption process, a decrease of the gas pressure as well as an increase of the mass of the solid in the enclosed volume can be observed. The plot of the adsorbed volume versus the relative pressure, p/p_0 (where p_0 is the saturation pressure at a certain temperature) is denoted as adsorption isotherm. N_2 adsorption at –196 °C is a commonly applied technique to characterize the micro- (< 2 nm), meso- (2 – 50 nm) and macroporosity (> 50 nm) of materials, as well as the particle external surface area.

The sorption measurements in this work were carried out on a TriStar instrument, provided by Micromeritics. The device is located at the University of Leuven. Typically, 16 mg of sample were outgassed for 10 min. at 30 °C, then heated to 200 °C with 10 °/min. and kept at this temperature for two hours. Contrary to the typical procedure, the outgassing was done under nitrogen flow, prior the measurements.

The isotherm analysis was performed with the TriStar 3000 V6.03 software. From the N_2 adsorption isotherm, several characteristics of the porosity of the material as total sum of the outer and inner surfaces, total pore volume (which includes micro- and mesopores) or micropore volume (using the *t*-plot method) can be obtained. The BET isotherm method was first introduced by Brunauer, Emmett and Teller [BE38], who presented a model to describe adsorption processes on solid surfaces. They presumed that the monomolecular layer which is formed as a result of interactions among the adsorptive molecules is covered with other layers during adsorption. The BET equation can be written:

$$\frac{p / p_0}{V_{ads}\,(1 - p / p_0)} = \frac{1}{V_{mono}\,C} + \frac{C - 1}{V_{mono}\,C}\; p / p_0$$

It contains the relative pressure, p/p_0, the adsorbed volume, V_{ads}, the monolayer volume, V_{mono}, and the BET constant, C.

The *t*-plot method compares the adsorption isotherm of a porous material with that of a non-porous material of similar chemical characteristics. By multiplying the ratio between the specific adsorbate volume, V_{ads}, of the non-porous material and the volume of the first adsorbed monolayer, V_{mono}, with the monolayer thickness, t_i, the thickness of the layer, t, is obtained:

$$t = \frac{V_{ads}}{V_{mono}} t_i$$

The volume of the monolayer can be calculated from the BET equation presented before. The plot of the thickness of the layer, t, over the relative pressure results in the standard isotherm. To characterize the microporosity, the specific adsorbate volume, V_{ads}, of the test material is plotted over the thickness of the layer, t [HD02].

Ultraviolet-visible spectroscopy

Room temperature UV-vis measurements were recorded on a UV Vis NIR spectrophotometer Cary 5E provided by Varian Company.

All samples were measured in diffuse reflection, using the Kubelka-Munk theory [KM31], which provides an equation that relates the reflection of a sample under diffuse illumination to certain of its properties, and does not take boundary reflectance into account [KO69]. In this way all spectra were transformed into units of the Kubelka-Munk function (see equation below):

$$F(R_\infty) = (1- R_\infty)^2 / 2 R_\infty = k / s$$

where: $F(R_\infty)$ = Kubelka-Munk function

R = reflectivity

k = absorption coefficient

s = scattering coefficient.

The Praying-Mantis™ device was used as accessory for the diffuse reflectance measurements. Its typical optical configuration is shown in Fig. 3.3.1.

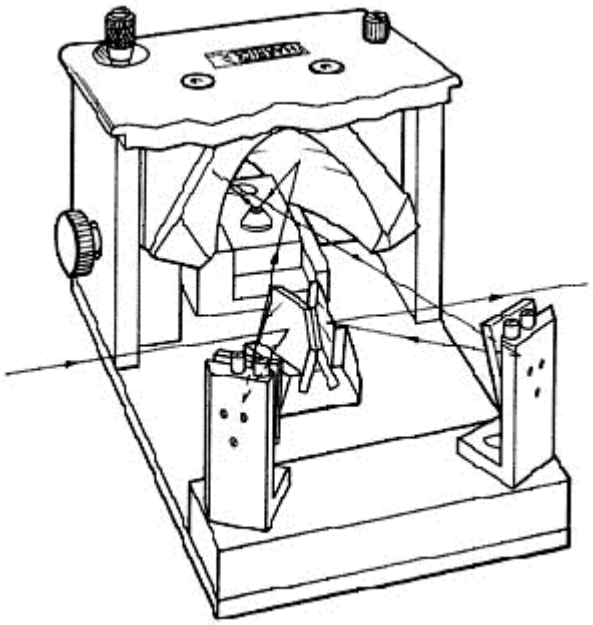

Fig. 3.3.1. Praying-Mantis™ accessory.

For the measurements of UV-vis spectra of solids, the samples were normally diluted with BaSO4, which was also considered as reference material. But in the case of zeosils inserted with iodine, mercury(II) halides or gold(III) chloride, the samples were measured as they were, using the respective calcined hosts as reference. Spectra of all compounds were collected at room temperature from 200 to 500 ~ 800 nm, depending on the guest. As the materials are air-sensitive, a special chamber was used (see Fig. 3.3.2.). This was made in the atelier of the Institute for Inorganic Chemistry, Hannover, and was designed for studying samples in a controlled environment. The samples can be loaded in a glove-box, the chamber can then be sealed, removed from the glove-box and inserted in the Praying Mantis™ for analysis. This chamber features a removable stainless steel dome with three windows (one for observation).

Fig. 3.3.2. Special chamber for air-sensitive samples for UV-vis measurements.

Raman spectroscopy

Raman spectra were recorded on a FRA 106 device, attached at one side of the FT-IR spectrometer from Bruker; the 1064 nm line of a Nd:YAG laser with a maximum power of 700 mW was used for excitation. Measurements were performed in the 180° backscattering geometry, whereby the samples were held in standard melting-point tubes made out of glass and having a diameter of approximately 1 mm. Different numbers of scans were considered in order to obtain high-quality spectra with a laser power between 150 and 700 mW. The measurements of the selenium-loaded samples were carried out on a similar Raman spectrometer, which however had a higher laser power (measurements were done at 900 mW). In the case of mercury(II) halide insertion compounds, due to the fast desorption of the guest, spectra were taken with only 60 scans (maximum) and with low laser power (max. 200 mW). Higher laser power or higher number of scans lead to a desorption of the guest for all insertion compounds. This can be observed for the coloured samples, as a white spot develops in the position where the beam touched the sample. For calibration, a sulphur sample was used as standard. For the evaluation of the spectra, the program OPUS 3.0.1. was used.

4. RESULTS AND DISCUSSIONS

4.1. Insertion compounds

4.1.1. Iodine insertion compounds

Upon insertion, the originally white zeosils change their colour in a reproducible and significant way. The characteristic colours of the zeosils after insertion, violet to brownish (see Fig. 4.1.1.1.) and the thermogravimetric results, shown in Table 4.1.1.2., are two valid proofs that iodine was successfully filled into the porous host systems.

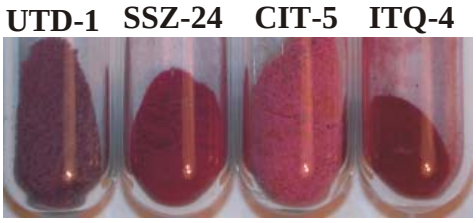

Fig. 4.1.1.1. Colour of iodine-inserted zeosils.

As shown in ref. [WP96] regarding the iodine insertion compounds of zeosils with medium size pores (4 – 5.5 Å), the colour gives an indication about the degree of interaction between the iodine molecules inside the voids of zeosils. Iodine–UTD-1 and iodine–ITQ-4 have a dark violet-to-brownish colour, which resembles that of iodine–MFI. This colour again is similar to that of liquid iodine and indicates rather strong interactions between the iodine molecules in the large channels of UTD-1 and in the cage-like corrugations of the channels of ITQ-4 (as well as in the cage-like cross-sections of the channels of MFI [WP96] [WI98]). Iodine–CIT-5 possesses a violet, iodine–SSZ-24 a red-violet colour, indicative of isolated iodine molecules. This is similar to I_2 in the vapour phase and to the insertion compound iodine–DDR [WP96] [WI98]. The isolated nature of I_2 molecules in DDR is understandable, as the pore system of zeosil DDR consists of small cages. However, it is difficult to correlate the violet colour with the rather large channels of SSZ-24 and CIT-5. The colour of the compounds is an especially important indicator for the properties of the loaded materials based on large-pore zeosils, because it turned out that these are much less stable than the composites based on medium pore zeosils. After opening the ampoule in which they were synthesized, they lose iodine rapidly, as can be

observed by the colour changing from brown or violet to white. This fact hampers the application of further characterization methods as powder X-ray diffraction, thermogravimetric analysis, UV-vis and Raman spectroscopy.

Table 4.1.1.2. Thermogravimetric results for iodine insertion compounds of large pore zeosils.

zeosil	unit cell composition $I_2 : SiO_2$
ITQ-4	1.75 : 32
SSZ-24	1.45 : 24
CIT-5	1.13 : 32
UTD-1	1.61 : 64

Thermogravimetric analysis gives the composition of iodine insertion compounds and allows to draw first quantitative conclusions. The data presented in Table 4.1.1.2. show that in case of the 14 MR zeosils CIT-5 and UTD-1, the loading is inferior to the one obtained for the 12 MR zeosils ITQ-4 and SSZ-24. This was not to be expected, but can be explained by the fact that the inserted materials based on extra-large pore zeosils are quite unstable, and iodine can easily desorb from the pores (channels) of the host during transfer of the sample.

Figs. 4.1.1.3., 4.1.1.4., 4.1.1.5. and 4.1.1.6. show the powder X-ray diffraction patterns of the calcined and iodine–inserted materials. They were recorded at RT. The diffraction data show significant differences in the reflection intensities of the loaded samples as compared to the calcined zeosils. Generally, the diffraction peaks in the low 2Θ region are suppressed upon insertion and this can be interpreted in terms of an increased electron density within the channels after filling. Powder XRD gives also information concerning the host-guest interactions which, when using zeosils as host materials, are weak so that the zeosil structure is not perturbed upon loading. This can be seen in the case of UTD-1 host system. The as-synthesized material has a monoclinic structure at room temperature which changes to orthorhombic upon calcination (chapter 3.1.1.B). The iodine loading within the channels of this host retains the orthorhombic structure. This was not the case when MFI was filled with different inorganic or organic species. The as-synthesized material has an orthorhombic structure at room temperature. Calcination causes a transition of the crystal system to

monoclinic symmetry [KJ90] and the full loading of the material with organic or inorganic compounds induces a back-transformation to orthorhombic symmetry [WL79] [FK84] [KJ96]. In contrast, with iodine inserted into its voids, MFI retains the monoclinic structure. This was observed also when other inorganic species, like IBr or Br_2, were loaded into MFI [WI98]. The invariance of the framework symmetry with respect to iodine insertion reflects the weak host-guest interactions due to the electroneutral SiO_2 framework of zeosils.

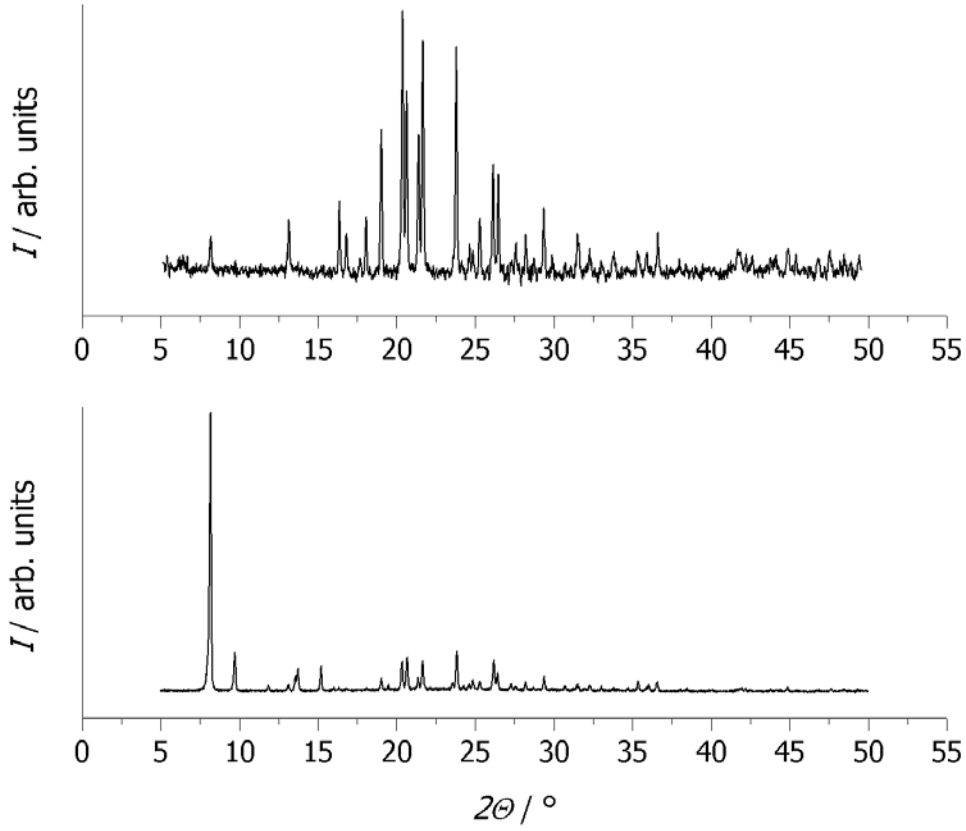

Fig. 4.1.1.3. Powder X-ray diffraction pattern of calcined ITQ-4 (lower trace) and of its insertion compound with iodine (upper trace).

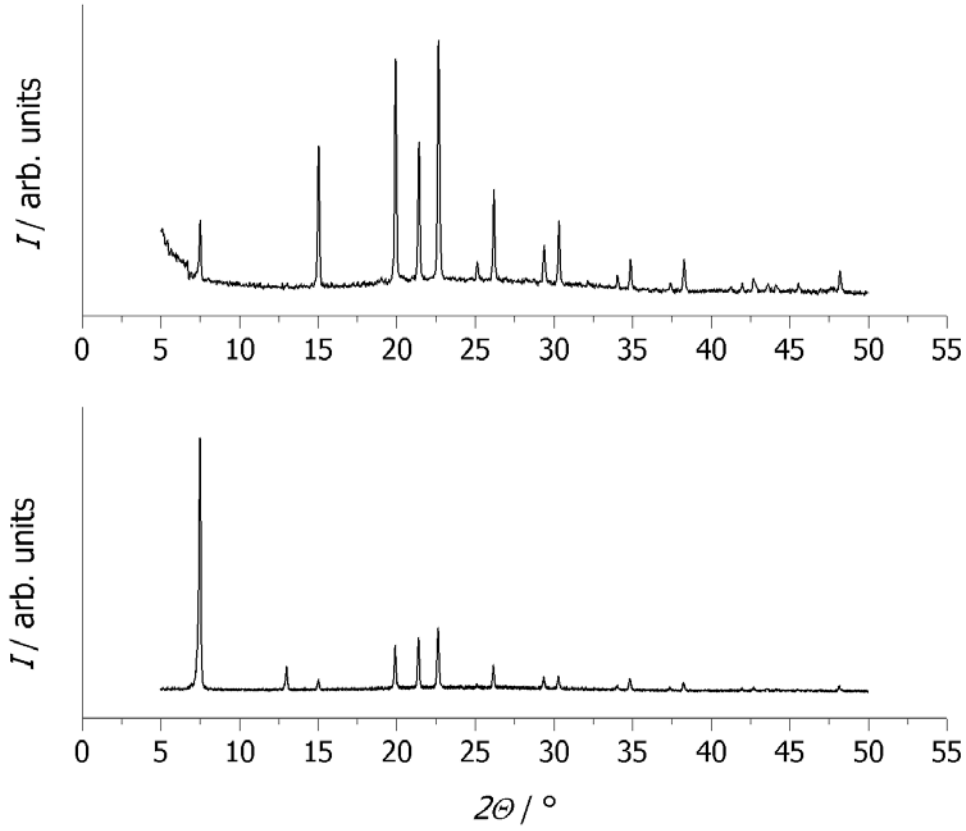

Fig. 4.1.1.4. Powder X-ray diffraction pattern of calcined SSZ-24 (lower trace) and of its insertion compound with iodine (upper trace).

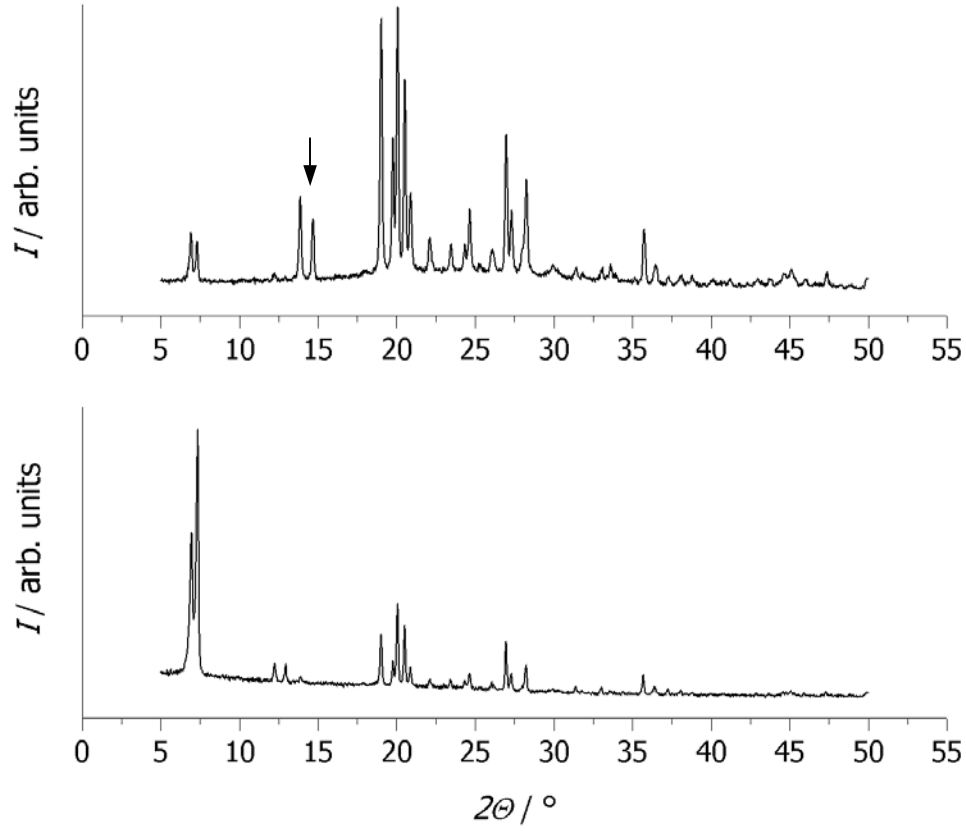

Fig. 4.1.1.5. Powder X-ray diffraction pattern of calcined CIT-5 (lower trace) and of its insertion compound with iodine (upper trace).

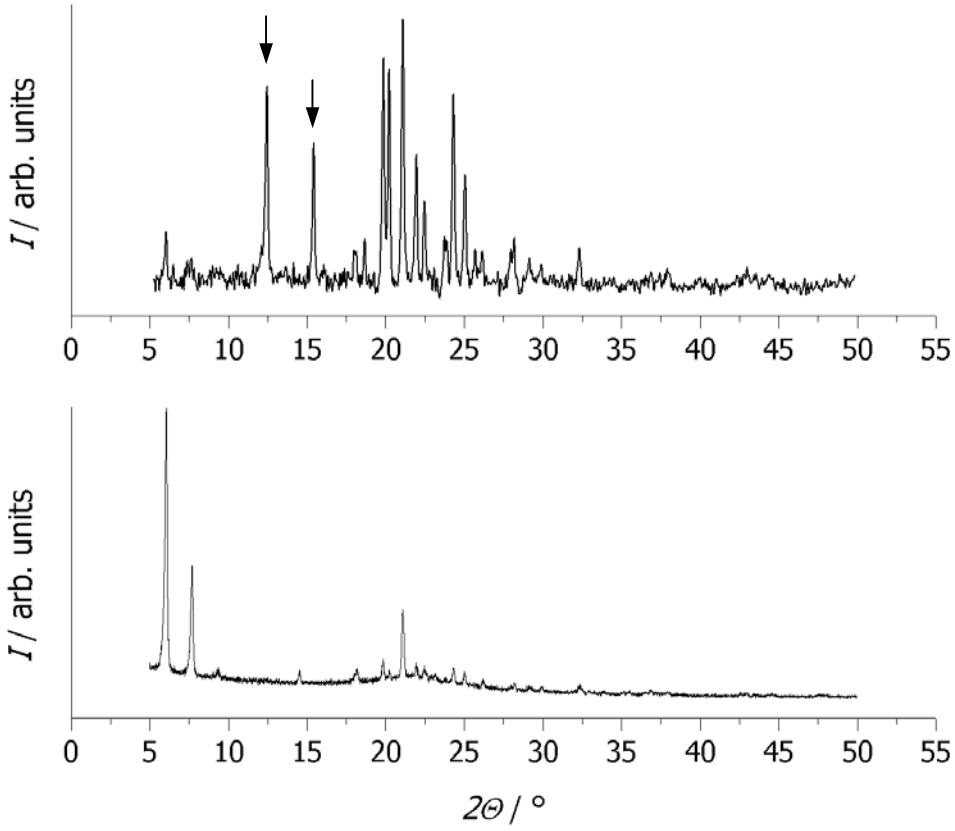

Fig. 4.1.1.6. Powder X-ray diffraction pattern of calcined UTD-1 (lower trace) and of its insertion compound with iodine (upper trace).

As can be observed in the XRD data of CIT-5 and UTD-1, some new peaks appeared in the patterns after insertion. For I_2 in CIT-5, a new peak was observed at 14.69 °2Θ (Fig. 4.1.1.5.). For iodine loaded into UTD-1, two additional peaks were detected at 12.45 and 15.42 °2Θ (Fig. 4.1.1.6.). These peaks were finally indexed as belonging to the zeosil structure. A list of all reflections and peak indexing is given in appendices A7, A10, A16 and A23 for iodine insertion compounds of ITQ-4, SSZ-24, CIT-5 and UTD-1, respectively.

Despite the fact that some conclusions can be drawn from the XRD data, the standard methods for the characterization of iodine–loaded compounds are the spectroscopic investigations. They are better suited since they probe the local state of the inserted guest molecules. The UV-vis spectra of the insertion compounds, shown in Fig. 4.1.1.7., reveal the general problem of their characterization. All spectra look very similar, especially in the visible region. This finding is in contrast to the different colours of the compounds that they exhibit when are still in the ampoules used for preparation. In fact, all spectra exhibit a relatively strong band at 516 nm and are very similar to that of iodine–DDR [WP96] [WI98] which in turn resembles that of gaseous iodine or iodine in weakly coordinating solvents. All spectra show also one band in the region between 400 and 260 nm where liquid iodine also has its strongest absorption [YN88]. Possibly, the insertion compounds have become partially deinserted during sample preparation or during measurement. Upon lowering the concentration of the iodine molecules within the channels, the interactions between them will be reduced. Correspondingly, spectral characteristics of isolated molecules are observed.

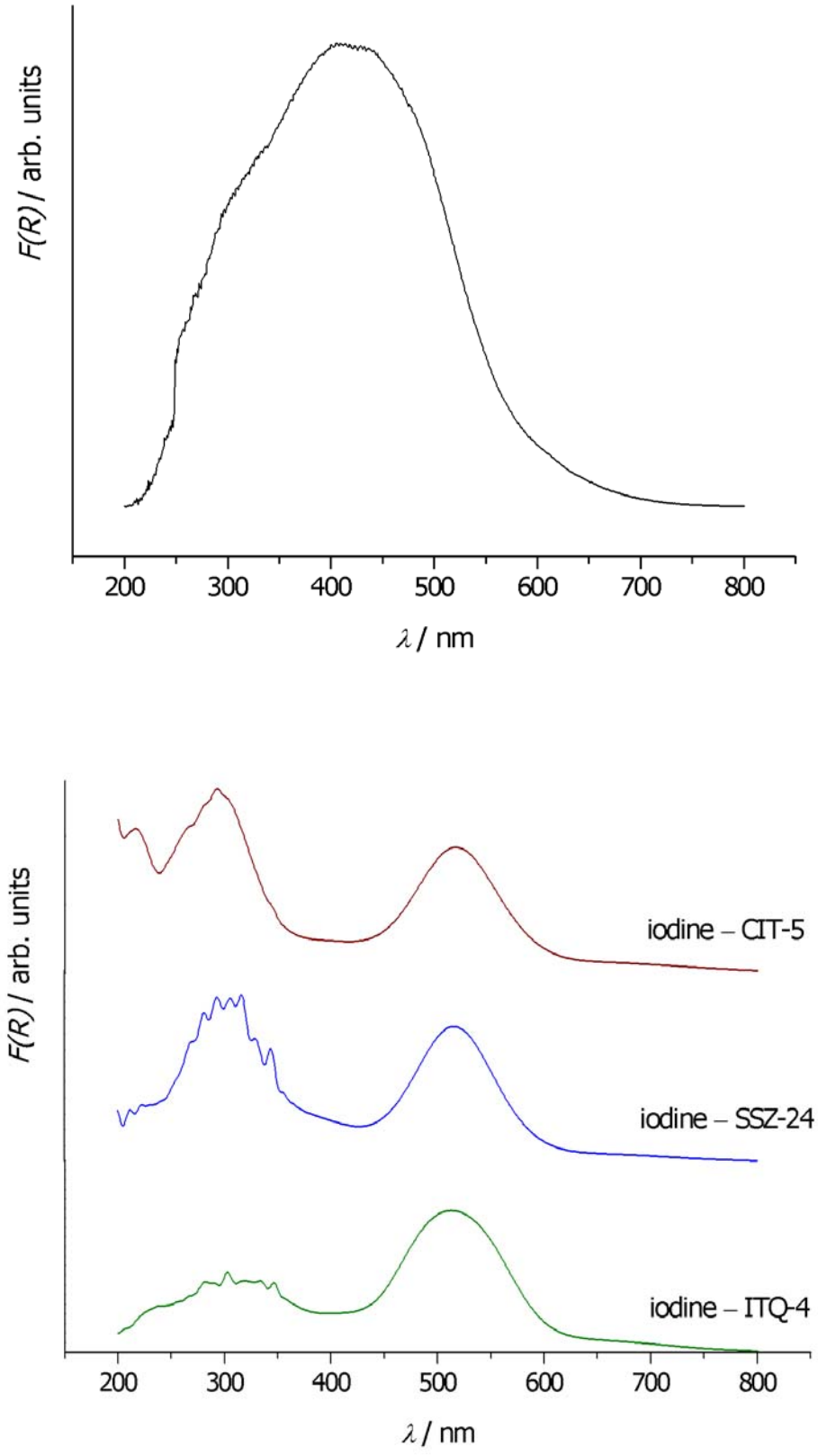

Fig. 4.1.1.7. UV-vis spectra (converted to Kubelka-Munk function $F(R)$) of solid iodine and iodine inserted zeosils.

A very sensitive method to investigate possible interactions between the occluded iodine molecules is Raman spectroscopy, since interactions between the molecules modify their vibrational properties. For example, for gaseous iodine the stretching vibration occurs at 213 cm^{-1}, whereas for solid iodine, due to intermolecular interactions, it appears at 188 and 181 cm^{-1}, as confirmed by inelastic neutron scattering [SN75] and Raman spectroscopy [SL81]. The Raman spectra of iodine–loaded zeosils are shown in Fig. 4.1.1.8.

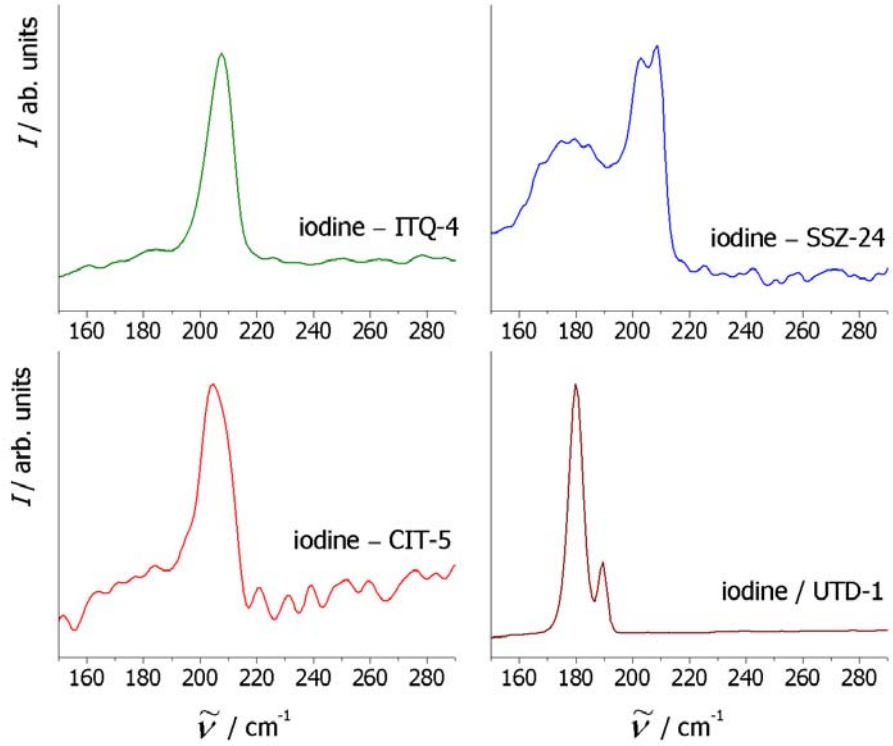

Fig. 4.1.1.8. Raman spectra of iodine–inserted zeosils.

Intermolecular interactions between the inserted iodine molecules cause a weakening of the intramolecular bonds and lead to a shift of the stretching vibrations to lower frequencies as compared to the isolated molecule in the gas phase (Table 4.1.1.9.). Iodine–ITQ-4 shows a single band at 207 cm^{-1}. This is characteristic of isolated I_2 molecules; for iodine–DDR this band was observed at 208 cm^{-1} [WP96] [WI98] and for gaseous iodine at 213 cm^{-1} [HM70]. The results furthermore support the idea that non-interacting iodine in zeosils are present in a nearly unperturbed state, like in vapour phase or in weakly coordinating solvents. No further bands have been detected, indicating that the concentration of iodine that reacts with the hydroxyl groups (on the crystal surface or within the crystal, due to defects) is negligible.

Iodine–SSZ-24 appears to be more stable. In addition to the peak at 207 cm^{-1}, there is a signal at 202 cm^{-1}, characteristic of iodine molecules interacting in one dimension, i.e. having a chain-like arrangement (similar to iodine–TON insertion compound [WP96]); in addition a broad emission band is located around 180 cm^{-1}. This band is similar to the Raman spectrum of liquid iodine [ML85] [YN88] and thus characteristic of strongly interacting iodine molecules. The shifts are attributed to the presence of intermolecular iodine-iodine interactions, causing a weakening of the intramolecular iodine-iodine bond and so a decrease of its force constant. However, these interactions are much weaker than in bulk iodine [SL81].

For the insertion compound of CIT-5, a band at 204 cm^{-1} was observed, which is again attributed to a chain-like arrangement of iodine molecules.

The Raman spectrum of iodine inserted in zeosil UTD-1 resembles the one observed for solid iodine, showing bands at 179 and 189 cm^{-1} characteristic for strongly interacting molecules. This finding must be viewed with regard to the instability of the loaded sample. Probably during sample preparation or during measurement, the iodine became deinserted and is observed as a bulk phase in the Raman spectrum.

Table 4.1.1.9. Raman bands of iodine and iodine insertion compounds.

compound	Raman shift / cm^{-1}	references
I_2 gaseous	213	[HM70]
I_2 in CCl_4	211	[KB73]
I_2 in C_6H_6	205	[KL67]
I_2 liquid	180, 194	[ML85]
I_2 solid	181, 188	[SL81]
I_2-ITQ-4	207	this work
I_2-SSZ-24	180, 202, 207	this work
I_2-CIT-5	204	this work
I_2-UTD-1	179, 189	this work

To conclude, the results presented in this chapter demonstrate the successful insertion of iodine into large and extra-large pore zeosils. The interactions between the iodine molecules can be also finely tuned by occlusion in microporous SiO_2 modifications when varying the pore dimensionality. The problem when using host compounds with larger channel diameters, is the instability of the loaded materials, even when the samples were prepared and measured in closed surroundings excluding air. After opening the ampoules in which they were synthesized, they partially or completely lose the inserted iodine, as can be directly observed by the colour changes.

The results described in this section have been published [NB05].

4.1.2. Insertion experiments with selenium

For the sorption experiments with selenium, commercial black selenium was used. The brittle, opaque, dark red-brown to bluish-black lustrous solid quickly transforms to hexagonal selenium when heated at 180-190 °C. In the gaseous phase, predominantly small Se_2, Se_3 molecules are present, which condense to larger molecules upon cooling. The kind of selenium species present inside the channels of the zeosils will depend on the dimensionality of the host. We examined the behavior of selenium molecules as guest materials in insertion experiments using the zeosils SSZ-24, CIT-5 and UTD-1 as hosts. The loaded zeosils exhibit characteristic colours after insertion, SSZ-24 and CIT-5 zeosils show an intensively yellow colour, whereas UTD-1 displays a grey colour after loading. Figure 4.1.2.1. shows the colours of the three zeosils after insertion.

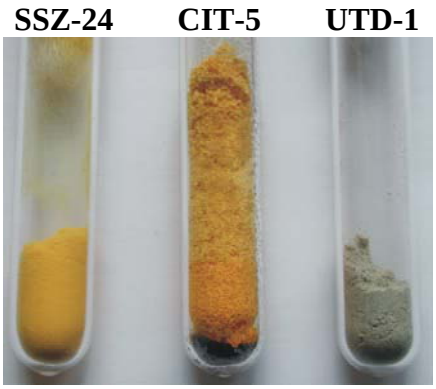

Fig. 4.1.2.1. Colour of SSZ-24, CIT-5 and UTD-1 after Se insertion experiments.

Powder X-ray diffraction patterns of the calcined and loaded zeosils were recorded at room temperature. X-ray diffraction analyses showed that the lattice parameters of CIT-5 are the same in the pure and the inserted state. However, the relative intensities of the reflections are different, an observation which can be interpreted by the presence of the strongly scattering selenium inside the zeosil channels (Fig. 4.1.2.2.). As in the case of iodine–inserted zeosils, the diffraction peaks in the low 2Θ region are suppressed upon insertion and this can be interpreted in terms of an increased electron density within the channels after filling. Also, an additional peak was detected in the powder pattern of Se–inserted CIT-5 at 14.67 °2Θ. The *d* spacing and the indexing of the experimental pattern are presented in appendix A17.

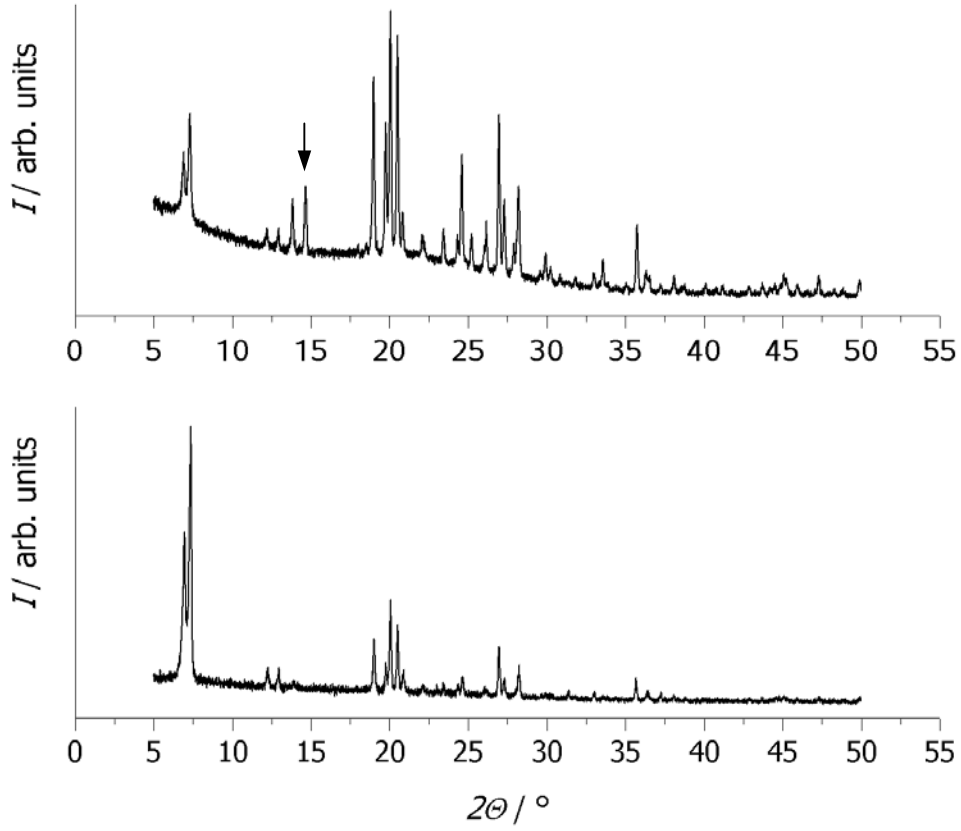

Fig. 4.1.2.2. Powder X-ray diffraction pattern of Se–CIT-5 (upper trace) in comparison to that of calcined CIT-5 (lower trace).

In case of selenium/SSZ-24, no differences in the peak intensities were observed in the X-ray diffraction pattern of the zeosil after insertion as compared to the calcined material (see Fig. 4.1.2.3). However, 13 new small reflections appeared, which did not belong to the structure of the zeosil; a large part of them could be indexed as belonging to four different selenium modifications, as shown in Table 4.1.2.4. (appendix A11).

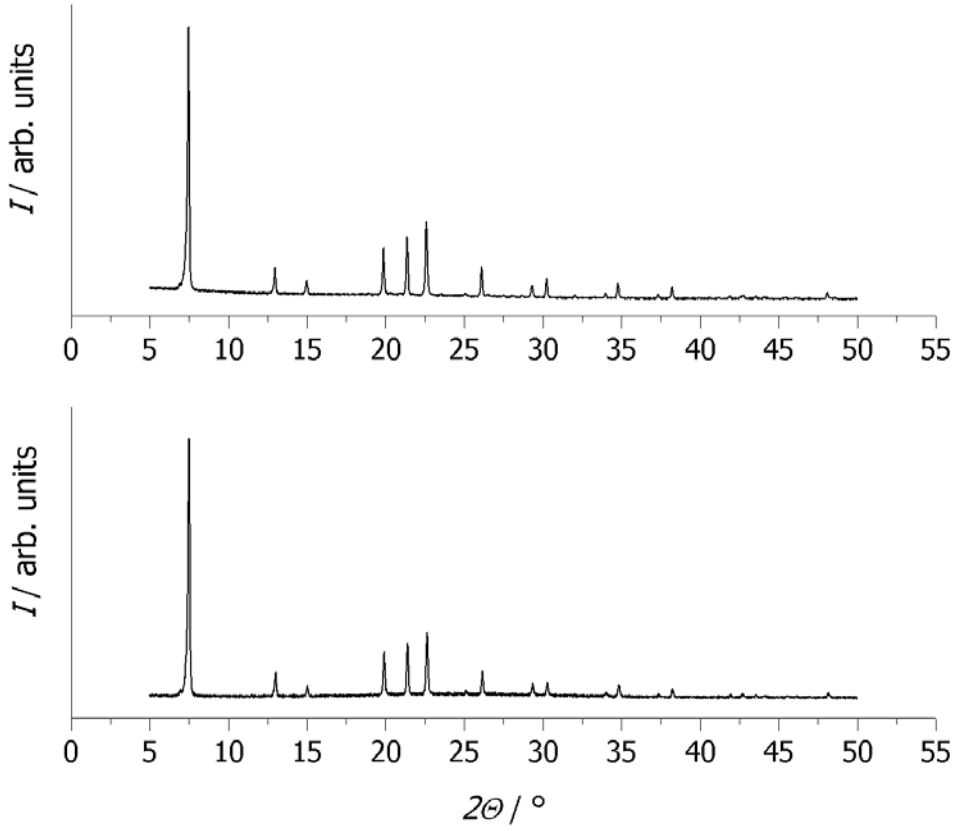

Fig. 4.1.2.3. Powder X-ray diffraction patterns of Se/SSZ-24 (upper trace) and calcined SSZ-24 (lower trace).

Thus, a mixture of SSZ-24 powder and selenium was obtained after the insertion experiment. One explanation for the presence of reflections due to bulk selenium could be that during sample preparation or during measurements, selenium became deinserted from a previously formed insertion compound, or secondly, that the new reflections are due to selenium externally adsorbed on the surface of the SSZ-24 crystals. This result is puzzling, as the Se insertion into isostructural aluminium phosphate $AlPO_4$-5 is possible. Thus, there are obviously no spatial restrictions [PK99].

Table 4.1.2.4. Comparison of the non-indexed peaks of Se/SSZ-24 and Se.

Se/SSZ-24 °2Θ	Se modification °2Θ	ascribed to Se modification:
18.956	10.097	monoclinic, β
20.275	20.442	monoclinic, β
20.948	21.015	monoclinic, α
23.530	23.523	monoclinic, β
26.555	-	no assignment possible
26.915	26.914	rhombic
27.494	-	no assignment possible
28.024	28.037	trigonal
28.686	-	no assignment possible
31.094	31.016	monoclinic, β
32.045	32.043	monoclinic, β
40.601	40.606	monoclinic, β
48.584	-	no assignment possible

The X-ray diffraction pattern of the grey Se–inserted UTD-1 sample does not show any differences when compared to the white, calcined zeosil. The two diffractograms are identical, no new peaks and no changes in the reflection intensities being observed (appendix A24). Fig. 4.1.2.5. shows the powder XRD of the Se/UTD-1 sample. The explanation can be that selenium either was not loaded into the channels of UTD-1, although these offer enough space for selenium to form even large rings or chains, or the guest was deinserted during cooling and condensed on the walls of the ampoule. The grey colour of the sample after insertion and the similarity between the two XRD patterns suggest that amorphous selenium was formed.

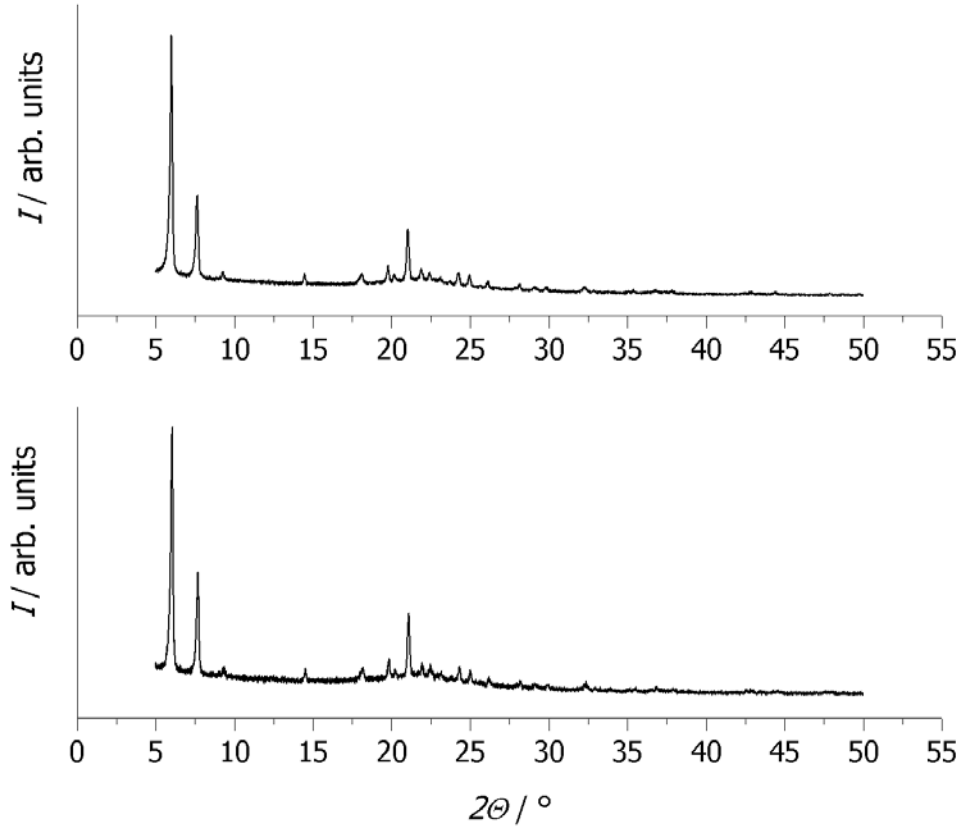

Fig. 4.1.2.5. X-ay diffraction patterns of calcined UTD-1 (lower trace) and Se/UTD-1 (upper trace).

Based on the results obtained by X-ray diffraction, only CIT-5 has formed an insertion compound with selenium and only this sample will be considered for further characterization experiments.

Thermogravimetric analysis was employed to determine the composition of the loaded material. The measurement was performed by heating the sample from room temperature to 900 °C, under helium atmosphere and revealed two weight losses (Fig. 4.1.2.6.). The first one, of 5.4 %, appeared at 400 °C and was followed by a second weight loss at 755 °C, of 2.5 %, giving a total weight loss of 7.9 %. This corresponds to a unit cell composition for the selenium loaded CIT-5 of 2.1 Se to 32 SiO_2. Based on the results obtained up to now, two explanations can be given for the appearance of these two weight losses. One can be that different selenium species are formed inside the channels of zeosil CIT-5 and the observed weight losses correspond to the deinsertion of these different molecules. The second explanation is that the weight loss at 420 °C corresponds to the evacuation of selenium from the channels of CIT-5, when a mixture of

liquid Se and powder zeosil is obtained. At ca. 680 °C, the boiling temperature of Se, selenium vaporizes and upon cooling, bulk selenium is formed.

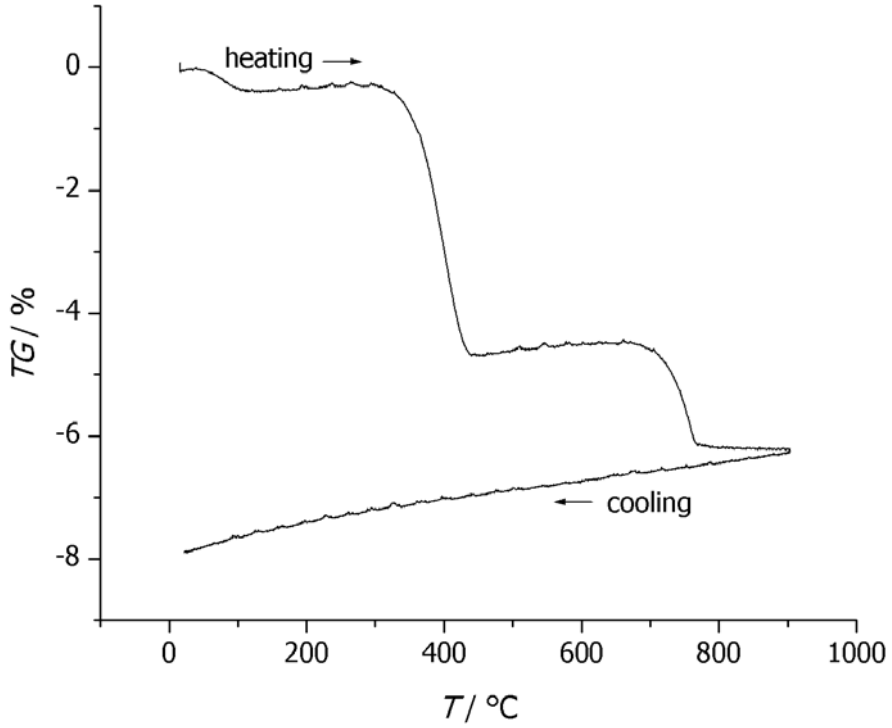

Fig. 4.1.2.6. Thermogravimetric results of Se-CIT-5;
hellium atmosphere; heating-rate: 4K/min.

For the elucidation of selenium species trapped in the micropores of CIT-5, Raman spectroscopy was used. Because the Raman activity of the zeosil framework is very weak compared to that of selenium species, Raman spectroscopy should be a well-suited method for the characterization of selenium–inserted zeosils. Unfortunately, this method, normally a powerful tool for the characterization of composite materials, cannot be applied for selenium–CIT-5 compound to its full extent using the apparatus available. The reason is the experimental limitation to a lower frequency limit of 150 cm^{-1} and the fact that many selenium species exhibit vibrational bands below this limit.

Trigonal selenium, rhombohedral selenium and the three kinds of monoclinic selenium are composed of polymeric chains, Se_6 ring and Se_8 ring molecules, respectively. Trigonal selenium exhibits Raman bands at 142.5, 233 and 237.5 cm^{-1} assigned to the low-frequency E mode (E' mode), the high frequency E mode (E" mode) and the A_1 mode, respectively [RR73] [MW69]. Rhombohedral selenium shows signals at 66, 71, 100, 129, 246 cm^{-1} assigned to the normal

modes of the Se_6 ring molecule and to the rotation of the Se_6 ring molecule [NI81]. Although selenium vapour consist of mixtures of selenium clusters in the range Se_2-Se_9 [SS84] only few experimental information is available on most of these species. Only Se_6 and Se_8 rings crystallize, allowing structural characterization of the building units [KG98]. No information regarding the Raman spectrum of cyclic Se_7 molecules could be found.

A typical Raman spectrum of a selenium–CIT-5 compound obtained with a laser power of 700 mW and 30 scans is shown in Figure 4.1.2.7. As usually observed for Raman spectra of microporous materials, especially SiO_2 modifications, a broad luminescence covers almost the whole spectral range of interest. However, one band at 266 together with one shoulder peaking at 255, and another band at 156 cm^{-1} are clearly detected. After longer measurement times, performed with a laser power of 700 mW and 500 scans, another band appeared in the spectrum of Se–CIT-5, at 236 cm^{-1} (Fig. 4.1.2.8.). Obviously, under stronger laser power and with longer measurement times, a deinsertion of selenium from the voids of the zeosil takes place. This can be seen in the Raman spectrum as a band in the region 230-240 cm^{-1} where crystalline trigonal selenium, the most stable allotrope, has its Raman scattering (237 cm^{-1}) [NI83]. Bands assignable to Se_2 (around 392 cm-1) or Se_3 (around 312 cm-1) vibrations were not detected [NA86] and hence the existence of those molecules within the channels of CIT-5 can be excluded. The fact that only few bands were detected in the Raman spectrum suggest that the occluded species have a high symmetry. For this reason, substantial amounts of Se_5 can be excluded; for this, more than four Raman active modes are to be expected [OJ96].

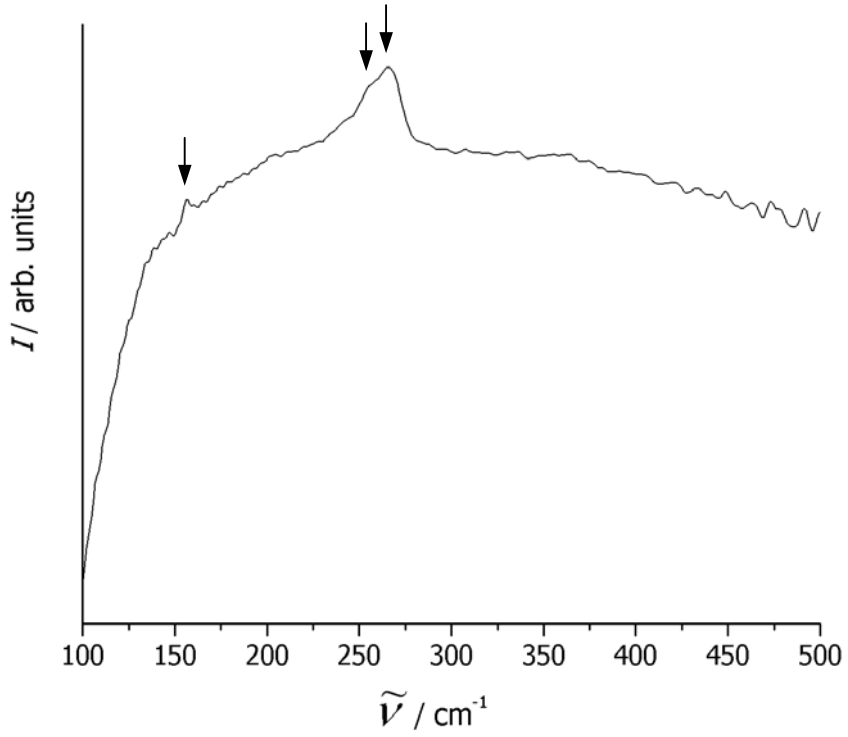

Fig. 4.1.2.7. Raman spectrum of Se-CIT-5; 700 mW laser power and 30 scans.

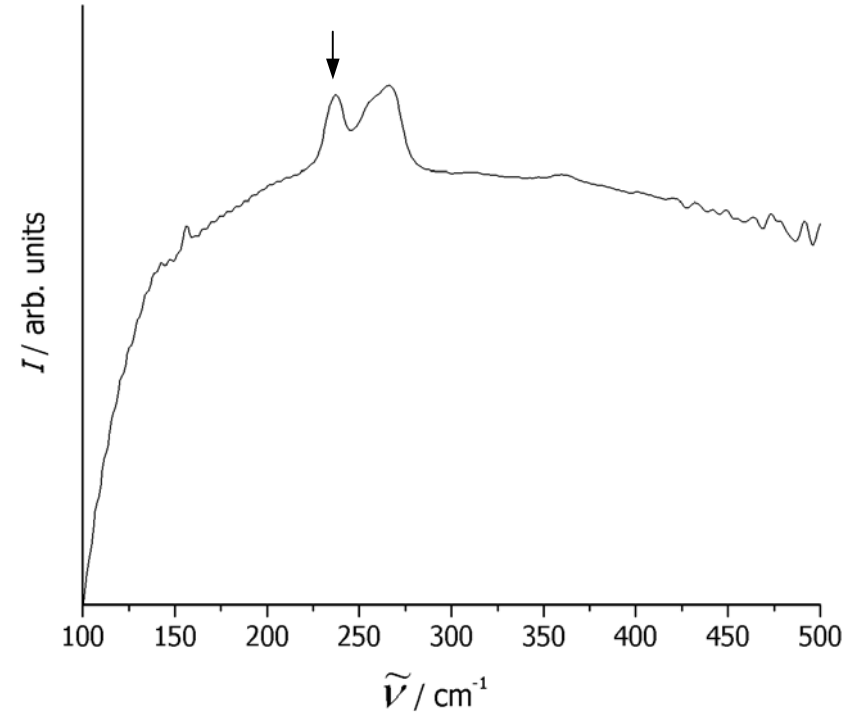

Fig. 4.1.2.8. Raman spectrum of Se-CIT-5; 700 mW laser power and 500 scans.

An overview of all Raman frequencies is given in Table 4.1.2.9.

Table. 4.1.2.9. Summary of experimental Raman frequencies and symmetry assignments for trigonal Se, Se_6 rings, Se_8 rings in α-monoclinic Se, Se–mordenite, Se–$AlPO_4$-5, Se–DDR and Se loaded in CIT-5.

trigonal Se [LM67]	Se_6 ring [NI81]	Se_8 ring in α-Se [LM67]	Se in mordenite [PK97]	Se in $AlPO_4$-5 [PK99]	Se in DDR [WI98]	Se in CIT-5
143; E mode	102; E_g	50; E_2	233-237	237	102	156
233; E mode	129; A_{1g}	84; E_2	256	259	133	255
237; A_1 mode	221; E_g	114; A_1	267	268	263	266
	247; A_{1g}	128; E_3	274		276	
		239; E_3				
		249; A_1				
		254; E_2				

Special attention should be paid to the frequency of the active A_1 symmetric stretching mode. According to the data of Richter et.al. [RR73] and to the calculations of Martin et.al. [ML76], the A_1 mode frequency strongly depends on the interchain interactions in trigonal Se [BP85]. This effect can be seen in the case of Se–mordenite [PK97], which exhibits a Raman band at 256 cm^{-1}, considerably higher than the A_1 mode frequency of trigonal Se (237 cm^{-1}). Also for Se–$AlPO_4$-5 composites, this band was detected at 259 cm^{-1} and was assigned to the symmetric bond-stretching mode of single Se chains. The other two Raman bands, observed at 237 and 268 in the spectrum of Se–$AlPO_4$-5 were attributed to the symmetric bond-stretching mode of Se chains incorporated into the channels and to the Se_8 rings, respectively [PK99]. The band at ca. 233-237 cm^{-1} observed in the case of Se inserted into mordenite is due to the superposition of symmetric and antisymmetric bond-stretching modes of bulk trigonal selenium on the surface of the crystals. The other band, at 274 cm^{-1}, was assigned to Se_6 rings. The Raman bands of bulk and zeolite encapsulated Se_6 and Se_8 are significantly displaced when compared to the calculated values of the isolated molecules [KG98] [WF99b]. This is due to interactions between clusters in the bulk. G. Wirnsberger et.al. [WF99b] found that selenium was inserted into the voids of DDR-composite as Se_6 rings, giving four bands in the Raman spectrum at 276,

263, 133 and 102 cm^{-1}. For selenium loaded in CIT-5, two bands were detected in the region 250-270 cm^{-1}, at 255 and 266 cm^{-1}, respectively (Table 4.1.2.9.). Based on the results presented above, we can assign the band at 255 cm^{-1} to the vibrations of inserted Se chains and the one at 266 cm^{-1} to inserted Se_8 rings. No assignment for the band at 155 cm^{-1} could be found.

These experimental results support the idea that selenium species occluded into the channels of CIT-5 are Se_8 rings and Se chains. The small Se_2 or Se_3 molecules, which are present in the gas phase at that insertion temperature, penetrate into the channels of the zeosil, where they become stabilized as chains and Se_8 rings.

This result explains also the appearance of two weight losses in the thermogravimetric measurements. They correspond to the deinsertion from the channels of CIT-5 of the two different selenium species. Based on these findings, the other explanation for the two-step weight-loss, namely the formation of liquid selenium and its boiling, is probably not correct.

4.1.3. Insertion compounds of mercury(II) halides

In comparison to iodine or selenium insertion compounds into large and extra-large pore zeosils, mercury(II) bromide loaded materials were colourless, so no qualitative information can be obtained in this way. The powder X-ray diffraction patterns of the zeosils after insertion are shown in Figs. 4.1.3.2., .4.1.3.3., 4.1.3.4. and 4.1.3.5. together with the respective calcined zeosils. The XRD pattern of solid $HgBr_2$ is given as comparison in Fig. 4.1.3.1.

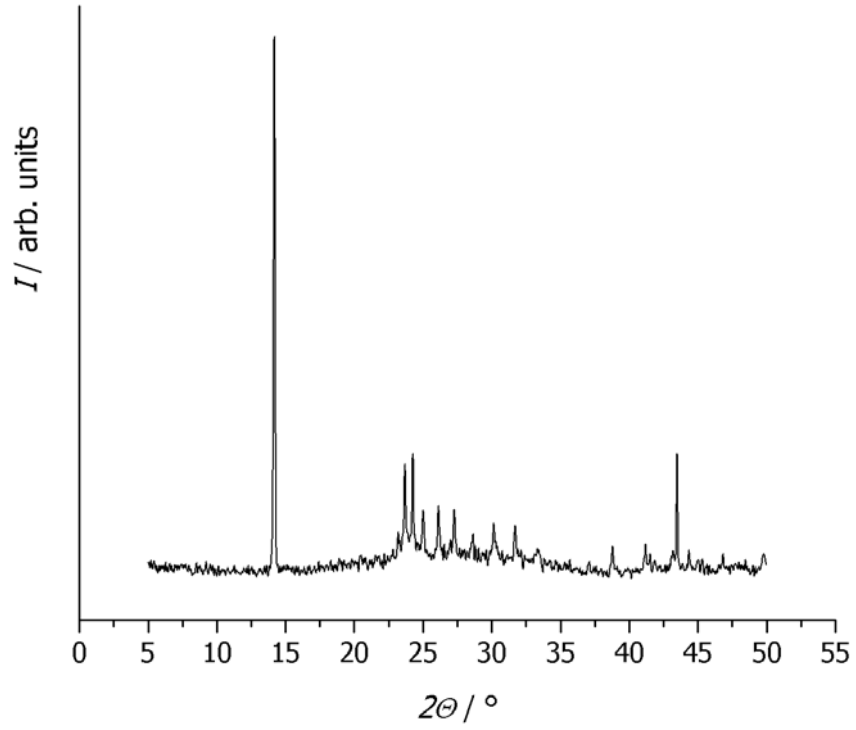

Fig. 4.1.3.1. X-ray powder pattern of solid mercury(II) bromide (experimental).

For all $HgBr_2$–zeosils strong differences in the reflection intensities of the loaded samples were observed when compared to the calcined zeosils (Fig. 4.1.3.2., 4.1.3.3., 4.1.3.4 and 4.1.3.5).

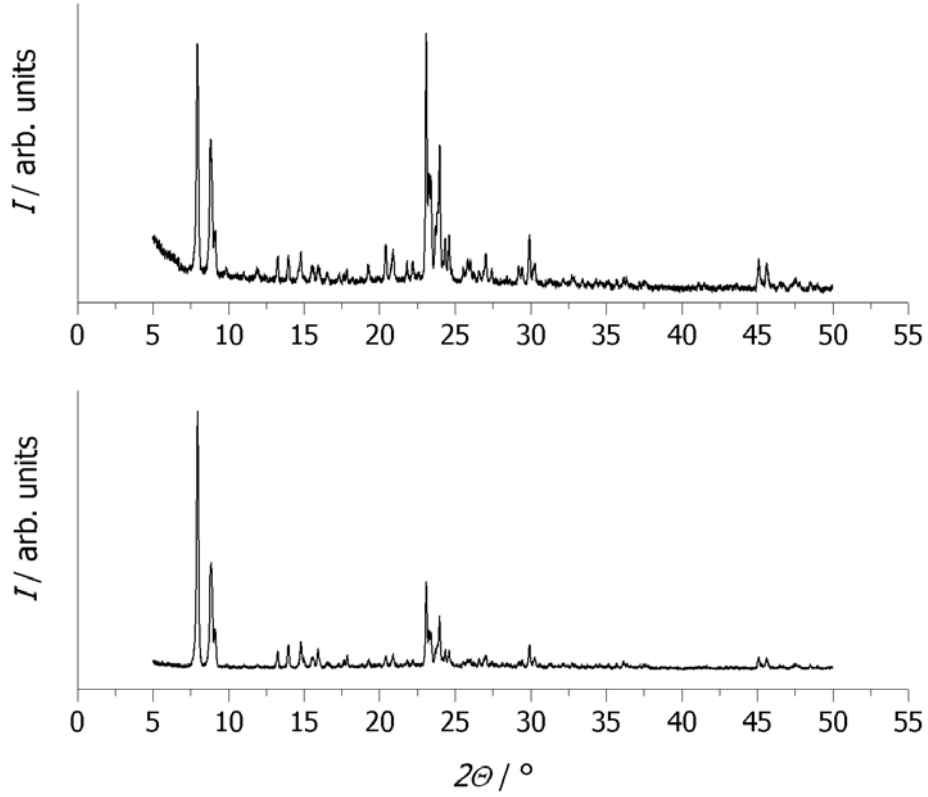

Fig. 4.1.3.2. X-ray powder patterns of calcined Silicalite-1 (lower trace) and $HgBr_2$–Silicalite-1 (upper trace).

In case of $HgBr_2$–SSZ-24, some new peaks appeared after loading which could not be indexed as belonging to the zeosil structure (see appendix A12), but had to be attributed to bulk $HgBr_2$ (see Fig. 4.1.3.1. and appendix A27). This sample thus consists of a mixture of $HgBr_2$–SSZ-24 and bulk mercury(II) bromide, either externally adsorbed on the surface of the zeosil or having become deinserted during X-ray measurements.

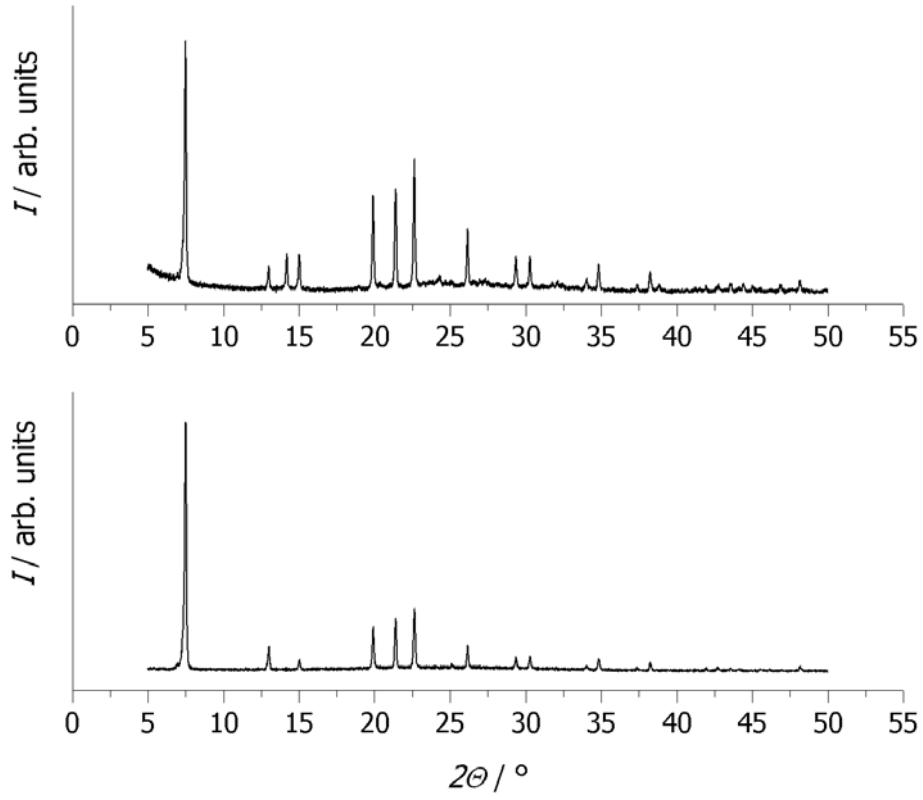

Fig. 4.1.3.3. X-ray powder pattern of calcined SSZ-24 (lower trace) and $HgBr_2$–SSZ-24 (upper trace).

A new peak was detected also in the X-ray powder pattern of $HgBr_2$–CIT-5 at 14.69 °2Θ (Fig. 4.1.3.4.). It could be indexed as belonging to the zeosil structure (see appendix A18). This supports the interpretation that a pure insertion compound was formed.

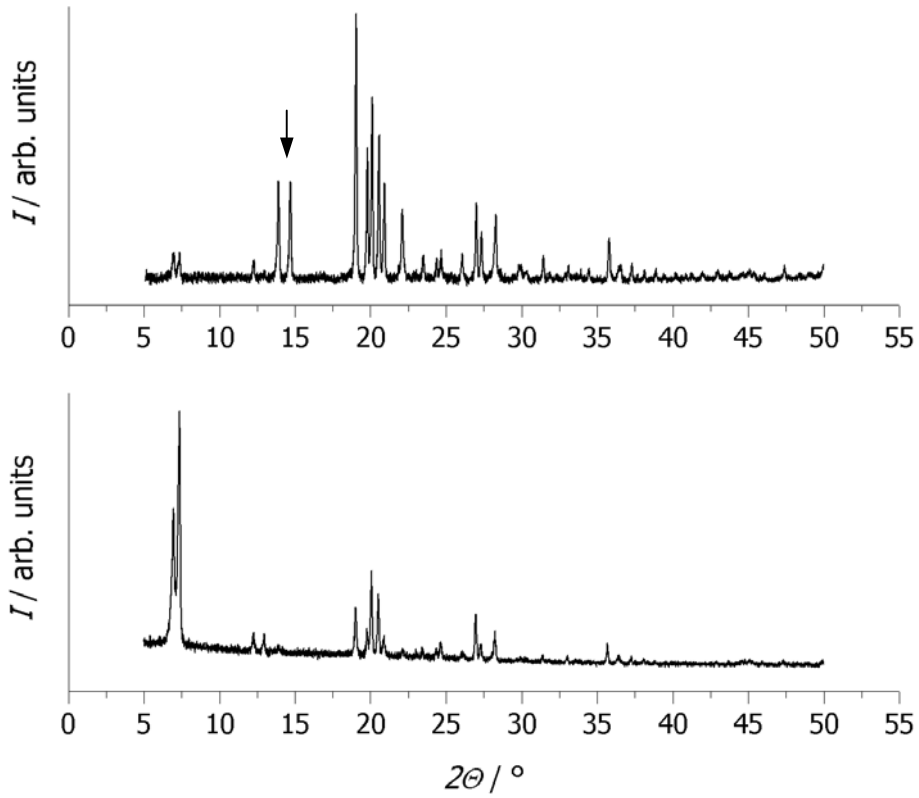

Fig. 4.1.3.4. X-ray powder pattern of calcined CIT-5 (lower trace) and $HgBr_2$–CIT-5 (upper trace).

For the UTD-1 insertion compound with $HgBr_2$, together with the differences observed in the reflection intensities after loading, three new peaks appeared at 12.14, 12.47 and 15.40 °2Θ (Fig. 4.1.3.5.). Again these could be indexed as belonging to the structure of the zeosil (appendix A25).

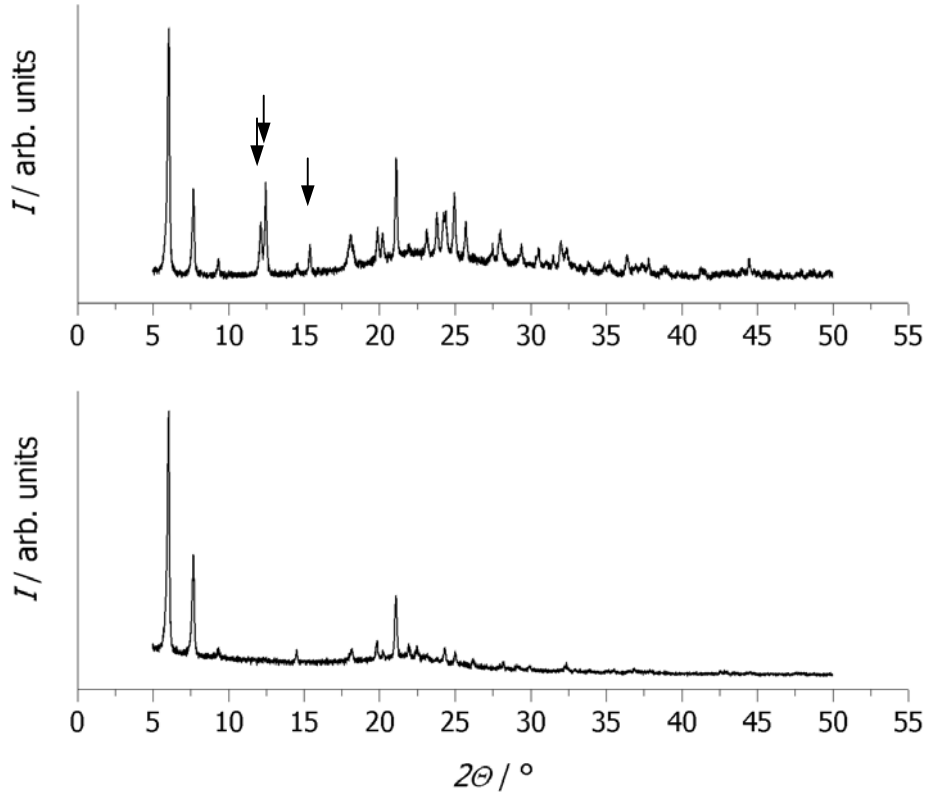

Fig. 4.1.3.5. X-ray powder pattern of calcined UTD-1 (lower trace) and $HgBr_2$–UTD-1 (upper trace).

As in the case of other insertion compounds presented here, some observations regarding the host-guest interactions can be drawn from the XRD experiments. The as-synthesized zeosil has a monoclinic structure, which changes to orthorhombic after calcination. Upon insertion of mercury(II) bromide, the material again retains the orthorhombic symmetry. Host-guest interactions are thus obviously weak.

In case of $HgBr_2$/ITQ-4, no additional peaks were observed in the X-ray diffraction pattern of the zeosil after insertion (not shown).

For further characterization of $HgBr_2$–zeosil compounds, we turn to spectroscopic investigations, since they probe the local state of the occluded guest molecules and allow conclusions about host-guest and guest-guest interactions.

The UV-vis spectra of $HgBr_2$–composites are characterized by strong absorptions observed in the spectral region down to 200 nm (Table 4.1.3.8.). This correspond to the electronic transition from the $^1\Sigma_g^+$ ground state to the $1\Pi_u$ state ($4\sigma_g \leftarrow 1\pi_u$) [WA80]. UV-vis spectra of mercury(II) insertion compounds in large-pore zeosils are shown in Fig. 4.1.3.7. in comparison to that of an insertion compound of a medium-pore zeosil (Silicalite-1). The UV-vis spectra of solid $HgBr_2$ is given as comparison (Fig. 4.1.3.6.).

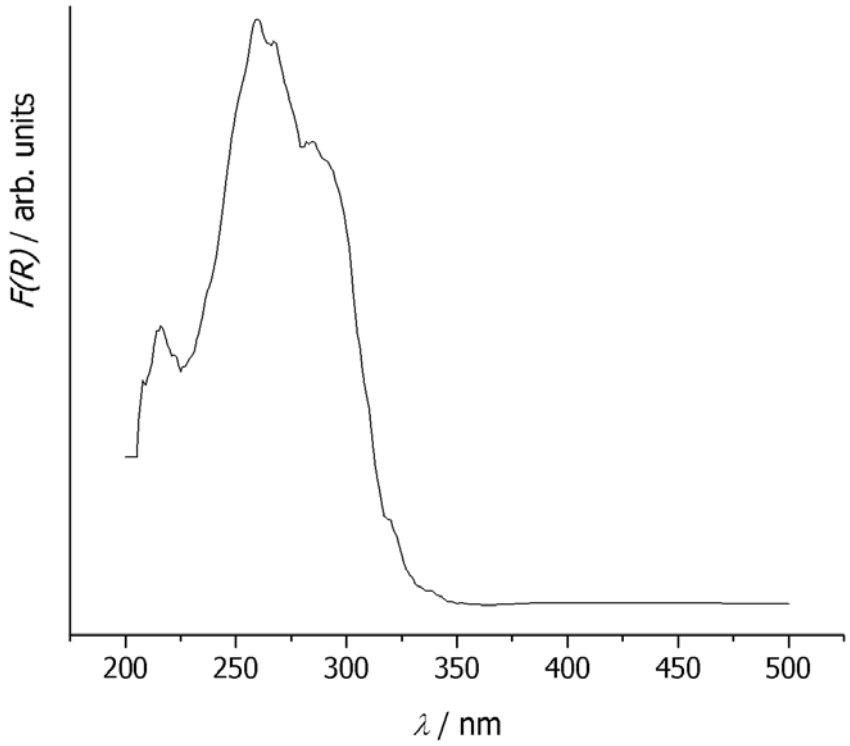

Fig. 4.1.3.6. UV-vis spectra (as Kubelka-Munk function) of solid $HgBr_2$.

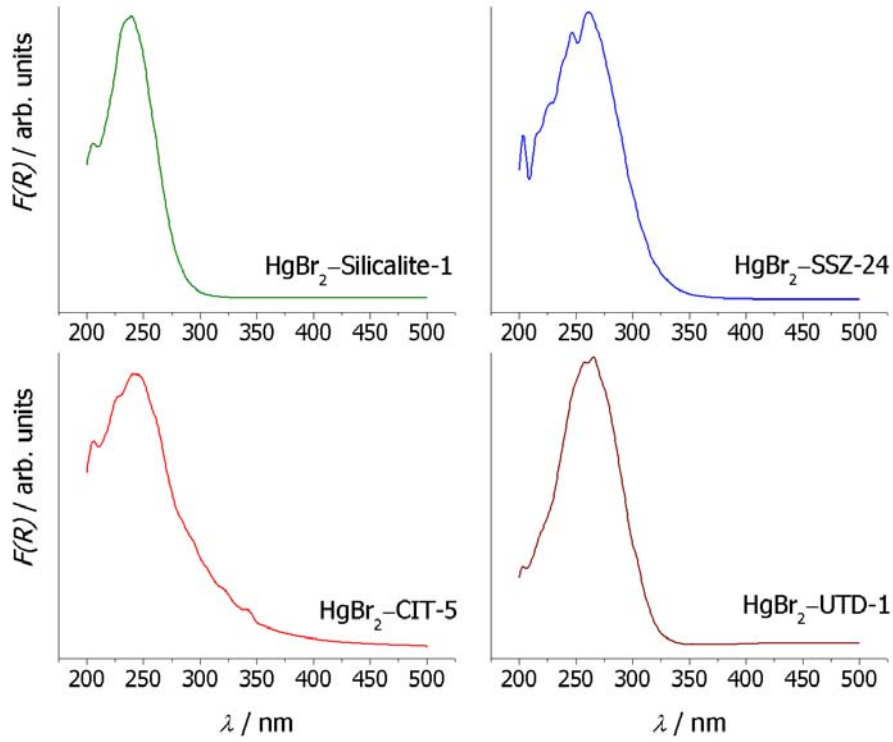

Fig. 4.1.3.7. UV-vis spectra (as Kubelka-Munk functions) of $HgBr_2$ insertion compounds of Silicalite-1, SSZ-24, CIT-5 and UTD-1.

Table 4.1.3.8. Electronic transitions of $HgBr_2$ and $HgBr_2$–insertion compounds (in nm).

$HgBr_2$ gaseous [TD72]	$HgBr_2$ in solvents [GA79]	$HgBr_2$ solid	$HgBr_2$– Silicalite-1	$HgBr_2$– SSZ-24	$HgBr_2$– CIT-5	$HgBr_2$– UTD-1
229.8	237-240	259	239	261	244	264

For $HgBr_2$–Silicalite-1 composite, it is known that the molecules are isolated, residing in the cross-sections of the pore system [WI98] [WP02]. The peak maximum of the band in the UV-vis spectrum is similar to the one obtained for mercury bromide in non-interacting solvents. In case of $HgBr_2$–CIT-5, the spectra resembles that of $HgBr_2$ in weakly interacting solvents, but the small shift of the absorption band to a higher wavelength indicates increased interactions between the guest molecules, comparative to the ones present in the liquid phase. In case of $HgBr_2$–SSZ-24 and $HgBr_2$–UTD-1, the bands appear at higher wavelengths, indicating possible interactions between the occluded $HgBr_2$ molecules, similar to those observed for the solid

halide (259 nm). This is probably due to the desorption of $HgBr_2$ from the zeosil channels. For $HgBr_2$–UTD-1 the guest molecules were located inside the voids of the zeosil immediately after insertion, as shown by the powder X-ray diffraction pattern. But exposed to air and under the radiation of the spectrometer, the inserted samples lost the $HgBr_2$ from the pores, resulting in the appearance of bands characteristic for bulk halide in the UV-vis spectrum. Also in the case of $HgBr_2$–SSZ-24, immediately after insertion some bulk halide could be already observed in the X-ray diffraction pattern, but other guest molecules were still located inside the voids of the zeosil (as shown by the differences in the reflection intensities of the loaded sample when compared to the calcined zeosil). The absence of bands in the region 230-240 nm from the UV-vis spectrum, where gaseous and liquid bromide exhibit their absorption bands and the only band observed at 261 nm, where bulk halide has its absorption, reflects the total desorption of the guest molecules from the voids of the host material during the UV-vis measurements.

Whereas UV-vis probes the energy difference between the electronic ground state and the excited states, Raman spectroscopy is sensitive to changes in the vibrational spacing within the ground state. Since the intermolecular interactions between the inserted halide molecules cause a weakening of the intramolecular bonds, a shift to lower frequencies is expected when interactions are present, as compared to the gas phase.
Upon condensation or dilution a shift to lower frequencies can be noticed in the Raman spectra (Table 4.1.3.9.). This reflects intermolecular interactions between the $HgBr_2$ molecules in the solid and in the liquid phase or when dissolved in various solvents.

Table. 4.1.3.9. Raman frequencies (in cm^{-1}) of solid, liquid and gaseous $HgBr_2$ [VP94] and of $HgBr_2$ molecules in various solvents [PS87].

$HgBr_2$ solid	$HgBr_2$ liquid	$HgBr_2$ gas	$HgBr_2$ in benzene	$HgBr_2$ in furan	$HgBr_2$ in 1,4-dioxane
187	197	220	213	212	204

Figs. 4.1.3.10. and 4.1.3.11. show the typical Raman spectra of solid $HgBr_2$ (experimentally measured) and of mercury(II) bromide occluded in the voids (channels) of the large pore zeosils SSZ-24 and UTD-1, in comparison to the one of a medium pore zeosil, Silicalite-1.
As in the case of all other insertion compounds presented up to now, no bands due to the SiO_2 framework and no peaks characteristic for other mercury halide species, e.g. Hg_2Br_2 were

detected. For $HgBr_2$ loaded into Silicalite-1, the Raman frequency is only slightly shifted (218 cm^{-1}) in comparison to the vapour phase value (220 cm^{-1}). HgB_2–SSZ-24 gives a Raman band in the region 186 cm^{-1}, which corresponds to solid $HgBr_2$, and a very weak signal at 205 cm^{-1}, similar to the one obtained for $HgBr_2$ solved in 1,4-dioxane. These findings confirm once again that the sample is a mixture of powder SSZ-24 and bulk mercury(II) bromide. For mercury(II) bromide in UTD-1, the frequencies of the Raman bands are found at 193 cm^{-1}, similar to the one observed for the liquid halide, describing increased interactions between the occluded molecules, and another band at 218 cm^{-1}, showing an unperturbed state of the mercury halide molecules. Despite serious attempts, spectra from the $HgBr_2$–CIT-5 compound could not be obtained. This is possibly due to very small amounts of organic residues formed during calcination, which have a strong fluorescence and obscure the proper Raman spectra.

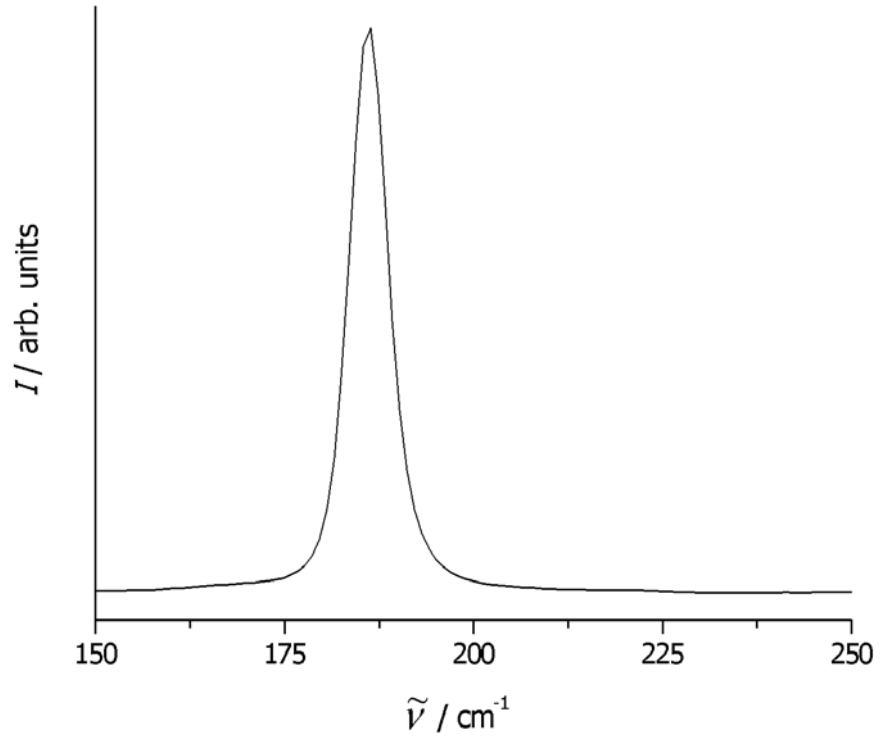

Fig. 4.1.3.10. Raman spectra of solid $HgBr_2$.

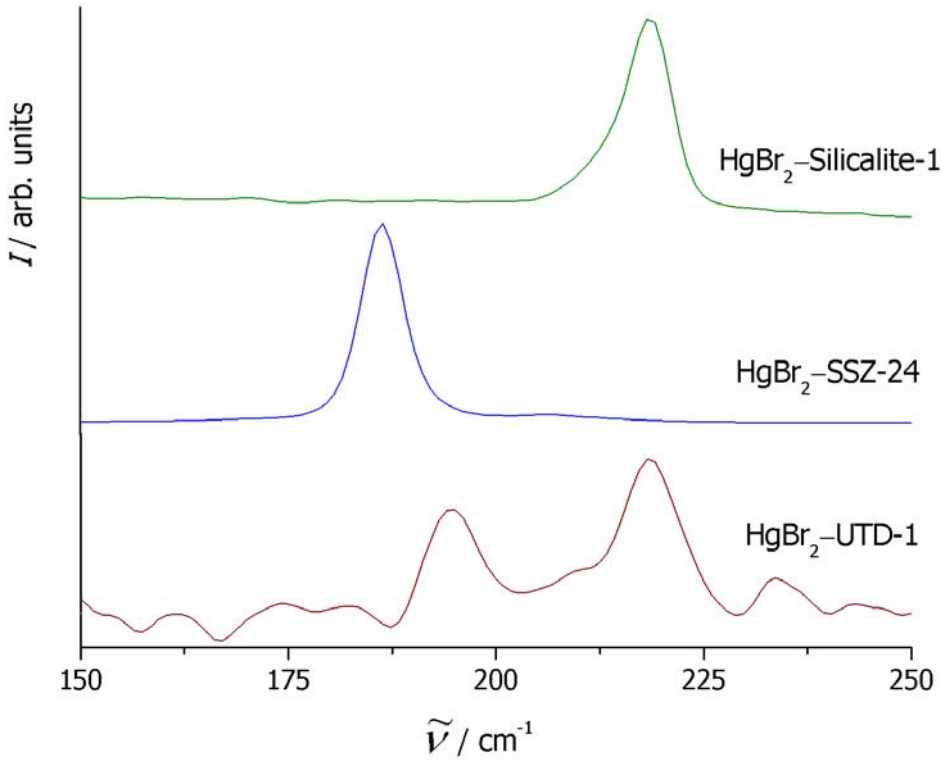

Fig. 4.1.3.11. Raman spectra of mercury(II) bromide–inserted zeosils.

To summarize, the results presented in this chapter prove the successful incorporation of $HgBr_2$ molecules into the voids of the large and extra-large pore zeosils SSZ-24, CIT-5 and UTD-1. Their UV-vis and Raman spectra exhibit differences in comparison to the ones obtained for the medium-pore zeosils, indicating possible interactions between the $HgBr_2$ molecules, for example in $HgBr_2$–UTD-1. However, the compounds are considerably less stable than those obtained on the basis of medium pore zeosils [WP02], possible due to reduced host-guest interactions, and desorption can take place immediately when exposed to air. This instability hampers the spectroscopic characterization of the compounds under study.

No stable insertion compounds of $HgCl_2$ or HgI_2 could be obtained when using larger-pore materials as hosts.

4.1.4. Gold(III) chloride insertion compounds

Based on the experiences with mercury(II) halides insertion compounds in zeosils, the next step was to try to synthesize compounds using larger molecules as guests, e.g. Au_2Cl_6. It is expected that only the extra-large pore zeosils are able to give access for the Au_2Cl_6 molecules to enter their channels; on the other hand, with larger guest molecules the host-guest contacts will possibly improve, leading to more stable insertion compounds. The present work shows that gold(III) chloride can be incorporated into extra-large pore zeosils. We loaded the activated zeosils CIT-5 and UTD-1 by sublimation of $AuCl_3$ in a closed ampoule. After the insertion experiments, the loaded zeosils exhibit characteristic colours, as shown in Figure 4.1.4.1. All inserted materials have a yellow-orange colour.

Fig. 4.1.4.1. Colours of Au_2Cl_6–CIT-5 (left) and Au_2Cl_6–UTD-1 (right) insertion compounds.

For the insertion experiments where no chlorine was added to the ampoules in order to avoid the decomposition of Au_2Cl_6, the different colours obtained at one end of the ampoule indicate the formation of different gold compounds as decomposition products of the gold(III) chloride (Fig. 4.1.4.2.). When zeolite A was inserted by gold(III) chloride in a closed ampoule [KC03], it was observed that, at the beginning of the loading procedure, a dark brown-red layer was deposited at the cooler part of the ampoule. As the temperature was increased, the layer vanished and a uniform thin light-yellow layer was deposited on the whole area of the ampoule but disappeared gradually as the loading reaction proceeded. After this, a lustrous gold layer was often observed for some time. The colour patterns indicated that these layers consisted of $AuCl_3$, AuCl and Au. Based on these observations, we can assign the different colours observed (on the walls of the ampoules in our loading experiments where no chlorine was added to the tubes): the red-brown colour is due to the presence of gold(III) chloride, whereas the yellow one is the result of AuCl

and Au formation. This means that some decomposition of gold(III) chloride occurred during reaction.

Fig. 4.1.4.2. Insertion of UTD-1 with gold(III) chloride in the absence of chlorine.

To avoid the decomposition of gold(III) chloride, further insertion experiments were carried out in the presence of chlorine. We obtained insertion compounds of zeosils CIT-5 and UTD-1.
From the total weight loss observed in thermogravimetric experiments, we can determine the gold(III) chloride contents of the insertion compounds. The unit cell compositions are presented in Table 4.1.4.3. It should be mentioned that these values are well reproducible, even when slight alterations are used in the insertion procedure.

Table 4.1.4.3. Unit cell composition of zeosils after insertion with Au_2Cl_6.

zeosil	unit cell composition $Au_2Cl_6 : SiO_2$
CIT-5	0.24 Au_2Cl_6 : 32 SiO_2
UTD-1	0.61 Au_2Cl_6 : 64 SiO_2

With UTD-1 as host material, higher loadings are obtained. The large channels (7.5 x 10 Å) of this zeosil offer enough space for the gold(III) chloride molecules.
The theoretical maximal loading of zeosils CIT-5 and UTD-1 with gold(III) chloride, expressed as the maximum number of Au_2Cl_6 molecules per channel per unit cell, can be calculated i.e. by dividing the length of the channel (8.427 Å for UTD-1 and 5.022 Å for CIT-5, respectively) by

the length of a Au_2Cl_6 molecule (10.22 Å). So, there will be ca. 0.82 molecules per channel per unit cell of UTD-1 and 0.49 Au_2Cl_6 molecules per channel per unit cell of CIT-5. This means 1.65 and 0.98 Au_2Cl_6 molecules per unit cell UTD-1 and CIT-5, respectively, because both zeosils contain two channels in the unit cell (Table 4.1.4.4.).

Table 4.1.4.4. Theoretical maximal loading of zeosils CIT-5 and UTD-1 with gold(III) chloride.

zeosil	unit cell composition	channel length / Å	Au_2Cl_6 length / Å	Au_2Cl_6 per channel per unit cell	Au_2Cl_6 molec. per unit cell
CIT-5	$Si_{32}O_{64}$	5.022	10.22	0.49	0.98
UTD-1	$Si_{64}O_{128}$	8.427	10.22	0.82	1.65

The TG curves for CIT-5 and UTD-1 inserted with Au_2Cl_6 are shown in Fig. 4.1.4.5. and 4.1.4.6., respectively. In both cases, the weight loss occurs in two steps, the first one at 210 to 230 °C and the second one at 290 to 310 °C. These temperatures correspond to the decomposition temperatures given for pure Au_2Cl_6 [CS65] [FB28] [SO56], as follows:

$$\text{210-230 °C:} \quad AuCl_3\,(s) \rightarrow AuCl\,(s) + Cl_2\,(g)$$

$$\text{290-310 °C:} \quad 2\,AuCl\,(s) \rightarrow 2\,Au\,(s) + Cl_2\,(g)$$

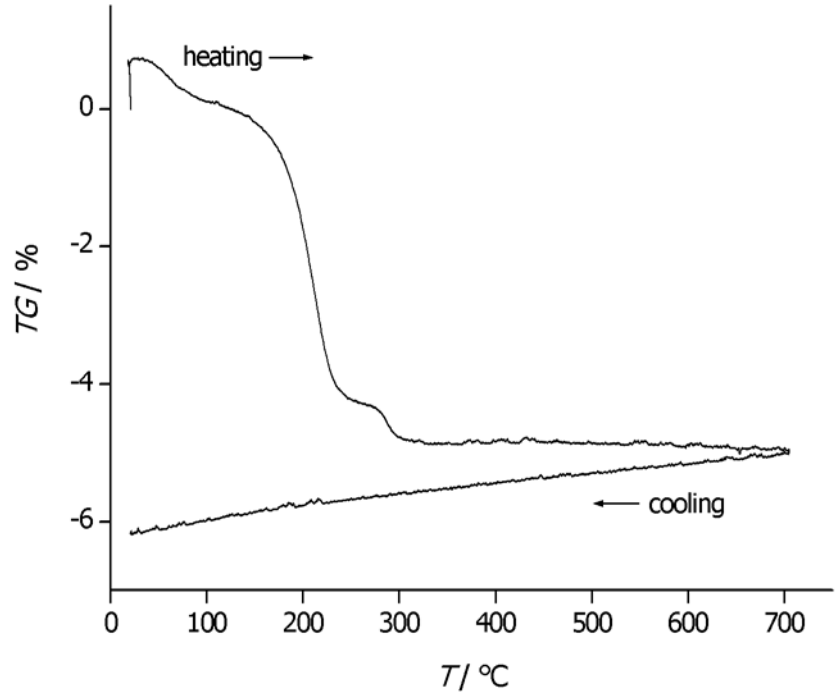

Fig. 4.1.4.5. Thermogravimetry of the Au_2Cl_6–CIT-5 insertion compound; helium atmosphere; heating-rate 4 K/min.

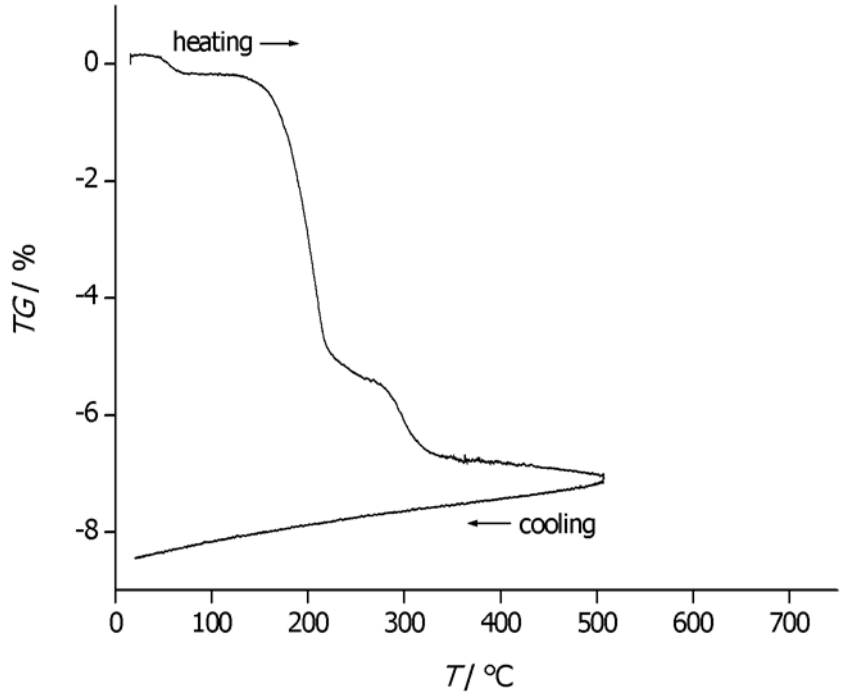

Fig. 4.1.4.6. Thermogravimetry of the Au_2Cl_6–UTD-1 insertion compound; helium atmosphere; heating-rate 4 K/min.

After the thermal treatment during the thermogravimetric measurements, the samples still had a light mauve colour, similar to that observed in case of gold-loaded zeolite A [KC03]. It was shown that very lowly loaded samples exhibit a mauve colour, and all gold-loaded zeolites change their colour to mauve when heated under vacuum. According to the authors, this colour is typical for gold clusters. We do not expect, however, that the clusters are situated in the pores of our materials.

When the insertion experiments were carried out without chlorine, the weight of the samples after insertion was superior to the one obtained when chlorine was used, but in this case a mixture of powder zeosil or partially loaded zeosil and different gold chloride species was probably obtained, as shown by the different colours in Fig. 4.1.4.2.

We now turn to the characterization of Au_2Cl_6–zeosil composites. Firstly, the samples were analyzed by X-ray powder diffraction. The patterns of the calcined and loaded zeosils are presented in Figs. 4.1.4.10. and 4.1.4.11. All XRD patterns of Au_2Cl_6–zeosils show that the loading of zeosils does not damage their structure. For comparison, the X-ray diffraction patterns of solid Au_2Cl_6 (Fig. 4.1.4.7.) and gold(III) chloride insertion compounds of Silicalite-1 and SSZ-24 (Figs. 4.1.4.8 and 4.1.4.9.) are shown. The smaller channels of these zeosils (5.1 x 5.5 Å and 5.3 x 5.6 Å for the 10 MR Silicalite-1; 7.3 x 7.3 Å in the case of SSZ-24) do not allow Au_2Cl_6 molecules to enter. Correspondingly, no insertion compounds based on these zeosils could be obtained and the XRD patterns of Au_2Cl_6/Silicalite-1 and Au_2Cl_6/SSZ-24 do not show any differences in the reflection intensities when compared to the calcined zeosils; they only show some new peaks that could be indexed as belonging to bulk gold(III) chloride. For comparison, a list of all reflections and peak indexing is shown in appendices A4, A13, A28, A29 and A30, corresponding to the Au_2Cl_6–Silicalite-1, Au_2Cl_6–SSZ-24, $AuCl_3$, AuCl and $HAuCl_4$, respectively.

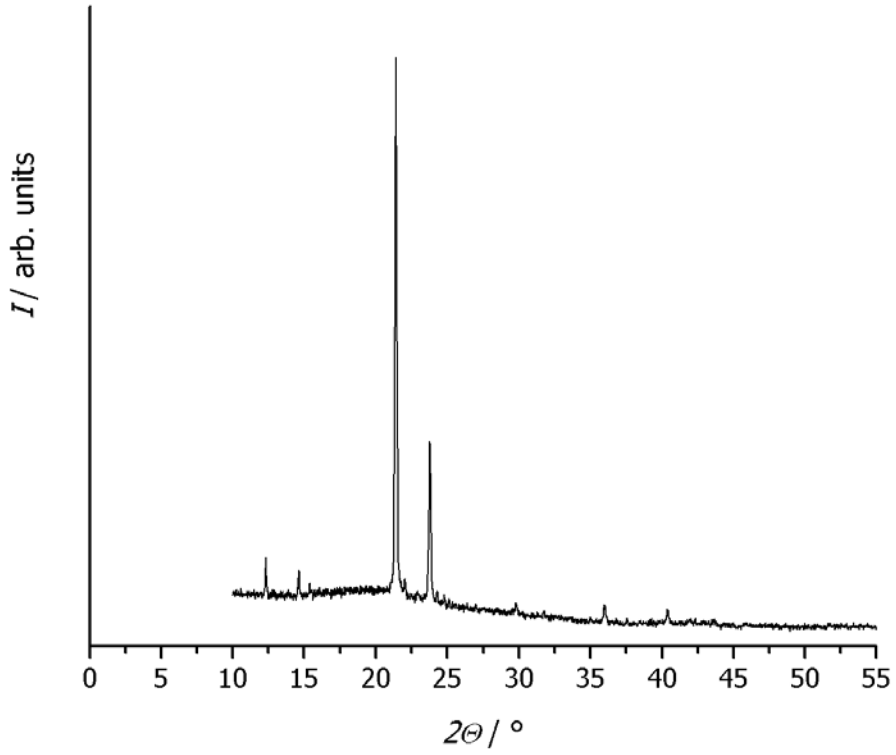

Fig. 4.1.4.7. X-ray diffraction pattern of Au_2Cl_6 solid.

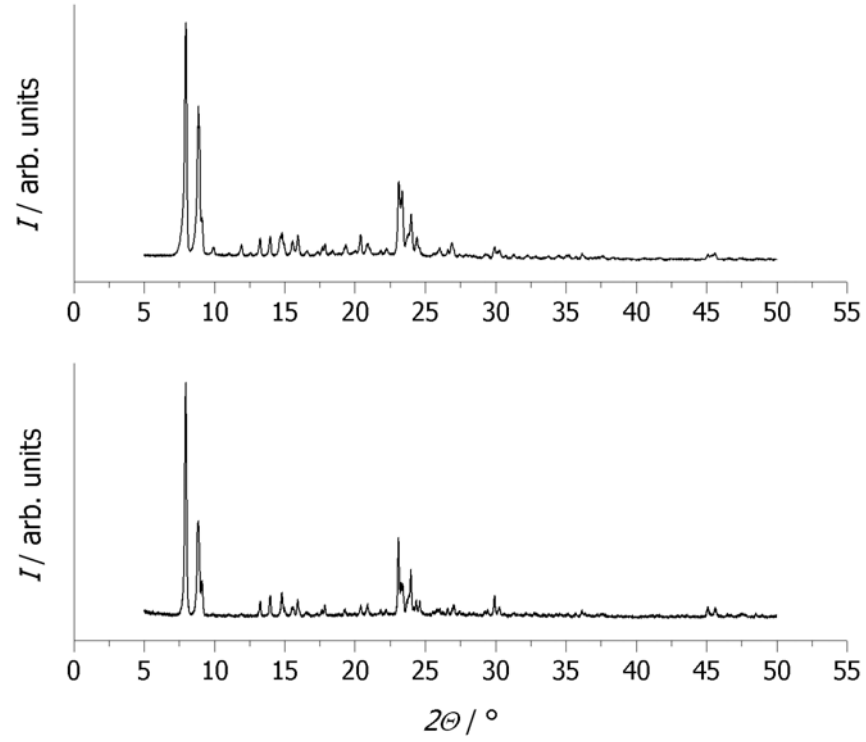

Fig. 4.1.4.8. Powder X-ray diffraction patterns of calcined Silicalite-1 (lower trace) and Au_2Cl_6/Silicalite-1 (upper trace).

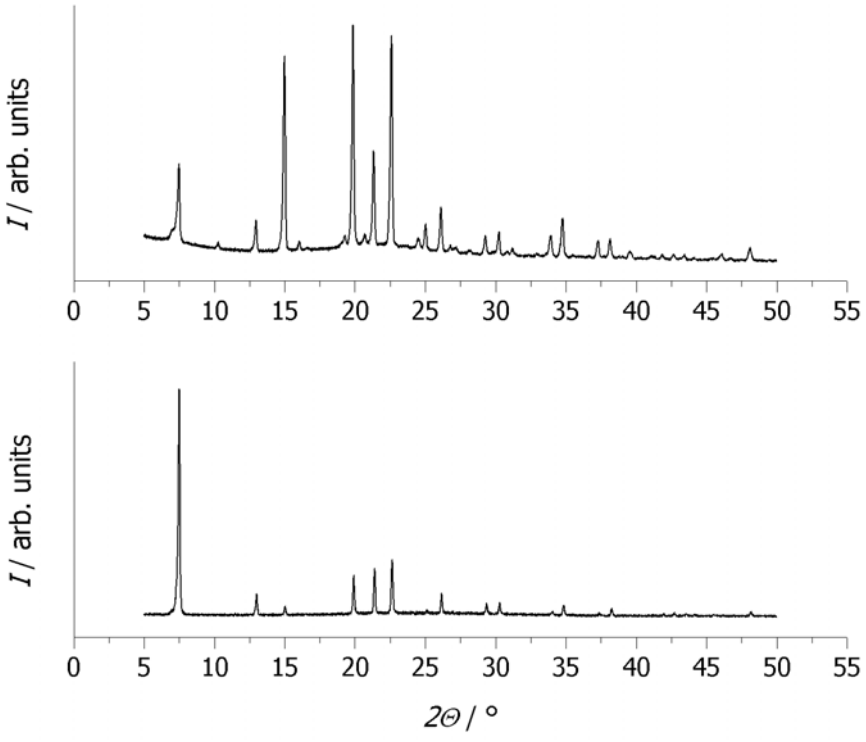

Fig. 4.1.4.9. Powder X-ray diffraction patterns of calcined SSZ-24 (lower trace) and Au_2Cl_6/SSZ-24 (upper trace).

On the other hand, in case of CIT-5 and UTD-1 insertion compounds, no Au_2Cl_6 phase was observed, but all loaded materials showed drastic changes in the reflection intensities. Also, new peaks could be observed in the XRD powder pattern of Au_2Cl_6–CIT-5 (Fig. 4.1.4.10.) and Au_2Cl_6–UTD-1 (Fig. 4.1.4.11.) and they were indexed as belonging to the structure of the respective zeosils (see appendices 19 and 26, respectively). This provides strong evidence that true insertion compounds have formed, and that, probably, Au_2Cl_6 molecules occupy well-defined positions with regard to the zeosil structure.

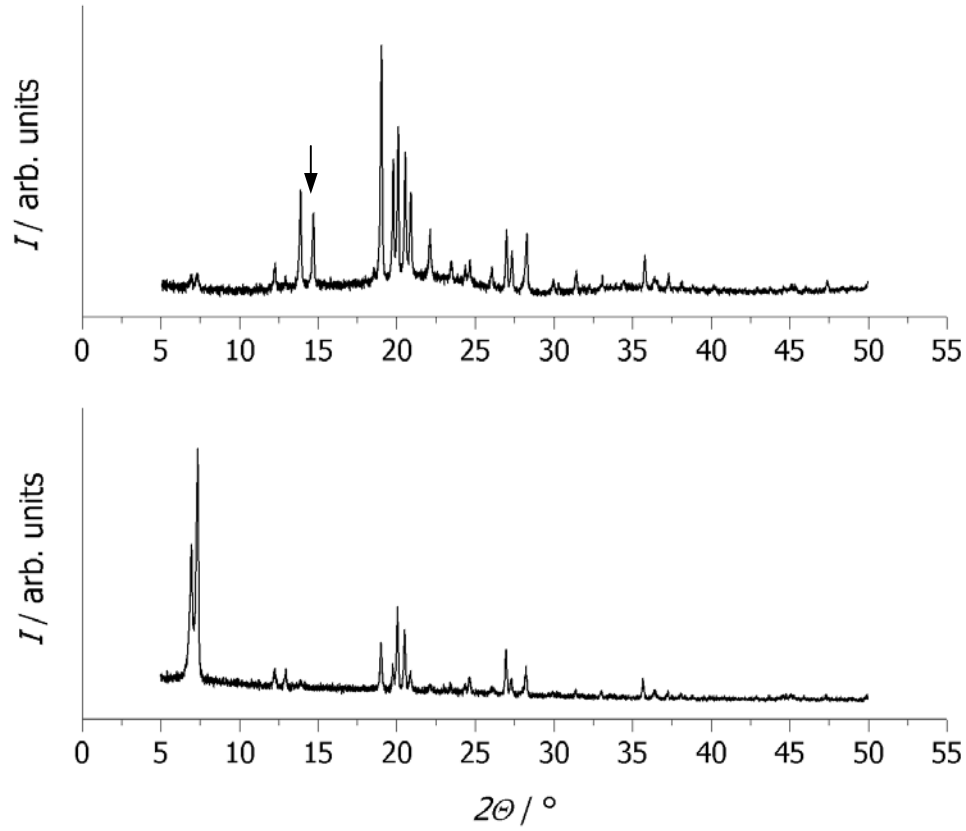

Fig. 4.1.4.10. Powder X-ray diffraction patterns of calcined CIT-5 (lower trace) and Au_2Cl_6–CIT-5 (upper trace).

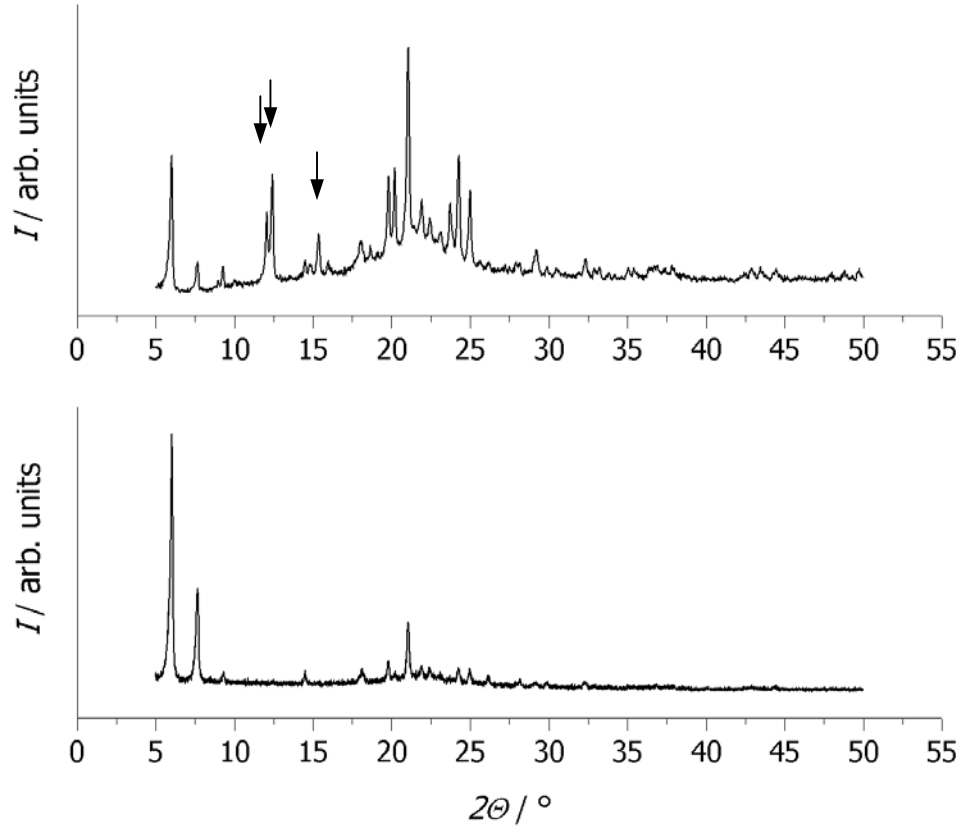

Fig. 4.1.4.11. Powder X-ray diffraction patterns of calcined UTD-1 (lower trace) and Au_2Cl_6–UTD-1 (upper trace).

The UV-vis absorption spectrum of dimeric gold(III) chloride in the gas phase was reported by D. S. Rustad et.al. [RG91]. In solid gold(III) chloride, planar Au_2Cl_6 molecular units are observed [CT58]. The spectrum of a solid gold(III) chloride film [SB78] shows four distinct peaks at 293 K: 230, 320, 358 and 438 nm, and three distinct peaks at 83 K: 230, 320 and 438 nm. Solid gold(III) chloride, experimentally measured in this work, showed two distinct bands in the UV-vis spectrum, at 230 and 320 nm, and a very weak band at around 430 nm (see Fig. 4.1.4.12.) In contrast, Au_2Cl_6 (g) has three distinct peaks, observed at 222, 244 and in the visible region at 460 nm. The first two have similar large molar absorptivities; the third one is much weaker. The presence of the two different absorption bands in the UV part of the spectrum can possibly be associated with the different electron-donating abilities of the bridging and terminal chlorine ligands. Mason and Grey have pointed out that the ligand-to-metal charge transfer transitions from the "bridging" ligands have lower energy than those from the terminal ligands [MG68].

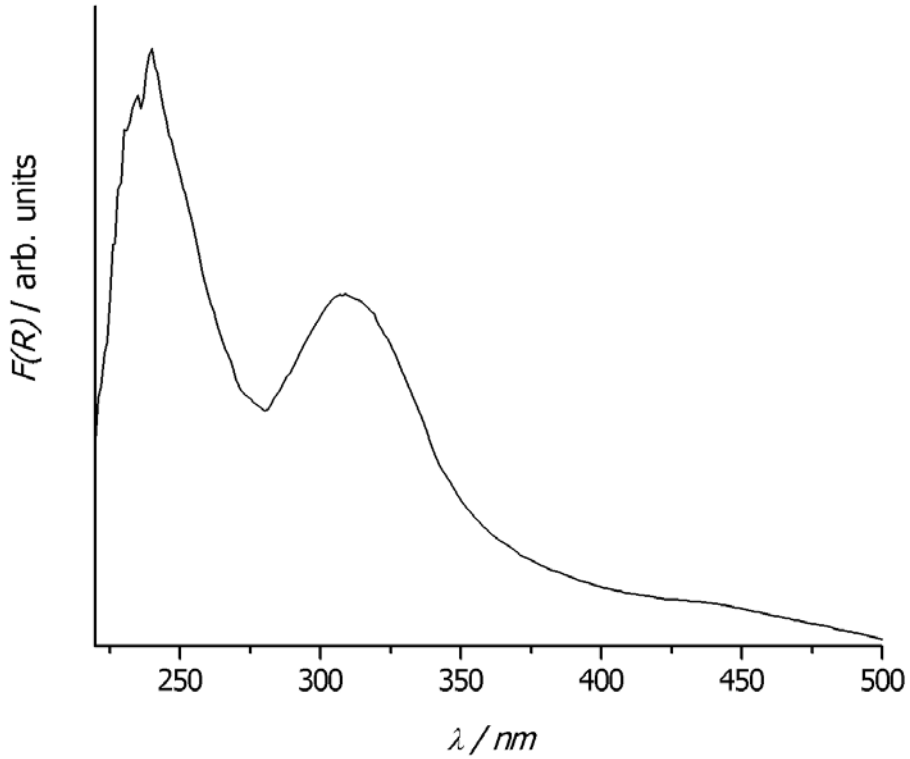

Fig. 4.1.4.12. UV-vis spectra of solid Au_2Cl_6 experimentally measured.

The UV-vis spectra of Au_2Cl_6–CIT-5 and Au_2Cl_6–UTD-1 insertion compounds obtained under chlorine atmosphere are shown in Fig. 4.1.4.13.

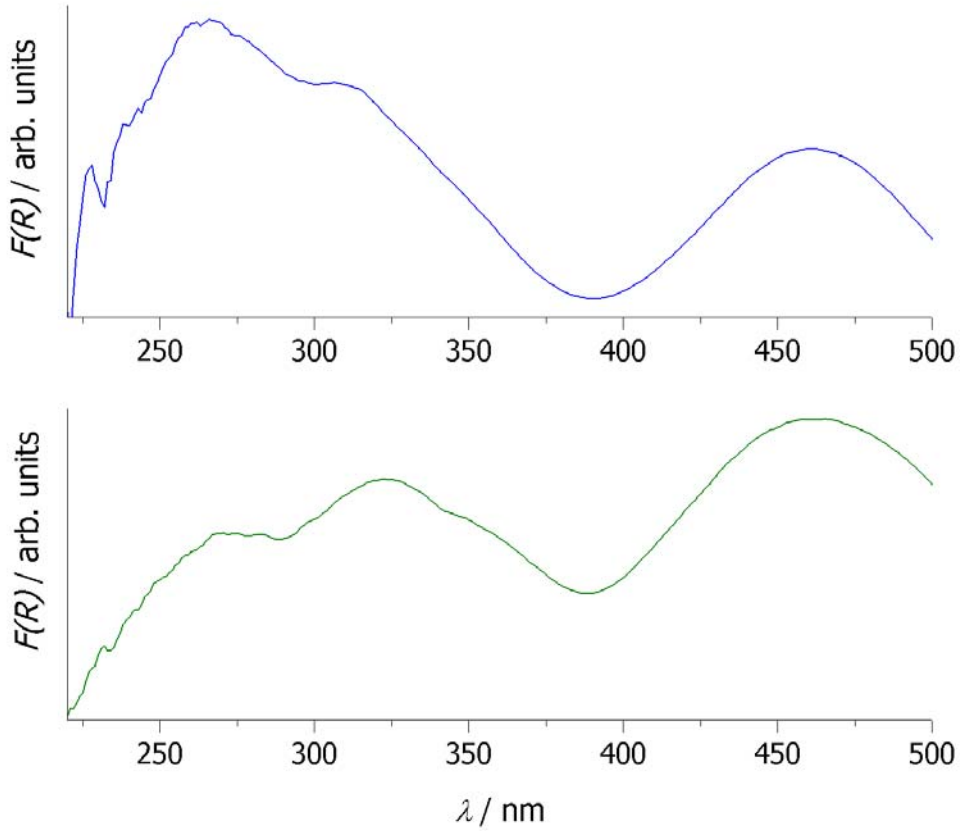

Fig. 4.1.4.13. UV-vis spectra of Au_2Cl_6 insertion compounds of CIT-5 (upper trace) and UTD-1 (lower trace).

In the region between 300 and 350 nm, the absorption spectra of the loaded zeosils show bands at ca 320 nm (Fig. 4.1.4.13.). This is an evidence that Au_2Cl_6 is present inside the channels of CIT-5 and UTD-1, respectively. The shift of the absorption bands of the loaded zeosils in the region 270 nm cannot be really explained. Chlorine gas gives a broad absorption band between 250 and 480 nm, with a maximum at 330 nm [SB64] [BN63] [GB33]. The presence of one absorption band at 460 nm in the UV-vis spectra of the loaded zeosils can be explained if gaseous chlorine used in the insertion experiments in order to avoid the decomposition of gold(III) chloride, became partially inserted in the large channels of CIT-5 and UTD-1, in between the Au_2Cl_6 molecules. The absence from the UV-vis spectrum of bands in the region 500-550 nm (not shown) means that no gold clusters have been formed inside the voids

(channels) of the zeosils. Band in this area are typical for the plasmon absorption of gold clusters [LS99] [KA00].

An overview of all UV-vis maxima of Au_2Cl_6 and Au_2Cl_6 insertion compounds in zeosils is given in Table 4.1.4.14.

Table. 4.1.4.14. Absorption band positions (in nm) in the UV/vis absorption spectra of solid and gaseous Au_2Cl_6 [GM92] [RG91] [SB78] and of Au_2Cl_6–CIT-5 and Au_2Cl_6–UTD-1 [this work].

Au_2Cl_6 (s)	Au_2Cl_6 (s) experim.	Au_2Cl_6 in diethylether	Au_2Cl_6 (g)	Au_2Cl_6–CIT-5 experim.	Au_2Cl_6–UTD-1 experim.
230	230		222	not measured	not measured
			244		
				268	270
320	320	~ 322		315	323
358				350 (sh)	350 (sh)
438	437		460	461	460

The Raman frequencies for Au_2Cl_6, as reported by R. Forneris et.al. [FH70], are presented in Table 4.1.4.16. They are believed to be accurate to ± 3 cm^{-1}. The values for gaseous Au_2Cl_6 are given for comparison. The Raman spectra of Au_2Cl_6–CIT-5 and Au_2Cl_6–UTD-1 insertion compounds obtained under chlorine atmosphere are shown in Fig. 4.1.4.15. Both of them look very similar to that of solid Au_2Cl_6.

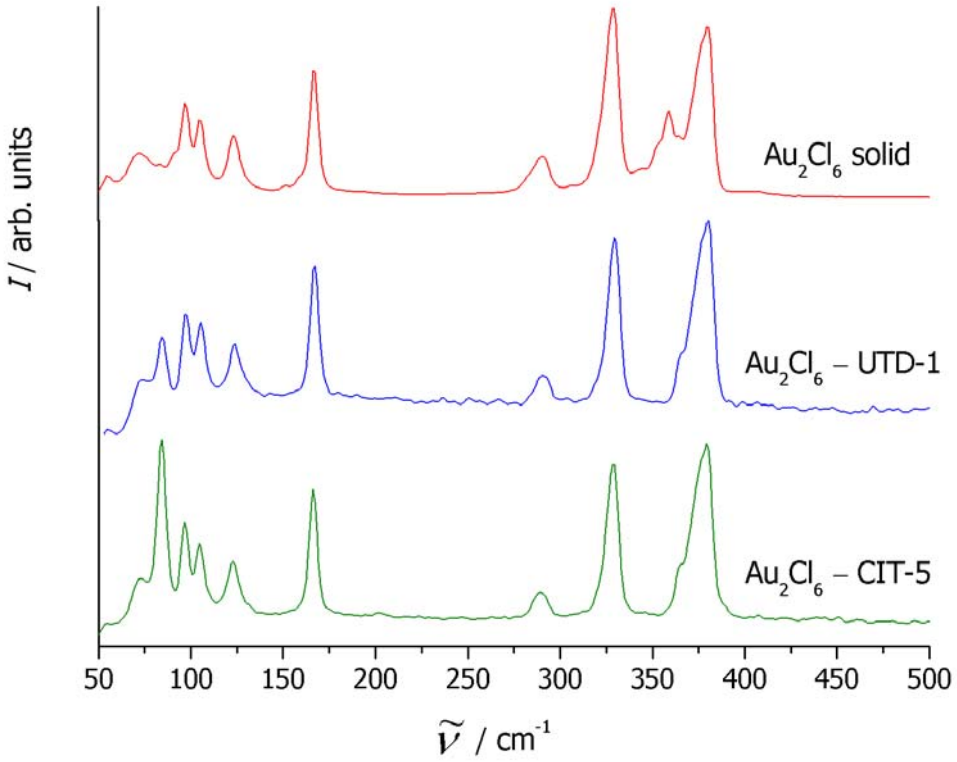

Fig. 4.1.4.15. Experimental Raman spectra of solid Au_2Cl_6 and gold(III) chloride inserted zeosils.

Table 4.1.4.16. Vibrational frequencies (in cm^{-1}) and assignments of vibrations of gold(III) chloride and Au_2Cl_6 in CIT-5 and UTD-1, respectively.

schematic description	Au_2Cl_6 cryst. [FH70]	Au_2Cl_6 experim.	Au_2Cl_6 gas [AT00]	Au_2Cl_6–CIT-5 experim.	Au_2Cl_6–UTD-1 experim.
ring deform.	96		96	97	97
twist	103	104		104	106
term. $AuCl_2$ wag	122	123		123	124
term. $AuCl_2$ rock	166	151 166	157	166	167
term. $AuCl_2$ scissors	189				
ring stretch	289	290		289	291
Au-Cl ring str. (breathing)	328	329		330	329
asym. stretch	350 [b]	344 353 sh 359			
term. $AuCl_2$ str., antisym.	366	365 vw		365	365 sh
term. $AuCl_2$ str., sym.	379	373 sh 380 s	386	380	380

where: v - very w, m, s - weak, medium, small sh - shoulder.

In comparison, figure 4.1.4.17. shows the Raman spectra of zeosils after the insertion experiments for which no gaseous chlorine was added in the ampoules. In this case, all spectra look very different; no true gold(III) chloride inserted zeosils were obtained.

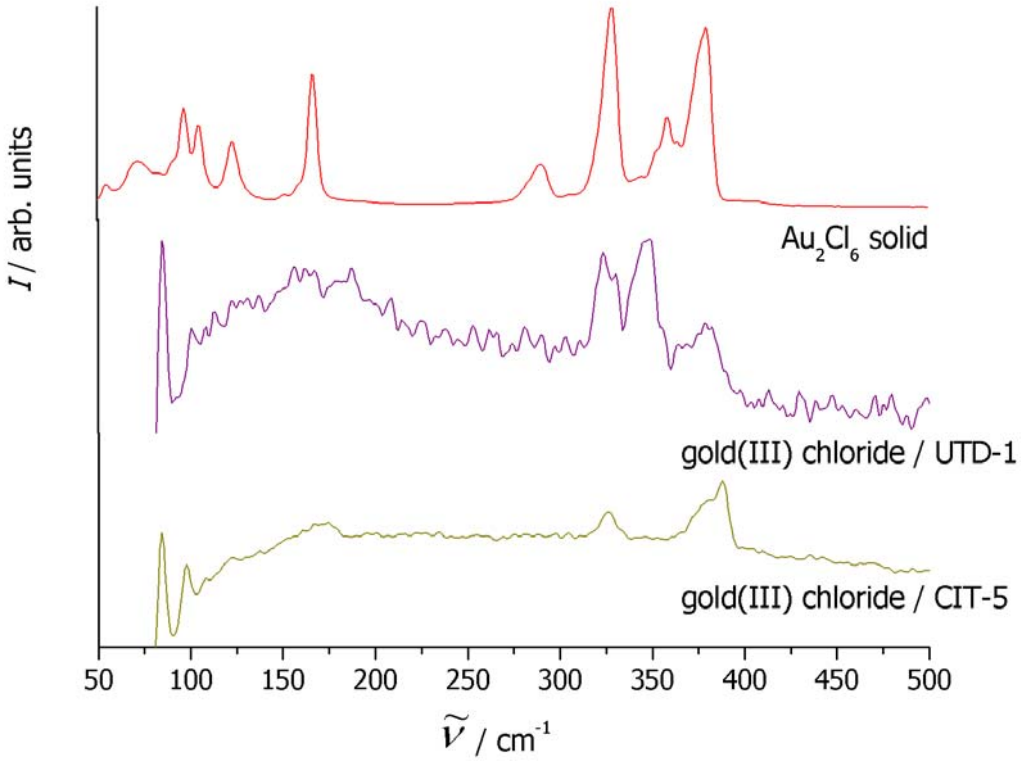

Fig. 4.1.4.17. Raman spectra of zeosils after the insertion experiments without chlorine and of solid Au_2Cl_6.

Based on the experimental data presented in Fig. 4.1.4.15. and Table 4.1.4.16., respectively, it is clear that the insertion compounds prepared under chlorine atmosphere contain Au_2Cl_6 molecules. Furthermore, the fact that no shifts are observed for the Raman excitations shows that the Au_2Cl_6 molecules in the zeosils are in a state which is very similar to that of those molecules in the bulk solid as well as for isolated dimmers in the vapour phase. The guest molecules appear like isolated molecules inside the large channels of CIT-5 and UTD-1. This behaviour is quite different from the one observed for inserted mercury(II) halides, for example $HgBr_2$. For these coordinetively under-saturated molecules, guest-guest interactions inside the zeosil channels could be clearly observed.

4.2. Characterization of zeodyes

The zeodyes were prepared as described in Chapter 3.2. They were then characterized by X-ray powder diffraction, thermogravimetry, N_2 adsorption experiments and UV-vis spectroscopy.

X-ray powder diffraction

The transmission XRD pattern of the as-synthesized zeodye-4.2, obtained with $C_4AzoC_2TMA^+$ as surfactant, revealed the presence of a crystalline, layered material showing first (001) and second (002) order diffractions (see Fig. 4.2.1.). The repeat distance was 3.5 nm.

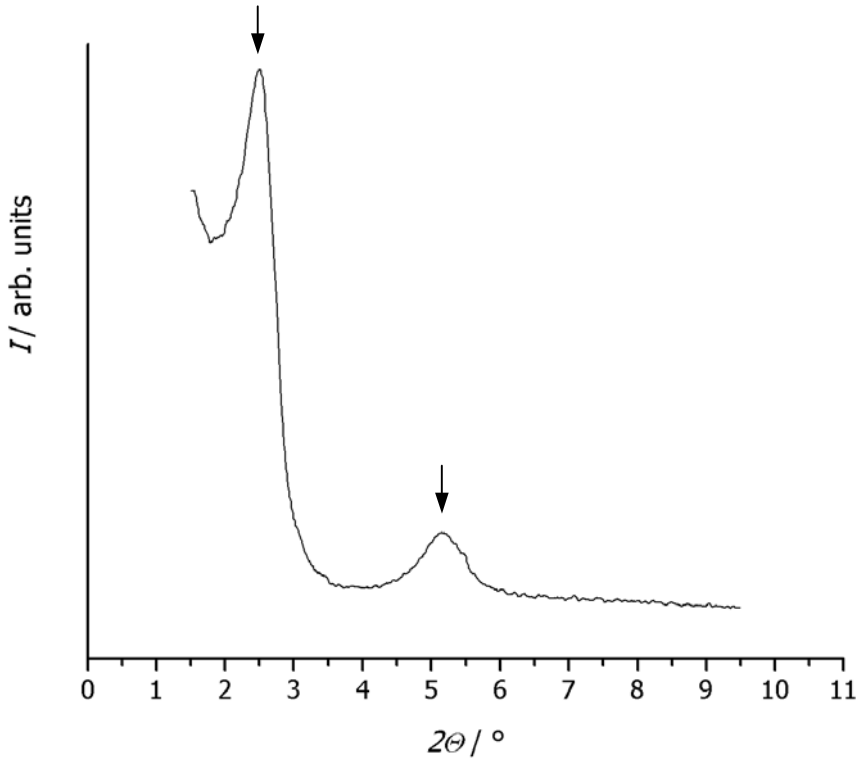

Fig. 4.2.1. Powder X-ray diffraction of the as-synthesized zeodye-4.2.

The XRD pattern of the zeodye-4.2 after heat treatment at 150 °C, intermediate stage, shows that the repeat distance has shrunk from the original 3.5 nm to 3.3 nm (Fig. 4.2.2.).

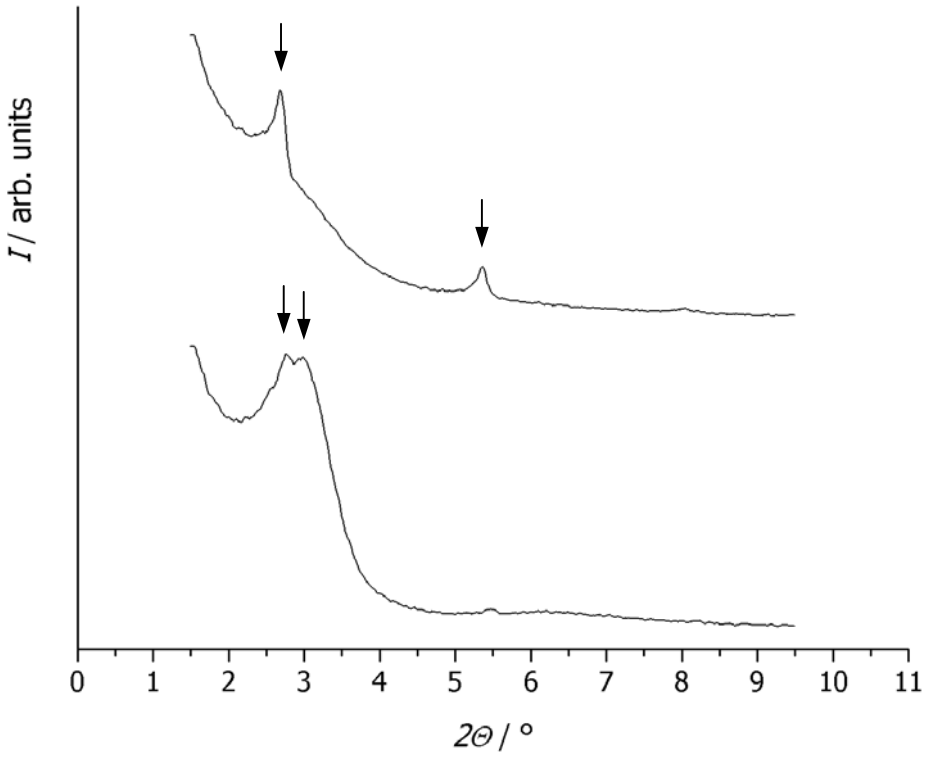

Fig. 4.2.2. Powder X-ray diffraction of the intermediary zeodye-4.2, heated to 150 °C; orange, upper trace and yellow, lower trace.

From the sample of zeodye-4.2 obtained after heating to 150 °C, two capillaries were filled. Both samples were kept in the same conditions, at room temperature in sealed glass capillaries. After approximately two weeks, one sample had a light-orange colour and the other one was yellow. As shown by the X-ray diffraction, the orange-coloured sample kept the layered structure of the as-synthesized material, whereas the other one rearranged itself in a structure similar to a tile. This shows in the XRD pattern several peaks as mentioned in the literature [KR04]. Although it is difficult to rationalize the differences between the two samples, in general it appears possible that a layered structure rearranges to another topology under ambient conditions.

The final sample, obtained after calcination of zeodye-4.2, indicated also a repeat distance of 3.3 nm, but in this case only the first reflection (001) of the superstructure was observed as a very broad peak. Bragg-type diffraction of the crystalline material at wider angles was not detected (Fig. 4.2.3.).

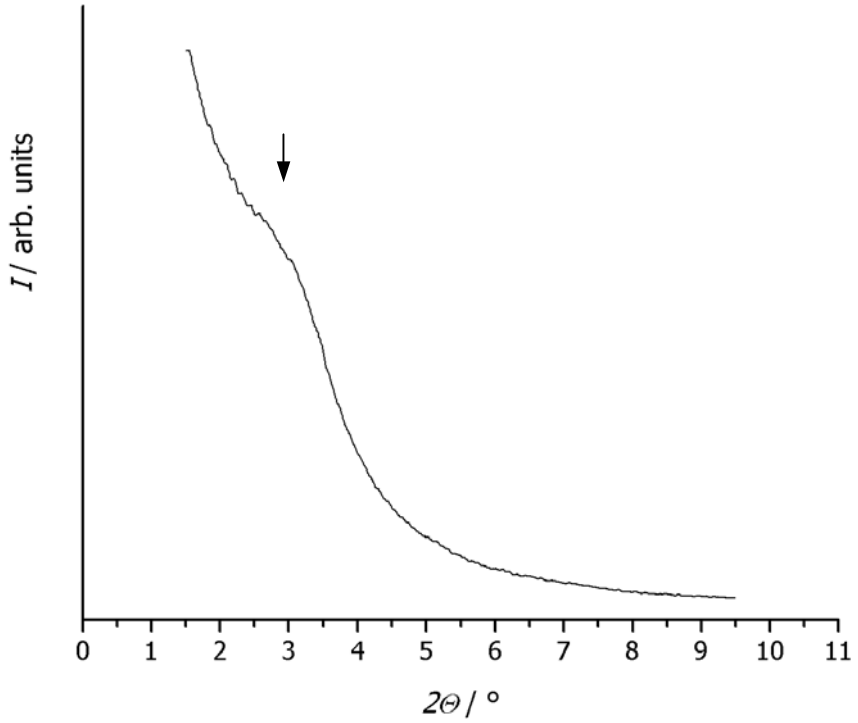

Fig. 4.2.3. Powder X-ray diffraction of the calcined zeodye-4.2.

The absence of Bragg reflections shows that no domains larger than 15 nm with undisturbed Silicalite-1 structure were formed [JD81] [KR99c].

In the case of zeodye-8.6 obtained after one day at 70 °C, the X-ray diffraction pattern of the as-synthesized material revealed a layered structure with the repeat distance of 4.1 nm (Fig. 4.2.4.).

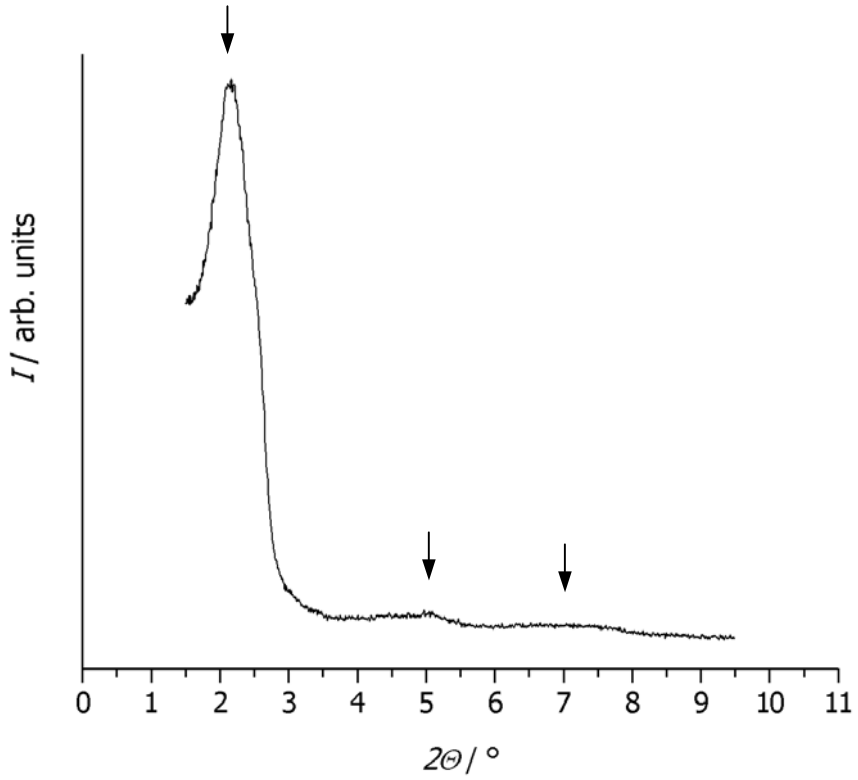

Fig. 4.2.4. Powder X-ray diffraction of the as-synthesized zeodye-8.6. after one day reaction time.

The sample synthesized in the same conditions but kept at 70 °C for two days, maintained the layered structure, but a more ordered material, showing first (001), second (002) and a small third (003) order diffraction peaks, and a repeat distance of 4.4. nm (Fig. 4.2.5.) was obtained.

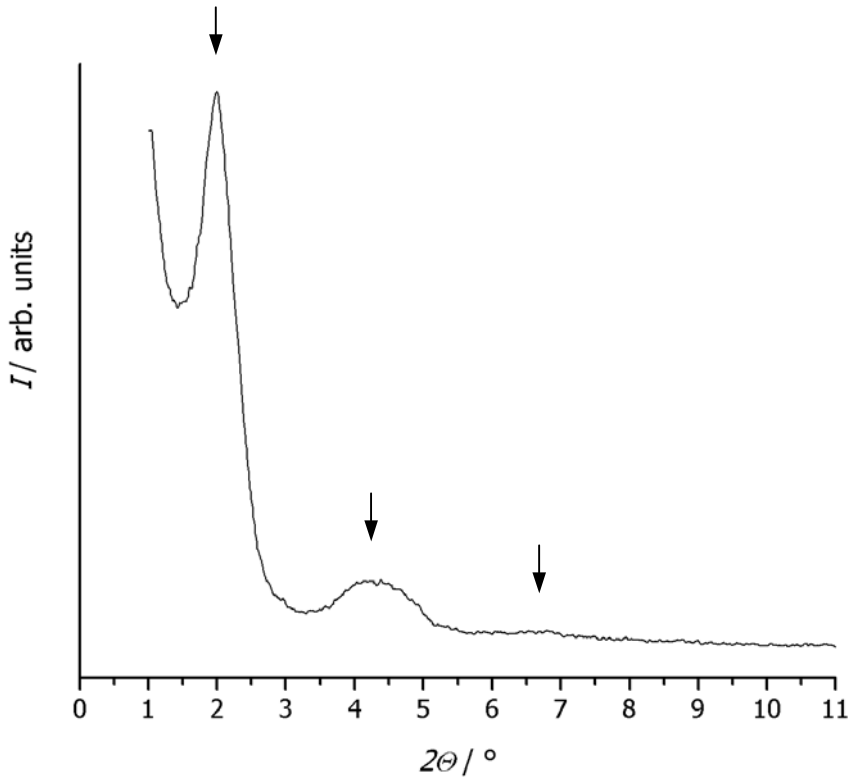

Fig. 4.2.5. Powder X-ray diffraction of the as-synthesized zeodye-8.6. after two days reaction time.

An explanation for this observation is that when longer azo-dye molecules are used as surfactants in the synthesis of zeodye materials, longer reaction times permit the formation of more ordered structure. The respective repeat distances also indicate that in the beginning, the distance between the layers is smaller, as just a few surfactant molecules had time to enter and become incorporated; at this point the layered structure is not yet very ordered. With increasing reaction time, more and more azo-dye molecules enter in between the layers, aggregating to form a more ordered and stable structure, as shown in Fig. 4.2.6. The result is the observed increase of the repeat distance.

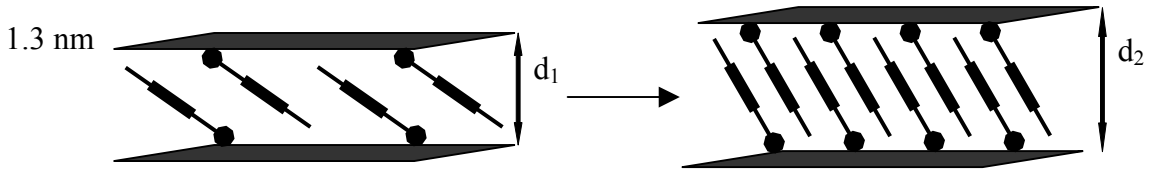

Fig. 4.2.6. Structure of zeodye-8.6 after 1 and 2 days, respectively.

Figures 4.2.7. and 4.2.8. show the XRD patterns of the as-synthesized zeodye-3.2 and zeodye-10.8, obtained with C_3AzoC_2TMABr and $C_{10}AzoC_8TMABr$ as surfactants, respectively. In case of these two zeodyes, no suitable synthesis conditions have been found up to now. In these cases, their XRD powder patterns reveal only the presence of the first order diffraction (001) with $2\Theta = 2.18°$ ($d = 40.5$ Å) in the case of zeodye-3.2 and $2\Theta = 1.91°$ ($d = 46.3$ Å) for zeodye-10.8, respectively.

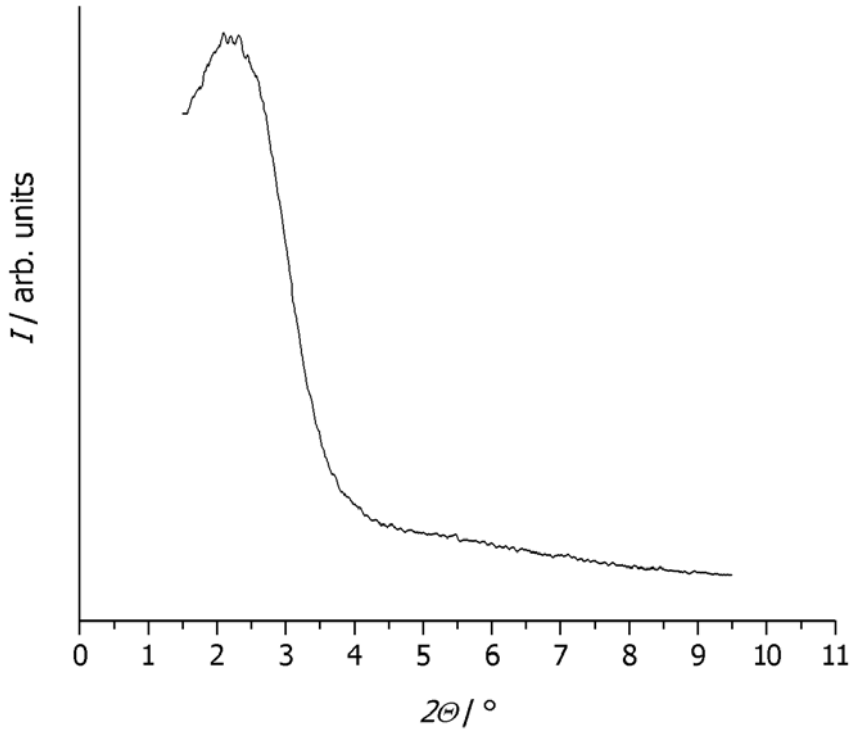

Fig. 4.2.7. Powder X-ray diffraction of the as-synthesized zeodye-3.2.

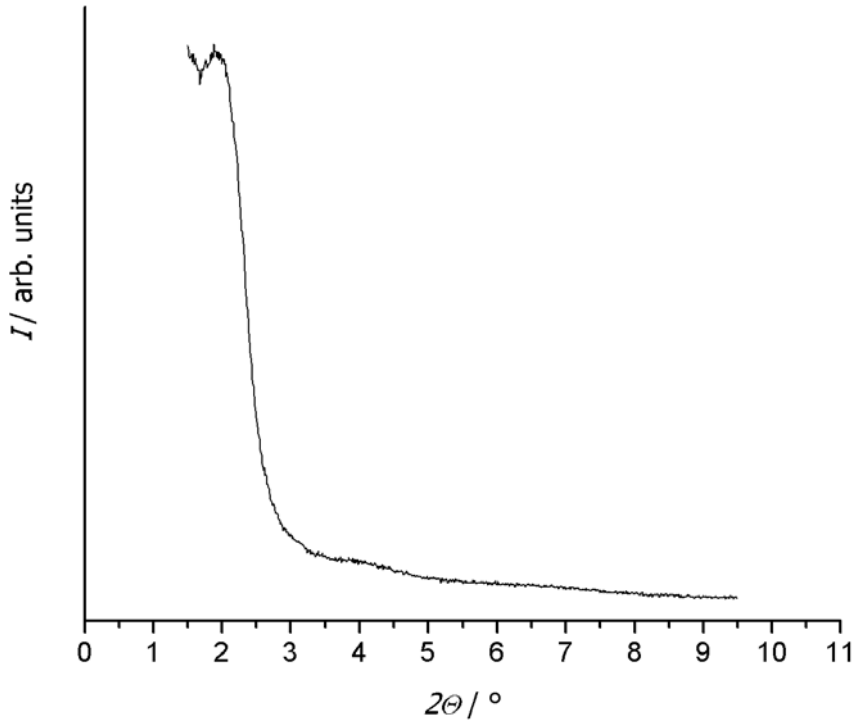

Fig. 4.2.8. Powder X-ray diffraction of the as-synthesized zeodye-10.8.

Some syntheses were carried out under hydrothermal conditions. The X-ray diffraction patterns of the materials obtained from such syntheses taking place at 100 °C for two or three days, showed that no crystalline phases were obtained. It is known that when heating the clear solution to 100 °C for one to two days, it transforms into a turbid suspension of Silicalite-1 crystals with sizes of ca. 100 nm [PS94] [RK98]. The transformation of Silicalite-1 nanoslabs into colloidal crystals was followed by in situ XRS (X-ray scattering) by C. Kirschhock et.al. [KR99c]. The absence of the crystalline phase in zeodye synthesis at 100 °C reveals that the presence of the surfactant in the reaction mixture inhibits the formation of the crystalline porous material. The direct synthesis of a zeodye by heating a mixture of tetraethylorthosilicate (TEOS), TPA (molar ratio of Si : TPA = 25 : 9) and surfactant in water at 100 °C failed. Also in this case, no crystalline phases were detected after synthesis.

Thermogravimetry

The as-synthesized zeodye-4.2 and zeodye-8.6 were subjected to TGA measurements. They were performed in air by heating the sample from ambient temperature to 1000 °C with a heating-rate of 5 °/min. The total weight loss was 66.0 % for zeodye-4.2 and 70.1 % in case of zeodye-8.6. (Figs. 4.2.9. and Fig. 4.2.10., respectively).

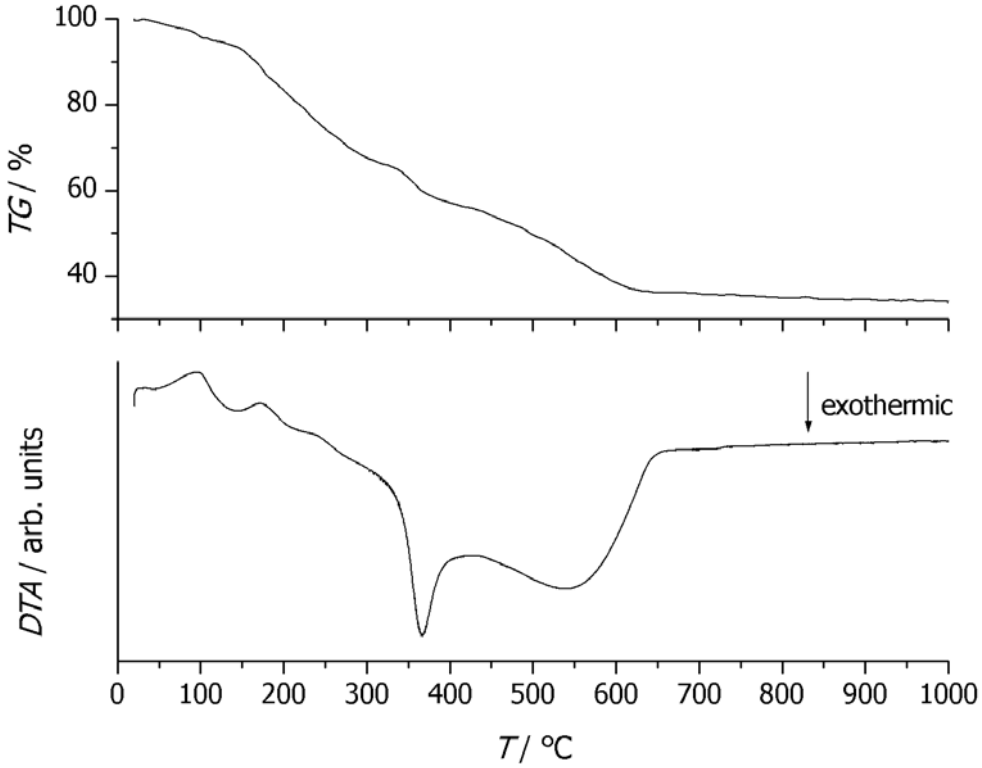

Fig. 4.2.9. Thermogravimetric and differential thermal analysis of zeodye-4.2; under air; heating-rate 5 K/min.

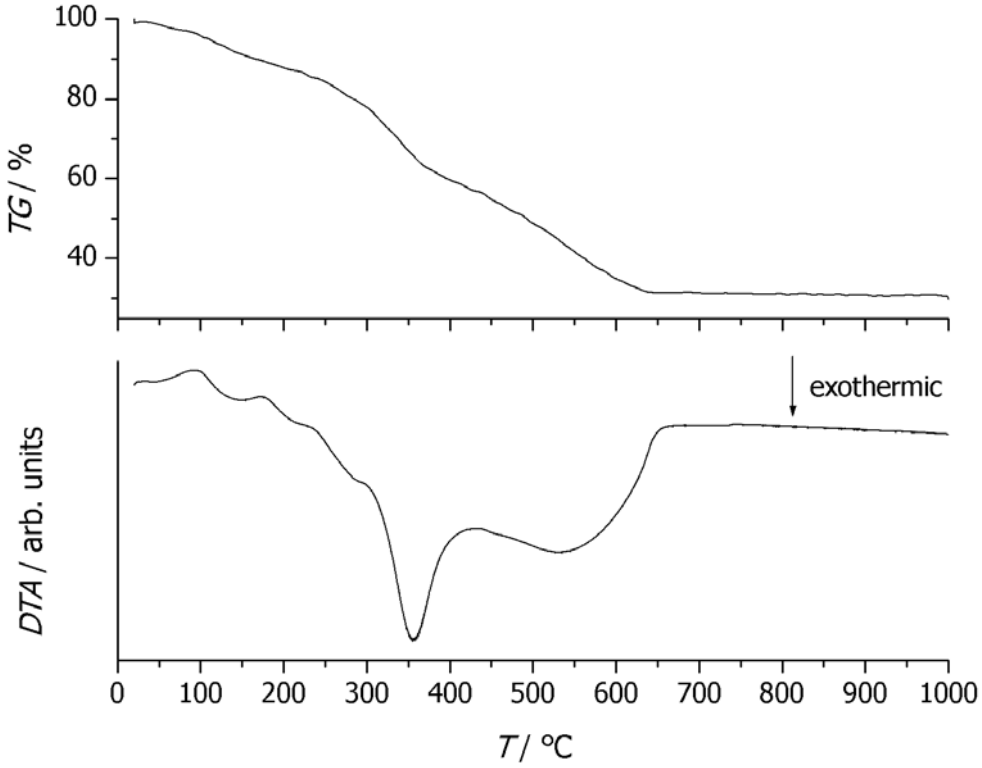

Fig. 4.2.10. Thermogravimetric and differential thermal analysis of zeodye-8.6; under air; heating-rate 5 K/min.

It is difficult to say at which temperatures occurred exactly the weight losses. Among all these weight losses, only two of them coincide with exothermal effects, according to the DTA trace.

N_2 adsorption

The N_2 adsorption isotherm of zeodye-4.2 is displayed in Fig. 4.2.11.

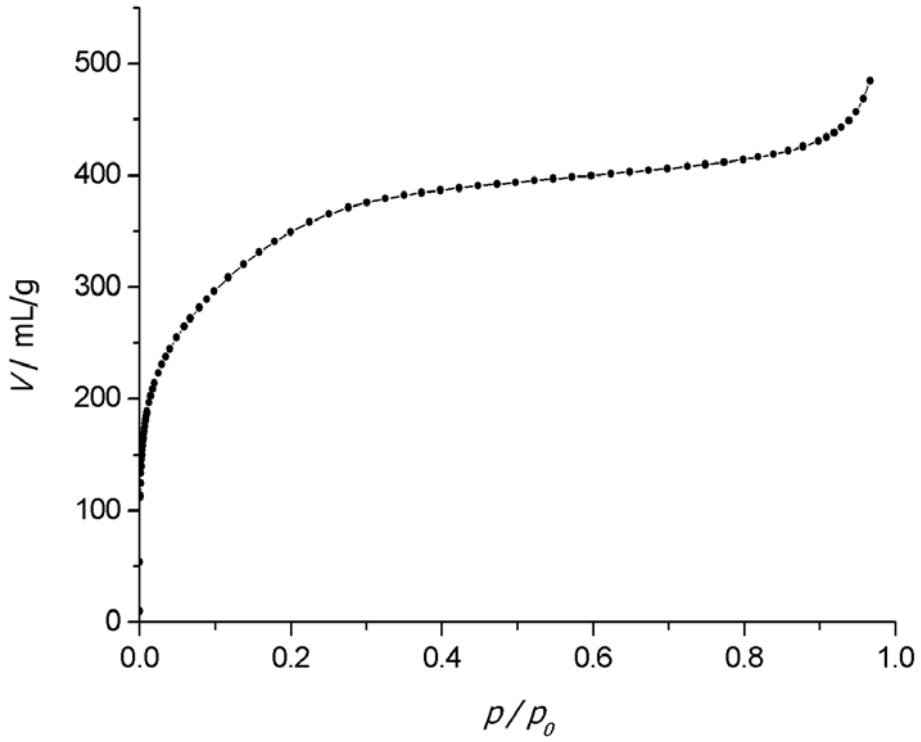

Fig. 4.2.11. N_2 adsorption isotherm of calcined zeodye-4.2.

Pure microporous materials exhibit a type I adsorption isotherm. This is characterized by a steep of the adsorbed volume at very low relative pressures and a pronounced plateau. The rise indicates the microporosity of the sample and the plateau can be interpreted as a sign of a small external surface for the adsorbent. A type II adsorption isotherm is characterized by a concave shape at low relative pressures, which is followed by a linear range and by a small upward deviation at p/p_0 higher than 0.9, owing to capillary condensation in the void spaces in between the crystallites.

In our case, the adsorption isotherm is a combination of these two. It reveals the presence in the calcined zeodye of micropores, and together with these, mesopores with no well-defined dimensions. An explanation for this result can be that during surfactant extraction and calcination, the nanoplates fuse and empty spaces with no well-defined dimensions are left in between. The total pore volume of the calcined zeodye-4.2 was found to be 0.383 mL/g. The BET measurements report a surface area of 19.313 m^2/g The *t*-plot indicates a micropore

volume of 0.075 mL/g with a micropore area of 142.352 m^2/g and a external surface area of 1050.061 m^2/g.

UV-vis spectroscopy

In the UV-vis spectra of azo-dyes, three bands are observed. The $n–\pi^*$ transition has a small intensity and occurs at the longest wavelength. The $\pi–\pi^*$ transition band is of higher intensity. Another band occurs at shorter wavelength, corresponding to $\phi–\phi^*$ transition [BJ66] [KB68] [JY58]. The present work deals with microporous materials based on azo-dyes / SiO_2. The azo-dye molecules that form these porous materials are present as aggregates, so that they come close enough to each other in order to interact These interactions are responsible for different shifts in the UV-vis absorption spectra of these materials [KA63] [BJ66]. The UV-vis spectra obtained on zeodyes are shown in Figs. 4.2.12. and 4.2.13.

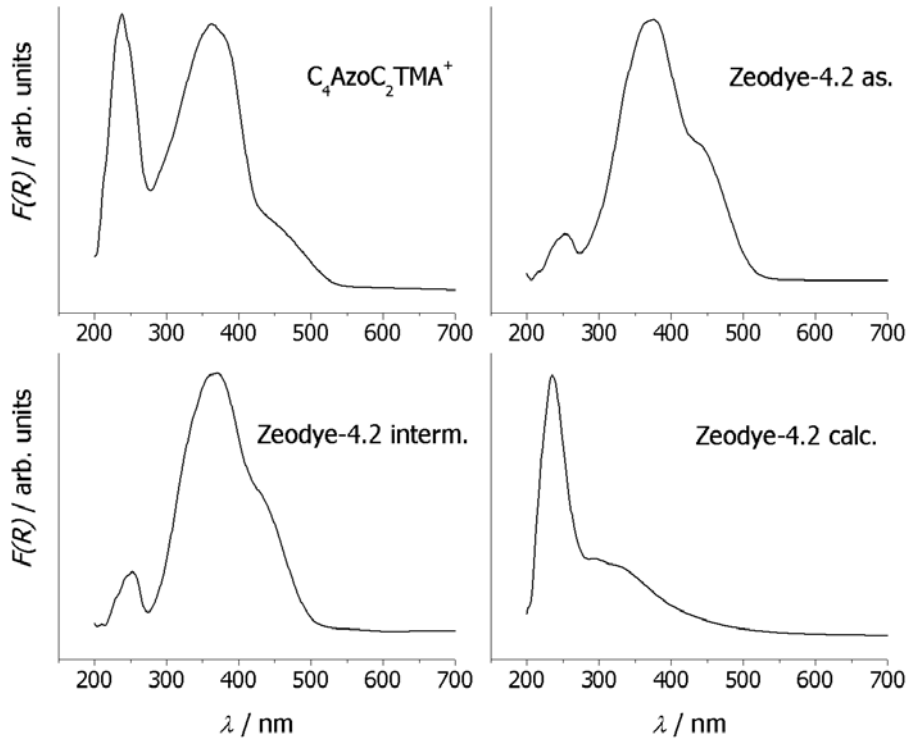

Fig. 4.2.12. UV-vis spectra of pure solid azo-dye C_4AzoC_2TMABr together with the as-synthesized, intermediary and calcined zeodye-4.2.

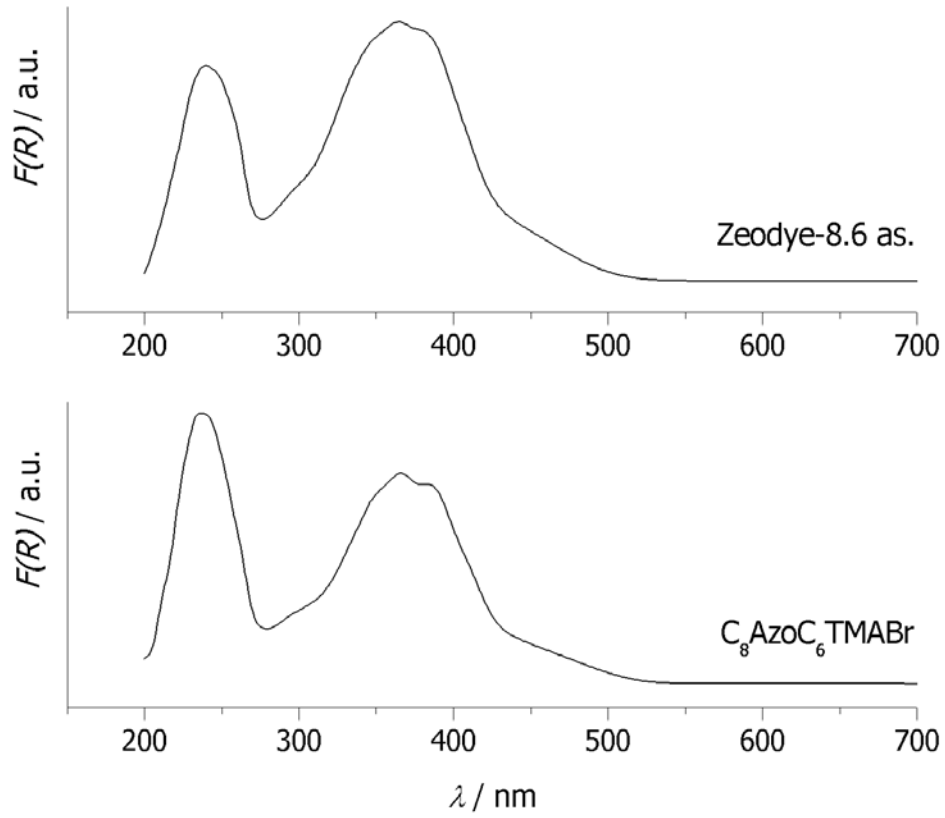

Fig. 4.2.13. UV-vis spectra of pure solid azo-dye C_8AzoC_6TMABr together with the as-synthesized zeodye-8.6.

The UV-vis spectrum of calcined zeodye-4.2 shows no significant absorption bands, proving once again the total elimination of the azo-dye molecules from between the layers upon calcination.

Formation mechanism of zeodyes

The following model can be proposed for the formation of the zeodyes prepared here: first, the Silicalite-1 nanoslabs condense into nanoplates and then layers, controlled by the surfactant molecules. Second, during calcination, the layers fuse leaving empty spaces in between them. The shrinkage observed upon calcination is probably due to the removal of the surfactant from between the nanoslab layers. The repeat distance of 3.3 nm could be explained if the nanoslabs belonging to different layers were connected in the *a* direction, while leaving gaps. With respect to the facial linking of nanoslabs, it must be noted that the two large faces of a nanoslab are different [KR04]. In order to allow linking of two slabs in the *a* direction, the slabs must have

an opposite orientation so that the same type of surfaces are facing each other (see Fig. 4.2.14.). The weakening of the second order diffraction after removal of the surfactant indicates a loss of ordering.

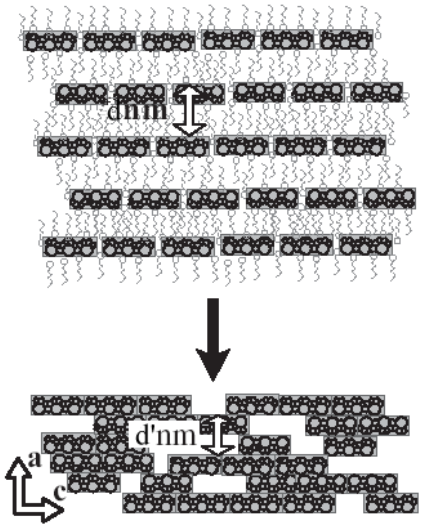

Fig. 4.2.14. Formation of zeodyes.

Structure of zeodyes

The nanoslabs occlude TPA in complete and some incomplete channel intersections. From a previous thermogravimetric analysis of nanoslabs [RK99a], it is known that TPA desorbs from incomplete channel intersections in the temperature range between 150 to 240 °C. The fully occluded TPA molecules give rise to exothermal weight losses at temperatures exceeding 240 °C. Thermogravimetric analysis of the as-synthesized zeodye-4.2 and zeodye-8.6 showed a total weight loss of 66.0 and 70.1 %, respectively, ascribed to the complete removal of the organic molecules (Figures 4.2.9. and 4.2.10.). Due to the shape of the TG curves, no exact explanation can be given regarding the calcinations steps and their corresponding weight losses.

According to XRD results, zeodyes 4.2 and 8.6 have layered structures with repeat distances of 3.5 and 4.4 nm, respectively. Silicalite-1 nanoslabs have dimensions of 1.3, 4.0 and 4.0 nm in the *a*, *b* and *c* crystallographic directions of Silicalite-1, respectively [KR04]. The repeat distances in the as-synthesized zeodyes are interpreted as the thickness of a nanoslab, 1.3 nm, plus the thickness of the surfactant layer. The negative surface charge of the nanoslabs in suspension provides a driving force for the interaction with the surfactant. After heating to 150

°C, the repeat distance in zeodye-4.2 shrunk from 3.5 to 3.3 nm (Fig. 4.2.2.). The repeat distance did not change any more upon calcination at 400 °C (Fig. 4.2.3.). The shrinkage could be explained by removal of the surfactant from between the nanoslab layers. The weakening of the second order diffraction after removal of the surfactant (Fig. 4.2.3.) indicated a loss of ordering compared to as-synthesized zeodye-4.2. The proposed condensation of nanoslabs in the *a* direction, while leaving gaps of various sizes between the individual slabs in the *b* and *c* directions, matched with the observed spacing, with the loss of higher order diffraction and with the absence of diffraction on other planes but (001). Together with this, nitrogen adsorption investigations on calcined zeodye-4.2 showed the presence of some larger pores, mesopores with no well-defined dimensions. These were formed in between the nanoplates during surfactant removal.

Depending on the arrangement of the surfactant molecules in between the nanoslab layers, the porous composite can form J or H aggregate, respectively (see Fig. 4.2.15) [GL99]. The distance obtained from the XRD experiments and the π–π^* band position in the UV-vis spectra can give information about the type of aggregate.

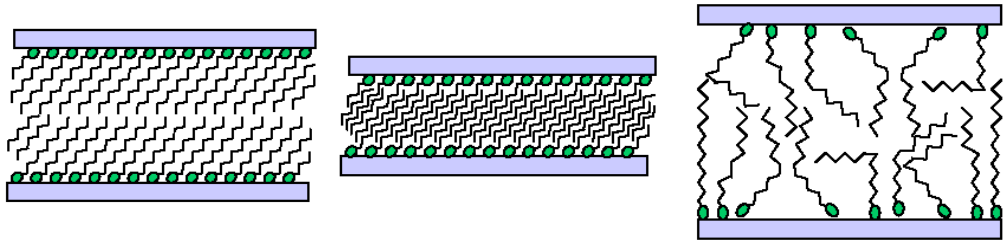

Fig. 4.2.15. J-aggregate double-layer; H-aggregate mono-layer; liquid-crystalline mono-layer (from left to right).

For example, in case of zeodye-4.2, the gallery height between the nanoslab layers was found to be 2.25 nm, obtained from the difference 3.55 – 1.3 nm, where 3.55 nm represents the repeat distance in zeodye-4.2 (see Table 4.2.16.) and 1.3 nm the thickness of the nanoslab in the *a* direction. The length of the corresponding azo-dye, C_4AzoC_2TMABr, was calculated and found to be 2.00 nm; this means that the gallery height can only be filled by a double-layer, a J-aggregate. It was shown also that a shift of the π–π^* absorption band, i.e. that appears in the 370-390 nm region in the case of a J-aggregate, takes place when compared to the non-aggregated azo-dye [GL99]. In case of zeodye-4.2 the band appeares indeed at 372 nm, whereas for the pure azo-dye C_4AzoC_2TMABr, the band is observed at 362 nm. The case for zeodye-8.6

is different, however. Here, the π–π^* transition band appears at 364 nm for the pure azo-dye, and no shift was observed upon formation of the zeodye. But also in this case, the presence of a J-aggregate is probable, the repeat distance obtained from the XRD measurements being 4.44 nm, corresponding to a gallery height of 3.14 nm. The calculated length of the azo-dye C_8AzoC_6TMABr is 3.02 nm, so only a double-layer can fill the gallery height.

Table 4.2.16. Azo-dye lengths and repeat distances in zeodyes.

azo-dye	azo-dye length / Å [GL99]	zeodye	repeat distance / Å [XRD this work]
$C_3AzoC_2TMA^+$	18.7	zeodye-3.2 as-synth.	40.5
$C_4AzoC_2TMA^+$	20.0	zeodye-4.2 as-synth.	35.5
$C_4AzoC_2TMA^+$	20.0	zeodye-4.2 intermed.	32.9
$C_4AzoC_2TMA^+$	20.0	zeodye-4.2 calc.	33.0
$C_8AzoC_6TMA^+$	30.2	zeodye-8.6 (1 day)	41.1
$C_8AzoC_6TMA^+$	30.2	zeodye-8.6 (2 days)	44.4
$C_{10}AzoC_8TMA^+$	35.2	zeodye-10.8 as-synth.	46.3

Knowing the length of the surfactant and the gallery height, the inclination angle of the surfactant inside the composite material can be calculated for zeodye-4.2 and zeodye-8.6 (Fig. 4.2.17.). This was found to be 34.01° and 31.33°, respectively.

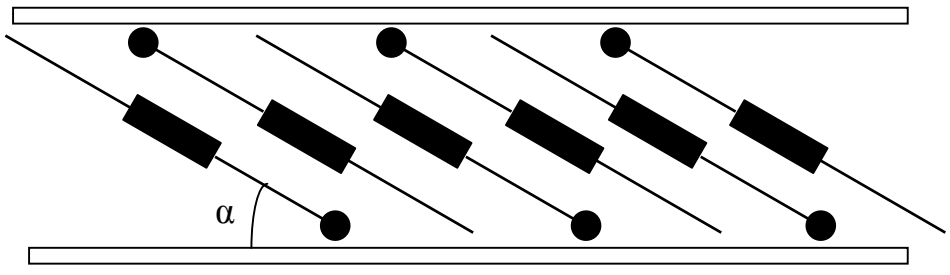

Fig. 4.2.17. Inclination angle of the azo-dye molecules inside the composite material.

Due to the disordered character of the synthesized zeodyes, no correlation between the α-angle, calculated on the basis of the XRD experiments, and the shift ($\Delta\lambda$) of the π–π^* absorption band in the UV-vis spectrum could be made [GL99] [MU04].

5. GENERAL CONCLUSIONS

The main aim of the present work was the synthesis and characterization of new host-guest compounds. Pure silica frameworks, i.e. zeosils, were used for the insertion of iodine, selenium, mercury(II) halides and gold(III) chloride. The zeosil frameworks are uncharged and so, only weak van der Waals interactions can occur between the host and the guest components. In contrast to previous work in our group, the focus here was on large and extra-large pore zeosils. Four members of these groups, namely ITQ-4, SSZ-24, CIT-5 and UTD-1 were practically used. In addition, the medium pore zeosil Silicalite-1 (MFI) was in some cases used for comparison.

As a general result, it was found that many of the insertion compounds of the large and, more pronounced, of the extra-large pore zeosils, were unstable when being removed from the saturated vapors of the substance to be inserted, i.e. when the ampoule was opened. This was observed especially for the insertion compounds of iodine and of mercuric halides. As similar insertion compounds of medium pore zeosils, like MFI, had been shown to be stable [WP96] [WI98], we ascribe this behaviour to a reduced host-guest interaction in the larger pores. On the other hand, the larger pore systems allow for the introduction of larger guest species as for example gold(III) chloride, which cannot be inserted into Silicalite-1. The reduced stability of some insertion compounds hampered their analytical characterization. Nevertheless, also in these cases at least a basic characterization was possible. Based on their different pore geometries, the arrangement of the guest molecules and their interactions inside the host void system could be investigated. The insertion compounds of iodine and selenium serve as an impressive example of this concept.

In the case of iodine insertion compounds, the different guest-guest interactions inside the different zeosil channels could be monitored first of all by the changes in colour after insertion (and before opening the ampoule). The loaded material has, in the case of I_2–UTD-1 and I_2–ITQ-4, a violet-to-brownish colour which indicates strong interactions between the occluded iodine molecules. This is not the case for I_2–CIT-5 and I_2–SSZ-24; their violet colour resembles that of isolated iodine molecules. More accurate information regarding these interactions could be drawn from Raman spectroscopy. The large channel diameters permit interactions between the inserted iodine molecules and these intermolecular interactions appear in the Raman spectrum as shifts of the stretching vibrations to lower frequencies when compared to the isolated molecules. In this sense, for I_2–SSZ-24, the two vibration bands located at 202 and 180

cm^{-1} were attributed to iodine molecules interacting in one dimension and to even stronger interacting molecules (similar to a liquid phase), respectively. Also for I_2–CIT-5, the band present at 204 cm^{-1} was described as characterizing a chain-like arrangement of the iodine molecules.

When selenium was loaded into zeosils, the small Se_2 and Se_3 molecules, which are present in the gaseous phase at the insertion temperature, condensed during cooling and formed Se chains and Se_8 rings. The formation and stabilization of these large entities inside the void system was possibly due to the large channel diameters of zeosil CIT-5. This was not possible when medium-size zeosils were used as hosts.

In the case of mercury(II) halides insertion compounds in zeosils, the instability of the loaded materials, due to the reduced host-guest interactions, made their characterization more difficult. However, we can say that some interactions between the occluded HgX_2 molecules are present. For example, the UV-vis spectrum of $HgBr_2$–CIT-5 resembles that of $HgBr_2$ in weakly interacting solvents. The small shift of the absorption band to higher wavelengths when compared to the gaseous phase characterizes interacting mercury(II) bromide molecules. For $HgBr_2$–UTD-1, the frequencies of the two Raman bands (193 and 218 cm^{-1}) correspond to interacting $HgBr_2$ molecules (193 cm^{-1}) occluded together with unperturbed ones (218 cm^{-1}).

The use of extra-large pore zeosils as hosts permitted the insertion of larger molecules as Au_2Cl_6. In order to avoid the decomposition of gold(III) chloride during loading, gaseous chlorine had to be added. No interactions between the guest species were detected inside the large channels of CIT-5 and UTD-1. One explanation for this can be that even in the solid state, the interactions between these saturated molecules are very weak.

In the second part of this work was presented the successful synthesis of so-called zeodyes. They were prepared by heating the “clear solution”, in fact a Silicalite-1 nanoslab suspension, together with azo-surfactants. The surfactants can be generally represented as C_mAzoC_nTMABr, where C_m is the number of carbon atoms in the alkyl tail and C_n represent the number of C-atoms in the alkyl spacer. Practically, we used solutions with different concentrations of C_3AzoC_2TMABr, C_4AzoC_2TMABr, C_8AzoC_6TMABr and $C_{10}AzoC_8TMABr$ in ethanol. The reaction mixture was heated for some time and the yellow precipitate was then filtered, washed, dried and characterized. The main characterization method was powder X-ray diffraction. This showed in every case the presence of a layered material, more or less ordered, depending on the surfactant type and on the synthesis conditions. Best results were obtained when using C_4AzoC_2TMABr and C_8AzoC_6TMABr as surfactants. In the first case, the optimum reaction time was one day at a temperature of 60 °C. When using C_8AzoC_6TMABr at temperatures of 70

°C and two days synthesis time, we obtained a layered material that showed pronounced first and second order diffractions in the X-ray diffraction pattern. The calcination of the as-synthesized sample caused a shrinking of the repeat distance and together with this, a loss of ordering. As shown by the nitrogen adsorption experiment, micropores together with some mesopores with no well-defined dimensions are present in the calcined structure. The presence of these larger cavities can be explained by the fact that during surfactant removal, the nanoplates fused leaving empty spaces in between. These empty spaces with no well-defined pore sizes can be responsible for the mesoporosity in the zeodyes.

References

[AP97] [O. Axelsson, D. Peters, *Journal of Heterocyclic Chemistry* **1997**, *34*(2), 461–463]

[AT00] [Z. Akdeniz, M. P. Tosi, *Z. Naturforsch*. **2000**, *55 A*, 495-498]

[AW70] [Table of Atomic Weights, 1969, IUPAC Commission on Atomic Weights; *Pure Appl. Chem.* **1970**, *21*, 95]

[BA82] [R. M Barrer, Hydrothermal Synthesis of Zeolites, Academic Press, London, United Kingdom, 1982]

[BB97] [K. J. Balkus Jr., M. Biscotto, A. G. Gabrielov, The Synthesis and Characterization of UTD-1: The First Large Pore Zeolite Based on a 14 Membered Ring System, in: H. Chon, S.-K. Ihm, Y. S. Uh (Herausgeber), Progress in Zeolite and Microporous Materials, Band 105A, Studies in Surface Science and Catalysis, Elsevier Science B. V., 1997, p. 415-421]

[BC83] [J. M. Bennett, J. P. Cohen, E. M. Flanigen, J. J. Pluth, J. V. Smith, *ACS Sym. Ser.* **1983**, *218***,** 109-118]

[BC97a] [U. Buontempo, A. Di Cicco, A. Filipponi, M. Nardone, P. Postornio, *J. Chem. Phys*. **1997**, *107*, 5720]

[BC97b] [P. A. Barrett, M. A. Camblor, A. Corma, R. H. Jones, L. A. Villaescusa, *Chem. Mater*. **1997**, *9*, 1713-1715]

[BD98a] [L.W. Beck, M. E. Davis, *Microporous and Mesoporous Materials* **1998**, *22*, 107–114]

[BD98b] [P. A. Barrett, M. J. Díaz-Cabañas, M. A. Camblor, R. H. Jones, *J. Chem. Soc., Faraday Trans.* **1998**, *94*, 2475-2481]

[BE38] [S. Brunauer, P. H. Emmet, E. Teller, *J. Amer. Chem. Soc.* **1938**, *60*, 309]

[BG95] [K. J. Balkus Jr., A. G. Gabrielov, S. I. Zones, in: Symposium on Synthesis of Zeolites, Layered Compounds and Other Microporous Solids, Presented Before the Division of Petroleum Chemisty, Inc., 209th National Meeting, Band 40, Petr. Preprints, American Chemical Society, Anaheim, CA, 1995, p. 296–297]

[BG96] [K. J. Balkus Jr., A. G. Gabrielov, S. I. Zones, I. Y. Chan, Synthesis and Characterization of UTD-1: A Novel Zeolite Molecular Sieve, in: M. Occelli, H. Kessler (Herausgeber), Library of Congress Cataloging-in-Publication Data,

Synthesis of Microporous Materials, ACS Symp. Ser., Marcel Dekker, New York, 1996, p. 77-91]

[BG97] [P. Behrens, A. Glaue, C. Haggenmüller, G. Schechner, *Solid State Ionics* **1997**, *101*, 255]

[BH01] [P. Behrens, M. Hartl, G. Wirnsberger, A. Popitsch, B. Pillep, *Stud. Surf. Sci. Catal.* **2001**, *135,* 10]

[BJ66] [D. L. Beveridge, H. H. Jaffe, *J. Am. Chem. Soc.* **1966**, *88*, 1948]

[BK67] [F. van Bolhuis, P. B. Koster, T. Migchelsen, *Acta Cryst*. **1967**, *23*, 90]

[BM91] [R. Bialek, W. M. Meier, M. Davis, M. J. Annen, *Zeolites* **1991**, *11*, 438-442]

[BM01] [C. Baerlocher, W. M. Meier, D. H. Olson, Atlas of Zeolite Structure Types, 5th Ed., Elsevier, Amsterdam, The Netherlands, 2001]

[BN63] [G. Burns, R. G. W. Norrish, *Proc. R. Soc. (Lond.), Ser. A* **1963**, *271*, 289]

[BP85] [V. N. Bogomolov, V. V. Poborchii, S. G. Romanov, S. I. Shagin, *J. Phys. C: Solid State Phys*. **1985**, *18*, L313-L317]

[BP97] [P. Behrens, C. Panz, V. Hufnagel, B. Lindlar, C. C. Freyhardt, G. van de Goor, *Solid State Ionics* **1997**, *101-103*, 229]

[BS96] [P. Behrens, G. D. Stucky, in: Comprehensive Supramolecular Chemistry, Vol. 7, Eds. J. L. Atwood, D. D. MacNicol, J. E. D. Davies, F. Vögtle, Pergamon, Oxford, 1996, p.721-772]

[BU51] [R. D. Burbank, *Acta Cryst*. **1951***, 4*, 140]

[BU52] [R. D. Burbank, *Acta Cryst.* **1952**, *5*, 236-246]

[CO73a] [Comprehensive Inorganic Chemistry, Vol. 2, Pergamon Press, 1973, p. 1172]

[CO73b] [Comprehensive Inorganic Chemistry, Vol. 3, Pergamon Press, 1973, p. 297-300]

[CO75] [Comprehensive Inorganic Chemistry, Vol. 2, Pergamon Press, 1975, p. 935-949]

[CR56] [A. F. Cronstedt, *Kongl. Vetenskaps, Acad. Handl. Stockh*. **1756**, 17, 120]

[CS65] [L. Capella, C. Schwab, *Compt. Rend.* **1965**, *260*, 4337]

[CS98] [T. M. Cooper, M. O. Stone, *Langmuir* **1998**, *14*, 6662]

[CT58] [E. S. Clark, D. H. Templeton, C. H. MacGillavry, *Acta Cryst.* **1958**, *11*, 284-288]

[CU67] [P. Cherin, P. Unger, *Inorg. Chem.* **1967**, *6*, 1589]

[CU72] [P. Cherin, P. Unger, *Acta Cryst. B* **1972**, *28*, 313-317]

[CV90] [A. T. Casey, A. M. Vecchio, *Applied Organometallic Chemistry* **1990**, *4*, 513-522]

[CV99] [M. A. Camblor, L. A. Villaescusa, M. J. Díaz-Cabañas, *Topics in Catalysis* **1999**, *9*, 59-76]

[DA62] [A. S. Davydov, Theory of Molecular Excitons, McGraw-Hill, New York, 1962]

[DL92] [M. E. Davis, R. F. Lobo, *Chem. Matter*. **1992**, *4*, 756-768]

[DM87] [J. M. Delgado, R. K. McMullan, B. J. Wuensch, *Transactions of the American Crystallographic Association* **1987**, *23*, 93-95]

[DO74] [J. Donohue, The Structure of Elements, New-York-London-Sydney-Toronto, 1974, p. 385-386]

[EV72] [D. H. Everett, *Pure Appl. Chem.* **1972**, *31*, 577–638]

[FB28] [W. Fischer, W. Blitz, *Z. Anorg. und Allgem. Chem.* **1928**, *176*, 81]

[FB99] [G. Flachenecker, P. Behrens, G. Knopp, M. Schmitt, T. Siebert, A. Vierheilig, G. Wirnsberger, A. Materny, *J. Phys. Chem. A* **1999**, *103*, 3854-3863]

[FH70] [R. Forneris, J. Hiraishi, F. A. Miller, *Spectrochimica Acta* **1970**, *26 A*, 581-591]

[FJ80] [O. Foss, V. Janickis, *J. Chem. Soc. Dalton Trans*. **1980**, *4*, 624]

[FK84] [C. A. Fyfe, G. J. Kennedy, C. T. De Schutter, G. T. Kokotailo, *J. Chem. Soc., Chem. Commun*. **1984**, 541]

[FL88] [K. R. Franklin, B. M. Lowe, *Zeolites* **1988**, *8*, 508–516]

[FR31] [J. Frenkel, *Phys. Rev*. **1931**, *37*, 17, 1276]

[FT96] [C. C. Freyhardt, M. Tsapatsis, R. F. Lobo, K. J. Balkus Jr., M. E. Davis, *Nature* **1996**, *381*, 295–298]

[GA79] [T. R. Griffiths, R. A. Anderson, *J. Chem. Soc. Faraday Trans. II* **1979**, *75*, 957]

[GB33] [G. E. Gibson, N. S. Bayliss, *Phys. Rev*. **1933**, *44*, 188]

[GB96] [C. S. Gittleman, A. T. Bell, C. J. Radke, *Catalysis Letters* **1996**, *38*(1/2), 1-9]

[GI92] [J. P. Gilson, Organic and Inorganic Agents in the Synthesis of Molecular Sieves, in Zeolite Microporous Solids: Synthesis, Structure and Reactivity, Vol. 352, Derouane, Lemas, Naccache, Ramoa, Ribeiro, Eds., NATO ASI Series, 1992, p. 19]

[GK86] [J. L. Guth, H. Kessler, R. Wey, Proceedings of the 7th International Zeolite Conference, New Route to Pentasil-Type Zeolites Using a Non Alkaline Medium in the Presence of Fluoride Ions, in: Y. Murakami, Iijima A und J. W. Ward (Herausgeber), New Developments in Zeolite Science and Technology, Kodansha Elsevier, Tokyo, 1986, p. 121–128]

[GL99] [A. Glaue, *PhD Thesis*, Ludwig-Maximilians Universität München, **1999**]

[GM98] [H. Gies, B. Marler, U. Werthmann, Synthesis of Porosils: Crystalline Silicas with Cage- and Channel-like Voids Structures, in: Molecular Sieves, Vol. 1, Springer-Verlag Berlin Heidelberg, 1998]

[GM92] [Gmelin Handbook of Inorganic and Organometallic Chemistry, Au Suppl. Vol. B 1, 1992, p.198]

[GO95] [G. van de Goor, *PhD Thesis*, Universität Konstanz, **1995**]

[GS99] [H. Ghobarkar, O. Schäf, U. Guth, *Prog. Solid St. Chem*. **1999**, *27*, 29-73]

[HA02] [M. Hartl, *PhD Thesis*, Universität Hannover, **2002**]

[HD02] [V. Hauer, C. Day, Cryosorbent Characterization of Activated Charcoal in the COOLSORP Facility, in: Final Report on Subtask 8 of Task VP1: Cryopump Development and Testing (ITER Task no. 448), Forschungzentrum Karlsruhe GmbH, 2002]

[HM70] [W. Holzer, W. F. Murphy, H. J. Bernstein, *J. Chem. Phys.* **1970**, *52*, 399]

[HU00] [V. Hufnagel, *PhD Thesis*, Universität München, **2000**]

[JA02] [R. Jäger, *PhD Thesis*, Universität Hannover, **2002**]

[JD81] [P. A. Jacobs, E. G. Derouane, J. Weitkamp, *Chem. Commun*. **1981**, *591*]

[JV67] [G. A. Jeffrey, M. Vlasse, *Inorg. Chem.* **1967**, *6*, 396-399]

[JY58] [H. H. Jaffe, S. J. Yeh, R. W. Gardner, *J. Molec. Spectr*. **1958**, *2*, 120-136]

[KA63] [M. Kasha, *Radiat. Res.* **1963**, *20*, 55]

[KA00] [K. Kuge, M. Arisawa, N. Aoki, A. Hasegawa, *Jpn. J. Appl. Phys.,* Part. 1, **2000**, *39*, 6550]

[KB68] [J. Kroner, H. Bock, *Chem. Ber.* **1968**, *101*, 1922]

[KB73] [W. Kiefer, H. J. Bernstein, *J. Raman Spectr*. **1973**, *1*, 417]

[KC03] [K. Ken'ichi, G. Calzaferri, *Microporous Mesoporous Mater*. **2003**, *66*, 15-20]

[KG98] [S. Kohara, A. Goldbach, N. Koura, M.-L. Saboungi, L. A. Curtiss, *Chem. Phys. Lett*. **1998**, *287*, 282-288]

[KH77] [R. Keller, W. B. Holzapfel, H. Schulz, *Physical Review 3 B - Solid State* **1977**, *16*, 4404-4412]

[KJ90] [H. van Koningsveld, J. C. Jansen, H. van Bekkum, *Zeolites* **1990**, *10*, 235]

[KJ96] [H. van Koningsveld, J. C. Jansen, *Micropor. Mater*. **1996**, *6*, 159]

[KK80] [U. Kölle, F. Khouzami, *Angewandte Chemie* **1980**, *92*(8), 658-659]

[KK81] [U. Kölle, F. Khouzami, *Chemische Berichte* **1981**, *114*, 2929-2937]

[KL67] [P. Klaboe, *J. Am. Chem. Soc.* **1967**, *89*, 3667]

[KL78] [G. T. Kokotailo, S. L. Lawton, D. H. Olson, W. M. Meier, *Nature,* **1978***, 272***,** 437-438]

[KL92] [C. Kresge, M. Leonowicz, W. Roth, J. Vartuli, J. Beck, *Nature* **1992**, *359*, 710]

[KM31] [P. Kubelka, F. Munk, *Zeitschrift für Technische Physik*, **1931**, *12*, 593-601]

[KM98] [R. Kumar, P. Mukherjee, R. K. Pandey, P. Rajmohanan, A. Bhaumik, *Microporous and Mesoporous Materials* **1998**, *22*, 23–31]

[KO69] [G. Kortüm, Reflexionsspektroskopie, Grundlagen, Methodik, Anwen-dungen, Springer-Verlag, Heidelberg, 1969]

[KR51] [H. Krebs, *Z. Anorg. Chem*. **1951**, *265*, 156]

[KR99a] [C.E.A. Kirschhock, R. Ravishankar, F. Verspeurt, P.J. Grobet, P.A. Jacobs, J.A. Martens, *J. Phys. Chem. B* **1999**, *103*, 4965]

[KR99b] [C.E.A. Kirschhock, R. Ravishankar, L. van Looveren, P.A. Jacobs, J.A. Martens, *J. Phys. Chem. B* **1999**, *103*, 4972]

[KR99c] [C.E.A. Kirschhock, R. Ravishankar, P.A. Jacobs, J.A. Martens, *J. Phys. Chem. B* **1999**, *103*, 11021]

[KR04] [S. Kremer, *PhD Thesis*, Katholieke Universiteit Leuven, **2004**]

[KT00] [Y. Kubota, S. Tawada, K. Nakagawa, C. Naitoh, N. Sugimoto, Y. Fukushima, T. Hanaoka, Y. Imada, Y. Sugi, *Microporous and Mesoporous Materials* **2000**, *37*, 291–301]

[KU81] [M. Kageyama, S. Ueda, M. Koizumi, *Nippon Kagaku Kaishi* **1981**, *9*, 1510]

[LD94] [R. F. Lobo, M. E. Davis, *Microporous Materials* **1994**, *3*, 61-69]

[LG86] [F. Liebau, H. Gies, R.P. Gunawardane, B. Marler, *Zeolites* **1986**, *6*, 373]

[LM67] [G. Lucovsky, A. Mooradian, W. Taylor, G. B. Wright, R. C. Keezer, *Solid State Commun.* **1967**, *5*, 113-117]

[LS99] [S. Link, M. A. El Sayed, *J. Phys. Chem. B* **1999**, *103*, 8410]

[LZ95] [R. F. Lobo, S. I. Zones, M. E. Davis, *J. Inclusion Phenom. Mol. Recognit. Chem.* **1995**, *21*, 47]

[MB70] [A. R. Monahan, D. F. Blossey, *J. Phys. Chem.* **1970**, *74*, 4014]

[MD99] [J. Martinez-Triguero, M. J. Díaz-Cabañas, M. A. Camblor, V. Fornes, Th. L. M. Maesen, A. Corma, *J. Catal.* **1999**, *182*, 463-469]

[MG68] [W. R. Mason, H. B. Gray, *J. Am. Chem. Soc.* **1968**, *90*, 5721]

[MI77] [Y. Miyamoto, *Jpn. J. Appl Phys*. **1977**, *16*, 2257]

[MI80] [Y. Miyamoto, *Jpn. J. Appl Phys.* **1980**, *19/10*, 1813-1819]

[ML76] [R. M. Martin, G. Lucovsky, K. Helliwell, *Phys. Rev. B* **1976**, *13*, 1383]

[ML85] [R. J. Magana, J. S. Lannin, *Phys. Rev. B* **1985**, *32*, 3819]

[MP53] [R. E. Marsh, L. Pauling, J. D. McCullough, *Acta Cryst*. **1953**, *6*, 71]

[MU04] [O. Musolf, *PhD Thesis*, Universität Hannover, **2004**]

[MW69] [A. Mooradian, G. B. Wright, The Physics of Selenium and Tellurium, Pergamon, London, 1969, p. 269]

[NA86] [K. Nakamoto, Infrared and Raman Spectra of Inorganic and Coordinating Compounds, 4th Edition, Willey, New-York, 1986]

[NA93] [Y. Nakagawa, *U.S. Patent* **1993**, *5, 271, 922*]

[NB05] [R. Nechifor, P. Behrens, in Organosilicon VI, N. Auner, J. Weiss, Willey-VCH, Weinheim 2005, p. 930-936]

[NI81] [K. Nagata, T. Ishikawa, Y. Miyamoto, *Jpn. J. Appl. Phys*. **1981**, *20*, 463]

[NI83] [K. Nagata, T. Ishikawa, Y. Miyamoto, *Jpn. J. Appl. Phys*. **1983**, *22*, 1129-1132]

[NT81] [K. Nagata, H. Tashiro, Y. Miyamoto, *Jpn. J. Appl Phys.* **1981**, *20*, 2265]

[OG89] [G. A. Ozin, C. Gil, *Chem. Rev.* **1989**, *89*, 1749-1746]

[OJ96] [C. Oligschleger, R. O. Jones, S. M. Reimann, H. R. Schober, *Phys. Rev. B* **1996**, *53*, 6165]

[OK81] [D. H. Olson, G. T. Kokotailo, S. L. Lawton, W. M. Meier, *J. Phys. Chem.,* **1981***, 85***,** 2238-2243]

[OP71] [D. E. O'Reilly, E. M. Peterson, C. E. Scheie, J. M. Williams, *J. Chem. Phys.***1971**, *55*, 5629-5635]

[OS00] [R. W. Owens, D. A. Smith, *Langmuir* **2000**, *16*, 562]

[OZ92] [G. A. Ozin, *Adv. Mater*. **1992**, *4*, 612]

[PG90] [V. I. Pakhomov, A. V. Goryunov, I. N. Ivanova-Korfini, A. A. Boguslavskii, R. Sh. Lotfullin, *Zhurnal Neorganicheskoi Khimii* **1990**, *35*, 2476-2478 and *Phase Transition* **1992**, *38*, 127-220]

[PI99] [B. Pillep, *PhD Thesis*, Universität München, **1999**]

[PK97] [V. V. Poborchii, A. V. Kolobov, H. Oyanagi, S. G. Romanov, K. Tanaka, *Chem. Phys. Letters* **1997**, *280*, 10-16]

[PK99] [V. V. Poborchii, A. V. Kolobov, J. Caro, V. V. Zhuravlev, K. Tanaka, *Phys. Rev. Lett.* **1999**, *82*(9), 1955-1958]

[PM92] [C. Petrillo, O. Moze, R. M. Ibberson, *Physik* (Berlin) **1992**, *180*, 639-641]

[PS87] [I. Persson, M. Sandstöm, P. L. Goggin, *Inorg. Chim. Acta* **1987**, *129*, 183]

[PS94] [A. E. Persson, B.J. Schoeman, J. Sterte, J.E. Otterstedt, *Zeolites* **1994**, *14*, 557]

[RA94] [J. Rouquérol, D. Avnir, C. W. Fairbridge, D. H. Everett, J. H. Haynes, N. Pericone, J. D. F. Ramsay, K. S. W. Sing, K. K. Unger, *Pure Appl. Chem.* **1994**, *66*, 1739–1758]

[RB98] [A. R. Ramsaran, K. J. Balkus Jr., M. A. Biscotto, J. E. Sheats, K. T. Micai, S. Furyk, A. Hamilton, *Preprints - American Chemical Society, Division of Petroleum Chemistry* **1998**, *43*(2), 289-291]

[RE41] [E. Rabinowitch, L. F. Epstein, *J. Am. Chem. Soc.* **1941**, *63*, 69]

[RE82] [J. L. Robbins, N. Edelstein, B. Spencer, J. C. Smart, *J. Am. Chem. Soc.* **1982**, *104*(7), 1882-1893]

[PG90] [V. I. Pakhomov, A. V. Goryunov, I. N. Ivanova-Korfini, A. A. Boguslavskii, R. Sh. Lotfullin, *Zhurnal Neorganicheskoi Khimii* **1990**, *35*, 2476-2478; *Phase Transition* **1992**, *38*, 127-220]

[RG91] [D. S. Rustad, N. W. Gregory, *Polyhedron* **1991**, *10*, 633-643]

[RK52] [H. Richter, W. Kulcke, H. Specht, *Z. Naturforsch*. **1952***, 7a*, 511]

[RK98] [R. Ravishankar, C.E.A. Kirschhock, B.J. Schoeman, P. Vanoppen, P.J. Grobet, S. Storck, W.F. Maier, J.A. Martens, F.C.E.A. De Schryver, P.A. Jacobs, *J. Phys. Chem. B* **1998**, *102*, 2633]

[RK99a] [R. Ravishankar, C.E.A. Kirschhock, B.J. Schoeman, D. De Vos, P.J. Grobet, P.A. Jacobs, J.A. Martens, Synthesis, isolation and characterisation of nano-powder of Silicalite-1 type molecular sieves, in Proceedings of the 12th International Zeolite Conference, Vol. III, Treacy, Marcus, Bisher, Higgins, Eds., Materials Research Society, Warrendale, Pennsylvania, USA, 1999, p. 1825]

[RK99b] [R. Ravishankar, C.E.A. Kirschhock, P.P. Knops-Gerrits, E.J.P. Feijen, P.J. Grobet, P. Vanoppen, F.C.E.A. De Schryver, G. Miehe, H. Fuess, B.J. Schoeman, P.A. Jacobs, J.A. Martens, *J. Phys. Chem. B* **1999**, *103*, 4960]

[RN99] [R. Ricceri, C. Neto, A. Abbotto, A. Facchetti, G. A. Pagani, *Langmuir* **1999**, *15*, 2149]

[RR73] [W. Richter, J. B. Renucci, M. Cardona, *Phys. Status Solidi (b)* **1973**, *56*, 223]

[RR99] [F. Rouquerol, J. Rouquerol, S. King, Adsorption by Powders & Porous Solids, Principles, Methodology and Applications, Academic Press, San Diego, California, USA, 1999, p. 223]

[SB64] [D. J. Seery, D. Britton, *J. Phys. Chem*. **1964**, *68*, 2266]

[SB78] [T. N. Silukova, P. A. Babin, S. F. Voropaev, *Fiz. Kondensiv. Sostoyaniya Veshchestva, Khabarovsk* **1978**, 14]

[SD90] [G. D. Stucky, J. E. MacDougall, *Science* **1990**, *247*, 69]

[SH79] [J. E. Sheats, The Chemistry of Cobaltocene, Cobalticinium Salts and Other Cobalt Sandwich Compounds, in: D. Seyferth, A. G. Davies, E. O. Fischer, J. F. Normant, O. A. Reutov (Herausgeber), Organomet. Chem. Rev., Band 7, J. Organomet. Chem. Libr., Elsevier, Amsterdam-Oxford-New York, 1979, p. 461-521]

[SL74] [J. Straehle, K. P. Loercher, *Z. Naturforschung*, Teil B. Anorganische Chemie, Organische Chemie **1974**, *29*, 266-267]

[SL81] [B. V. Shanabrook, J. S. Lannin, *Solid State Commun.* **1981**, *38*, 49]

[SN75] [H. G. Smith, M. Nielsen, C. B. Clark, *Chem Phys. Lett.* **1975**, *33*, 75]

[SO56] [S. A. Shchukarev, M. A. Oranskaya, V. M. Tsintsius, *Zh. Neorg. Khim.* **1956**, *1*, 881]

[SO99] [J. O. Smith, D. A. Olson, B. A. Armitage, *J. Am. Chem. Soc.* **1999**, *121*, 2686]

[SS80] [V. Subramanian, K. Seff, *Acta Cryst. B* **1980**, *36*, 2132-2135]

[SS84] [R. Steudel, E. M. Strauss, *Advan. Inorg. Chem. Radiochem*. **1984**, *28*, 135]

[SS93] [B.J. Schoeman, J. Sterte, J.E. Otterstedt, *Chem. Commun*. **1993**, 994]

[SS94a] [B.J. Schoeman, J. Sterte, J.E. Otterstedt, *Zeolites* **1994**, *14*, 110]

[SS94b] [B.J. Schoeman, J. Sterte, J.E. Otterstedt, *Zeolites* **1994**, *14*, 568]

[SW02] [G. Schulz-Ekloff, D. Wöhrle, B. van Duffel, R. A. Schoonheydt, *Microporous Mesoporous Materials* **2002**, *51*, 91]

[TA73] [C. Tanford, The Hydrophobic Effect, John Willey & Sons, New York, 1973]

[TD72] [P. Templet, J. R. McDonald, S. P. McGlynn, C. H. Kendrow, J. L. Roebber, K. Weiss, *J. Chem. Phys*. **1972**, *56*, 5746]

[TI58] [Chemical Society Special Publications Nos. 11 and 18, Tables of Interatomic Distances and Configurations in Molecules and Ions, London, 1958, 1965]

[TT60] [JANAF Thermochemical Tables, The Dow Chemical Company, Midland, Michigan, 1960-68]

[TT65] [D. R. Stull (Ed.), JANAF Thermochemical Tables, Dow Chemical Co., Midland, Michigan, 1965-67]

[UC67] [P. Unger, P Cherin, *Phys. Selenium Tellurium Proc. Intern. Symp. Montreal* **1967 (1969)**, 223-229]

[UC69] [P. Unger, P. Cherin, *The Physics of Selenium and Tellurium*, Pergamon, London, **1969**, p.223]

[UF03] [B. Ufer, *Diplomarbeit*, Universität Hannover, **2003**]

[UK79] [S. Ueda, M. Koizumi, *Am. Mineral*. **1979**, *64*, 172]

[UK84] [S. Ueda, N. Kageyama, M. Koizumi, S. Kobayashi, Y. Fujiwara, Y. Kyoguku, *J. Phys. Chem*. **1984**, *88*, 2128]

[UM80] [S. Ueda, H. Murata, M. Koizumi, H. Nishimura, *Am. Mineral.* **1980**, *65*, 1012]

[VP94] [G. A. Voyiatzis, G. N. Papatheodorou, Ber. Bunsenges. *Phys. Chem*. **1994**, *98*, 683]

[VP99] [V. Valtchev, J.-L. Paillaud, H. Kessler, E. J. Creyghton, *Microporous and Mesoporous Materials* **1999**, *3* (1-3), 143-148]

[WA80] [W. R. Wadt, *J. Chem. Phys*. **1980**, *72*, 2469]

[WB99a] [T. Wessels, C. Baerlocher, L. B. McCusker, *Science* **1999**, *284*, 477-479]

[WB99b] [T. Wessels, C. Baerlocher, L. B. McCusker, E. J. Creyghton, *J. Am. Chem. Soc.,* **1999***, 121***,** 6242-6247]

[WE62] [A. F. Wells, Structural Inorganic Chemistry, 3rd Ed., Oxford University Press, 1962]

[WF99a] [G. Wirnsberger, H.P. Fritzer, H. Koller, P. Behrens, A. Popitsch, *J. Molec. Str.* **1999**, *480-481,* 699-704]

[WF99b] [G. Wirnsberger, H.P. Fritzer, R. Zink, A. Popitsch, B. Pillep, P. Behrens, *J. Phys. Chem. B* **1999**, *103,* 5797-5801]

[WI98] [G. Wirnsberger, *PhD Thesis,* Graz University of Technology, **1998**]

[WL79] [E. L. Wu, S. L. Lawton, D. H. Olson, A. C. Rohrman Jr., G. T. Kokotailo, *J. Phys. Chem.* **1979**, *83*, 2777]

[WP96] [G. Wirnsberger, A. Popitsch, H.P. Fritzer, G. van de Goor, P. Behrens, *Angew. Chem. Intern. Ed. Engl*. **1996**, *35*, 2777-2779]

[WP02] [G. Wirnsberger, B. M. Pillep, A. Popitsch, P. Knoll, P. Behrens, *Chem. Eur. J*. **2002**, *8/17*, 3927]

[WY97] [P. Wagner, M. Yoshikawa, M. Lovallo, K. Tsuji, M. Tsapatsis, M. E. Davis, *Chem. Commun*. **1997**, *22*, 2179-2180]

[YN88] [M. Yao, N. Nakamura, H. Endo, *Z. Phys. Chem*. **1988**, *157*, 569]

[YP68] [R. Yamdagni, R. F. Porter, *J. Electrochem. Soc.* **1968**, *115*, 601]

[YW98] [M. Yoshikawa, P. Wagner, M. Lovallo, K. Tsuji, T. Takewaki, C. Y. Chen, L. W. Beck, C. Jones, M. Tsapatsis, S. I. Zones, M. E. Davis, *J. Phys. Chem. B* **1998***, 102***,** 7139-7147]

[ZL96] [X. S. Zhao, G. Q. Lu, G. J. Millar, *Ind. Eng. Chem. Res.* **1996**, *35*, 2075]

Table of acronyms

AFI	structure code of AlPO-5 / SSZ-24
Å	Angström, 10^{-10} m
as-synth.	as-synthesized
calc.	calcined
BET	Brunauer-Emmett-Teller model
CFI	structure code of CIT-5
CIT-5	California Institute of Technology-5
cp	cyclopentadyenyl
*cp**	pentamethylcyclopentadienyl
CTMA	cetyltrimethylammonium
CTAB	cetyltrimethylammonium bromide
d	day(s)
d	diffraction length in XRD
DDR	structure code of decadodecasil 3R
DON	structure code of UTD-1(F)
DTA	differential thermal analysis
DTG	differential thermogravimetry
EtOH	ethanol
HR-TEM	high-resolution transmission electron microscopy
I	intensity
IFR	structure code of ITQ-4
IR	infrared
ITQ-4	Instituto de Tecnología Química-4
IZA	International Zeolite Association
λ	wavelength
MFI	structure code of ZSM-5 / Silicalite-1
MO	molecular orbital
MS	*N*(16)-methylsparteinium cation
puriss.	purity ~ 99 % for analysis
purum	purity ~ 98 %
Raman	Raman spectroscopy
REM	resonance electron microscopy

SDA	structure-directing agent
SEM	scanning electron microscopy
SSZ-24	Socal (Standard Oil of California) Synthetic Zeolite-24
t	time
T	temperature
TEOS	tetraethylorthosilicate
TG	thermogravimetry
TGA	thermogravimetric analysis
TPA	tetrapropylammonium
TPAOH	tetrapropylammonium hydroxide
UTD-1	University of Texas Dallas-1
UV	ultraviolet
UV-vis	ultraviolet-visible spectroscopy
$\widetilde{\nu}$	wavenumber
XRD	X-ray diffraction
XRS	X-ray scattering

A1. Silicalite-1 as-synthesized

Symmetry : Orthorhombic *P*
Space group : *P n m a* (No. 62)

Refined cell parameters:
a : 20.020(6)
b : 19.916(5)
c : 13.3664(24)

N	2Θ[obs]	H	K	L	2Θ[calc]	obs-calc	Int.	*d*[obs]	*d*[calc]
1	7.978	1	0	1	7.947	0.0317	82.6	11.0724	11.1165
		0	1	1	7.960	0.0188			11.0985
2	8.872	0	2	0	8.873	-0.0011	34.9	9.9591	9.9579
3	9.127	1	1	1	9.103	0.0235	24.1	9.6818	9.7067
4	9.896	2	1	0	9.881	0.0145	7.7	8.9308	8.9439
5	11.935	2	1	1	11.896	0.0384	13.5	7.4094	7.4333
		1	2	1	11.922	0.0125			7.4172
6	12.550	2	2	0	12.528	0.0218	7.3	7.0475	7.0597
7	13.247	0	0	2	13.237	0.0100	10.9	6.6781	6.6832
8	13.976	1	0	2	13.959	0.0174	19.9	6.3315	6.3393
9	14.672	1	1	2	14.652	0.0199	12.1	6.0325	6.0407
10	14.848	3	0	1	14.825	0.0227	10.6	5.9616	5.9706
11	15.550	1	3	1	15.535	0.0157	14.1	5.6939	5.6996
12	15.959	2	0	2	15.932	0.0268	17.7	5.5490	5.5582
		0	2	2	15.958	0.0008			5.5492
13	16.558	2	1	2	16.545	0.0126	5.4	5.3496	5.3536
		1	2	2	16.564	-0.0062			5.3476
14	17.322	3	2	1	17.304	0.0183	7.2	5.1153	5.1207
		2	3	1	17.333	-0.0117			5.1119
15	17.790	0	4	0	17.800	-0.0097	7.7	4.9816	4.9789
16	19.321	3	1	2	19.302	0.0193	10.8	4.5903	4.5949
		1	3	2	19.345	-0.0238			4.5847
17	19.994	3	3	1	19.985	0.0088	6.4	4.4374	4.4393
18	20.414	1	0	3	20.404	0.0105	15.7	4.3468	4.3491
		0	1	3	20.409	0.0054			4.3480
19	20.912	1	1	3	20.890	0.0220	14.4	4.2445	4.2489
		4	2	1	20.930	-0.0180			4.2409
20	21.823	2	0	3	21.817	0.0065	5.0	4.0693	4.0705
21	22.243	4	3	0	22.226	0.0169	10.0	3.9935	3.9965
		0	4	2	22.247	-0.0044			3.9927
		2	1	3	22.274	-0.0309			3.9880
22	22.690	1	4	2	22.691	-0.0009	3.8	3.9158	3.9156
23	23.188	5	0	1	23.171	0.0170	100.0	3.8329	3.8356
		4	3	1	23.211	-0.0238			3.8290
24	23.720	1	5	1	23.709	0.0112	27.3	3.7480	3.7497
25	24.000	2	4	2	23.976	0.0245	61.7	3.7049	3.7086
		3	0	3	23.996	0.0042			3.7055
		2	5	0	24.026	-0.0259			3.7009
		0	3	3	24.036	-0.0353			3.6995
26	24.452	3	1	3	24.414	0.0376	45.7	3.6375	3.6430
		1	3	3	24.449	0.0030			3.6379
27	24.862	5	2	1	24.856	0.0063	3.9	3.5784	3.5793
28	25.629	3	2	3	25.630	-0.0012	4.7	3.4730	3.4728
		2	3	3	25.651	-0.0218			3.4701
29	25.961	4	3	2	25.956	0.0046	13.8	3.4294	3.4300
		3	4	2	25.985	-0.0240			3.4263

30	26.319	5	1	2	26.309	0.0098	3.2	3.3836	3.3848
31	26.400	1	5	2	26.405	-0.0048	3.5	3.3733	3.3727
32	26.753	4	0	3	26.767	-0.0143	11.6	3.3296	3.3279
33	27.026	1	0	4	27.031	-0.0051	13.1	3.2966	3.2960
34	27.416	1	1	4	27.406	0.0099	3.4	3.2506	3.2518
		5	2	2	27.446	-0.0308			3.2470
35	27.535	2	5	2	27.528	0.0079	5.3	3.2367	3.2376
		6	0	1	27.530	0.0055			3.2374
		3	3	3	27.545	-0.0100			3.2356
36	28.127	2	0	4	28.130	-0.0034	4.0	3.1700	3.1696
		0	2	4	28.145	-0.0186			3.1680
37	28.499	2	1	4	28.492	0.0070	5.5	3.1295	3.1303
		1	2	4	28.503	-0.0042			3.1290
38	28.975	6	2	1	28.979	-0.0036	2.1	3.0791	3.0787
39	29.315	3	5	2	29.310	0.0048	14.0	3.0442	3.0447
40	30.020	5	0	3	29.980	0.0396	12.1	2.9743	2.9781
		4	3	3	30.012	0.0074			2.9750
		0	6	2	30.035	-0.0153			2.9728
		3	4	3	30.037	-0.0175			2.9726
41	30.207	3	1	4	30.222	-0.0145	3.3	2.9563	2.9549
42	30.402	1	6	2	30.372	0.0299	9.3	2.9378	2.9406
		1	5	3	30.406	-0.0041			2.9374
43	31.316	5	2	3	31.325	-0.0092	3.2	2.8541	2.8533
44	32.200	4	0	4	32.183	0.0168	2.8	2.7777	2.7791
		0	4	4	32.237	-0.0368			2.7746
45	32.865	3	3	4	32.844	0.0208	5.0	2.7230	2.7247
		6	3	2	32.869	-0.0039			2.7227
46	33.512	2	4	4	33.487	0.0248	2.2	2.6719	2.6738
		6	0	3	33.527	-0.0145			2.6708
47	33.788	1	0	5	33.800	-0.0127	1.8	2.6507	2.6498
		0	1	5	33.804	-0.0159			2.6495
48	34.442	5	5	2	34.451	-0.0090	9.7	2.6019	2.6012
49	34.718	2	0	5	34.705	0.0137	3.4	2.5818	2.5828
		6	2	3	34.748	-0.0301			2.5796
50	34.967	5	0	4	34.945	0.0225	3.7	2.5639	2.5655
		4	3	4	34.973	-0.0056			2.5635
		3	4	4	34.995	-0.0273			2.5620
		2	1	5	35.005	-0.0371			2.5613
51	35.254	5	1	4	35.243	0.0104	3.0	2.5438	2.5445
		7	2	2	35.276	-0.0220			2.5423
52	35.845	8	0	0	35.854	-0.0092	4.2	2.5031	2.5025
53	36.162	5	2	4	36.125	0.0370	6.4	2.4820	2.4844
		8	1	0	36.146	0.0158			2.4830
		3	0	5	36.168	-0.0058			2.4816
		2	5	4	36.188	-0.0266			2.4802
		0	3	5	36.195	-0.0331			2.4798
54	36.482	3	1	5	36.457	0.0248	2.1	2.4609	2.4625
		1	3	5	36.481	0.0008			2.4610
		8	0	1	36.499	-0.0172			2.4598
55	36.744	7	3	2	36.734	0.0104	2.1	2.4439	2.4446
56	36.982	1	8	1	36.974	0.0082	2.4	2.4288	2.4293
		8	2	0	37.009	-0.0271			2.4271
		4	4	4	37.015	-0.0331			2.4267
57	37.307	3	2	5	37.314	-0.0069	3.7	2.4084	2.4079
		2	3	5	37.329	-0.0216			2.4070
		7	0	3	37.332	-0.0245			2.4068
58	37.588	5	3	4	37.554	0.0336	5.1	2.3910	2.3931
		3	5	4	37.601	-0.0133			2.3902
		7	1	3	37.613	-0.0254			2.3894
		6	5	2	37.623	-0.0352			2.3888
59	37.734	1	7	3	37.753	-0.0193	2.7	2.3821	2.3809

60	38.155	4	0	5	38.134	0.0212	2.0	2.3567	2.3580
		0	6	4	38.186	-0.0303			2.3549
61	38.386	6	1	4	38.359	0.0276	2.0	2.3431	2.3447
		8	0	2	38.377	0.0090			2.3436
		8	3	0	38.410	-0.0241			2.3417
		4	1	5	38.411	-0.0245			2.3416
62	38.782	4	7	2	38.790	-0.0076	2.2	2.3201	2.3197
63	39.172	3	8	1	39.175	-0.0030	1.9	2.2979	2.2977
		6	2	4	39.180	-0.0085			2.2974
64	40.543	6	3	4	40.518	0.0253	1.5	2.2233	2.2246
		5	0	5	40.543	0.0002			2.2233
		4	3	5	40.567	-0.0245			2.2220
65	41.016	1	1	6	40.981	0.0348	1.8	2.1987	2.2005
		4	8	1	41.018	-0.0021			2.1986
66	41.570	1	9	1	41.578	-0.0081	1.5	2.1707	2.1703
		5	2	5	41.587	-0.0163			2.1699
		8	1	3	41.605	-0.0351			2.1689
67	41.727	4	7	3	41.734	-0.0077	1.7	2.1629	2.1625
		2	1	6	41.752	-0.0249			2.1617
		1	2	6	41.760	-0.0329			2.1613
68	42.357	6	4	4	42.331	0.0258	1.4	2.1322	2.1334
		2	9	1	42.340	0.0176			2.1330
		8	2	3	42.374	-0.0170			2.1313
		4	4	5	42.379	-0.0223			2.1311
		4	6	4	42.384	-0.0272			2.1309
69	42.542	2	2	6	42.518	0.0237	1.6	2.1233	2.1245
		2	8	3	42.533	0.0090			2.1238
		7	2	4	42.551	-0.0093			2.1229
70	42.985	3	1	6	43.010	-0.0254	2.6	2.1025	2.1013
71	43.305	1	9	2	43.271	0.0336	1.9	2.0877	2.0892
		5	8	1	43.293	0.0112			2.0882
		6	0	5	43.335	-0.0306			2.0863
72	43.609	3	9	1	43.584	0.0244	3.1	2.0738	2.0749
		6	1	5	43.584	0.0242			2.0749
		8	3	3	43.631	-0.0223			2.0728
73	43.773	3	2	6	43.759	0.0144	2.3	2.0664	2.0671
		2	3	6	43.772	0.0015			2.0665
		3	8	3	43.773	0.0000			2.0664
		7	3	4	43.804	-0.0307			2.0650
		9	2	2	43.810	-0.0372			2.0648
74	43.896	7	6	2	43.893	0.0037	2.2	2.0609	2.0611
		3	7	4	43.907	-0.0105			2.0604
		7	5	3	43.917	-0.0211			2.0600
		6	7	2	43.926	-0.0297			2.0596
75	44.579	6	5	4	44.575	0.0043	1.2	2.0309	2.0311
		5	4	5	44.598	-0.0190			2.0301
		5	6	4	44.603	-0.0237			2.0299
76	45.220	3	9	2	45.216	0.0035	13.1	2.0036	2.0038
		8	0	4	45.233	-0.0130			2.0031
		10	0	0	45.258	-0.0381			2.0020
77	45.478	7	7	1	45.439	0.0395	10.8	1.9928	1.9945
		4	2	6	45.450	0.0284			1.9940
		4	8	3	45.464	0.0145			1.9934
		8	1	4	45.474	0.0047			1.9930
		2	4	6	45.480	-0.0016			1.9928
		10	1	0	45.499	-0.0203			1.9920
		0	10	0	45.508	-0.0302			1.9916
		7	4	4	45.511	-0.0329			1.9915
78	46.278	1	10	1	46.275	0.0030	2.1	1.9602	1.9604
79	46.601	7	6	3	46.573	0.0276	4.0	1.9474	1.9485
		0	7	5	46.580	0.0202			1.9482

		6	7	3	46.605	-0.0043			1.9472
		5	0	6	46.618	-0.0176			1.9467
		4	3	6	46.640	-0.0397			1.9458
80	47.458	8	6	2	47.450	0.0072	3.9	1.9142	1.9145
		8	5	3	47.474	-0.0161			1.9136
81	47.606	5	8	3	47.568	0.0377	3.5	1.9086	1.9100
		10	1	2	47.596	0.0101			1.9090
		0	10	2	47.605	0.0006			1.9086
		2	5	6	47.605	0.0004			1.9086
		7	5	4	47.636	-0.0298			1.9075
82	48.081	1	1	7	48.043	0.0375	1.2	1.8909	1.8923
83	48.689	5	3	6	48.706	-0.0169	6.4	1.8687	1.8680
		2	1	7	48.724	-0.0350			1.8674
84	48.928	8	7	1	48.909	0.0188	2.0	1.8601	1.8608
		5	9	2	48.924	0.0037			1.8602
		7	8	1	48.944	-0.0167			1.8595
85	49.581	7	7	3	49.569	0.0124	2.7	1.8371	1.8375
		1	9	4	49.578	0.0034			1.8372
		3	0	7	49.618	-0.0370			1.8358
86	49.819	3	1	7	49.843	-0.0237	1.5	1.8289	1.8281

A2. Silicalite-1 calcined

Symmetry : Monoclinic *B*

Refined cell parameters:
a : 19.847(15)
b : 20.059(16)
c : 13.33(3)
β : 90.43(18)

N	2Θ[obs]	H	K	L	2Θ[calc]	obs-calc	Int.	*d*[obs]	*d*[calc]
1	7.964	-1	0	1	7.956	0.0076	100.0	11.0932	11.1038
		0	1	1	7.958	0.0058			11.1012
		1	0	1	8.012	-0.0485			11.0261
2	8.848	0	2	0	8.810	0.0385	42.3	9.9859	10.0295
		2	0	0	8.904	-0.0562			9.9231
3	9.100	-1	1	1	9.096	0.0046	16.6	9.7098	9.7147
		1	1	1	9.145	-0.0446			9.6625
4	9.892	1	2	0	9.873	0.0185	2.5	8.9346	8.9514
		2	1	0	9.937	-0.0450			8.8942
5	11.058	0	2	1	11.031	0.0269	2.3	7.9946	8.0140
		-2	0	1	11.067	-0.0085			7.9885
6	11.927	-1	2	1	11.881	0.0465	1.9	7.4139	7.4428
		-2	1	1	11.915	0.0124			7.4216
		1	2	1	11.919	0.0087			7.4193
		2	1	1	11.990	-0.0629			7.3751
7	13.258	0	3	0	13.231	0.0269	7.4	6.6728	6.6863
		0	0	2	13.275	-0.0172			6.6642
8	13.980	1	3	0	13.965	0.0144	10.2	6.3299	6.3364
		-1	0	2	13.975	0.0049			6.3321
		0	1	2	13.992	-0.0123			6.3243
		1	0	2	14.039	-0.0595			6.3032
9	14.801	0	3	1	14.811	-0.0102	11.6	5.9805	5.9765
10	14.994	3	0	1	14.984	0.0104	5.2	5.9038	5.9078
11	15.527	-1	3	1	15.457	0.0703	4.7	5.7022	5.7280
		1	3	1	15.486	0.0411			5.7173
		-3	1	1	15.537	-0.0096			5.6987
12	15.614	-3	1	1	15.537	0.0774	4.7	5.6706	5.6987
		3	1	1	15.624	-0.0097			5.6671
13	15.921	-2	0	2	15.950	-0.0291	8.2	5.5620	5.5519
		0	2	2	15.954	-0.0328			5.5506
		2	3	0	15.970	-0.0491			5.5450
14	16.506	-1	2	2	16.543	-0.0369	3.1	5.3661	5.3543
		-2	1	2	16.554	-0.0479			5.3507
15	17.306	-2	3	1	17.281	0.0253	2.4	5.1199	5.1273
		-3	2	1	17.329	-0.0228			5.1132
		2	3	1	17.333	-0.0271			5.1119
16	17.673	0	4	0	17.672	0.0007	4.0	5.0146	5.0147
17	17.863	4	0	0	17.863	0.0003	5.8	4.9614	4.9615
18	19.280	-1	3	2	19.290	-0.0102	4.2	4.6000	4.5976
		-3	1	2	19.331	-0.0512			4.5879
		1	3	2	19.337	-0.0574			4.5865
19	20.415	-1	0	3	20.435	-0.0198	5.5	4.3467	4.3425
		0	1	3	20.458	-0.0428			4.3377
20	20.919	2	3	2	20.867	0.0521	6.3	4.2431	4.2536
		-2	4	1	20.898	0.0204			4.2472
		-1	1	3	20.914	0.0054			4.2442

		3	2	2	20.940	-0.0209		4.2390
		2	4	1	20.942	-0.0233		4.2385
		1	1	3	20.979	-0.0601		4.2311
21	21.843	-2	0	3	21.839	0.0038	3.8	4.0658	4.0665
		0	2	3	21.862	-0.0199		4.0621
22	22.203	0	5	0	22.140	0.0631	4.1	4.0005	4.0118
		0	4	2	22.167	0.0363		4.0070
		3	4	0	22.227	-0.0238		3.9963
		-4	0	2	22.239	-0.0355		3.9942
23	22.581	1	5	0	22.594	-0.0124	2.7	3.9344	3.9323
		-1	4	2	22.600	-0.0184		3.9312
		1	4	2	22.640	-0.0589		3.9243
24	23.098	-3	3	2	23.070	0.0282	35.3	3.8475	3.8521
		0	5	1	23.134	-0.0362		3.8416
25	23.278	-4	3	1	23.243	0.0349	14.5	3.8182	3.8239
		3	4	1	23.247	0.0304		3.8231
		-5	0	1	23.316	-0.0382		3.8120
		4	3	1	23.322	-0.0440		3.8111
26	23.414	5	0	1	23.414	-0.0008	15.1	3.7964	3.7963
27	23.713	2	2	3	23.706	0.0074	8.6	3.7491	3.7502
		-5	1	1	23.739	-0.0260		3.7450
28	23.978	2	5	0	23.906	0.0720	20.9	3.7083	3.7193
		-4	2	2	23.962	0.0162		3.7108
		2	4	2	23.969	0.0087		3.7096
		-3	0	3	24.024	-0.0464		3.7013
		0	3	3	24.030	-0.0521		3.7004
29	24.356	-1	3	3	24.422	-0.0664	8.0	3.6516	3.6419
30	24.605	3	1	3	24.605	-0.0001	8.0	3.6152	3.6152
31	25.549	-2	3	3	25.619	-0.0703	3.4	3.4838	3.4744
32	25.839	3	2	3	25.796	0.0436	4.6	3.4452	3.4510
		0	5	2	25.902	-0.0624		3.4371
33	26.010	3	5	0	25.954	0.0568	4.3	3.4230	3.4303
		-4	3	2	25.964	0.0467		3.4290
		-5	0	2	26.021	-0.0104		3.4216
		3	4	2	26.030	-0.0196		3.4204
		-4	4	1	26.078	-0.0679		3.4142
		5	3	0	26.087	-0.0762		3.4131
34	26.313	-1	5	2	26.277	0.0364	2.9	3.3843	3.3889
		1	5	2	26.312	0.0012		3.3844
35	26.582	5	1	2	26.578	0.0034	4.7	3.3507	3.3511
		0	6	0	26.642	-0.0609		3.3432
36	27.036	5	3	1	26.987	0.0491	5.7	3.2954	3.3013
		4	0	3	27.019	0.0168		3.2974
		1	6	0	27.025	0.0111		3.2967
		-1	0	4	27.079	-0.0434		3.2902
		0	1	4	27.106	-0.0696		3.2871
37	27.401	4	1	3	27.389	0.0120	3.4	3.2523	3.2537
		-2	5	2	27.406	-0.0054		3.2517
		-1	1	4	27.448	-0.0474		3.2468
		2	5	2	27.474	-0.0731		3.2438
38	29.229	-3	5	2	29.210	0.0194	3.3	3.0529	3.0549
		6	2	1	29.232	-0.0029		3.0526
		-5	3	2	29.297	-0.0680		3.0460
		3	5	2	29.306	-0.0763		3.0451
39	29.452	-5	4	1	29.408	0.0439	3.1	3.0303	3.0348
		4	5	1	29.413	0.0392		3.0343
		5	3	2	29.456	-0.0046		3.0299
		5	4	1	29.487	-0.0354		3.0268
40	29.927	0	6	2	29.876	0.0504	9.8	2.9833	2.9882
		-3	0	4	29.909	0.0176		2.9850
		3	6	0	29.922	0.0048		2.9838

		0	3	4	29.937	-0.0104		2.9823
		-3	4	3	29.982	-0.0550		2.9780
		0	5	3	29.986	-0.0596		2.9775
41	30.271	4	3	3	30.196	0.0746	5.2	2.9502	2.9573
		-1	6	2	30.206	0.0649		2.9564
		6	0	2	30.232	0.0388		2.9539
		1	6	2	30.237	0.0339		2.9534
		-3	1	4	30.246	0.0243		2.9525
		-1	3	4	30.250	0.0202		2.9521
		5	0	3	30.284	-0.0138		2.9489
		-1	5	3	30.307	-0.0363		2.9468
		1	3	4	30.312	-0.0416		2.9463
42	31.244	0	7	0	31.187	0.0572	2.7	2.8604	2.8656
		-2	6	2	31.205	0.0397		2.8640
		-2	3	4	31.233	0.0114		2.8615
		-3	2	4	31.238	0.0063		2.8610
		2	6	2	31.265	-0.0204		2.8586
		-2	5	3	31.295	-0.0510		2.8559
43	32.146	-7	0	1	32.204	-0.0577	2.6	2.7823	2.7774
		-4	0	4	32.221	-0.0750		2.7759
44	32.739	4	1	4	32.768	-0.0286	2.7	2.7332	2.7309
		7	2	0	32.800	-0.0610		2.7282
		-3	6	2	32.818	-0.0793		2.7268
45	33.406	-2	4	4	33.445	-0.0384	1.5	2.6801	2.6771
		-7	2	1	33.451	-0.0444		2.6767
		-4	2	4	33.467	-0.0612		2.6754
46	33.765	4	2	4	33.693	0.0718	2.4	2.6525	2.6580
		-1	6	3	33.810	-0.0448		2.6491
47	34.298	1	1	5	34.239	0.0584	2.0	2.6125	2.6168
		-7	0	2	34.249	0.0485		2.6160
		-1	7	2	34.322	-0.0240		2.6107
		7	3	0	34.328	-0.0305		2.6102
		1	7	2	34.350	-0.0517		2.6086
48	35.167	3	4	4	35.116	0.0520	1.8	2.5498	2.5535
		1	2	5	35.130	0.0372		2.5524
		6	5	0	35.135	0.0324		2.5521
		2	1	5	35.183	-0.0157		2.5487
		4	3	4	35.187	-0.0194		2.5485
		4	5	3	35.203	-0.0350		2.5474
		-2	7	2	35.216	-0.0489		2.5464
		6	4	2	35.234	-0.0663		2.5452
49	35.710	-5	6	1	35.693	0.0176	2.5	2.5123	2.5135
		-6	5	1	35.755	-0.0444		2.5093
		5	6	1	35.760	-0.0492		2.5090
		0	8	0	35.783	-0.0725		2.5074
50	36.142	1	8	0	36.077	0.0646	3.5	2.4833	2.4876
		-2	5	4	36.111	0.0305		2.4853
		-5	2	4	36.162	-0.0200		2.4820
		4	7	0	36.170	-0.0281		2.4814
		-3	6	3	36.177	-0.0355		2.4809
		8	0	0	36.180	-0.0382		2.4808
		-3	0	5	36.206	-0.0643		2.4790
		2	5	4	36.217	-0.0753		2.4783
51	37.233	8	1	1	37.156	0.0767	2.1	2.4130	2.4178
		4	4	4	37.190	0.0421		2.4156
		8	2	0	37.310	-0.0771		2.4082
		0	7	3	37.311	-0.0782		2.4081
52	45.100	3	9	2	45.020	0.0796	5.2	2.0087	2.0120
		4	1	6	45.031	0.0691		2.0116
		-4	9	1	45.050	0.0497		2.0108
		4	9	1	45.094	0.0056		2.0089

		8	5	2	45.120	-0.0199		2.0078
		0	10	0	45.165	-0.0654		2.0059
53	45.623	-7	4	4	45.557	0.0658	4.8	1.9868	1.9896
		-6	3	5	45.571	0.0521		1.9890
		-8	1	4	45.612	0.0111		1.9873
		2	4	6	45.617	0.0064		1.9871
		4	7	4	45.629	-0.0059		1.9866
		10	0	0	45.677	-0.0540		1.9846
		3	6	5	45.679	-0.0557		1.9845
		0	10	1	45.703	-0.0796		1.9836
54	46.470	-2	9	3	46.423	0.0472	1.8	1.9526	1.9545
		2	9	3	46.487	-0.0174		1.9519
		0	7	5	46.490	-0.0207		1.9518
		10	1	1	46.497	-0.0274		1.9515
		-6	7	3	46.519	-0.0491		1.9506
		-7	0	5	46.548	-0.0787		1.9495
55	47.543	-7	2	5	47.473	0.0710	2.5	1.9110	1.9137
		-8	3	4	47.474	0.0691		1.9136
		2	7	5	47.488	0.0554		1.9131
		-1	10	2	47.510	0.0337		1.9122
		-8	6	2	47.518	0.0255		1.9119
		6	4	5	47.523	0.0207		1.9117
		6	8	2	47.528	0.0159		1.9116
		1	10	2	47.531	0.0126		1.9114
		-8	5	3	47.550	-0.0066		1.9107
		9	5	1	47.552	-0.0085		1.9106
		5	8	3	47.564	-0.0200		1.9102
		-5	7	4	47.574	-0.0308		1.9098
		-2	5	6	47.581	-0.0377		1.9095
		-3	9	3	47.587	-0.0432		1.9093
		-5	2	6	47.590	-0.0463		1.9092
56	48.516	8	7	0	48.498	0.0180	2.3	1.8749	1.8756
		4	4	6	48.510	0.0053		1.8751
		-3	7	5	48.518	-0.0026		1.8748
		-2	0	7	48.580	-0.0643		1.8726
		-10	2	2	48.582	-0.0665		1.8725
57	48.982	-4	8	4	48.910	0.0715	2.0	1.8582	1.8607
		4	10	0	48.940	0.0423		1.8597
		2	1	7	48.950	0.0319		1.8593
		-9	5	2	48.950	0.0319		1.8593
		-8	7	1	48.966	0.0164		1.8587
		7	8	1	48.971	0.0113		1.8586
		7	3	5	48.972	0.0103		1.8585
		5	3	6	49.035	-0.0527		1.8563
		8	7	1	49.048	-0.0663		1.8558
		-8	4	4	49.060	-0.0777		1.8554

A3. Mercury(II) bromide – Silicalite-1

Symmetry : Monoclinic *B*

Refined cell parameters:
a : 19.8(153)
b : 20.1(153)
c : 13.3(35)
β : 90.3(2)

N	2Θ[obs]	H	K	L	2Θ[calc]	obs-calc	Int.	*d*[obs]	*d*[calc]
1	7.955	0	1	1	7.960	-0.0048	96.8	11.1053	11.0987
		-1	0	1	7.967	-0.0126			11.0878
		1	0	1	8.012	-0.0570			11.0265
2	8.834	0	2	0	8.795	0.0387	60.1	10.0023	10.0462
		2	0	0	8.903	-0.0697			9.9241
3	9.123	-1	1	1	9.102	0.0205	26.9	9.6860	9.7077
		1	1	1	9.141	-0.0184			9.6665
4	9.861	1	2	0	9.860	0.0007	12.8	8.9628	8.9635
		2	1	0	9.933	-0.0721			8.8979
5	11.014	0	2	1	11.024	-0.0103	10.6	8.0270	8.0195
		-2	0	1	11.079	-0.0652			7.9799
6	11.885	-1	2	1	11.878	0.0076	13.4	7.4401	7.4448
		1	2	1	11.908	-0.0223			7.4262
		-2	1	1	11.924	-0.0381			7.4164
7	13.254	0	3	0	13.209	0.0454	16.2	6.6747	6.6975
		0	0	2	13.289	-0.0351			6.6571
8	13.965	1	3	0	13.944	0.0210	17.3	6.3365	6.3459
		-1	0	2	13.995	-0.0298			6.3230
		0	1	2	14.003	-0.0381			6.3193
		1	0	2	14.046	-0.0807			6.3002
9	14.788	1	1	2	14.724	0.0644	18.0	5.9856	6.0116
		0	3	1	14.794	-0.0060			5.9832
10	15.535	1	3	1	15.467	0.0676	12.9	5.6995	5.7243
		-3	1	1	15.546	-0.0111			5.6955
		3	1	1	15.615	-0.0799			5.6705
11	15.623	-3	1	1	15.546	0.0766	13.3	5.6677	5.6955
		3	1	1	15.615	0.0078			5.6705
12	15.932	2	3	0	15.952	-0.0198	13.2	5.5584	5.5515
		0	2	2	15.958	-0.0262			5.5493
		-2	0	2	15.974	-0.0420			5.5439
13	16.527	-1	2	2	16.552	-0.0258	10.8	5.3596	5.3513
		-2	1	2	16.575	-0.0481			5.3442
		1	2	2	16.596	-0.0691			5.3375
14	17.313	-2	3	1	17.272	0.0415	10.0	5.1179	5.1301
		2	3	1	17.313	0.0001			5.1179
		-3	2	1	17.331	-0.0182			5.1125
		3	2	1	17.393	-0.0802			5.0944
15	17.642	0	4	0	17.642	-0.0000	10.8	5.0231	5.0231
16	17.861	4	0	0	17.861	0.0000	12.2	4.9621	4.9621
17	18.206	1	4	0	18.203	0.0027	9.0	4.8689	4.8696
		-2	2	2	18.263	-0.0568			4.8539
18	19.245	-1	3	2	19.289	-0.0444	14.3	4.6082	4.5977
		1	3	2	19.327	-0.0817			4.5890
19	20.414	-1	0	3	20.463	-0.0484	21.2	4.3469	4.3367
		0	1	3	20.477	-0.0629			4.3336
20	20.907	-3	2	2	20.824	0.0833	19.1	4.2454	4.2622

		2	3	2	20.852	0.0553			4.2566
		-2	4	1	20.880	0.0278			4.2510
		2	4	1	20.914	-0.0068			4.2441
		3	2	2	20.928	-0.0205			4.2413
		-1	1	3	20.939	-0.0318			4.2391
		1	1	3	20.991	-0.0835			4.2287
21	21.822	-2	0	3	21.871	-0.0495	15.1	4.0696	4.0605
		0	2	3	21.876	-0.0544			4.0596
22	22.203	0	4	2	22.152	0.0516	14.8	4.0005	4.0097
		3	4	0	22.202	0.0010			4.0007
		-4	0	2	22.263	-0.0597			3.9899
		4	3	0	22.279	-0.0762			3.9870
23	22.576	1	5	0	22.557	0.0191	11.1	3.9353	3.9386
		-1	4	2	22.589	-0.0129			3.9331
		1	4	2	22.621	-0.0450			3.9276
24	23.097	-3	3	2	23.077	0.0204	100.0	3.8476	3.8510
		0	5	1	23.101	-0.0032			3.8471
		3	3	2	23.171	-0.0738			3.8355
		-3	4	1	23.173	-0.0752			3.8353
25	23.275	3	4	1	23.220	0.0551	46.3	3.8187	3.8276
		-4	3	1	23.239	0.0358			3.8245
		4	3	1	23.301	-0.0266			3.8144
		-5	0	1	23.326	-0.0514			3.8104
26	23.404	-5	0	1	23.326	0.0777	47.7	3.7979	3.8104
		5	0	1	23.404	0.0000			3.7979
27	23.709	2	2	3	23.706	0.0025	28.6	3.7498	3.7502
		-5	1	1	23.748	-0.0393			3.7437
28	23.979	2	4	2	23.947	0.0324	59.5	3.7081	3.7131
		-4	2	2	23.979	0.0002			3.7082
		0	3	3	24.035	-0.0565			3.6996
		-3	0	3	24.059	-0.0805			3.6959
29	24.348	-1	3	3	24.433	-0.0857	23.3	3.6528	3.6402
30	24.603	3	1	3	24.603	0.0000	25.5	3.6155	3.6155
31	25.553	-2	3	3	25.635	-0.0823	12.4	3.4832	3.4722
32	25.839	3	2	3	25.790	0.0491	16.4	3.4453	3.4517
		0	5	2	25.877	-0.0380			3.4403
		-3	4	2	25.921	-0.0816			3.4346
		3	5	0	25.921	-0.0818			3.4346
33	26.014	-4	3	2	25.973	0.0409	16.0	3.4225	3.4278
		3	4	2	26.005	0.0091			3.4236
		-5	0	2	26.045	-0.0306			3.4185
		-4	4	1	26.066	-0.0517			3.4158
		5	3	0	26.073	-0.0589			3.4149
		4	3	2	26.086	-0.0715			3.4133
34	26.231	5	0	2	26.185	0.0460	10.6	3.3947	3.4005
		-1	5	2	26.256	-0.0249			3.3915
		1	5	2	26.284	-0.0528			3.3880
35	26.586	5	1	2	26.564	0.0217	11.7	3.3502	3.3529
		0	6	0	26.597	-0.0115			3.3487
36	27.040	5	3	1	26.967	0.0731	18.1	3.2950	3.3037
		1	6	0	26.980	0.0595			3.3021
		4	0	3	27.013	0.0270			3.2982
		-1	0	4	27.115	-0.0756			3.2859
37	27.426	4	1	3	27.381	0.0452	11.9	3.2494	3.2546
		-2	5	2	27.390	0.0368			3.2536
		0	6	1	27.442	-0.0152			3.2476
		2	5	2	27.443	-0.0168			3.2474
		-1	1	4	27.482	-0.0561			3.2429
38	28.419	6	2	0	28.382	0.0366	7.7	3.1381	3.1421
		4	2	3	28.460	-0.0415			3.1336
39	28.622	-4	4	2	28.547	0.0742	8.3	3.1163	3.1243

		-1	2	4	28.558	0.0636			3.1231
		-2	1	4	28.558	0.0633			3.1231
		4	5	0	28.560	0.0612			3.1229
		1	2	4	28.610	0.0121			3.1176
		5	4	0	28.639	-0.0172			3.1145
		4	4	2	28.650	-0.0288			3.1133
		2	1	4	28.661	-0.0398			3.1121
40	29.211	-6	2	1	29.141	0.0700	13.3	3.0548	3.0620
		-3	5	2	29.197	0.0135			3.0562
		6	2	1	29.217	-0.0059			3.0542
		3	5	2	29.273	-0.0622			3.0484
41	29.441	4	5	1	29.378	0.0630	13.2	3.0315	3.0378
		-5	4	1	29.398	0.0430			3.0358
		5	3	2	29.434	0.0065			3.0321
		5	4	1	29.461	-0.0197			3.0295
42	29.920	0	6	2	29.842	0.0775	25.4	2.9840	2.9916
		3	6	0	29.881	0.0391			2.9878
		0	3	4	29.953	-0.0334			2.9807
		-3	0	4	29.954	-0.0345			2.9806
		0	5	3	29.973	-0.0531			2.9788
		-3	4	3	29.993	-0.0727			2.9769
43	30.266	4	3	3	30.180	0.0861	14.4	2.9507	2.9589
		1	6	2	30.200	0.0664			2.9570
		6	0	2	30.216	0.0497			2.9554
		-1	3	4	30.273	-0.0067			2.9500
		5	0	3	30.273	-0.0069			2.9500
		-3	1	4	30.290	-0.0239			2.9484
		-1	5	3	30.298	-0.0323			2.9476
		1	3	4	30.322	-0.0556			2.9454
		1	5	3	30.335	-0.0690			2.9441
44	31.213	0	7	0	31.134	0.0795	7.1	2.8632	2.8704
		-2	6	2	31.178	0.0354			2.8664
		2	6	2	31.225	-0.0122			2.8621
		-2	3	4	31.261	-0.0475			2.8590
		-3	2	4	31.277	-0.0639			2.8575
		-2	5	3	31.292	-0.0783			2.8562
45	31.344	-2	3	4	31.261	0.0832	7.4	2.8516	2.8590
		-3	2	4	31.277	0.0668			2.8575
		-2	5	3	31.292	0.0524			2.8562
		2	3	4	31.356	-0.0117			2.8505
		2	5	3	31.363	-0.0188			2.8499
		-6	2	2	31.387	-0.0434			2.8477
		-5	2	3	31.407	-0.0627			2.8460
		3	2	4	31.419	-0.0754			2.8449
46	32.163	-1	7	1	32.188	-0.0242	8.6	2.7808	2.7788
		1	7	1	32.199	-0.0358			2.7778
		-7	0	1	32.213	-0.0492			2.7767
		4	6	0	32.223	-0.0598			2.7758
		0	4	4	32.236	-0.0729			2.7747
47	32.729	4	1	4	32.766	-0.0365	10.1	2.7340	2.7310
		7	2	0	32.793	-0.0634			2.7289
		-3	6	2	32.795	-0.0662			2.7286
48	32.894	-3	3	4	32.863	0.0302	9.9	2.7207	2.7231
		3	6	2	32.864	0.0299			2.7231
		-3	5	3	32.898	-0.0050			2.7203
		-4	6	1	32.913	-0.0192			2.7192
		4	6	1	32.958	-0.0646			2.7155
		-6	3	2	32.969	-0.0753			2.7147
49	33.442	-7	2	1	33.455	-0.0134	8.5	2.6774	2.6763
		-2	4	4	33.463	-0.0219			2.6757
		0	6	3	33.496	-0.0542			2.6732

		-4	2	4	33.509	-0.0679			2.6721
50	33.780	-1	6	3	33.791	-0.0106	7.8	2.6513	2.6505
		1	6	3	33.824	-0.0439			2.6480
		6	0	3	33.867	-0.0866			2.6447
51	34.326	1	1	5	34.267	0.0586	8.3	2.6104	2.6147
		-7	0	2	34.272	0.0537			2.6143
		-1	7	2	34.282	0.0444			2.6137
		1	7	2	34.303	0.0225			2.6120
		7	3	0	34.316	0.0098			2.6111
		-5	5	2	34.415	-0.0893			2.6038
52	34.592	5	5	2	34.524	0.0674	8.3	2.5909	2.5958
		-7	1	2	34.570	0.0213			2.5925
53	35.137	-5	0	4	35.049	0.0877	7.7	2.5519	2.5581
		6	2	3	35.057	0.0800			2.5576
		-6	4	2	35.076	0.0612			2.5563
		-5	4	3	35.093	0.0438			2.5550
		-2	1	5	35.096	0.0411			2.5548
		-1	2	5	35.101	0.0360			2.5545
		3	4	4	35.105	0.0322			2.5542
		6	5	0	35.108	0.0289			2.5540
		1	2	5	35.155	-0.0176			2.5507
		4	5	3	35.173	-0.0356			2.5494
		4	3	4	35.177	-0.0400			2.5491
		-2	7	2	35.180	-0.0424			2.5490
		2	1	5	35.203	-0.0660			2.5473
		6	4	2	35.205	-0.0674			2.5472
		2	7	2	35.222	-0.0852			2.5460
54	35.690	-5	6	1	35.665	0.0251	8.5	2.5137	2.5154
		5	6	1	35.718	-0.0277			2.5118
		0	8	0	35.721	-0.0312			2.5116
		-6	5	1	35.738	-0.0482			2.5104
55	36.159	2	2	5	36.070	0.0890	9.1	2.4821	2.4880
		-2	5	4	36.120	0.0391			2.4847
		4	7	0	36.122	0.0375			2.4846
		-3	6	3	36.167	-0.0077			2.4816
		8	0	0	36.176	-0.0164			2.4810
		2	5	4	36.204	-0.0445			2.4792
		-5	2	4	36.206	-0.0466			2.4790
56	36.335	-3	0	5	36.261	0.0740	8.2	2.4705	2.4754
		3	6	3	36.261	0.0736			2.4754
		0	3	5	36.275	0.0593			2.4745
		-6	3	3	36.311	0.0239			2.4721
		7	4	0	36.355	-0.0202			2.4692
		0	8	1	36.373	-0.0383			2.4680
		5	2	4	36.414	-0.0797			2.4653
		3	0	5	36.417	-0.0821			2.4652
57	37.211	8	1	1	37.142	0.0691	7.5	2.4144	2.4187
		4	4	4	37.175	0.0362			2.4166
		0	7	3	37.277	-0.0666			2.4102
58	37.561	2	3	5	37.477	0.0841	7.3	2.3926	2.3978
		-7	0	3	37.507	0.0539			2.3959
		-2	8	1	37.511	0.0499			2.3957
		2	8	1	37.532	0.0297			2.3945
		3	2	5	37.537	0.0246			2.3941
		-3	5	4	37.539	0.0219			2.3940
		-1	7	3	37.546	0.0150			2.3936
		-5	6	2	37.568	-0.0069			2.3922
		1	7	3	37.577	-0.0153			2.3917
		-5	3	4	37.608	-0.0471			2.3897
		-6	5	2	37.633	-0.0720			2.3882
		-5	5	3	37.650	-0.0884			2.3872

59	41.104	-5	7	2	41.026	0.0779	6.9	2.1942	2.1982
		-8	4	1	41.070	0.0342			2.1960
		-1	1	6	41.117	-0.0129			2.1936
		5	7	2	41.120	-0.0159			2.1934
		8	3	2	41.139	-0.0353			2.1924
		9	1	0	41.144	-0.0401			2.1922
		8	4	1	41.145	-0.0408			2.1922
		5	1	5	41.145	-0.0413			2.1921
		-7	5	2	41.159	-0.0556			2.1914
		1	1	6	41.173	-0.0691			2.1907
60	45.101	4	9	1	45.026	0.0749	15.8	2.0086	2.0118
		4	1	6	45.043	0.0573			2.0111
		-3	3	6	45.057	0.0435			2.0105
		8	5	2	45.083	0.0176			2.0094
		0	10	0	45.086	0.0146			2.0092
		0	8	4	45.190	-0.0894			2.0049
61	45.625	-4	2	6	45.546	0.0785	14.1	1.9868	1.9900
		4	7	4	45.590	0.0349			1.9882
		-7	4	4	45.592	0.0321			1.9881
		-6	3	5	45.625	-0.0004			1.9868
		0	10	1	45.625	-0.0006			1.9868
		2	4	6	45.631	-0.0068			1.9865
		3	6	5	45.661	-0.0369			1.9853
		-8	1	4	45.663	-0.0382			1.9852
		-1	9	3	45.670	-0.0450			1.9849
		10	0	0	45.672	-0.0475			1.9848
		8	4	3	45.682	-0.0579			1.9844
		1	9	3	45.695	-0.0709			1.9839
		8	0	4	45.703	-0.0786			1.9835
62	46.460	-2	9	3	46.376	0.0843	7.3	1.9530	1.9563
		-10	1	1	46.396	0.0644			1.9555
		2	9	3	46.427	0.0332			1.9543
		0	7	5	46.481	-0.0200			1.9522
		10	1	1	46.481	-0.0207			1.9521
		-6	7	3	46.509	-0.0489			1.9510
63	46.728	5	9	0	46.639	0.0886	7.1	1.9424	1.9459
		4	9	2	46.647	0.0809			1.9456
		6	7	3	46.662	0.0658			1.9450
		-1	7	5	46.697	0.0311			1.9436
		-3	4	6	46.699	0.0285			1.9435
		-4	3	6	46.714	0.0138			1.9429
		0	5	6	46.724	0.0039			1.9426
		-9	2	3	46.729	-0.0015			1.9423
		1	7	5	46.739	-0.0112			1.9420
		-5	0	6	46.740	-0.0123			1.9419
		7	6	3	46.749	-0.0214			1.9416
		-5	5	5	46.750	-0.0217			1.9415
64	47.495	-1	10	2	47.440	0.0546	8.6	1.9128	1.9149
		-9	5	1	47.445	0.0498			1.9147
		1	10	2	47.457	0.0379			1.9143
		2	7	5	47.467	0.0275			1.9139
		6	8	2	47.468	0.0265			1.9138
		6	4	5	47.503	-0.0087			1.9125
		5	8	3	47.507	-0.0122			1.9124
		-8	6	2	47.509	-0.0148			1.9123
		-8	3	4	47.518	-0.0229			1.9119
		9	5	1	47.520	-0.0255			1.9119
		-7	2	5	47.533	-0.0389			1.9113
		-3	9	3	47.544	-0.0497			1.9109
		-8	5	3	47.564	-0.0697			1.9102
		-5	7	4	47.575	-0.0809			1.9098

65	47.583	6	4	5	47.503	0.0794	9.4	1.9095	1.9125
		5	8	3	47.507	0.0759			1.9124
		-8	6	2	47.509	0.0733			1.9123
		-8	3	4	47.518	0.0652			1.9119
		9	5	1	47.520	0.0626			1.9119
		-7	2	5	47.533	0.0492			1.9113
		-3	9	3	47.544	0.0384			1.9109
		-8	5	3	47.564	0.0184			1.9102
		-5	7	4	47.575	0.0072			1.9098
		-2	5	6	47.615	-0.0324			1.9083
		3	9	3	47.620	-0.0368			1.9081
		8	6	2	47.643	-0.0604			1.9072
		-5	2	6	47.659	-0.0758			1.9066
66	47.798	2	5	6	47.715	0.0827	7.3	1.9014	1.9045
		5	7	4	47.742	0.0556			1.9035
		-3	10	1	47.747	0.0505			1.9033
		10	3	0	47.755	0.0434			1.9030
		8	5	3	47.765	0.0334			1.9026
		3	10	1	47.772	0.0255			1.9023
		0	0	7	47.780	0.0174			1.9020
		8	3	4	47.785	0.0134			1.9019
		7	2	5	47.825	-0.0275			1.9004
		10	0	2	47.863	-0.0647			1.8990
		-9	3	3	47.875	-0.0774			1.8985
67	48.522	8	7	0	48.458	0.0642	7.5	1.8747	1.8770
		4	4	6	48.511	0.0112			1.8751
		-3	7	5	48.525	-0.0027			1.8746
		-10	2	2	48.601	-0.0785			1.8718
68	48.984	3	5	6	48.896	0.0882	6.4	1.8581	1.8612
		-4	8	4	48.897	0.0874			1.8612
		7	8	1	48.914	0.0700			1.8606
		-8	7	1	48.936	0.0483			1.8598
		1	2	7	48.942	0.0422			1.8596
		-9	5	2	48.951	0.0327			1.8593
		7	3	5	48.952	0.0322			1.8592
		2	1	7	48.987	-0.0030			1.8580
		8	7	1	49.001	-0.0171			1.8575
		4	8	4	49.027	-0.0434			1.8565
		5	3	6	49.033	-0.0493			1.8563

A4. Gold(III) chloride – Silicalite-1

Symmetry : Monoclinic *B*

Refined cell parameters:
a : 19.818(12)
b : 20.039(14)
c : 13.352(12)
β : 90.35(10)

N	2Θ[obs]	H	K	L	2Θ[calc]	obs-calc	Int.	*d*[obs]	*d*[calc]
1	7.973	0	1	1	7.951	0.0219	100.0	11.0806	11.1111
		-1	0	1	7.956	0.0169			11.1040
		1	0	1	8.000	-0.0278			11.0421
2	8.865	0	2	0	8.818	0.0465	64.2	9.9672	10.0197
3	9.117	-1	1	1	9.098	0.0190	17.7	9.6924	9.7126
		1	1	1	9.137	-0.0202			9.6711
4	9.938	2	1	0	9.950	-0.0118	5.8	8.8929	8.8824
5	11.044	0	2	1	11.032	0.0123	3.5	8.0051	8.0140
		-2	0	1	11.079	-0.0347			7.9801
6	11.933	-1	2	1	11.887	0.0459	7.2	7.4104	7.4389
		1	2	1	11.917	0.0158			7.4202
		-2	1	1	11.928	0.0056			7.4139
7	12.569	2	2	0	12.554	0.0153	3.7	7.0370	7.0455
8	13.251	0	3	0	13.244	0.0069	9.7	6.6763	6.6798
		0	0	2	13.252	-0.0013			6.6757
9	13.975	-1	0	2	13.962	0.0134	10.7	6.3319	6.3380
		0	1	2	13.972	0.0034			6.3335
		1	3	0	13.980	-0.0046			6.3299
		1	0	2	14.013	-0.0380			6.3149
10	14.689	-1	1	2	14.647	0.0420	10.6	6.0258	6.0429
		1	1	2	14.696	-0.0070			6.0229
11	14.802	0	3	1	14.817	-0.0158	11.8	5.9802	5.9738
12	15.568	-3	1	1	15.559	0.0093	8.5	5.6874	5.6908
13	15.950	0	2	2	15.940	0.0099	10.9	5.5521	5.5555
		-2	0	2	15.950	-0.0004			5.5520
		2	3	0	15.988	-0.0386			5.5388
14	16.596	-2	1	2	16.555	0.0406	4.4	5.3375	5.3505
		1	2	2	16.580	0.0153			5.3424
		2	1	2	16.642	-0.0463			5.3227
15	17.354	2	3	1	17.340	0.0139	4.2	5.1059	5.1099
		-3	2	1	17.352	0.0021			5.1065
16	17.687	0	4	0	17.689	-0.0028	6.3	5.0106	5.0098
17	17.880	4	0	0	17.889	-0.0087	7.4	4.9569	4.9545
18	18.428	4	1	0	18.432	-0.0042	4.8	4.8108	4.8097
19	19.344	1	3	2	19.327	0.0173	7.0	4.5848	4.5889
		-3	1	2	19.344	0.0003			4.5849
20	20.016	4	2	0	19.976	0.0401	4.6	4.4324	4.4412
		-3	3	1	19.996	0.0200			4.4368
		3	3	1	20.051	-0.0343			4.4249
21	20.412	-1	0	3	20.409	0.0022	11.1	4.3474	4.3479
		0	1	3	20.425	-0.0135			4.3446
22	20.900	2	3	2	20.857	0.0432	7.6	4.2469	4.2556
		-1	1	3	20.889	0.0107			4.2491
		-2	4	1	20.920	-0.0194			4.2430
		3	2	2	20.928	-0.0275			4.2414
		1	1	3	20.942	-0.0414			4.2386

23	21.832	-2	0	3	21.825	0.0065	4.7	4.0678	4.0690
		0	2	3	21.834	-0.0027			4.0673
24	22.251	3	4	0	22.253	-0.0019	5.3	3.9921	3.9918
		-4	0	2	22.262	-0.0116			3.9900
		-1	2	3	22.271	-0.0199			3.9886
		-2	1	3	22.276	-0.0254			3.9876
25	23.133	-3	3	2	23.088	0.0457	32.8	3.8417	3.8492
		0	5	1	23.152	-0.0187			3.8386
		3	3	2	23.182	-0.0490			3.8337
26	23.348	4	3	1	23.338	0.0105	29.4	3.8069	3.8085
		-5	0	1	23.354	-0.0054			3.8060
27	23.788	-5	1	1	23.777	0.0111	11.5	3.7374	3.7391
28	24.000	2	4	2	23.966	0.0335	19.4	3.7050	3.7101
		-4	2	2	23.987	0.0128			3.7069
		0	3	3	24.008	-0.0084			3.7037
		-3	0	3	24.024	-0.0239			3.7013
29	24.402	-1	3	3	24.408	-0.0054	9.8	3.6448	3.6440
		-3	1	3	24.436	-0.0340			3.6398
30	24.580	3	1	3	24.571	0.0090	6.1	3.6188	3.6201
31	26.019	3	5	0	25.983	0.0368	5.6	3.4218	3.4265
		-4	3	2	25.991	0.0284			3.4255
		3	4	2	26.029	-0.0099			3.4205
		-5	0	2	26.055	-0.0355			3.4172
32	26.622	5	1	2	26.577	0.0452	5.1	3.3457	3.3513
		0	6	0	26.669	-0.0472			3.3399
33	26.905	3	5	1	26.861	0.0441	7.9	3.3112	3.3165
		-5	3	1	26.940	-0.0356			3.3069
34	27.440	-1	1	4	27.412	0.0282	3.2	3.2478	3.2511
		-2	5	2	27.424	0.0156			3.2496
		1	1	4	27.465	-0.0256			3.2448
		2	5	2	27.478	-0.0382			3.2434
35	27.912	-1	6	1	27.873	0.0391	3.1	3.1940	3.1983
		1	6	1	27.886	0.0258			3.1969
36	28.167	-6	1	1	28.123	0.0438	2.7	3.1656	3.1704
		-2	0	4	28.136	0.0308			3.1690
		0	2	4	28.156	0.0105			3.1667
		2	6	0	28.173	-0.0059			3.1649
		6	1	1	28.202	-0.0350			3.1617
37	28.431	6	2	0	28.429	0.0015	2.6	3.1368	3.1370
		4	2	3	28.446	-0.0147			3.1352
38	29.280	-3	5	2	29.235	0.0449	3.3	3.0477	3.0523
		6	2	1	29.259	0.0215			3.0499
		3	5	2	29.311	-0.0312			3.0446
39	29.934	0	6	2	29.890	0.0446	6.1	2.9826	2.9869
		-3	0	4	29.895	0.0393			2.9864
		0	3	4	29.901	0.0333			2.9858
		3	6	0	29.955	-0.0202			2.9806
		0	5	3	29.979	-0.0449			2.9782
40	30.277	-3	1	4	30.233	0.0442	4.7	2.9496	2.9538
		6	0	2	30.237	0.0400			2.9534
		1	6	2	30.248	0.0296			2.9524
		5	0	3	30.261	0.0159			2.9511
		1	3	4	30.271	0.0061			2.9502
		-1	5	3	30.306	-0.0282			2.9469
41	30.728	-3	6	1	30.692	0.0361	2.5	2.9073	2.9107
		3	6	1	30.728	-0.0003			2.9073
42	31.288	2	6	2	31.275	0.0123	3.0	2.8566	2.8577
		-2	5	3	31.302	-0.0140			2.8553
		2	3	4	31.310	-0.0224			2.8546
43	32.259	-4	0	4	32.220	0.0388	2.7	2.7728	2.7760
		-7	0	1	32.257	0.0025			2.7730

		-1	7	1	32.267	-0.0076			2.7721
		1	7	1	32.278	-0.0192			2.7711
		4	6	0	32.299	-0.0401			2.7694
44	32.839	-3	3	4	32.824	0.0151	2.1	2.7251	2.7263
		7	2	0	32.847	-0.0079			2.7245
		-3	6	2	32.848	-0.0089			2.7244
45	33.764		---	not	indexed	---	2.3	2.6525	
46	34.485	7	0	2	34.456	0.0283	2.6	2.5987	2.6008
		-5	5	2	34.463	0.0219			2.6003
47	35.024	-4	3	4	34.974	0.0495	2.6	2.5599	2.5635
		-4	6	2	35.008	0.0160			2.5611
		-7	3	1	35.008	0.0157			2.5611
		-2	1	5	35.008	0.0154			2.5610
		-5	0	4	35.012	0.0114			2.5608
		-1	2	5	35.016	0.0083			2.5605
		6	2	3	35.064	-0.0397			2.5571
		-4	5	3	35.064	-0.0402			2.5571
		1	2	5	35.070	-0.0457			2.5567
48	35.203	6	5	0	35.180	0.0234	2.7	2.5473	2.5489
		4	5	3	35.193	0.0100			2.5480
		5	0	4	35.228	-0.0246			2.5456
		-1	5	4	35.234	-0.0310			2.5451
		-2	7	2	35.244	-0.0410			2.5444
		6	4	2	35.248	-0.0444			2.5442
49	35.727	-5	6	1	35.739	-0.0118	2.2	2.5112	2.5104
50	36.166	-5	2	4	36.176	-0.0103	3.4	2.4817	2.4810
		-3	0	5	36.178	-0.0124			2.4809
		2	5	4	36.188	-0.0221			2.4802
		-3	6	3	36.197	-0.0312			2.4796
		0	3	5	36.199	-0.0332			2.4795
		4	7	0	36.210	-0.0447			2.4787
51	37.606	-5	3	4	37.587	0.0193	2.4	2.3899	2.3911
		-1	7	3	37.588	0.0185			2.3910
		-2	8	1	37.605	0.0009			2.3899
		1	7	3	37.618	-0.0120			2.3892
		2	8	1	37.626	-0.0195			2.3887
		-5	6	2	37.628	-0.0223			2.3885
		3	5	4	37.650	-0.0435			2.3872
52	38.310	-6	4	3	38.279	0.0306	1.7	2.3476	2.3494
		6	6	0	38.294	0.0157			2.3485
		4	6	3	38.307	0.0032			2.3478
		-1	6	4	38.345	-0.0349			2.3455
		0	8	2	38.350	-0.0397			2.3452
		4	0	5	38.359	-0.0488			2.3447
53	38.415	1	6	4	38.385	0.0304	1.7	2.3414	2.3432
		3	8	0	38.402	0.0134			2.3422
		-1	4	5	38.415	0.0004			2.3414
		-2	7	3	38.416	-0.0009			2.3413
		6	0	4	38.426	-0.0111			2.3407
		-4	1	5	38.432	-0.0166			2.3404
		6	4	3	38.459	-0.0440			2.3388
		-6	1	4	38.459	-0.0441			2.3388
		1	4	5	38.465	-0.0495			2.3385
54	39.452	-2	8	2	39.433	0.0193	1.4	2.2822	2.2833
		4	2	5	39.437	0.0148			2.2830
		-4	5	4	39.455	-0.0028			2.2821
		2	8	2	39.472	-0.0197			2.2811
		-7	5	1	39.485	-0.0332			2.2804
		-5	4	4	39.489	-0.0371			2.2802
55	40.571	-3	4	5	40.544	0.0262	1.5	2.2218	2.2232
		-4	3	5	40.561	0.0091			2.2223

		0	5	5	40.563	0.0073		2.2222
		-6	3	4	40.588	-0.0172		2.2209
		-5	0	5	40.590	-0.0196		2.2208
		8	4	0	40.594	-0.0234		2.2206
		3	6	4	40.602	-0.0309		2.2202
56	41.514	-9	0	1	41.489	0.0255	1.4	2.1735	2.1748
		-2	0	6	41.505	0.0094		2.1740
		0	7	4	41.524	-0.0097		2.1730
		2	9	0	41.535	-0.0213		2.1724
		0	2	6	41.538	-0.0238		2.1723
57	41.723	-7	0	4	41.674	0.0495	1.6	2.1631	2.1655
		6	7	0	41.719	0.0046		2.1633
		4	7	3	41.730	-0.0070		2.1627
		-9	1	1	41.744	-0.0205		2.1621
		-2	1	6	41.760	-0.0365		2.1613
		-7	4	3	41.765	-0.0418		2.1610
		-1	7	4	41.766	-0.0425		2.1610
		-1	2	6	41.770	-0.0473		2.1607
58	45.104	-4	9	1	45.102	0.0014	3.1	2.0085	2.0086
		3	3	6	45.124	-0.0207		2.0076
		4	9	1	45.137	-0.0336		2.0071
		8	5	2	45.150	-0.0469		2.0065
59	45.609	7	7	1	45.565	0.0444	3.6	1.9874	1.9893
		-6	3	5	45.587	0.0214		1.9883
		-7	4	4	45.600	0.0087		1.9878
		4	7	4	45.616	-0.0066		1.9871
		3	6	5	45.639	-0.0302		1.9862
60	47.550	-7	2	5	47.500	0.0496	1.7	1.9107	1.9126
		-8	3	4	47.527	0.0227		1.9116
		-9	5	1	47.530	0.0201		1.9115
		-2	5	6	47.544	0.0057		1.9109
		-1	10	2	47.550	-0.0006		1.9107
		6	8	2	47.560	-0.0103		1.9103
		1	10	2	47.567	-0.0174		1.9101
		5	8	3	47.577	-0.0267		1.9097
		-5	2	6	47.577	-0.0269		1.9097
		-8	6	2	47.587	-0.0369		1.9093
61	48.227	-4	4	6	48.240	-0.0133	1.1	1.8855	1.8850
		-2	10	2	48.242	-0.0151		1.8849
		2	10	2	48.275	-0.0484		1.8837
62	49.490	-4	10	1	49.481	0.0086	1.2	1.8403	1.8406
		6	0	6	49.487	0.0023		1.8404
		-9	4	3	49.495	-0.0049		1.8401
		6	5	5	49.512	-0.0221		1.8395
		4	10	1	49.514	-0.0240		1.8394
		2	2	7	49.524	-0.0343		1.8391

A5. ITQ-4 as-synthesized

Symmetry : Monoclinic *B*

Refined cell parameters:
a : 18.476(4)
b : 13.425(3)
c : 7.7065(19)
β : 101.618(21)

N	2Θ[obs]	H	K	L	2Θ[calc]	obs-calc	Int.	*d*[obs]	*d*[calc]
1	8.184	1	1	0	8.194	-0.0097	100.0	10.7950	10.7823
2	9.752	2	0	0	9.767	-0.0147	30.2	9.0625	9.0488
3	13.456	0	1	1	13.446	0.0096	30.6	6.5751	6.5798
4	15.187	-2	1	1	15.183	0.0035	20.9	5.8294	5.8307
5	16.090	3	1	0	16.094	-0.0042	21.3	5.5040	5.5026
6	16.423	2	2	0	16.429	-0.0060	24.6	5.3931	5.3911
7	16.816	-3	0	1	16.851	-0.0356	16.6	5.2681	5.2571
8	17.719	-1	2	1	17.691	0.0283	15.8	5.0016	5.0095
9	18.964	1	2	1	18.966	-0.0014	32.8	4.6759	4.6755
10	19.604	4	0	0	19.605	-0.0013	16.8	4.5247	4.5244
11	20.431	1	3	0	20.427	0.0037	58.0	4.3434	4.3442
12	20.587	3	0	1	20.599	-0.0117	44.0	4.3108	4.3084
13	21.457	-3	2	1	21.452	0.0051	33.7	4.1379	4.1388
14	21.785	-4	1	1	21.781	0.0043	51.0	4.0764	4.0772
15	23.597	0	0	2	23.552	0.0450	46.9	3.7672	3.7743
		-2	0	2	23.624	-0.0264			3.7631
16	24.758	3	3	0	24.752	0.0068	15.1	3.5931	3.5941
17	25.038	-5	0	1	25.030	0.0082	16.2	3.5536	3.5547
18	25.456	5	1	0	25.467	-0.0112	15.8	3.4963	3.4947
19	25.918	1	1	2	25.909	0.0091	37.3	3.4349	3.4361
20	26.538	0	4	0	26.537	0.0015	25.3	3.3561	3.3563
21	27.160	-2	2	2	27.145	0.0160	11.6	3.2806	3.2825
22	27.551	-4	0	2	27.537	0.0141	12.0	3.2349	3.2365
23	28.396	-5	2	1	28.388	0.0078	13.2	3.1406	3.1414
24	28.855	-4	3	1	28.844	0.0108	9.7	3.0917	3.0928
25	29.581	6	0	0	29.592	-0.0115	14.4	3.0174	3.0163
26	29.913	1	4	1	29.923	-0.0091	8.9	2.9846	2.9837
27	30.479	2	2	2	30.473	0.0065	9.2	2.9305	2.9311
28	30.632	-1	3	2	30.592	0.0390	8.0	2.9163	2.9199
		-4	2	2	30.641	-0.0099			2.9154
29	31.622	-3	4	1	31.602	0.0200	9.1	2.8271	2.8289
30	31.781	5	3	0	31.771	0.0102	8.5	2.8133	2.8142
31	32.356	5	2	1	32.354	0.0026	6.7	2.7646	2.7649
32	33.211	4	4	0	33.209	0.0022	10.2	2.6954	2.6956
33	33.822	4	0	2	33.826	-0.0040	11.1	2.6481	2.6478
		3	4	1	33.828	-0.0056			2.6477
34	34.091	-6	0	2	34.082	0.0092	5.8	2.6278	2.6285
35	34.986	-1	0	3	34.972	0.0144	11.6	2.5626	2.5636
36	35.453	0	5	1	35.456	-0.0033	8.5	2.5300	2.5297
37	35.777	-3	0	3	35.763	0.0136	9.7	2.5078	2.5087
		0	4	2	35.773	0.0040			2.5081
		-2	4	2	35.821	-0.0448			2.5048
38	36.188	-2	5	1	36.190	-0.0019	6.1	2.4802	2.4801
39	36.760	-5	4	1	36.800	-0.0402	11.1	2.4430	2.4404
40	37.796	-4	1	3	37.815	-0.0198	5.9	2.3783	2.3771
41	40.264	7	3	0	40.253	0.0108	6.6	2.2381	2.2386

		0	6	0	40.274	-0.0104			2.2375
42	41.349	7	2	1	41.340	0.0094	5.4	2.1818	2.1822
43	41.574	2	6	0	41.542	0.0317	5.9	2.1705	2.1721
		3	0	3	41.542	0.0316			2.1721
		-5	2	3	41.572	0.0021			2.1706
44	42.124	-1	6	1	42.097	0.0266	5.6	2.1434	2.1447
		8	2	0	42.117	0.0064			2.1437
		1	5	2	42.144	-0.0200			2.1425
45	42.443	-6	1	3	42.395	0.0484	4.7	2.1280	2.1304
46	43.806	3	2	3	43.770	0.0365	3.8	2.0649	2.0666
47	44.147	6	2	2	44.116	0.0310	4.9	2.0498	2.0512
		2	3	3	44.125	0.0214			2.0507
		-9	0	1	44.178	-0.0314			2.0484
48	44.903	-7	0	3	44.887	0.0153	4.0	2.0170	2.0177
49	45.158	-6	5	1	45.161	-0.0028	5.5	2.0062	2.0061
		4	6	0	45.171	-0.0132			2.0056
50	46.727	-6	3	3	46.698	0.0287	4.1	1.9424	1.9436
51	47.196	0	6	2	47.183	0.0131	5.9	1.9242	1.9247
		-9	1	2	47.188	0.0090			1.9245
		-2	6	2	47.222	-0.0258			1.9232
52	47.931	-1	1	4	47.889	0.0419	4.6	1.8964	1.8980
		-3	1	4	47.966	-0.0351			1.8951
		5	0	3	47.971	-0.0403			1.8949
53	49.181	9	0	1	49.141	0.0398	4.8	1.8511	1.8525
		-2	2	4	49.161	0.0199			1.8518
		4	3	3	49.206	-0.0248			1.8502
54	49.555	-2	7	1	49.531	0.0240	5.2	1.8380	1.8388

A6. ITQ-4 calcined

Symmetry : Monoclinic *B*
Space group: *I* 1 2/*m* 1 (No. 12)

Refined cell parameters:
a : 18.644(3)
b : 13.4922(20)
c : 7.6385(17)
β : 101.953(15)

N	2Θ[obs]	H	K	L	2Θ[calc]	obs-calc	Int.	*d*[obs]	*d*[calc]
1	8.150	1	1	0	8.144	0.0052	100.0	10.8403	10.8472
2	9.700	2	0	0	9.690	0.0094	12.3	9.1112	9.1201
3	11.842	-1	0	1	11.822	0.0204	3.2	7.4670	7.4798
4	13.114	0	2	0	13.113	0.0009	3.8	6.7457	6.7461
5	13.543	0	1	1	13.534	0.0088	6.4	6.5329	6.5372
6	13.688	1	0	1	13.693	-0.0051	7.3	6.4639	6.4615
7	15.175	-2	1	1	15.165	0.0100	9.0	5.8337	5.8375
8	15.981	3	1	0	15.976	0.0051	2.5	5.5415	5.5432
9	16.347	2	2	0	16.330	0.0166	2.6	5.4181	5.4236
10	16.767	-3	0	1	16.771	-0.0039	2.2	5.2833	5.2821
11	18.061	2	1	1	18.057	0.0044	2.2	4.9076	4.9088
12	19.006	1	2	1	19.003	0.0023	5.4	4.6658	4.6664
13	19.455	4	0	0	19.451	0.0048	3.0	4.5589	4.5600
14	20.316	1	3	0	20.321	-0.0052	12.1	4.3677	4.3666
15	20.631	3	0	1	20.638	-0.0070	10.4	4.3018	4.3004
16	21.343	-3	2	1	21.347	-0.0042	4.4	4.1597	4.1589
17	21.631	-4	1	1	21.630	0.0008	9.8	4.1051	4.1053
18	23.537	4	2	0	23.530	0.0077	3.5	3.7767	3.7779
19	23.791	-2	0	2	23.772	0.0191	12.0	3.7369	3.7399
		0	0	2	23.795	-0.0032			3.7365
20	24.200	-1	1	2	24.199	0.0006	2.3	3.6748	3.6749
21	24.591	3	2	1	24.529	0.0625	3.7	3.6172	3.6262
		3	3	0	24.601	-0.0100			3.6157
22	24.808	-5	0	1	24.823	-0.0157	3.6	3.5861	3.5839
23	25.274	5	1	0	25.270	0.0047	3.3	3.5209	3.5216
24	26.140	-3	1	2	26.102	0.0381	9.2	3.4063	3.4112
		1	1	2	26.143	-0.0028			3.4059
25	26.385	0	4	0	26.402	-0.0173	7.2	3.3752	3.3731
26	27.245	-2	2	2	27.242	0.0027	2.9	3.2706	3.2709
		0	2	2	27.262	-0.0169			3.2686
27	27.541	-4	0	2	27.529	0.0116	2.1	3.2361	3.2375
		2	0	2	27.587	-0.0468			3.2308
28	28.170	-5	2	1	28.172	-0.0022	3.3	3.1652	3.1650
		2	4	0	28.185	-0.0148			3.1636
29	28.662	-4	3	1	28.666	-0.0040	1.6	3.1120	3.1116
30	29.041	-1	4	1	29.016	0.0252	1.6	3.0722	3.0749
31	29.356	6	0	0	29.356	-0.0002	4.1	3.0400	3.0400
		5	0	1	29.361	-0.0055			3.0395
32	29.878	1	4	1	29.857	0.0210	1.2	2.9881	2.9902
33	30.067	-6	1	1	30.065	0.0026	1.1	2.9697	2.9699
34	30.668	-4	2	2	30.605	0.0635	2.2	2.9129	2.9188
		2	2	2	30.658	0.0106			2.9138
		-1	3	2	30.687	-0.0183			2.9112
35	31.194	-5	1	2	31.200	-0.0055	1.6	2.8649	2.8645
		3	1	2	31.269	-0.0749			2.8583

36	31.440	-3	4	1	31.443	-0.0033	2.6	2.8431	2.8429
37	31.930	4	3	1	31.942	-0.0118	1.4	2.8006	2.7995
38	32.265	-3	3	2	32.236	0.0293	2.1	2.7723	2.7747
		1	3	2	32.269	-0.0045			2.7719
		6	2	0	32.273	-0.0079			2.7716
		5	2	1	32.278	-0.0128			2.7712
39	32.996	4	4	0	33.005	-0.0091	1.9	2.7125	2.7118
40	33.737	3	4	1	33.744	-0.0069	1.7	2.6546	2.6540
41	33.972	-6	0	2	33.915	0.0563	1.3	2.6368	2.6410
		-7	0	1	33.982	-0.0103			2.6360
		4	0	2	33.996	-0.0243			2.6350
42	34.708	6	1	1	34.696	0.0119	1.4	2.5825	2.5834
43	35.054	7	1	0	35.045	0.0087	1.2	2.5578	2.5585
44	35.318	-1	0	3	35.314	0.0039	3.7	2.5393	2.5396
		0	5	1	35.336	-0.0181			2.5380
45	35.857	-2	4	2	35.821	0.0358	2.0	2.5024	2.5048
		0	4	2	35.836	0.0205			2.5038
46	36.002	-2	1	3	35.944	0.0581	2.4	2.4926	2.4965
		-3	0	3	35.992	0.0097			2.4933
		-2	5	1	36.029	-0.0274			2.4908
47	36.542	-6	2	2	36.507	0.0350	3.3	2.4570	2.4593
		-5	4	1	36.553	-0.0116			2.4563
		-5	3	2	36.562	-0.0200			2.4557
		-7	2	1	36.569	-0.0275			2.4552
		4	2	2	36.582	-0.0406			2.4544
48	36.604	-5	4	1	36.553	0.0508	3.0	2.4530	2.4563
		-5	3	2	36.562	0.0424			2.4557
		-7	2	1	36.569	0.0349			2.4552
		4	2	2	36.582	0.0218			2.4544
		3	3	2	36.622	-0.0180			2.4518
		0	1	3	36.657	-0.0527			2.4496
49	37.943	-4	1	3	37.961	-0.0183	0.9	2.3695	2.3684
50	38.368	-7	1	2	38.354	0.0134	1.2	2.3442	2.3450
		5	1	2	38.441	-0.0735			2.3399
51	39.823	1	2	3	39.800	0.0230	0.9	2.2618	2.2631
		6	4	0	39.889	-0.0661			2.2582
		5	4	1	39.893	-0.0702			2.2580
52	40.057	0	6	0	40.065	-0.0074	1.3	2.2491	2.2487
53	41.825	8	2	0	41.786	0.0391	1.4	2.1581	2.1600
		-8	0	2	41.891	-0.0664			2.1548
		4	5	1	41.903	-0.0780			2.1542
54	41.917	-8	0	2	41.891	0.0262	1.5	2.1535	2.1548
		4	5	1	41.903	0.0146			2.1542
		3	0	3	41.911	0.0067			2.1538
		-1	6	1	41.918	-0.0004			2.1535
		6	0	2	41.985	-0.0680			2.1502
55	42.126	-3	5	2	42.136	-0.0098	1.0	2.1433	2.1429
		1	5	2	42.163	-0.0366			2.1416
56	42.382	-6	1	3	42.377	0.0057	1.2	2.1309	2.1312
57	43.742	-3	6	1	43.715	0.0270	1.2	2.0678	2.0690
		-9	0	1	43.757	-0.0141			2.0672
58	44.335	8	1	1	44.349	-0.0141	0.8	2.0415	2.0409
59	44.829	-7	0	3	44.790	0.0391	1.5	2.0202	2.0218
		-6	5	1	44.846	-0.0173			2.0194
		4	6	0	44.908	-0.0788			2.0168
60	45.439	4	1	3	45.422	0.0171	0.9	1.9945	1.9952
		3	6	1	45.481	-0.0422			1.9927
61	46.644	-6	3	3	46.640	0.0033	1.2	1.9457	1.9458
62	47.536	-2	0	4	47.579	-0.0430	1.2	1.9112	1.9096
		7	4	1	47.591	-0.0546			1.9092
63	47.625	-2	0	4	47.579	0.0462	1.3	1.9079	1.9096

		7	4	1	47.591	0.0346			1.9092
64	48.395	-3	1	4	48.345	0.0499	1.0	1.8793	1.8811
		-1	1	4	48.369	0.0259			1.8803
65	48.830	0	7	1	48.752	0.0778	0.8	1.8636	1.8664
		9	0	1	48.900	-0.0702			1.8611
66	49.254	-2	5	3	49.221	0.0325	0.9	1.8485	1.8497
		9	3	0	49.277	-0.0227			1.8477
		-2	7	1	49.288	-0.0338			1.8473
		-4	6	2	49.300	-0.0467			1.8469

A7. Iodine – ITQ-4

Symmetry : Monoclinic *B I*

Refined cell parameters:
a : 18.622(8)
b : 13.456(5)
c : 7.640(4)
β : 101.73(3)

N	2Θ[obs]	H	K	L	2Θ[calc]	obs-calc	Int.	*d*[obs]	*d*[calc]
1	8.187	1	1	0	8.160	0.0273	29.1	10.7909	10.8269
2	13.161	0	2	0	13.148	0.0128	34.7	6.7216	6.7281
3	16.368	2	2	0	16.361	0.0073	38.8	5.4111	5.4135
4	16.804	-3	0	1	16.808	-0.0033	28.9	5.2717	5.2707
5	17.686	-1	2	1	17.722	-0.0359	22.0	5.0109	5.0008
6	18.073	2	1	1	18.032	0.0415	35.8	4.9043	4.9155
7	19.032	1	2	1	19.009	0.0235	65.3	4.6593	4.6650
8	20.380	1	3	0	20.373	0.0066	98.9	4.3541	4.3555
9	20.644	3	0	1	20.601	0.0428	77.0	4.2990	4.3078
10	21.406	-3	2	1	21.398	0.0072	65.1	4.1478	4.1491
11	21.677	-4	1	1	21.677	-0.0009	95.7	4.0965	4.0964
12	23.800	0	0	2	23.769	0.0309	100.0	3.7356	3.7403
		-2	0	2	23.787	0.0131			3.7376
13	24.647	3	3	0	24.648	-0.0005	34.1	3.6091	3.6090
14	24.864	-5	0	1	24.873	-0.0084	29.8	3.5781	3.5769
15	25.297	5	1	0	25.284	0.0129	41.1	3.5179	3.5197
16	26.142	1	1	2	26.107	0.0349	64.4	3.4060	3.4105
		-3	1	2	26.140	0.0022			3.4063
17	26.470	0	4	0	26.474	-0.0044	56.5	3.3646	3.3640
18	27.598	-4	0	2	27.580	0.0178	35.8	3.2296	3.2316
19	28.227	-5	2	1	28.233	-0.0061	38.3	3.1590	3.1583
		2	4	0	28.254	-0.0267			3.1560
20	28.766	-4	3	1	28.736	0.0303	31.1	3.1010	3.1042
21	29.365	5	0	1	29.324	0.0404	43.1	3.0391	3.0432
		6	0	0	29.368	-0.0027			3.0388
22	29.893	1	4	1	29.909	-0.0155	29.8	2.9866	2.9851
23	30.739	-1	3	2	30.718	0.0209	27.6	2.9064	2.9083
24	31.512	-3	4	1	31.524	-0.0125	37.5	2.8368	2.8357
25	32.295	5	2	1	32.259	0.0357	31.3	2.7698	2.7728
		1	3	2	32.270	0.0248			2.7719
		-3	3	2	32.297	-0.0021			2.7696
		6	2	0	32.299	-0.0038			2.7695
26	33.030	4	4	0	33.068	-0.0379	25.0	2.7098	2.7067
27	33.793	3	4	1	33.779	0.0144	25.6	2.6503	2.6514
28	35.421	0	5	1	35.418	0.0028	23.3	2.5321	2.5323
29	35.883	0	4	2	35.874	0.0094	28.4	2.5006	2.5012
		-2	4	2	35.886	-0.0028			2.5004
30	36.619	-6	2	2	36.591	0.0275	30.8	2.4520	2.4538
		3	3	2	36.599	0.0200			2.4533
		0	1	3	36.622	-0.0034			2.4518
		-7	2	1	36.637	-0.0184			2.4508
		-5	4	1	36.642	-0.0234			2.4505
		-5	3	2	36.647	-0.0282			2.4502
31	37.975	-4	1	3	38.007	-0.0320	23.6	2.3675	2.3656
32	38.816	7	0	1	38.821	-0.0051	18.4	2.3182	2.3179
33	41.714	5	5	0	41.677	0.0369	23.9	2.1636	2.1654

		-5	2	3	41.689	0.0241			2.1648
34	44.140	6	2	2	44.111	0.0288	23.1	2.0501	2.0514
		-8	2	2	44.183	-0.0434			2.0482
35	44.894	-7	0	3	44.884	0.0097	25.3	2.0174	2.0178
36	46.793	7	1	2	46.830	-0.0368	25.3	1.9399	1.9384
37	47.523	1	7	0	47.524	-0.0003	26.5	1.9117	1.9117
		-2	0	4	47.567	-0.0437			1.9101
38	48.472	8	3	1	48.468	0.0039	26.1	1.8765	1.8767
39	49.434	2	6	2	49.398	0.0361	25.0	1.8422	1.8435
		-10	1	1	49.409	0.0252			1.8431
		4	3	3	49.414	0.0197			1.8429
		-2	7	1	49.425	0.0095			1.8425
		-4	6	2	49.426	0.0077			1.8425

A8. SSZ-24 as-synthesized

Symmetry : Hexagonal *P*
Space group: *P* 6 (No. 168)

Refined cell parameters:
a : 13.636(8)
c : 8.280(3)

N	2Θ[obs]	H	K	L	2Θ[calc]	obs-calc	Int.	*d*[obs]	*d*[calc]
1	7.491	1	0	0	7.480	0.0105	95.9	11.7925	11.8091
2	12.979	1	1	0	12.974	0.0044	8.3	6.8157	6.8180
3	14.998	2	0	0	14.992	0.0061	40.7	5.9022	5.9046
4	19.884	2	1	0	19.876	0.0082	86.3	4.4616	4.4634
5	21.453	0	0	2	21.446	0.0069	80.5	4.1387	4.1400
6	22.620	2	1	1	22.613	0.0069	100.0	3.9278	3.9290
7	25.160	1	1	2	25.145	0.0146	4.9	3.5367	3.5387
8	26.124	2	2	0	26.119	0.0049	44.8	3.4084	3.4090
9	29.358	2	1	2	29.402	-0.0444	13.9	3.0398	3.0353
10	30.250	4	0	0	30.249	0.0016	26.4	2.9521	2.9523
11	31.292	3	0	2	31.331	-0.0387	1.8	2.8562	2.8527
12	34.037	2	2	2	34.040	-0.0025	6.4	2.6318	2.6317
13	34.786	4	1	0	34.785	0.0009	21.4	2.5769	2.5770
		3	2	1	34.814	-0.0282			2.5749
14	37.389	4	0	2	37.382	0.0076	4.8	2.4032	2.4037
15	38.303	2	1	3	38.312	-0.0085	11.1	2.3480	2.3475
16	41.218	4	1	2	41.231	-0.0131	1.3	2.1884	2.1878
17	41.876	4	2	1	41.891	-0.0143	4.5	2.1555	2.1548
18	42.576	5	1	0	42.591	-0.0154	3.4	2.1217	2.1210
19	43.697	0	0	4	43.693	0.0041	3.8	2.0698	2.0700
20	44.125	5	0	2	44.109	0.0164	2.5	2.0508	2.0515
21	45.497	3	3	2	45.493	0.0040	2.4	1.9921	1.9922
22	46.093	6	0	0	46.080	0.0128	1.8	1.9677	1.9682
23	46.993	3	2	3	46.958	0.0349	0.7	1.9321	1.9334
24	48.087	5	2	0	48.078	0.0098	7.9	1.8906	1.8910
		4	3	1	48.100	-0.0126			1.8902

A9. SSZ-24 calcined

Symmetry : Hexagonal *P*
Space group: *P* 6 (No. 168)

Refined cell parameters:
a : 13.624(9)
c : 8.312(3)

N	2Θ[obs]	H	K	L	2Θ[calc]	obs-calc	Int.	*d*[obs]	*d*[calc]
1	7.484	1	0	0	7.487	-0.0027	100.0	11.8026	11.7984
2	12.983	1	1	0	12.986	-0.0034	13.9	6.8136	6.8118
		1	0	1	13.019	-0.0359			6.7949
3	15.006	2	0	0	15.006	0.0001	7.7	5.8991	5.8992
4	19.897	2	1	0	19.894	0.0028	19.1	4.4587	4.4594
5	21.370	0	0	2	21.364	0.0061	22.7	4.1547	4.1558
6	22.617	3	0	0	22.591	0.0265	26.6	3.9282	3.9328
		2	1	1	22.610	0.0075			3.9295
7	25.090	1	1	2	25.081	0.0091	3.5	3.5464	3.5477
8	26.139	2	2	0	26.143	-0.0038	10.9	3.4064	3.4059
9	29.336	3	1	1	29.309	0.0271	5.8	3.0421	3.0448
		2	1	2	29.354	-0.0177			3.0403
10	30.270	4	0	0	30.277	-0.0075	6.1	2.9503	2.9496
11	34.004	2	2	2	34.005	-0.0012	2.6	2.6343	2.6343
12	34.814	4	1	0	34.818	-0.0039	5.9	2.5749	2.5746
		3	2	1	34.831	-0.0167			2.5737
13	37.339	4	0	2	37.356	-0.0170	2.0	2.4064	2.4053
14	38.219	2	1	3	38.213	0.0060	4.0	2.3530	2.3533
15	41.937	4	2	1	41.917	0.0201	1.6	2.1526	2.1535
16	42.692	3	1	3	42.729	-0.0375	1.8	2.1162	2.1145
17	43.530	0	0	4	43.519	0.0116	1.7	2.0774	2.0779
18	44.082	5	1	1	44.066	0.0165	1.7	2.0526	2.0534
		5	0	2	44.097	-0.0150			2.0520
19	45.498	3	3	2	45.484	0.0138	1.2	1.9920	1.9926
20	48.133	5	2	0	48.124	0.0090	2.3	1.8889	1.8892
		4	3	1	48.134	-0.0008			1.8889
		5	1	2	48.164	-0.0303			1.8878

A10. Iodine – SSZ-24

Symmetry : Hexagonal *P*
Space group: *P* 6 (No. 168)

Refined cell parameters:
a : 13.604(6)
c : 8.292(3)

N	2Θ[obs]	H	K	L	2Θ[calc]	obs-calc	Int.	*d*[obs]	*d*[calc]
1	7.514	1	0	0	7.497	0.0163	32.9	11.7563	11.7817
2	13.050	1	1	0	13.005	0.0449	11.7	6.7789	6.8022
		1	0	1	13.045	0.0042			6.7810
3	15.049	2	0	0	15.027	0.0221	61.4	5.8823	5.8909
4	19.945	2	1	0	19.922	0.0227	94.1	4.4481	4.4531
5	21.426	0	0	2	21.414	0.0115	62.3	4.1439	4.1461
6	22.675	3	0	0	22.623	0.0520	100.0	3.9184	3.9272
		2	1	1	22.647	0.0281			3.9232
		1	0	2	22.718	-0.0433			3.9110
7	25.138	3	0	1	25.069	0.0690	17.9	3.5397	3.5493
		1	1	2	25.134	0.0041			3.5403
8	26.198	2	2	0	26.181	0.0178	45.0	3.3988	3.4011
		2	0	2	26.264	-0.0653			3.3905
9	29.395	3	1	1	29.355	0.0404	23.0	3.0360	3.0401
		2	1	2	29.411	-0.0157			3.0345
10	30.335	4	0	0	30.321	0.0143	33.1	2.9441	2.9454
11	32.165	4	0	1	32.226	-0.0612	10.8	2.7807	2.7755
12	34.059	2	2	2	34.068	-0.0087	12.9	2.6302	2.6296
13	34.885	4	1	0	34.869	0.0167	18.6	2.5698	2.5710
		3	2	1	34.885	0.0007			2.5698
		3	1	2	34.933	-0.0474			2.5664
14	37.403	4	0	2	37.422	-0.0192	10.9	2.4024	2.4012
15	38.300	2	1	3	38.295	0.0044	19.2	2.3482	2.3484
16	41.241	3	3	1	41.244	-0.0034	8.6	2.1873	2.1871
		4	1	2	41.286	-0.0451			2.1850
17	41.994	4	2	1	41.982	0.0128	10.2	2.1497	2.1504
18	42.702	5	1	0	42.695	0.0066	11.9	2.1157	2.1161
19	43.628	0	0	4	43.626	0.0024	9.6	2.0729	2.0731
20	44.125	5	1	1	44.134	-0.0087	10.1	2.0507	2.0504
		5	0	2	44.174	-0.0482			2.0486
21	45.569	3	3	2	45.562	0.0069	9.4	1.9891	1.9893
22	48.212	5	2	0	48.197	0.0151	14.2	1.8860	1.8866
		4	3	1	48.209	0.0028			1.8861
		5	1	2	48.246	-0.0341			1.8848

A11. Selenium – SSZ-24

Symmetry : Hexagonal *P*

Refined cell parameters:
a : 13.6338(17)
c : 8.3026(11)

N	2Θ[obs]	H	K	L	2Θ[calc]	obs-calc	Int.	*d*[obs]	*d*[calc]
1	7.466	1	0	0	7.481	-0.0149	100.0	11.8308	11.8072
2	12.962	1	1	0	12.976	-0.0143	11.8	6.8244	6.8169
		1	0	1	13.025	-0.0629			6.7916
3	14.985	2	0	0	14.995	-0.0097	7.2	5.9074	5.9036
4	18.956		---	not	indexed	---	2.7	4.6778	
5	19.869	2	1	0	19.879	-0.0094	19.1	4.4648	4.4627
6	20.275		---	not	indexed	---	3.0	4.3764	
7	20.948		---	not	indexed	---	2.7	4.2373	
8	21.372	0	0	2	21.387	-0.0156	23.2	4.1543	4.1513
9	22.591	3	0	0	22.573	0.0172	29.1	3.9328	3.9357
		2	1	1	22.602	-0.0113			3.9309
10	23.530		---	not	indexed	---	2.3	3.7779	
11	25.085	3	0	1	25.018	0.0665	2.7	3.5471	3.5564
		1	1	2	25.096	-0.0110			3.5456
12	26.115	2	2	0	26.123	-0.0083	12.1	3.4095	3.4085
13	26.555		---	not	indexed	---	2.1	3.3540	
14	26.915		---	not	indexed	---	1.9	3.3099	
15	27.494		---	not	indexed	---	2.0	3.2415	
16	28.024		---	not	indexed	---	1.8	3.1815	
17	28.686		---	not	indexed	---	1.8	3.1094	
18	29.325	3	1	1	29.294	0.0317	5.6	3.0431	3.0463
		2	1	2	29.361	-0.0353			3.0395
19	30.247	4	0	0	30.254	-0.0066	7.8	2.9524	2.9518
20	31.094		---	not	indexed	---	1.4	2.8739	
21	32.045		---	not	indexed	---	1.9	2.7908	
22	33.286	1	0	3	33.223	0.0636	1.3	2.6895	2.6945
23	33.996	2	2	2	34.005	-0.0094	2.7	2.6350	2.6343
24	34.780	4	1	0	34.791	-0.0109	6.1	2.5773	2.5766
		3	2	1	34.810	-0.0301			2.5752
25	37.344	4	0	2	37.351	-0.0066	2.1	2.4061	2.4057
26	38.225	2	1	3	38.236	-0.0107	4.7	2.3526	2.3520
27	40.601		---	not	indexed	---	1.1	2.2202	
28	41.186	3	3	1	41.153	0.0325	1.1	2.1900	2.1917
		4	1	2	41.203	-0.0173			2.1892
29	41.885	4	2	1	41.889	-0.0038	1.6	2.1551	2.1549
30	42.595	5	1	0	42.598	-0.0034	1.5	2.1208	2.1206
31	42.747	3	1	3	42.744	0.0036	1.8	2.1136	2.1138
32	43.564	0	0	4	43.569	-0.0049	1.5	2.0759	2.0756
33	44.074	5	1	1	44.036	0.0377	1.5	2.0530	2.0547
		5	0	2	44.083	-0.0094			2.0526
34	45.468	3	3	2	45.468	0.0000	1.2	1.9932	1.9932
35	46.115	6	0	0	46.088	0.0269	1.0	1.9668	1.9679
		4	2	2	46.149	-0.0338			1.9654
36	46.908	3	2	3	46.896	0.0121	0.9	1.9354	1.9358
37	48.093	5	2	0	48.086	0.0072	2.8	1.8904	1.8907
		4	3	1	48.101	-0.0075			1.8901
		5	1	2	48.145	-0.0516			1.8885
38	48.584		---	not	indexed	---	1.2	1.8724	

39	51.916	6	1	1	51.921	-0.0046	1.3	1.7598	1.7597
		4	3	2	51.962	-0.0463			1.7584
40	52.655	4	2	3	52.648	0.0067	1.4	1.7369	1.7371
41	53.200	5	2	2	53.191	0.0089	1.2	1.7204	1.7206
42	55.548	7	0	1	55.551	-0.0025	0.8	1.6530	1.6530
		6	1	2	55.590	-0.0423			1.6519
43	56.126	6	2	0	56.127	-0.0004	1.8	1.6374	1.6374
44	57.325	6	2	1	57.307	0.0184	1.3	1.6060	1.6064
45	57.981	4	3	3	57.988	-0.0072	1.5	1.5894	1.5892
46	59.023	7	1	0	59.016	0.0066	1.2	1.5637	1.5639
		7	0	2	59.067	-0.0445			1.5627
47	59.322	2	1	5	59.335	-0.0125	2.4	1.5566	1.5563
48	60.342	3	3	4	60.349	-0.0071	0.7	1.5327	1.5325
49	60.766	6	2	2	60.758	0.0081	1.3	1.5230	1.5232
50	61.379	6	1	3	61.378	0.0005	1.7	1.5093	1.5093
51	62.670	3	1	5	62.681	-0.0106	0.9	1.4812	1.4810
52	63.514	6	3	1	63.480	0.0335	0.8	1.4636	1.4643
		7	1	2	63.517	-0.0032			1.4635
53	64.658	7	0	3	64.662	-0.0041	0.6	1.4404	1.4403
54	65.687	7	2	1	65.641	0.0458	0.7	1.4203	1.4212
		5	4	2	65.677	0.0098			1.4205
55	66.275	6	2	3	66.271	0.0042	1.6	1.4091	1.4092
56	68.822	5	5	0	68.803	0.0182	1.4	1.3631	1.3634
		8	1	1	68.815	0.0064			1.3632
		7	2	2	68.850	-0.0287			1.3626
57	69.322	6	4	0	69.326	-0.0037	0.7	1.3544	1.3544

A12. Mercury(II) bromide – SSZ-24

Symmetry : Hexagonal *P*
Space group: *P* 6 (No. 168)

Refined cell parameters:
a : 13.618(5)
c : 8.3081(22)

N	2Θ[obs]	H	K	L	2Θ[calc]	obs-calc	Int.	*d*[obs]	*d*[calc]
1	7.494	1	0	0	7.490	0.0042	100.0	11.7868	11.7934
2	12.996	1	1	0	12.992	0.0044	12.9	6.8066	6.8089
		1	0	1	13.024	-0.0281			6.7920
3	14.195	---	not indexed	---			17.6	6.2341	
4	15.018	2	0	0	15.012	0.0058	18.2	5.8944	5.8967
5	19.909	2	1	0	19.903	0.0063	40.6	4.4561	4.4575
6	21.412	0	0	2	21.373	0.0395	43.3	4.1465	4.1541
7	22.636	3	0	0	22.600	0.0355	54.2	3.9250	3.9311
		2	1	1	22.619	0.0164			3.9279
8	24.292	---	not indexed	---			9.1	3.6610	
9	25.087	1	1	2	25.091	-0.0049	6.2	3.5469	3.5462
10	26.157	2	2	0	26.154	0.0032	27.9	3.4040	3.4044
11	26.966	---	not indexed	---			8.4	3.3038	
12	27.347	---	not indexed	---			7.4	3.2587	
13	29.361	3	1	1	29.322	0.0394	16.4	3.0395	3.0435
		2	1	2	29.366	-0.0054			3.0390
14	30.285	4	0	0	30.290	-0.0049	16.8	2.9488	2.9483
15	31.757	---	not indexed	---			5.3	2.8155	
16	32.096	---	not indexed	---			6.8	2.7865	
17	34.028	2	2	2	34.020	0.0078	7.6	2.6325	2.6331
18	34.827	4	1	0	34.833	-0.0061	14.3	2.5740	2.5735
		3	2	1	34.846	-0.0189			2.5726
19	37.381	4	0	2	37.372	0.0089	5.5	2.4038	2.4043
20	38.250	2	1	3	38.229	0.0202	10.7	2.3511	2.3523
21	38.834	---	not indexed	---			5.9	2.3171	
22	40.662	---	not indexed	---			4.0	2.2170	
23	41.931	4	2	1	41.935	-0.0047	5.4	2.1529	2.1526
24	42.733	3	1	3	42.748	-0.0148	5.1	2.1143	2.1136
25	43.526	0	0	4	43.538	-0.0120	6.1	2.0776	2.0770
26	44.408	---	not indexed	---			6.1	2.0383	
27	45.018	---	not indexed	---			5.2	2.0121	
28	45.519	3	3	2	45.505	0.0140	4.1	1.9912	1.9917
29	46.878	3	2	3	46.910	-0.0318	5.6	1.9365	1.9353
30	48.174	5	2	0	48.146	0.0285	7.3	1.8874	1.8884
		4	3	1	48.156	0.0186			1.8881
		5	1	2	48.185	-0.0108			1.8870

A13. Gold(III) chloride – SSZ-24

Symmetry : Hexagonal *P*
Space group: *P* 6 (No. 168)

Refined cell parameters:
a : 13.643(5)
c : 8.328(4)

N	2Θ[obs]	H	K	L	2Θ[calc]	obs-calc	Int.	*d*[obs]	*d*[calc]
1	7.477	1	0	0	7.476	0.0008	42.8	11.8144	11.8156
2	10.266	---	not	indexed	---		10.6	8.6102	
3	12.958	1	1	0	12.967	-0.0088	19.7	6.8263	6.8217
		1	0	1	12.995	-0.0364			6.8073
4	14.987	2	0	0	14.984	0.0034	87.3	5.9065	5.9078
5	16.041	---	not	indexed	---		11.1	5.5207	
6	19.273	---	not	indexed	---		13.5	4.6016	
7	19.864	2	1	0	19.865	-0.0006	100.0	4.4660	4.4659
8	20.693	---	not	indexed	---		14.1	4.2889	
9	21.330	0	0	2	21.320	0.0099	48.0	4.1623	4.1642
10	22.593	3	0	0	22.557	0.0361	95.1	3.9323	3.9385
		2	1	1	22.573	0.0199			3.9357
		1	0	2	22.622	-0.0286			3.9274
11	24.511	---	not	indexed	---		12.6	3.6288	
12	25.024	3	0	1	24.989	0.0351	18.1	3.5556	3.5605
		1	1	2	25.033	-0.0090			3.5543
13	26.117	2	2	0	26.104	0.0123	25.0	3.4093	3.4109
		2	0	2	26.161	-0.0441			3.4036
14	26.772	---	not	indexed	---		9.4	3.3273	
15	27.167	3	1	0	27.190	-0.0234	8.9	3.2798	3.2770
16	28.173	2	2	1	28.251	-0.0772	7.6	3.1649	3.1564
17	29.271	3	1	1	29.263	0.0084	13.4	3.0486	3.0495
		2	1	2	29.301	-0.0296			3.0456
18	30.238	4	0	0	30.232	0.0060	15.1	2.9533	2.9539
19	30.841	---	not	indexed	---		7.2	2.8970	
20	31.203	3	0	2	31.234	-0.0311	8.1	2.8642	2.8614
21	32.930	3	2	0	33.019	-0.0888	6.6	2.7178	2.7107
22	33.923	2	2	2	33.947	-0.0239	13.6	2.6405	2.6387
23	34.765	4	1	0	34.766	-0.0009	20.8	2.5784	2.5784
		3	2	1	34.777	-0.0118			2.5776
		3	1	2	34.809	-0.0445			2.5752
24	37.289	4	0	2	37.292	-0.0032	11.5	2.4095	2.4093
25	38.143	2	1	3	38.139	0.0042	12.1	2.3575	2.3577
26	39.558	3	3	0	39.602	-0.0437	7.2	2.2763	2.2739
		5	0	1	39.612	-0.0534			2.2734
		3	2	2	39.641	-0.0826			2.2718
27	41.113	3	3	1	41.116	-0.0026	5.7	2.1937	2.1936
		4	1	2	41.144	-0.0309			2.1922
28	41.856	4	2	1	41.851	0.0050	5.7	2.1565	2.1568
		2	2	3	41.926	-0.0694			2.1531
29	42.663	3	1	3	42.650	0.0133	5.8	2.1176	2.1182
30	43.419	0	0	4	43.427	-0.0078	5.7	2.0824	2.0821
31	46.072	6	0	0	46.054	0.0189	6.2	1.9685	1.9693
		4	2	2	46.088	-0.0156			1.9679
32	46.698	4	3	0	46.726	-0.0287	4.4	1.9436	1.9425
33	48.096	5	2	0	48.050	0.0461	8.6	1.8903	1.8920
		4	3	1	48.058	0.0377			1.8917

		5	1	2	48.083	0.0127		1.8908
		4	1	3	48.125	-0.0290		1.8892
		2	1	4	48.183	-0.0874		1.8871
34	51.909	6	1	1	51.875	0.0335	5.4	1.7601	1.7611
		4	3	2	51.899	0.0098		1.7604
		3	3	3	51.939	-0.0297		1.7591
		3	1	4	51.994	-0.0848		1.7574
35	52.566	4	2	3	52.555	0.0116	4.4	1.7396	1.7399
36	53.126	5	2	2	53.127	-0.0006	4.7	1.7226	1.7225
37	56.110	6	2	0	56.084	0.0261	5.6	1.6378	1.6385
38	57.285	6	2	1	57.257	0.0275	4.2	1.6070	1.6077
		6	0	3	57.316	-0.0315			1.6062
39	57.901	4	3	3	57.893	0.0082	4.1	1.5913	1.5916
40	59.142	5	0	4	59.087	0.0554	6.6	1.5609	1.5622
		2	1	5	59.152	-0.0098			1.5607
41	60.195	7	1	1	60.108	0.0875	3.5	1.5361	1.5381
		3	3	4	60.215	-0.0198			1.5356
		3	0	5	60.280	-0.0842			1.5341
42	60.694	6	2	2	60.690	0.0050	3.6	1.5246	1.5247
		4	2	4	60.775	-0.0804			1.5228
43	61.283	5	4	0	61.218	0.0646	4.2	1.5114	1.5128
		6	1	3	61.282	0.0008			1.5114
44	62.493	5	1	4	62.436	0.0570	3.5	1.4850	1.4862
		3	1	5	62.499	-0.0060			1.4849
45	65.609	7	2	1	65.584	0.0258	3.3	1.4218	1.4223
		5	4	2	65.604	0.0053			1.4219
		4	3	4	65.686	-0.0765			1.4203
46	66.218	6	2	3	66.172	0.0461	4.0	1.4102	1.4111
47	68.807	5	5	0	68.748	0.0589	3.7	1.3633	1.3643
		8	1	1	68.755	0.0522			1.3642
		7	2	2	68.775	0.0323			1.3639
		7	1	3	68.808	-0.0010			1.3633
		6	1	4	68.855	-0.0476			1.3625

A14. CIT-5 as-synthesized

Symmetry : Orthorhombic *I*
Space group: *I m m a* (No. 74)

Refined cell parameters:
a : 13.780(4)
b : 5.0329(19)
c : 25.536(11)

N	2Θ[obs]	H	K	L	2Θ[calc]	obs-calc	Int.	*d*[obs]	*d*[calc]
1	6.872	0	0	2	6.918	-0.0456	55.2	12.8525	12.7680
2	7.243	1	0	1	7.284	-0.0405	78.3	12.1947	12.1270
3	13.849	0	0	4	13.861	-0.0114	27.6	6.3892	6.3840
4	14.612	2	0	2	14.597	0.0148	24.3	6.0574	6.0635
5	18.940	2	0	4	18.936	0.0038	74.3	4.6819	4.6828
6	19.622	3	0	1	19.621	0.0010	38.6	4.5205	4.5208
7	20.003	1	1	2	20.012	-0.0085	100.0	4.4352	4.4333
8	20.488	0	1	3	20.484	0.0039	69.5	4.3315	4.3323
9	20.890	0	0	6	20.855	0.0349	29.0	4.2490	4.2560
10	22.003	3	0	3	21.971	0.0321	15.7	4.0365	4.0423
11	23.393	1	1	4	23.396	-0.0025	25.4	3.7996	3.7992
12	24.236	2	1	3	24.248	-0.0125	26.5	3.6694	3.6675
13	24.546	2	0	6	24.566	-0.0195	26.7	3.6237	3.6209
14	25.796	4	0	0	25.841	-0.0453	13.8	3.4509	3.4450
15	26.774	4	0	2	26.782	-0.0086	59.7	3.3271	3.3261
16	27.180	3	1	2	27.174	0.0061	26.5	3.2783	3.2790
17	27.892	0	0	8	27.929	-0.0370	16.0	3.1961	3.1920
18	28.207	1	1	6	28.190	0.0168	31.5	3.1612	3.1630
19	29.844	3	1	4	29.798	0.0465	11.6	2.9914	2.9960
20	31.312	3	0	7	31.287	0.0248	9.9	2.8545	2.8567
21	33.017	2	1	7	32.968	0.0497	9.9	2.7108	2.7148
22	33.397	4	0	6	33.437	-0.0398	11.4	2.6808	2.6777
23	33.806	3	1	6	33.758	0.0474	8.8	2.6493	2.6530
24	35.672	0	2	0	35.649	0.0231	24.3	2.5149	2.5165
25	36.415	1	2	1	36.435	-0.0197	13.2	2.4653	2.4640
26	37.022	5	0	5	37.035	-0.0138	7.2	2.4263	2.4254
27	37.862	1	2	3	37.817	0.0446	13.8	2.3743	2.3770
		5	1	2	37.849	0.0127			2.3751
28	38.708	2	1	9	38.672	0.0363	5.0	2.3244	2.3265
		3	1	8	38.700	0.0079			2.3248
		2	2	2	38.710	-0.0021			2.3242
29	40.170	4	1	7	40.183	-0.0137	5.5	2.2431	2.2423
30	40.671	2	2	4	40.669	0.0015	10.5	2.2166	2.2167
31	43.731	2	2	6	43.773	-0.0417	7.7	2.0683	2.0664
32	44.795	6	0	6	44.806	-0.0104	11.0	2.0216	2.0212
33	45.847	5	0	9	45.865	-0.0184	3.9	1.9777	1.9769
		0	2	8	45.883	-0.0361			1.9762
34	46.241	7	0	1	46.215	0.0260	4.4	1.9617	1.9627
35	46.816	1	1	12	46.777	0.0389	7.2	1.9389	1.9405
36	47.111	5	1	8	47.122	-0.0110	6.1	1.9275	1.9271
37	49.642	4	2	6	49.677	-0.0352	9.4	1.8350	1.8338

A15. CIT-5 calcined

Symmetry : Orthorhombic *I*
Space group: *I m* 2 *a* (No. 46)

Refined cell parameters:
a : 13.709(4)
b : 5.0358(14)
c : 25.580(10)

N	2Θ[obs]	H	K	L	2Θ[calc]	obs-calc	Int.	*d*[obs]	*d*[calc]
1	6.897	0	0	2	6.906	-0.0089	61.2	12.8064	12.7898
2	7.286	1	0	1	7.310	-0.0244	100.0	12.1236	12.0832
3	12.208	1	0	3	12.214	-0.0065	11.6	7.2442	7.2404
4	12.879	2	0	0	12.905	-0.0255	10.1	6.8681	6.8546
5	13.817	0	0	4	13.837	-0.0194	6.1	6.4039	6.3949
6	18.965	2	0	4	18.964	0.0012	23.4	4.6757	4.6760
7	19.719	3	0	1	19.719	0.0002	11.1	4.4985	4.4985
8	20.006	1	1	2	20.010	-0.0043	35.0	4.4348	4.4338
9	20.460	0	1	3	20.466	-0.0061	26.8	4.3373	4.3360
10	20.809	0	0	6	20.819	-0.0098	11.3	4.2653	4.2633
11	22.036	3	0	3	22.051	-0.0150	5.5	4.0304	4.0277
12	23.405	1	1	4	23.383	0.0217	7.3	3.7977	3.8012
13	24.556	2	0	6	24.570	-0.0146	9.4	3.6223	3.6202
14	25.998	4	0	0	25.977	0.0211	4.8	3.4246	3.4273
15	26.912	4	0	2	26.910	0.0012	19.9	3.3103	3.3105
16	27.236	3	1	2	27.237	-0.0013	9.5	3.2717	3.2715
17	28.159	1	1	6	28.164	-0.0053	11.7	3.1665	3.1659
18	29.838	3	1	4	29.847	-0.0091	2.8	2.9920	2.9911
19	31.346	3	0	7	31.317	0.0289	3.3	2.8514	2.8540
20	31.753	4	1	1	31.749	0.0039	2.3	2.8158	2.8161
21	32.994	2	1	7	32.957	0.0368	3.6	2.7126	2.7156
22	33.500	4	0	6	33.521	-0.0210	2.8	2.6728	2.6712
23	33.799	3	1	6	33.790	0.0094	2.1	2.6498	2.6506
		1	1	8	33.818	-0.0183			2.6485
24	34.333	5	0	3	34.328	0.0051	2.8	2.6098	2.6102
25	35.633	0	2	0	35.628	0.0044	7.6	2.5176	2.5179
26	36.321	0	2	2	36.336	-0.0144	3.9	2.4714	2.4705

A16. Iodine – CIT-5

Symmetry : Orthorhombic *I*
Space group: *I m* 2 *a* (No. 46)

Refined cell parameters :
a : 13.671(5)
b : 5.0201(18)
c : 25.485(8)

N	2Θ[obs]	H	K	L	2Θ[calc]	obs-calc	Int.	*d*[obs]	*d*[calc]
1	6.925	0	0	2	6.931	-0.0066	25.7	12.7547	12.7426
2	7.317	1	0	1	7.332	-0.0150	22.7	12.0719	12.0472
3	12.214	1	0	3	12.257	-0.0428	11.6	7.2407	7.2155
4	13.880	0	0	4	13.888	-0.0084	36.5	6.3751	6.3713
5	14.685	2	0	2	14.694	-0.0090	30.3	6.0273	6.0236
6	19.022	2	0	4	19.027	-0.0041	95.5	4.6617	4.6607
7	19.765	3	0	1	19.775	-0.0097	57.2	4.4881	4.4859
8	20.070	1	1	2	20.073	-0.0038	100.0	4.4207	4.4199
9	20.529	0	1	3	20.534	-0.0048	76.5	4.3229	4.3219
10	20.896	0	0	6	20.897	-0.0008	38.6	4.2477	4.2475
11	22.119	3	0	3	22.118	0.0006	23.9	4.0156	4.0157
12	23.465	1	1	4	23.462	0.0039	21.5	3.7881	3.7887
13	24.357	2	1	3	24.346	0.0108	21.6	3.6514	3.6530
14	24.659	2	0	6	24.657	0.0028	33.0	3.6073	3.6077
15	25.320	1	0	7	25.295	0.0252	14.9	3.5147	3.5181
16	26.098	4	0	0	26.050	0.0476	19.9	3.4117	3.4178
17	26.978	4	0	2	26.988	-0.0099	57.5	3.3023	3.3011
18	27.320	3	1	2	27.320	-0.0004	32.4	3.2618	3.2618
19	28.016	0	0	8	27.986	0.0297	20.5	3.1823	3.1856
20	28.257	1	1	6	28.263	-0.0057	43.4	3.1557	3.1551
21	29.943	3	1	4	29.942	0.0011	14.8	2.9817	2.9818
22	31.396	3	0	7	31.425	-0.0290	14.5	2.8470	2.8444
23	31.852	4	1	1	31.843	0.0089	13.4	2.8072	2.8080
24	33.104	2	1	7	33.072	0.0320	15.9	2.7039	2.7064
25	33.614	4	0	6	33.630	-0.0157	15.8	2.6640	2.6628
26	35.748	0	2	0	35.743	0.0049	26.5	2.5097	2.5101
27	36.491	0	2	2	36.454	0.0376	14.9	2.4603	2.4627
		1	2	1	36.537	-0.0460			2.4573
28	37.284	5	0	5	37.290	-0.0060	12.1	2.4098	2.4094
		3	0	9	37.358	-0.0748			2.4052
29	38.101	5	1	2	38.106	-0.0052	11.9	2.3600	2.3596
		2	2	0	38.164	-0.0626			2.3562
30	38.760	2	1	9	38.784	-0.0240	11.4	2.3214	2.3200
		2	2	2	38.836	-0.0766			2.3170
31	40.163	5	1	4	40.098	0.0648	10.3	2.2434	2.2469
		6	0	2	40.172	-0.0089			2.2429
		1	1	10	40.195	-0.0323			2.2417
32	41.216	3	2	1	41.178	0.0385	10.5	2.1885	2.1905
		5	0	7	41.259	-0.0433			2.1863
33	42.969	0	1	11	42.960	0.0090	10.5	2.1032	2.1036
34	43.769	6	1	1	43.739	0.0303	9.3	2.0666	2.0680
		3	0	11	43.799	-0.0304			2.0652
35	44.613	2	0	12	44.644	-0.0307	12.8	2.0295	2.0281
36	45.105	2	1	11	45.055	0.0505	13.7	2.0084	2.0106
		6	0	6	45.119	-0.0131			2.0079
37	45.996	0	2	8	45.996	-0.0001	10.3	1.9716	1.9716

38	47.397	5	1	8	47.372	0.0252	13.1	1.9165	1.9175
39	48.249	3	2	7	48.320	-0.0708	7.9	1.8847	1.8821
40	48.948	1	2	9	48.906	0.0421	8.4	1.8594	1.8609

A17. Selenium – CIT-5

Symmetry : Orthorhombic *I*

Refined cell parameters:
a : 13.6778(14)
b : 5.0196(6)
c : 25.570(3)

N	2Θ[obs]	H	K	L	2Θ[calc]	obs-calc	Int.	*d*[obs]	*d*[calc]
1	6.900	0	0	2	6.908	-0.0081	52.8	12.7999	12.7848
2	7.297	1	0	1	7.324	-0.0270	66.3	12.1052	12.0606
3	12.203	1	0	3	12.226	-0.0222	27.6	7.2468	7.2337
4	12.926	2	0	0	12.935	-0.0087	27.1	6.8435	6.8389
5	13.832	0	0	4	13.842	-0.0106	38.2	6.3973	6.3924
6	14.665	2	0	2	14.678	-0.0123	42.5	6.0353	6.0303
7	18.015	0	1	1	17.995	0.0203	23.5	4.9201	4.9256
8	18.521	1	0	5	18.508	0.0134	23.4	4.7866	4.7901
9	18.983	2	0	4	18.988	-0.0050	78.6	4.6712	4.6700
10	19.751	3	0	1	19.764	-0.0123	64.7	4.4912	4.4885
11	20.055	1	1	2	20.066	-0.0109	100.0	4.4239	4.4215
12	20.507	0	1	3	20.517	-0.0106	90.4	4.3275	4.3252
13	20.832	0	0	6	20.827	0.0047	33.4	4.2607	4.2616
14	22.098	3	0	3	22.093	0.0053	26.4	4.0193	4.0202
15	23.428	1	1	4	23.434	-0.0064	27.8	3.7941	3.7931
16	24.326	2	1	3	24.329	-0.0032	26.2	3.6560	3.6555
17	24.590	2	0	6	24.594	-0.0030	53.0	3.6173	3.6169
18	25.222	1	0	7	25.215	0.0074	26.7	3.5281	3.5291
19	26.156	3	0	5	26.164	-0.0083	29.3	3.4042	3.4032
20	26.963	4	0	2	26.970	-0.0072	65.9	3.3042	3.3033
21	27.300	3	1	2	27.308	-0.0087	37.6	3.2642	3.2631
22	27.908	0	0	8	27.892	0.0163	23.1	3.1944	3.1962
23	28.204	1	1	6	28.211	-0.0070	42.9	3.1615	3.1608
24	29.590	4	0	4	29.603	-0.0138	14.3	3.0165	3.0152
25	29.914	3	1	4	29.915	-0.0007	19.3	2.9846	2.9845
26	30.235	0	1	7	30.236	-0.0008	15.6	2.9536	2.9535
27	30.851	2	0	8	30.856	-0.0048	11.9	2.8960	2.8956
28	31.825	4	1	1	31.833	-0.0074	12.3	2.8096	2.8089
29	32.993	2	1	7	33.009	-0.0158	13.8	2.7127	2.7115
30	33.567	4	0	6	33.575	-0.0078	18.6	2.6676	2.6670
31	35.053	0	0	10	35.066	-0.0131	10.4	2.5579	2.5570
32	35.739	0	2	0	35.747	-0.0083	29.8	2.5104	2.5098
33	36.308	4	1	5	36.290	0.0184	14.3	2.4723	2.4735
		0	1	9	36.305	0.0037			2.4725
34	36.519	1	2	1	36.540	-0.0209	12.8	2.4585	2.4572
35	37.245	5	0	5	37.247	-0.0017	10.0	2.4122	2.4121
		3	0	9	37.261	-0.0160			2.4112
36	38.090	5	1	2	38.089	0.0014	13.2	2.3606	2.3607
37	38.741	2	1	9	38.693	0.0477	9.8	2.3225	2.3252
		3	1	8	38.772	-0.0311			2.3207
38	40.107	5	1	4	40.068	0.0384	10.1	2.2464	2.2485
		1	1	10	40.089	0.0182			2.2474
		6	0	2	40.148	-0.0414			2.2442
39	41.175	3	2	1	41.175	-0.0000	9.6	2.1906	2.1906
		5	0	7	41.195	-0.0194			2.1896
40	41.745	0	2	6	41.732	0.0122	7.6	2.1620	2.1626
41	42.857	0	1	11	42.838	0.0185	9.5	2.1085	2.1093

42	43.707	3	0	11	43.674	0.0336	10.0	2.0694	2.0709
		6	1	1	43.720	-0.0128			2.0688
43	44.184	4	0	10	44.193	-0.0092	9.5	2.0482	2.0478
44	44.502	2	0	12	44.500	0.0021	9.9	2.0343	2.0343
45	45.076	6	0	6	45.066	0.0101	13.1	2.0097	2.0101
46	45.944	0	2	8	45.938	0.0060	9.9	1.9737	1.9740
47	47.302	5	1	8	47.301	0.0017	13.1	1.9201	1.9202
48	47.879	2	2	8	47.928	-0.0485	7.4	1.8983	1.8965
49	48.299	3	2	7	48.274	0.0256	8.6	1.8828	1.8838
50	48.847	1	2	9	48.834	0.0127	8.4	1.8630	1.8634
51	49.907	0	0	14	49.891	0.0163	11.2	1.8258	1.8264
		7	0	5	49.924	-0.0170			1.8253
52	50.538	3	0	13	50.494	0.0444	12.9	1.8045	1.8060
		6	1	7	50.535	0.0030			1.8046
53	51.623	2	1	13	51.627	-0.0037	7.2	1.7691	1.7690
54	52.195	7	1	4	52.191	0.0041	8.5	1.7511	1.7512
		5	1	10	52.207	-0.0124			1.7507
55	52.586	5	2	5	52.581	0.0055	7.3	1.7390	1.7391
		3	2	9	52.592	-0.0054			1.7388
56	53.107	7	0	7	53.113	-0.0065	6.6	1.7231	1.7229
57	53.573	8	0	0	53.557	0.0163	6.8	1.7092	1.7097
		4	2	8	53.563	0.0106			1.7096
58	53.820	1	1	14	53.786	0.0338	6.5	1.7020	1.7030
		6	0	10	53.834	-0.0138			1.7016
59	54.796	7	1	6	54.779	0.0172	6.7	1.6739	1.6744
		6	2	2	54.831	-0.0354			1.6729
60	55.605	8	0	4	55.599	0.0060	11.1	1.6515	1.6517
61	57.047	4	1	13	56.999	0.0477	7.7	1.6131	1.6144
		0	1	15	57.009	0.0374			1.6141
62	57.719	5	0	13	57.679	0.0401	8.2	1.5959	1.5970
		3	0	15	57.689	0.0298			1.5967
		2	3	3	57.697	0.0221			1.5965
63	58.770	2	1	15	58.726	0.0441	7.8	1.5699	1.5709
		3	3	0	58.733	0.0366			1.5708
		6	2	6	58.808	-0.0385			1.5689
64	59.226	3	3	2	59.219	0.0075	7.4	1.5589	1.5590
65	59.703	6	1	11	59.674	0.0285	8.9	1.5476	1.5482
		1	3	6	59.707	-0.0041			1.5475
66	60.675	3	3	4	60.661	0.0142	6.8	1.5251	1.5254
67	62.020	9	0	3	61.975	0.0442	6.5	1.4952	1.4962
		7	0	11	61.995	0.0246			1.4957
		1	0	17	62.024	-0.0049			1.4951
68	62.744	4	3	3	62.724	0.0204	6.6	1.4797	1.4801
		8	1	7	62.743	0.0015			1.4797
69	63.403	3	2	13	63.400	0.0033	6.5	1.4659	1.4659
70	64.375	5	0	15	64.341	0.0342	6.9	1.4461	1.4467
		9	1	2	64.416	-0.0415			1.4452
71	65.455	6	0	14	65.425	0.0303	6.3	1.4248	1.4254
72	65.780	5	3	2	65.778	0.0013	6.9	1.4185	1.4186
		9	1	4	65.792	-0.0125			1.4183
73	66.263	2	1	17	66.236	0.0266	6.2	1.4094	1.4099
		3	3	8	66.243	0.0196			1.4097
74	67.233	2	0	18	67.261	-0.0276	5.9	1.3914	1.3909
75	67.550	7	0	13	67.516	0.0339	6.2	1.3856	1.3862
76	68.036	9	1	6	68.053	-0.0173	6.9	1.3769	1.3766
77	68.556	10	0	0	68.552	0.0049	6.6	1.3677	1.3678
78	69.771	5	2	13	69.741	0.0302	6.6	1.3468	1.3473
		3	2	15	69.750	0.0209			1.3472
		6	3	1	69.761	0.0097			1.3470

A18. Mercury(II) bromide – CIT-5

Symmetry : Orthorhombic *I*
Space group: *I m* 2 *a* (No. 46)

Refined cell parameters:
a : 13.665(4)
b : 5.0155(15)
c : 25.460(7)

N	2Θ[obs]	H	K	L	2Θ[calc]	obs-calc	Int.	*d*[obs]	*d*[calc]
1	6.946	0	0	2	6.938	0.0080	42.1	12.7154	12.7300
2	7.348	1	0	1	7.336	0.0122	41.3	12.0205	12.0405
3	12.260	1	0	3	12.267	-0.0071	36.7	7.2136	7.2095
4	12.962	2	0	0	12.946	0.0155	33.3	6.8245	6.8326
5	13.911	0	0	4	13.902	0.0090	54.8	6.3609	6.3650
6	14.693	2	0	2	14.702	-0.0089	54.7	6.0239	6.0203
7	19.047	2	0	4	19.041	0.0062	100.0	4.6558	4.6573
8	19.790	3	0	1	19.784	0.0061	65.8	4.4825	4.4839
9	20.107	1	1	2	20.091	0.0160	79.5	4.4125	4.4160
10	20.567	0	1	3	20.553	0.0139	69.2	4.3150	4.3178
11	20.921	0	0	6	20.918	0.0035	56.0	4.2426	4.2433
12	21.848	3	0	3	22.130	-0.2821	34.7	4.0647	4.0135
13	22.106	3	0	3	22.130	-0.0242	49.2	4.0178	4.0135
		2	1	1	22.245	-0.1387			3.9931
14	23.488	1	1	4	23.483	0.0049	34.8	3.7845	3.7853
15	24.380	2	1	3	24.366	0.0141	31.5	3.6480	3.6501
16	24.671	2	0	6	24.677	-0.0062	32.6	3.6056	3.6047
		0	1	5	24.898	-0.2272			3.5732
17	25.350	1	0	7	25.319	0.0307	26.2	3.5106	3.5148
18	26.055	4	0	0	26.062	-0.0069	29.6	3.4172	3.4163
		3	0	5	26.229	-0.1738			3.3949
19	27.000	4	0	2	27.001	-0.0007	40.6	3.2996	3.2996
20	27.343	3	1	2	27.339	0.0039	32.9	3.2591	3.2596
21	28.282	0	0	8	28.014	0.2684	35.7	3.1529	3.1825
		2	1	5	28.160	0.1228			3.1664
		1	1	6	28.290	-0.0072			3.1521
22	29.828	4	0	4	29.654	0.1737	21.7	2.9930	3.0101
		3	1	4	29.964	-0.1364			2.9797
23	29.969	3	1	4	29.964	0.0047	22.1	2.9792	2.9797
24	30.318	0	1	7	30.332	-0.0131	19.9	2.9457	2.9444
25	31.438	3	0	7	31.450	-0.0121	22.0	2.8433	2.8422
26	31.854	4	1	1	31.863	-0.0092	17.8	2.8071	2.8063
27	32.294	1	0	9	32.290	0.0035	17.1	2.7699	2.7702
28	33.101	5	0	1	32.934	0.1665	18.4	2.7041	2.7174
		2	1	7	33.102	-0.0014			2.7040
29	33.911	4	0	6	33.653	0.2585	16.3	2.6414	2.6611
		3	1	6	33.930	-0.0187			2.6400
		1	1	8	33.973	-0.0619			2.6367
30	34.446	5	0	3	34.447	-0.0008	16.6	2.6015	2.6015
31	35.798	0	2	0	35.777	0.0210	24.2	2.5063	2.5078
32	36.449	4	1	5	36.353	0.0951	16.4	2.4631	2.4693
		0	1	9	36.435	0.0137			2.4640
		0	2	2	36.489	-0.0401			2.4605
		1	2	1	36.572	-0.1232			2.4551
33	37.295	5	0	5	37.311	-0.0162	16.1	2.4091	2.4081
		3	0	9	37.391	-0.0958			2.4032

34	38.133	1	2	3	37.958	0.1757	14.0	2.3580	2.3686
		5	1	2	38.129	0.0047			2.3583
		2	2	0	38.198	-0.0647			2.3542
35	38.532	0	2	4	38.555	-0.0238	12.4	2.3346	2.3332
		4	0	8	38.634	-0.1022			2.3286
		2	1	9	38.821	-0.2889			2.3179
36	38.897	4	0	8	38.634	0.2636	13.8	2.3135	2.3286
		2	1	9	38.821	0.0769			2.3179
		2	2	2	38.872	0.0259			2.3149
		3	1	8	38.880	0.0173			2.3145
37	39.386	1	0	11	39.455	-0.0686	12.8	2.2859	2.2820
		6	0	0	39.536	-0.1500			2.2775
38	40.164	5	1	4	40.123	0.0410	12.1	2.2434	2.2456
		6	0	2	40.191	-0.0266			2.2419
		1	1	10	40.236	-0.0713			2.2396
		4	1	7	40.409	-0.2445			2.2304
39	40.852	1	2	5	40.609	0.2437	11.4	2.2072	2.2198
		2	2	4	40.836	0.0164			2.2080
40	41.967	0	2	6	41.807	0.1601	11.6	2.1511	2.1589
		6	0	4	42.104	-0.1366			2.1444
41	42.982	0	1	11	43.004	-0.0221	11.7	2.1026	2.1016
42	43.765	6	1	1	43.762	0.0028	11.6	2.0668	2.0669
		3	0	11	43.839	-0.0742			2.0634
		2	2	6	43.948	-0.1827			2.0586
43	45.063	4	2	0	44.796	0.2674	11.9	2.0102	2.0216
		3	2	5	44.900	0.1631			2.0171
		6	1	3	44.963	0.1009			2.0145
		2	1	11	45.099	-0.0355			2.0087
		6	0	6	45.145	-0.0816			2.0068
		4	1	9	45.344	-0.2801			1.9984
44	45.376	2	1	11	45.099	0.2772	10.8	1.9971	2.0087
		6	0	6	45.145	0.2311			2.0068
		4	1	9	45.344	0.0326			1.9984
		4	2	2	45.389	-0.0124			1.9966
45	46.053	0	2	8	46.042	0.0105	10.1	1.9693	1.9697
		5	0	9	46.145	-0.0925			1.9656
46	47.401	4	2	4	47.131	0.2703	11.5	1.9164	1.9267
		6	1	5	47.291	0.1103			1.9206
		5	1	8	47.407	-0.0061			1.9161
47	47.988	7	0	3	47.768	0.2192	8.6	1.8943	1.9025
		2	2	8	48.032	-0.0448			1.8926

A19. Gold(III) chloride – CIT-5

Symmetry : Orthorhombic *I*

Refined cell parameters:
a : 13.6638(19)
b : 5.0138(10)
c : 25.487(4)

N	2Θ[obs]	H	K	L	2Θ[calc]	obs-calc	Int.	*d*[obs]	*d*[calc]
1	6.966	0	0	2	6.931	0.0355	41.9	12.6790	12.7437
2	7.328	1	0	1	7.335	-0.0073	41.7	12.0544	12.0424
3	12.262	1	0	3	12.258	0.0044	40.7	7.2123	7.2149
4	12.937	2	0	0	12.948	-0.0104	36.1	6.8374	6.8319
5	13.896	0	0	4	13.887	0.0086	59.1	6.3679	6.3719
6	14.705	2	0	2	14.700	0.0047	52.4	6.0193	6.0212
7	18.570	1	0	5	18.563	0.0065	34.9	4.7743	4.7760
8	19.038	2	0	4	19.030	0.0081	100.0	4.6578	4.6597
9	19.792	3	0	1	19.786	0.0062	66.2	4.4822	4.4836
10	20.104	1	1	2	20.094	0.0098	75.3	4.4133	4.4154
11	20.562	0	1	3	20.552	0.0098	67.2	4.3159	4.3180
12	20.914	0	0	6	20.895	0.0184	56.3	4.2442	4.2479
13	22.132	3	0	3	22.127	0.0048	42.9	4.0133	4.0141
14	23.478	1	1	4	23.479	-0.0007	33.5	3.7861	3.7860
15	24.366	2	1	3	24.366	0.0000	30.3	3.6500	3.6500
16	24.669	2	0	6	24.659	0.0102	32.0	3.6060	3.6074
17	26.061	4	0	0	26.065	-0.0037	28.9	3.4164	3.4160
18	26.999	4	0	2	27.002	-0.0026	38.7	3.2998	3.2995
19	27.344	3	1	2	27.342	0.0017	31.6	3.2590	3.2592
20	28.279	1	1	6	28.277	0.0028	35.6	3.1533	3.1536
21	29.978	3	1	4	29.962	0.0160	20.5	2.9783	2.9799
22	30.306	0	1	7	30.313	-0.0071	19.9	2.9468	2.9462
23	31.428	3	0	7	31.430	-0.0014	22.2	2.8441	2.8440
24	31.850	4	1	1	31.868	-0.0182	17.6	2.8074	2.8059
25	32.267	1	0	9	32.256	0.0108	17.8	2.7721	2.7730
26	33.090	2	1	7	33.086	0.0043	18.3	2.7050	2.7053
27	34.447	5	0	3	34.447	0.0001	16.4	2.6015	2.6015
28	35.798	0	2	0	35.790	0.0085	22.9	2.5063	2.5069
29	36.420	0	1	9	36.407	0.0126	16.0	2.4650	2.4658
30	37.310	5	0	5	37.305	0.0055	16.6	2.4081	2.4085
31	38.117	5	1	2	38.133	-0.0158	14.0	2.3590	2.3581
32	38.838	3	1	8	38.861	-0.0227	12.6	2.3168	2.3155
33	39.563	6	0	0	39.541	0.0221	11.6	2.2761	2.2773
34	40.224	6	0	2	40.194	0.0298	12.6	2.2402	2.2418
		1	1	10	40.204	0.0199			2.2413
35	40.853	2	2	4	40.842	0.0112	12.0	2.2071	2.2077
36	42.949	0	1	11	42.967	-0.0182	10.7	2.1042	2.1033
37	43.742	6	1	1	43.769	-0.0266	11.2	2.0678	2.0666
38	44.624	2	0	12	44.642	-0.0182	11.2	2.0290	2.0282
39	45.165	6	0	6	45.138	0.0276	11.1	2.0059	2.0071
40	45.304	4	1	9	45.322	-0.0186	11.3	2.0001	1.9993
41	46.041	0	2	8	46.032	0.0083	9.8	1.9698	1.9701
42	47.399	5	1	8	47.393	0.0058	10.9	1.9165	1.9167
43	48.340	3	2	7	48.360	-0.0196	9.2	1.8813	1.8806

A20. UTD-1 as-synthesized

Symmetry : Monoclinic *B*
Space group: *P* 2 (No. 3)

Refined cell parameters:
a : 14.85(6)
b : 8.373(17)
c : 30.37(4)
β : 101.54(22)

N	2*Θ*[obs]	H	K	L	2*Θ*[calc]	obs-calc	Int.	*d*[obs]	*d*[calc]
1	6.073	1	0	0	6.070	0.0029	69.3	14.5426	14.5494
2	7.574	-1	0	2	7.596	-0.0213	48.6	11.6623	11.6297
3	10.978	0	1	1	10.968	0.0103	20.5	8.0528	8.0604
4	12.107	0	1	2	12.119	-0.0120	33.6	7.3043	7.2971
		2	0	0	12.157	-0.0495			7.2747
		1	1	0	12.186	-0.0787			7.2574
5	12.288	-1	0	4	12.222	0.0664	29.8	7.1970	7.2360
		-1	1	1	12.252	0.0365			7.2184
6	14.666	2	0	2	14.573	0.0935	53.5	6.0350	6.0735
7	15.125	-2	0	4	15.225	-0.0995	21.2	5.8529	5.8148
8	17.874	0	0	6	17.871	0.0030	34.6	4.9585	4.9594
		1	1	4	17.892	-0.0179			4.9536
		-3	0	1	17.919	-0.0447			4.9463
9	19.540	-2	0	6	19.527	0.0124	50.5	4.5394	4.5423
		2	1	3	19.608	-0.0687			4.5237
10	20.369	3	0	2	20.347	0.0224	36.0	4.3564	4.3611
11	20.622	-1	0	7	20.545	0.0767	33.4	4.3036	4.3195
		-1	1	6	20.643	-0.0207			4.2993
12	21.202	3	1	0	21.153	0.0488	100.0	4.1871	4.1967
		-3	0	5	21.174	0.0275			4.1925
		0	2	0	21.204	-0.0022			4.1867
13	22.039	-2	0	7	21.990	0.0497	65.8	4.0299	4.0389
		0	2	2	22.038	0.0015			4.0302
		1	2	0	22.075	-0.0359			4.0234
		-1	2	1	22.112	-0.0731			4.0168
14	22.538	1	2	1	22.444	0.0946	47.6	3.9418	3.9582
		-1	2	2	22.553	-0.0149			3.9392
15	23.977	0	0	8	23.905	0.0721	29.9	3.7085	3.7195
		-4	0	2	23.976	0.0002			3.7085
		-4	0	1	24.028	-0.0512			3.7007
16	24.287	-4	0	3	24.301	-0.0141	53.4	3.6618	3.6598
		1	2	3	24.309	-0.0221			3.6586
		0	2	4	24.376	-0.0897			3.6486
17	24.682	-2	0	8	24.586	0.0960	39.9	3.6041	3.6180
		-2	2	2	24.646	0.0352			3.6092
18	26.321	-4	1	2	26.261	0.0599	36.7	3.3833	3.3908
		2	0	7	26.292	0.0293			3.3870
		-4	1	1	26.308	0.0127			3.3849
		4	0	2	26.341	-0.0200			3.3807
		-1	0	9	26.402	-0.0807			3.3731
19	28.050	-3	2	2	27.986	0.0638	21.6	3.1785	3.1856
		1	1	8	28.004	0.0465			3.1837
		3	1	5	28.034	0.0156			3.1803
		3	2	0	28.134	-0.0845			3.1692
		-4	1	5	28.140	-0.0898			3.1686

20	28.498	2	2	4	28.399	0.0987	28.0	3.1296	3.1403
		-3	2	3	28.400	0.0976			3.1401
		2	1	7	28.403	0.0949			3.1398
		4	1	2	28.449	0.0489			3.1349
		-1	1	9	28.505	-0.0076			3.1288
21	28.941	1	0	9	28.841	0.0998	21.7	3.0827	3.0931
		-4	0	7	28.916	0.0247			3.0853
		-2	2	6	28.981	-0.0402			3.0785
		0	1	9	29.013	-0.0721			3.0752
22	29.716	-1	2	7	29.693	0.0236	26.8	3.0040	3.0063
		4	1	3	29.755	-0.0383			3.0002
23	31.936	1	0	10	31.853	0.0828	18.3	2.8000	2.8071
		2	0	9	31.867	0.0693			2.8060
		0	1	10	31.892	0.0443			2.8038
		-2	1	10	31.946	-0.0094			2.7992
		-5	1	2	31.948	-0.0121			2.7990
		2	2	6	31.955	-0.0186			2.7985
		-3	0	10	31.961	-0.0246			2.7980
24	32.399	-5	0	6	32.383	0.0166	23.9	2.7611	2.7625
		-1	0	11	32.405	-0.0059			2.7606
		3	1	7	32.444	-0.0445			2.7574
		-4	2	3	32.468	-0.0685			2.7554
		5	0	2	32.486	-0.0870			2.7539
		-5	1	4	32.498	-0.0992			2.7529
25	33.984	2	2	7	34.019	-0.0352	15.3	2.6359	2.6332
		4	2	2	34.058	-0.0742			2.6303
26	34.099	2	2	7	34.019	0.0796	16.0	2.6272	2.6332
		4	2	2	34.058	0.0406			2.6303
		-1	2	9	34.106	-0.0076			2.6267
		-5	1	6	34.151	-0.0516			2.6234
		-1	1	11	34.172	-0.0731			2.6218
27	35.745	-2	3	4	35.652	0.0934	12.3	2.5099	2.5163
		3	0	9	35.769	-0.0239			2.5083
		-2	0	12	35.817	-0.0717			2.5051
28	36.857	-5	1	8	36.774	0.0832	16.5	2.4367	2.4420
		-5	0	9	36.810	0.0472			2.4397
		-1	3	6	36.832	0.0249			2.4383
		5	1	4	36.913	-0.0557			2.4332
		0	3	6	36.925	-0.0679			2.4324
		-3	3	1	36.950	-0.0923			2.4308
29	37.385	2	3	4	37.342	0.0431	14.5	2.4035	2.4062
		-3	3	3	37.343	0.0423			2.4061
		3	1	9	37.396	-0.0114			2.4028
		-2	1	12	37.442	-0.0575			2.4000
30	39.576	-2	2	11	39.482	0.0933	11.6	2.2754	2.2805
		1	1	12	39.528	0.0473			2.2780
		0	2	11	39.635	-0.0594			2.2721
		-4	0	12	39.652	-0.0766			2.2712
		3	2	8	39.669	-0.0929			2.2703
31	42.166	2	1	12	42.155	0.0116	13.3	2.1414	2.1419
		-5	1	11	42.179	-0.0124			2.1408
		-4	0	13	42.199	-0.0331			2.1398
32	43.201	-1	1	14	43.103	0.0972	13.6	2.0925	2.0970
		-6	0	10	43.119	0.0819			2.0963
		-6	2	5	43.125	0.0756			2.0960
		3	3	6	43.178	0.0223			2.0935
		0	4	0	43.181	0.0192			2.0934
		-4	2	11	43.225	-0.0244			2.0913
		-2	1	14	43.226	-0.0257			2.0913
		-3	2	12	43.255	-0.0542			2.0900
		0	4	1	43.293	-0.0929			2.0882

33	44.930	-4	0	14	44.846	0.0838	12.3	2.0159	2.0195
		-2	0	15	44.854	0.0755			2.0191
		3	3	7	44.886	0.0438			2.0177
		7	1	0	44.897	0.0325			2.0173
		-6	0	11	44.897	0.0322			2.0173
		1	4	3	44.909	0.0209			2.0168
		-5	3	4	44.927	0.0022			2.0160
		0	4	4	44.948	-0.0186			2.0151
		-2	4	1	44.958	-0.0289			2.0147
		5	3	0	44.967	-0.0371			2.0143
		-4	3	8	44.986	-0.0563			2.0135
		2	4	0	45.027	-0.0980			2.0117
34	46.343	-6	1	11	46.255	0.0881	11.5	1.9576	1.9611
		5	3	2	46.275	0.0679			1.9603
		2	2	12	46.326	0.0176			1.9583
		-5	2	11	46.348	-0.0047			1.9574
		7	0	3	46.353	-0.0097			1.9572
35	47.711	3	4	1	47.615	0.0956	11.2	1.9047	1.9083
		-5	0	14	47.631	0.0798			1.9077
		7	1	3	47.679	0.0320			1.9059
		7	0	4	47.689	0.0218			1.9055
		-4	2	13	47.693	0.0181			1.9053
		-2	4	6	47.804	-0.0928			1.9012
36	48.986	-6	0	13	48.914	0.0719	10.0	1.8580	1.8606
		-5	1	14	48.930	0.0554			1.8600
		0	0	16	48.937	0.0484			1.8598
		3	4	3	48.943	0.0423			1.8595
		-2	4	7	48.971	0.0147			1.8586
		7	1	4	48.987	-0.0015			1.8580
		-8	0	3	49.045	-0.0597			1.8559
		-7	2	6	49.050	-0.0645			1.8557

A21. UTD-1 calcined/extracted

Symmetry : Monoclinic *B*
Space group: *P* 2 (No. 3)

Refined cell parameters:
a : 14.6(19)
b : 8.1(2)
c : 30.3(56)
β : 105.1(27)

N	2*Θ*[obs]	H	K	L	2*Θ*[calc]	obs-calc	Int.	*d*[obs]	*d*[calc]
1	6.032	0	0	2	6.032	0.0000	100.0	14.6391	14.6391
2	7.675	1	0	1	7.640	0.0349	44.2	11.5098	11.5624
3	9.311	-	-	-	-		14.1	9.4902	
4	14.514	-1	1	3	14.514	-0.0000	12.3	6.0980	6.0980
5	18.069	0	0	6	18.165	-0.0956	12.5	4.9053	4.8797
6	19.826	3	0	1	19.918	-0.0916	18.2	4.4744	4.4540
7	20.207	-2	1	5	20.207	-0.0000	14.8	4.3911	4.3911
8	21.086	-	-	-	-		32.8	4.2099	
9	21.952	3	1	0	21.859	0.0934	17.0	4.0457	4.0628
10	22.472	-3	1	4	22.490	-0.0185	15.9	3.9533	3.9501
		2	1	4	22.493	-0.0217			3.9496
11	23.225	-1	2	2	23.128	0.0971	15.8	3.8268	3.8427
		1	2	1	23.178	0.0469			3.8345
		-1	1	7	23.262	-0.0373			3.8208
12	24.316	-2	0	8	24.298	0.0175	17.5	3.6575	3.6601
		0	0	8	24.301	0.0151			3.6598
		-2	1	7	24.325	-0.0092			3.6562
13	25.048	-1	2	4	25.039	0.0090	16.5	3.5522	3.5535
		0	2	4	25.040	0.0085			3.5534
		-4	0	4	25.048	-0.0001			3.5522
		3	0	4	25.052	-0.0041			3.5516
		-2	2	1	25.068	-0.0196			3.5495
		-3	1	6	25.143	-0.0942			3.5391
		1	2	3	25.148	-0.0996			3.5384
14	26.216	1	1	7	26.140	0.0758	12.6	3.3966	3.4062
		4	0	1	26.268	-0.0523			3.3899
15	28.211	-4	1	5	28.173	0.0388	12.7	3.1607	3.1650
		-1	2	6	28.197	0.0145			3.1623
16	29.198	4	0	3	29.113	0.0852	12.7	3.0561	3.0648
		-2	1	9	29.200	-0.0018			3.0559
		-2	2	6	29.268	-0.0693			3.0490
		-4	1	6	29.273	-0.0748			3.0484
17	32.311	-4	0	9	32.226	0.0853	11.5	2.7684	2.7755
		-1	2	8	32.268	0.0437			2.7720
		-4	1	8	32.271	0.0400			2.7717
		2	1	8	32.277	0.0345			2.7713
		-5	0	6	32.294	0.0171			2.7698
18	47.575	2	3	9	47.525	0.0500	6.9	1.9098	1.9117
		-6	1	12	47.554	0.0203			1.9106
		-2	2	14	47.559	0.0157			1.9104
		3	1	12	47.563	0.0114			1.9102

A22. UTD-1 calcined/extracted

Symmetry : Orthorhombic *B*
Space group: *B m m b* (No. 63)

Refined cell parameters:
a : 19.017(10)
b : 8.421(6)
c : 22.978(13)

N	2Θ[obs]	H	K	L	2Θ[calc]	obs-calc	Int.	*d*[obs]	*d*[calc]
1	6.032	1	0	1	6.028	0.0046	100.0	14.6391	14.6503
2	7.675	0	0	2	7.689	-0.0140	44.2	11.5098	11.4889
3	9.311	2	0	0	9.293	0.0179	14.1	9.4902	9.5084
4	14.514	3	0	1	14.484	0.0303	12.3	6.0980	6.1107
5	18.069	2	0	4	18.027	0.0426	12.5	4.9053	4.9168
6	19.826	1	0	5	19.860	-0.0332	18.2	4.4744	4.4670
7	20.207	4	0	2	20.198	0.0088	14.8	4.3911	4.3930
8	21.086	0	2	0	21.082	0.0040	32.8	4.2099	4.2107
9	21.952	1	2	1	21.946	0.0064	17.0	4.0457	4.0469
10	22.472	0	2	2	22.471	0.0011	15.9	3.9533	3.9535
		1	1	5	22.513	-0.0412			3.9462
11	23.225	0	0	6	23.207	0.0174	15.8	3.8268	3.8296
12	24.316	4	0	4	24.282	0.0339	17.5	3.6575	3.6626
		2	2	2	24.363	-0.0473			3.6506
13	25.048	2	0	6	25.047	0.0010	16.5	3.5522	3.5523
14	26.216	0	2	4	26.220	-0.0039	12.6	3.3966	3.3961
15	28.211	5	1	3	28.237	-0.0253	12.7	3.1607	3.1579
16	29.198	6	0	2	29.205	-0.0071	12.7	3.0561	3.0553
17	32.311	5	1	5	32.324	-0.0128	11.5	2.7684	2.7673

A23. Iodine – UTD-1

Symmetry : Orthorhombic *B*
Space group: *B m m b* (No. 63)

Refined cell parameters:
a : 18.999(15)
b : 8.418(9)
c : 22.989(16)

N	2Θ[obs]	H	K	L	2Θ[calc]	obs-calc	Int.	*d*[obs]	*d*[calc]
1	6.031	1	0	1	6.030	0.0010	93.5	14.6425	14.6450
2	12.450	1	0	3	12.445	0.0051	96.8	7.1039	7.1067
3	15.424	0	0	4	15.405	0.0194	86.9	5.7401	5.7473
4	18.059	2	0	4	18.025	0.0343	74.1	4.9081	4.9174
5	18.671	4	0	0	18.666	0.0047	76.5	4.7486	4.7498
		0	1	4	18.679	-0.0078			4.7466
6	19.862	1	0	5	19.851	0.0109	96.1	4.4664	4.4688
7	20.229	4	0	2	20.213	0.0159	95.0	4.3863	4.3898
8	21.095	3	1	3	21.020	0.0751	100.0	4.2082	4.2230
		0	2	0	21.089	0.0053			4.2092
9	21.957	1	2	1	21.954	0.0035	83.9	4.0448	4.0454
10	22.472	0	2	2	22.476	-0.0045	77.6	3.9533	3.9525
		1	1	5	22.507	-0.0355			3.9472
11	23.786	5	0	1	23.714	0.0718	68.5	3.7378	3.7489
12	24.306	4	0	4	24.291	0.0155	79.6	3.6590	3.6613
		2	2	2	24.372	-0.0656			3.6493
13	25.051	2	0	6	25.040	0.0115	67.4	3.5518	3.5534
14	25.689	3	2	1	25.686	0.0030	56.5	3.4651	3.4655
15	26.144	5	0	3	26.156	-0.0119	54.3	3.4058	3.4043
		3	1	5	26.165	-0.0210			3.4031
		0	2	4	26.222	-0.0778			3.3959
16	27.152	2	1	6	27.219	-0.0666	50.3	3.2816	3.2737
17	27.575	1	0	7	27.540	0.0342	46.0	3.2322	3.2362
18	27.982	3	2	3	27.967	0.0154	49.7	3.1861	3.1878
19	28.185	6	0	0	28.159	0.0269	50.3	3.1635	3.1665
		5	1	3	28.254	-0.0689			3.1560
20	29.115	1	2	5	29.121	-0.0061	43.6	3.0647	3.0640
21	29.903	4	0	6	29.939	-0.0351	41.6	2.9856	2.9822
22	32.329	6	0	4	32.251	0.0778	38.8	2.7669	2.7734
		5	1	5	32.336	-0.0069			2.7663
		4	2	4	32.383	-0.0537			2.7625
23	36.880	2	3	4	36.849	0.0306	28.0	2.4353	2.4372
		4	2	6	36.910	-0.0301			2.4334
		3	3	3	36.918	-0.0382			2.4328
24	37.443	5	2	5	37.374	0.0690	26.8	2.3999	2.4042
		3	2	7	37.495	-0.0525			2.3967
25	37.917	8	0	0	37.853	0.0643	28.7	2.3710	2.3749
		0	2	8	37.879	0.0382			2.3733
		3	0	9	37.952	-0.0347			2.3689
26	41.045	8	0	4	41.091	-0.0463	23.4	2.1972	2.1949

A24. Selenium – UTD-1

Symmetry : Orthorhombic *B*
Space group: *B m m b* (No. 63)

Refined cell parameters:
a : 19.016(8)
b : 8.436(4)
c : 23.087(12)

N	2Θ[obs]	H	K	L	2Θ[calc]	obs-calc	Int.	*d*[obs]	*d*[calc]
1	5.998	1	0	1	6.016	-0.0181	100.0	14.7225	14.6782
2	7.639	0	0	2	7.652	-0.0132	40.0	11.5634	11.5436
3	9.273	2	0	0	9.294	-0.0213	10.3	9.5299	9.5081
4	14.473	3	0	1	14.479	-0.0063	9.6	6.1152	6.1125
5	18.105	3	0	3	18.116	-0.0109	9.6	4.8956	4.8927
6	19.782	1	0	5	19.770	0.0122	12.3	4.4843	4.4870
7	20.173	4	0	2	20.184	-0.0115	9.2	4.3983	4.3959
8	21.035	0	2	0	21.044	-0.0091	26.3	4.2200	4.2182
9	21.892	1	2	1	21.906	-0.0136	11.0	4.0566	4.0541
10	22.414	0	2	2	22.422	-0.0078	10.0	3.9634	3.9620
		1	1	5	22.424	-0.0103			3.9616
11	23.086	2	2	0	23.048	0.0386	8.1	3.8494	3.8558
		0	0	6	23.096	-0.0097			3.8479
12	23.720	5	0	1	23.690	0.0295	6.7	3.7481	3.7527
13	24.249	4	0	4	24.235	0.0139	10.0	3.6675	3.6695
14	24.955	2	0	6	24.944	0.0114	9.0	3.5652	3.5668
15	25.641	3	2	1	25.638	0.0029	5.2	3.4714	3.4718
16	26.118	3	1	5	26.087	0.0314	6.6	3.4091	3.4131
		5	0	3	26.114	0.0039			3.4096
		0	2	4	26.145	-0.0269			3.4056
17	28.139	6	0	0	28.133	0.0062	5.5	3.1687	3.1694
18	29.046	1	2	5	29.030	0.0154	4.5	3.0718	3.0734
19	29.807	4	0	6	29.849	-0.0421	4.6	2.9951	2.9909
20	32.266	5	1	5	32.261	0.0052	4.4	2.7721	2.7726
		4	2	4	32.309	-0.0428			2.7686
21	32.870	2	2	6	32.857	0.0128	3.2	2.7226	2.7237

A25. Mercury(II) bromide – UTD-1

Symmetry : Orthorhombic *B*
Spacegroup : *B m m b* (No. 63)

Refined cell parameters:
a : 18.935(13)
b : 8.421(11)
c : 23.004(16)

N	2Θ[obs]	H	K	L	2Θ[calc]	obs-calc	Int.	*d*[obs]	*d*[calc]
1	6.052	1	0	1	6.041	0.0117	100.0	14.5913	14.6195
2	7.687	0	0	2	7.680	0.0064	39.5	11.4924	11.5019
3	9.335	2	0	0	9.334	0.0015	13.1	9.4661	9.4676
4	12.142	2	0	2	12.098	0.0443	26.7	7.2832	7.3098
		1	1	1	12.119	0.0236			7.2973
5	12.471	1	0	3	12.444	0.0266	41.3	7.0922	7.1073
6	14.568	3	0	1	14.541	0.0270	11.1	6.0755	6.0868
7	15.403	0	0	4	15.395	0.0085	17.9	5.7478	5.7509
8	18.094	2	0	4	18.033	0.0612	22.1	4.8987	4.9152
		3	0	3	18.190	-0.0956			4.8732
9	19.869	1	0	5	19.843	0.0258	24.7	4.4649	4.4707
10	20.207	4	0	2	20.270	-0.0627	21.9	4.3910	4.3776
11	21.107	3	1	3	21.046	0.0617	52.7	4.2057	4.2179
		0	2	0	21.082	0.0255			4.2107
12	21.973	1	2	1	21.949	0.0243	18.8	4.0418	4.0462
13	23.131	2	2	0	23.099	0.0323	23.9	3.8421	3.8474
		0	0	6	23.181	-0.0496			3.8340
14	23.810	5	0	1	23.793	0.0174	30.1	3.7341	3.7367
15	24.352	4	0	4	24.334	0.0181	30.7	3.6522	3.6549
		2	2	2	24.376	-0.0240			3.6487
16	24.963	2	0	6	25.038	-0.0750	37.9	3.5641	3.5536
17	25.714	3	2	1	25.705	0.0091	26.9	3.4617	3.4629
18	27.485	1	0	7	27.526	-0.0410	17.8	3.2426	3.2379
19	27.989	3	2	3	27.982	0.0074	23.4	3.1853	3.1861
20	29.399	6	0	2	29.323	0.0768	17.6	3.0356	3.0434
		4	2	2	29.409	-0.0091			3.0347
21	30.526	5	0	5	30.550	-0.0238	16.6	2.9261	2.9239
22	31.060	0	0	8	31.077	-0.0169	12.3	2.8770	2.8755
23	31.494	0	2	6	31.534	-0.0392	14.1	2.8383	2.8349
24	32.000	5	2	1	31.997	0.0033	19.7	2.7946	2.7949
		3	2	5	32.090	-0.0901			2.7870
25	32.372	6	0	4	32.332	0.0400	17.0	2.7633	2.7667
		5	1	5	32.386	-0.0144			2.7622
		4	2	4	32.411	-0.0387			2.7601
		1	3	1	32.451	-0.0792			2.7568
26	33.832	5	2	3	33.887	-0.0547	11.5	2.6473	2.6432
27	34.876	1	2	7	34.928	-0.0523	11.4	2.5705	2.5667
28	35.200	7	0	3	35.151	0.0484	11.2	2.5476	2.5510
		3	3	1	35.177	0.0222			2.5491
29	36.390	6	2	2	36.395	-0.0052	14.0	2.4669	2.4666
30	36.963	3	3	3	36.924	0.0386	10.4	2.4300	2.4324
		4	2	6	36.929	0.0334			2.4321
		1	1	9	37.031	-0.0685			2.4257
31	37.332	5	2	5	37.415	-0.0827	11.5	2.4068	2.4017
32	37.811	5	1	7	37.755	0.0557	13.6	2.3774	2.3808
		1	3	5	37.812	-0.0010			2.3774

		0	2	8	37.857	-0.0464		2.3746
33	38.800	8	0	2	38.813	-0.0125	10.8	2.3190	2.3183
34	39.715	0	3	6	39.765	-0.0501	8.7	2.2677	2.2649
		7	2	1	39.768	-0.0524			2.2648
35	41.275	8	0	4	41.211	0.0642	9.7	2.1855	2.1888
		7	2	3	41.349	-0.0736			2.1818
36	44.021	2	4	0	44.025	-0.0039	9.6	2.0553	2.0552
		5	1	9	44.039	-0.0172			2.0546
37	44.434	7	2	5	44.371	0.0624	12.4	2.0372	2.0399
		9	1	1	44.526	-0.0925			2.0332
38	48.740	0	1	12	48.675	0.0655	9.2	1.8668	1.8692
		10	0	2	48.697	0.0435			1.8684
		9	1	5	48.768	-0.0282			1.8658
		1	2	11	48.822	-0.0815			1.8639
39	49.141	4	3	8	49.238	-0.0967	8.4	1.8525	1.8491
40	49.747	5	4	1	49.663	0.0844	8.6	1.8313	1.8343
		2	1	12	49.677	0.0703			1.8338
		3	4	5	49.728	0.0195			1.8320
		5	0	11	49.767	-0.0194			1.8307

A26. Gold(III) chloride – UTD-1

Symmetry : Orthorhombic *P*

Refined cell parameters :
a : 23.035(9)
b : 19.002(12)
c : 8.223(11)

N	2Θ[obs]	H	K	L	2Θ[calc]	obs-calc	Int.	*d*[obs]	*d*[calc]
1	6.010	1	1	0	6.025	-0.0147	60.2	14.6939	14.6581
2	7.652	2	0	0	7.670	-0.0182	19.7	11.5448	11.5175
3	9.283	0	2	0	9.301	-0.0182	18.2	9.5195	9.5009
4	12.070	2	2	0	12.066	0.0038	39.0	7.3268	7.3291
5	12.418	3	1	0	12.423	-0.0052	52.5	7.1220	7.1191
6	14.495	1	3	0	14.492	0.0027	22.6	6.1061	6.1073
7	14.852	3	2	0	14.822	0.0296	17.3	5.9600	5.9719
8	15.373	4	0	0	15.374	-0.0011	30.5	5.7592	5.7587
9	15.944	2	3	0	15.956	-0.0123	19.5	5.5543	5.5500
10	18.025	4	2	0	17.998	0.0276	27.8	4.9172	4.9247
		1	3	1	18.079	-0.0533			4.9029
11	18.660	0	4	0	18.664	-0.0042	25.9	4.7515	4.7504
12	19.813	5	1	0	19.814	-0.0009	52.3	4.4775	4.4773
13	20.204	2	4	0	20.204	-0.0007	55.4	4.3917	4.3916
14	21.057	4	2	1	21.010	0.0473	100.0	4.2155	4.2249
		3	3	1	21.134	-0.0766			4.2004
15	21.914	1	4	1	21.932	-0.0184	42.7	4.0527	4.0493
		1	0	2	21.943	-0.0287			4.0474
		3	4	0	21.985	-0.0707			4.0398
16	22.450	1	1	2	22.441	0.0085	36.1	3.9572	3.9586
17	23.091	6	0	0	23.149	-0.0581	32.2	3.8487	3.8392
18	23.728	1	5	0	23.709	0.0185	41.3	3.7468	3.7497
19	24.272	4	4	0	24.269	0.0033	60.5	3.6640	3.6645
20	24.991	3	1	2	24.990	0.0010	46.1	3.5602	3.5603
		6	2	0	24.996	-0.0046			3.5595
21	25.599	6	0	1	25.587	0.0120	18.0	3.4771	3.4787
22	26.210	3	5	0	26.142	0.0681	19.3	3.3973	3.4060
		5	3	1	26.239	-0.0291			3.3936
23	27.226	6	2	1	27.279	-0.0533	20.4	3.2729	3.2666
24	29.211	7	0	1	29.207	0.0039	26.3	3.0547	3.0551
		2	6	0	29.222	-0.0109			3.0536
		6	3	1	29.267	-0.0554			3.0491
25	29.890	6	4	0	29.900	-0.0101	18.2	2.9869	2.9859
26	30.480	5	5	0	30.467	0.0133	16.3	2.9304	2.9316
		1	6	1	30.470	0.0101			2.9313
		3	6	0	30.509	-0.0284			2.9277
27	32.339	1	5	2	32.286	0.0524	21.0	2.7661	2.7705
		5	5	1	32.396	-0.0571			2.7614
		5	3	2	32.403	-0.0642			2.7608
28	32.908	1	0	3	32.881	0.0267	18.0	2.7196	2.7217
		8	0	1	32.933	-0.0250			2.7176
		0	7	0	32.970	-0.0629			2.7145
29	33.238	1	7	0	33.205	0.0326	18.5	2.6933	2.6959
		1	1	3	33.226	0.0116			2.6942
		6	2	2	33.266	-0.0283			2.6911
		8	1	1	33.277	-0.0396			2.6902
30	35.069	1	7	1	34.999	0.0702	17.5	2.5568	2.5617

		9	0	0	35.031	0.0380		2.5594
		3	7	0	35.033	0.0362		2.5593
		3	1	3	35.053	0.0162		2.5579
31	35.428	9	1	0	35.358	0.0702	17.0	2.5317	2.5365
32	37.819	7	5	1	37.750	0.0689	18.7	2.3769	2.3811
		7	3	2	37.756	0.0626			2.3807
		0	8	0	37.847	-0.0283			2.3752
		0	4	3	37.866	-0.0470			2.3741
		9	3	0	37.883	-0.0648			2.3730
33	42.919	4	7	2	42.865	0.0539	17.8	2.1056	2.1081
		7	0	3	42.908	0.0107			2.1061
		6	3	3	42.950	-0.0319			2.1041
		1	9	0	42.984	-0.0657			2.1025
34	43.437	11	1	0	43.440	-0.0036	18.4	2.0816	2.0815
35	44.450	2	6	3	44.376	0.0747	17.4	2.0365	2.0398
		1	9	1	44.440	0.0107			2.0370
		1	1	4	44.467	-0.0166			2.0358
		3	9	0	44.467	-0.0172			2.0358
36	48.008	3	3	4	47.974	0.0346	17.6	1.8935	1.8948
		8	3	3	47.985	0.0230			1.8944
		1	10	0	48.003	0.0056			1.8937
		8	6	2	48.061	-0.0528			1.8916
37	48.828	11	4	1	48.758	0.0701	18.1	1.8637	1.8662
		11	0	2	48.763	0.0650			1.8660
		7	7	2	48.764	0.0636			1.8659
		10	6	0	48.850	-0.0225			1.8629
		9	7	0	48.868	-0.0402			1.8622
		2	4	4	48.879	-0.0514			1.8618
		9	1	3	48.883	-0.0554			1.8617
38	49.727	12	2	1	49.666	0.0611	17.1	1.8320	1.8342
		11	5	0	49.668	0.0589			1.8341
		8	8	0	49.721	0.0064			1.8323
		3	4	4	49.725	0.0026			1.8321
		8	4	3	49.736	-0.0087			1.8317
		11	2	2	49.757	-0.0301			1.8310

A27. Mercury(II) bromide
[PG90]

Symmetry : Orthorhombic *C*
Space group: *C m c* 21

Cell parameters:
a : 4.6280
b : 6.8020
c : 12.4760

d	2*Θ*	*I*(rel)	*I*(abs)	*I*(int)	FWHM	H	K	L
6.238000	14.1865	94.90	94905	0.00	0.1000	0	0	2
3.826325	23.2278	14.17	14170	0.00	0.1000	1	1	0
3.658145	24.3116	100.00	100000	0.00	0.1000	1	1	1
3.401000	26.1812	0.20	202	0.00	0.1000	0	2	0
3.281265	27.1546	6.84	6836	0.00	0.1000	0	2	1
3.261622	27.3213	80.78	80784	0.00	0.1000	1	1	2
3.119000	28.5966	0.54	541	0.00	0.1000	0	0	4
2.986034	29.8990	13.30	13297	0.00	0.1000	0	2	2
2.815793	31.7529	65.06	65059	0.00	0.1000	1	1	3
2.632708	34.0259	56.99	56985	0.00	0.1000	0	2	3
2.417570	37.1596	13.57	13574	0.00	0.1000	1	1	4
2.314000	38.8881	34.40	34396	0.00	0.1000	2	0	0
2.298707	39.1574	17.73	17734	0.00	0.1000	0	2	4
2.169539	41.5933	14.97	14971	0.00	0.1000	2	0	2
2.090063	43.2528	29.13	29126	0.00	0.1000	1	1	5
2.079333	43.4873	10.35	10352	0.00	0.1000	0	0	6
2.036110	44.4592	22.84	22843	0.00	0.1000	1	3	0
2.011822	45.0252	21.29	21288	0.00	0.1000	0	2	5
2.009525	45.0795	9.03	9031	0.00	0.1000	1	3	1
1.935610	46.9017	23.27	23272	0.00	0.1000	1	3	2
1.913162	47.4855	0.13	135	0.00	0.1000	2	2	0
1.891057	48.0754	3.44	3443	0.00	0.1000	2	2	1
1.858396	48.9752	0.39	394	0.00	0.1000	2	0	4
1.829073	49.8134	6.72	6724	0.00	0.1000	2	2	2
1.828692	49.8245	4.95	4954	0.00	0.1000	1	3	3
1.826991	49.8740	14.64	14635	0.00	0.1000	1	1	6

A28. Gold(III) chloride
[CT58]

Symmetry : Monoclinic *B P*
Space group : *P* 1 21/*c* 1

Cell parameters:
a : 6.5700
b : 11.0400
c : 6.4400
β : 113.300

d	2*Θ*	*I*(rel)	*I*(abs)	*I*(int)	FWHM	H	K	L
6.034193	14.6683	100.00	100000	0.00	0.1000	1	0	0
5.520000	16.0433	20.71	20707	0.00	0.1000	0	2	0
5.294894	16.7301	3.10	3095	0.00	0.1000	1	1	0
5.213673	16.9926	1.49	1494	0.00	0.1000	0	1	1
4.874431	18.1850	14.77	14769	0.00	0.1000	-1	1	1
4.072903	21.8038	19.64	19644	0.00	0.1000	1	2	0
4.035587	22.0079	93.60	93603	0.00	0.1000	0	2	1
3.871973	22.9502	69.09	69089	0.00	0.1000	-1	2	1
3.401727	26.1756	1.23	1228	0.00	0.1000	1	1	1
3.203068	27.8307	11.04	11036	0.00	0.1000	-1	0	2
3.141828	28.3844	3.10	3097	0.00	0.1000	1	3	0
3.126313	28.5282	6.44	6440	0.00	0.1000	-2	1	1
3.124603	28.5442	16.38	16382	0.00	0.1000	0	3	1
3.076210	29.0030	0.05	50	0.00	0.1000	-1	1	2
3.046787	29.2893	0.84	843	0.00	0.1000	-1	3	1
3.017096	29.5841	4.27	4274	0.00	0.1000	2	0	0
3.001076	29.7456	38.94	38937	0.00	0.1000	1	2	1
2.957397	30.1953	7.22	7217	0.00	0.1000	0	0	2
2.910371	30.6951	0.07	67	0.00	0.1000	2	1	0
2.856676	31.2867	0.07	72	0.00	0.1000	0	1	2
2.806863	31.8566	5.88	5881	0.00	0.1000	-2	2	1
2.770434	32.2868	4.08	4083	0.00	0.1000	-1	2	2
2.760000	32.4123	6.36	6361	0.00	0.1000	0	4	0
2.716320	32.9482	14.78	14781	0.00	0.1000	-2	0	2
2.647447	33.8308	3.20	3199	0.00	0.1000	2	2	0
2.637655	33.9602	12.93	12933	0.00	0.1000	-2	1	2
2.606837	34.3741	5.99	5991	0.00	0.1000	0	2	2
2.564483	34.9599	1.57	1571	0.00	0.1000	1	3	1
2.509912	35.7454	9.43	9431	0.00	0.1000	1	4	0
2.501104	35.8755	15.50	15495	0.00	0.1000	0	4	1
2.460654	36.4858	12.28	12276	0.00	0.1000	-1	4	1
2.440103	36.8041	3.09	3086	0.00	0.1000	-2	3	1
2.437216	36.8493	6.59	6588	0.00	0.1000	-2	2	2
2.416055	37.1838	5.18	5179	0.00	0.1000	-1	3	2
2.333180	38.5557	5.74	5738	0.00	0.1000	2	3	0
2.317889	38.8202	23.06	23062	0.00	0.1000	1	0	2
2.305240	39.0419	0.86	859	0.00	0.1000	0	3	2
2.288300	39.3428	3.27	3272	0.00	0.1000	2	1	1
2.185444	41.2767	8.74	8736	0.00	0.1000	-2	3	2
2.184846	41.2885	13.17	13175	0.00	0.1000	1	4	1
2.153712	41.9132	18.69	18690	0.00	0.1000	2	2	1
2.144381	42.1043	7.22	7217	0.00	0.1000	-3	1	1
2.137123	42.2541	4.13	4126	0.00	0.1000	1	2	2
2.106387	42.9009	16.35	16351	0.00	0.1000	-2	4	1

2.101526	43.0051	1.91	1910	0.00	0.1000	-1	1	3
2.091885	43.2133	2.74	2740	0.00	0.1000	-3	0	2
2.090860	43.2355	5.42	5416	0.00	0.1000	-1	4	2
2.073542	43.6150	0.36	364	0.00	0.1000	1	5	0
2.068568	43.7253	0.11	107	0.00	0.1000	0	5	1
2.055313	44.0220	5.79	5789	0.00	0.1000	-3	1	2
2.045508	44.2441	1.28	1282	0.00	0.1000	-1	5	1
2.036451	44.4513	5.30	5295	0.00	0.1000	2	4	0
2.032443	44.5437	4.01	4005	0.00	0.1000	-3	2	1
2.031426	44.5672	9.48	9481	0.00	0.1000	-2	1	3
2.017793	44.8846	5.46	5458	0.00	0.1000	0	4	2
2.011398	45.0352	4.32	4321	0.00	0.1000	3	0	0
1.995844	45.4056	3.49	3493	0.00	0.1000	-1	2	3
1.978823	45.8183	2.47	2467	0.00	0.1000	3	1	0
1.974067	45.9350	2.38	2382	0.00	0.1000	2	3	1
1.961269	46.2521	0.06	62	0.00	0.1000	1	3	2
1.956131	46.3807	2.48	2483	0.00	0.1000	-3	2	2
1.940890	46.7665	0.72	725	0.00	0.1000	0	1	3
1.935987	46.8920	0.97	972	0.00	0.1000	-2	4	2
1.935504	46.9044	8.39	8388	0.00	0.1000	-2	2	3
1.889844	48.1082	1.49	1490	0.00	0.1000	3	2	0
1.879428	48.3919	0.07	72	0.00	0.1000	-3	3	1
1.878685	48.4122	0.26	257	0.00	0.1000	1	5	1
1.856719	49.0224	6.30	6303	0.00	0.1000	0	2	3
1.850375	49.2016	0.77	769	0.00	0.1000	-1	3	3
1.840000	49.4976	1.20	1202	0.00	0.1000	0	6	0
1.828100	49.8417	5.03	5026	0.00	0.1000	-2	5	1

A29. Gold(I) chloride
[SL74]

Symmetry : Tetragonal *I*
Space group : *I* 41/*a m d Z*

Cell parameters:
a : 6.7390
c : 8.6990

d	2*Θ*	*I*(rel)	*I*(abs)	*I*(int)	FWHM	H	K	L
5.327415	16.6273	100.00	100000	0.00	0.1000	1	0	1
3.369500	26.4304	3.95	3949	0.00	0.1000	2	0	0
3.212488	27.7474	4.07	4073	0.00	0.1000	1	1	2
2.847712	31.3878	68.79	68791	0.00	0.1000	2	1	1
2.663707	33.6181	95.78	95782	0.00	0.1000	2	0	2
2.663562	33.6200	13.70	13699	0.00	0.1000	1	0	3
2.382596	37.7255	22.94	22936	0.00	0.1000	2	2	0
2.174987	41.4843	11.28	11282	0.00	0.1000	3	0	1
2.174750	41.4890	12.70	12698	0.00	0.1000	0	0	4
2.089549	43.2640	36.76	36763	0.00	0.1000	2	1	3
1.913704	47.4713	1.53	1526	0.00	0.1000	3	1	2
1.827359	49.8633	19.26	19260	0.00	0.1000	3	2	1
1.827218	49.8674	0.04	38	0.00	0.1000	2	0	4

A30. Hydrogentetrachloroaurate(III) tetrahydrate
[OP71]

Symmetry : Monoclinic *B C*
Space group : *C* 1 2/*m* 1

Cell parameters:
a : 11.7800
b : 4.6200
c : 8.8900
β : 101.900

d	2*Θ*	*I*(rel)	*I*(abs)	*I*(int)	FWHM	H	K	L
8.698946	10.1605	100.00	100000	0.00	0.1000	0	0	1
5.763418	15.3615	39.49	39488	0.00	0.1000	2	0	0
5.338045	16.5939	35.06	35062	0.00	0.1000	-2	0	1
4.404563	20.1441	15.74	15738	0.00	0.1000	2	0	1
4.349473	20.4020	20.84	20838	0.00	0.1000	0	0	2
4.288373	20.6958	48.55	48546	0.00	0.1000	1	1	0
3.969034	22.3816	33.92	33921	0.00	0.1000	-1	1	1
3.877445	22.9174	10.44	10441	0.00	0.1000	-2	0	2
3.734441	23.8076	25.57	25566	0.00	0.1000	1	1	1
3.178031	28.0544	4.01	4014	0.00	0.1000	-1	1	2
3.171540	28.1130	5.85	5845	0.00	0.1000	2	0	2
2.954147	30.2293	25.92	25922	0.00	0.1000	3	1	0
2.942924	30.3474	46.52	46516	0.00	0.1000	1	1	2
2.921236	30.5782	12.61	12609	0.00	0.1000	-4	0	1
2.899648	30.8115	16.74	16739	0.00	0.1000	0	0	3
2.881709	31.0081	2.04	2036	0.00	0.1000	4	0	0
2.835668	31.5245	0.13	134	0.00	0.1000	-2	0	3
2.671269	33.5201	3.05	3047	0.00	0.1000	3	1	1
2.669023	33.5492	0.80	799	0.00	0.1000	-4	0	2
2.646563	33.8424	9.84	9837	0.00	0.1000	-3	1	2
2.581240	34.7257	0.30	301	0.00	0.1000	4	0	1
2.492432	36.0046	12.77	12770	0.00	0.1000	-1	1	3
2.399265	37.4536	9.01	9010	0.00	0.1000	2	0	3
2.320875	38.7683	8.74	8738	0.00	0.1000	1	1	3
2.310000	38.9582	9.54	9545	0.00	0.1000	0	2	0
2.294157	39.2382	1.05	1051	0.00	0.1000	-4	0	3
2.281437	39.4660	14.55	14548	0.00	0.1000	3	1	2
2.255862	39.9324	4.89	4892	0.00	0.1000	-3	1	3
2.232622	40.3660	2.00	2002	0.00	0.1000	0	2	1
2.202282	40.9469	1.09	1086	0.00	0.1000	4	0	2
2.189272	41.2012	5.06	5063	0.00	0.1000	-2	0	4
2.174736	41.4893	9.00	9004	0.00	0.1000	0	0	4
2.144186	42.1083	8.51	8515	0.00	0.1000	2	2	0
2.120010	42.6118	10.10	10095	0.00	0.1000	-2	2	1
2.095843	43.1275	6.70	6702	0.00	0.1000	-5	1	1
2.062810	43.8537	7.95	7946	0.00	0.1000	5	1	0
2.045727	44.2391	3.93	3927	0.00	0.1000	2	2	1
2.040125	44.3670	1.20	1204	0.00	0.1000	0	2	2
2.013176	44.9932	8.78	8779	0.00	0.1000	-5	1	2
2.002545	45.2453	5.91	5908	0.00	0.1000	-1	1	4
1.984517	45.6794	5.88	5877	0.00	0.1000	-2	2	2
1.963114	46.2061	5.45	5448	0.00	0.1000	-6	0	1
1.938722	46.8219	2.21	2215	0.00	0.1000	-4	0	4
1.928838	47.0762	2.16	2155	0.00	0.1000	5	1	1

1.922585	47.2386	7.11	7110	0.00	0.1000	3	1	3
1.921139	47.2763	1.41	1411	0.00	0.1000	6	0	0
1.908841	47.5997	9.50	9496	0.00	0.1000	2	0	4
1.901155	47.8041	8.95	8950	0.00	0.1000	-3	1	4
1.882213	48.3157	7.39	7393	0.00	0.1000	1	1	4
1.867221	48.7287	2.45	2445	0.00	0.1000	2	2	2
1.861096	48.8995	3.17	3171	0.00	0.1000	4	0	3
1.849796	49.2180	1.57	1567	0.00	0.1000	-5	1	3

List of publications

Chemical vapour deposition of mercury(II) halides into siliceous UTD-1 and SSZ-24 hosts

Ramona Nechifor, Monika Hartl, Peter Behrens

Contribution at the "15. Deutsche Zeolith-Tagung", Kaiserslautern, 5-7 March 2003

Chemical vapour deposition of mercury(II) halides into zeosils

Ramona Nechifor, Monika Hartl, Peter Behrens

Contribution at the "9th European Conference on Solid State Chemistry", Stuttgart, 3-6 September 2003

Chemical vapour deposition of iodine into pure silica hosts

Ramona Nechifor, Monika Hartl, Peter Behrens

Contribution at the "2nd European Organosilicon Days", München, 11-12 September 2003

Iodine and mercury bromide insertion into pure silica hosts with large pores

R. Nechifor, P. Behrens

Contribution at the "16. Deutsche Zeolith-Tagung", Dresden, 3-5 March 2004

Iodine insertion into pure silica hosts with large pores

*R. Nechifor, P. Behrens**

in Organosilicon Chemistry VI, Hrsg.: N. Auner, J. Weis, Wiley-VCH,

Weinheim 2005, p. 930-936

Curriculum Vitae

Personal information

Surname / First name:	Nechifor / Geanina Ramona
Date of birth:	22 December 1976
Place of birth:	Resita (Romania)

Education and training

Date (from – to):	01 / 2002 – 03 / 2005
Name of organisation providing education:	University of Hannover, Germany Institute of Inorganic Chemistry
Title of qualification awarded:	PhD (Dr. rer. nat.)
Principal subject:	Inorganic chemistry
Final project:	"Synthetic approaches utilizing zeosils: inorganic insertion compounds and hierarchical pore structures"
Date (from – to):	08 / 2004 – 10 / 2004
Name of organisation providing education:	Catholic University Leuven, Belgium Centre for Surface Chemistry and Catalysis Research at a foreign university, as required by the "Promotion Program"
Date (from – to):	10 / 2000 – 06 / 2001
Name of organisation providing education:	Polytechnic University of Timisoara, Romania Faculty of Chemical Engineering and Environment Protection
Title of qualification awarded:	Master Degree with specialization in Rubber Technology
Principal subject:	Macromolecular chemistry

Final project:	"Studies of vulcanization systems of the tire tread compounds and their influence on wear and winter performance"
Date (from – to):	10 / 1995 – 06 / 2000
Name of organisation providing education:	Polytechnic University of Timisoara, Romania Faculty of Chemical Engineering and Environment Protection
Title of qualification awarded:	University Diploma with specialization in Organic Chemistry
Principal subject:	Organic chemistry
Final project:	"Overview of the technological process to obtain isopropyl iodide and study of an innovative way to obtain hyper-branched polymers"

Grants and scholarships

Date (from – to):	01 / 2002 – 12 / 2004
Type:	"Georg Christoph Lichtenberg" fellowship, part of the Graduate Program "New Materials with Tailored Properties" sponsored by the State of Niedersachsen